FIBRILLAR COLLAGEN STRUCTURE IN OVINE LEATHER AND RELATED MATERIALS AND ITS RELATIONSHIP TO STRENGTH

A thesis presented in partial fulfilment of the
requirements for the degree of
Doctor of Philosophy in Engineering
at Massey University, Palmerston North, New Zealand

Melissa Basil-Jones

2013

ABSTRACT

Leather is used for a number of products including those of the garment, automotive and footwear industries. The footwear industry provides a consistent demand for leather. However, due to strength properties of leather produced from ovine skins, ovine leather is not currently used in significant quantities in this industry. A greater understanding of the structure of ovine leather could assist in designing processing steps to increase ovine leather strength. Fibrillar collagen is a major structural component of a number of tissues including skin and is the main component of leather. Small angle X-ray scattering (SAXS) is an X-ray diffraction technique that can be used to investigate fibrillar collagen structure and distribution.

A relationship is found between the orientation of collagen fibrils in ovine leather and tear strength. Stronger leather has a greater alignment of collagen fibrils parallel to the leather surface while weaker leather has more fibrils out of this plane. The fibrillar collagen structure is fairly consistent across the entire ovine leather skin, with the relationship between orientation index and tear strength maintained at all positions investigated. The fibrillar collagen structure of ovine skins changes during leather processing with the alignment of collagen fibrils, in the direction parallel to the skin surface, consistently increasing after the pickling stage.

Significant changes occur to the fibrillar collagen structure of ovine leather during uni-axial stretching. Initial strain results in reorientation of collagen fibrils followed by stretching of individual fibrils. The response to strain varies, with stretching of fibrils occurring more evenly across cross-sections in stronger samples than in weaker samples. The response of a different collagen rich material, a decellularized extracellular matrix biomaterial, to uni-axial strain is similar to that of leather.

The findings of this work greatly increase the knowledge of the fibrillar collagen structure of ovine leather. Through this work a fundamental relationship between fibrillar collagen orientation and tear strength has been identified. The results of this work can be used to develop appropriate processing techniques to create leather with desired characteristics.

The knowledge gained in this work is applicable to leathers produced from different species and may extend to other processed collagen rich tissues and tissue products.

ACKNOWLEDGEMENTS

I would like to thank a number of people whose help has made this work possible.

Firstly, I would like to thank the New Zealand Leather and Shoe Research Association Inc. (LASRA) who, in conjunction with the Foundation for Research Science and Technology (grant number LSRX0801), assisted financially with this project. I also wish to thank LASRA, and especially: Richard Edmonds; Sue Cooper; and Warren Bryson, for providing their assistance and input throughout this project.

I would like to thank my supervisor Richard Haverkamp for his significant assistance. Your continued support and positive outlook have been an enormous help. I would also like to acknowledge the contribution of my co-supervisor Gillian Norris.

This research was undertaken on the SAXS/WAXS beamline at the Australian Synchrotron, Victoria, Australia, with the NZ Synchrotron Group Ltd providing travel funding. I would like to thank everyone who helped with experimental work especially Katie Sizeland and Leah Graham for their assistance collecting data. I would also like to thank the SAXS/WAXS beamline staff, particularly; Nigel Kirby and Adrian Hawley, for their helpfulness and patience.

Finally, I wish to thank my partner, Michael, and my family for being so supportive of my decision to commence further study and for attempting to understand my work.

TABLE OF CONTENTS

Page

Page

Page

LIST OF FIGURES

Page

Page

Page

Page

Page

Page

Page

LIST OF TABLES

Page

LIST OF PUBLICATIONS

Journal Articles

Basil-Jones, M. M., Edmonds, R. L., Allsop, T. F., Cooper, S. M., Holmes, G., Norris, G. E., Cookson, D. J., Kirby, N., Haverkamp, R. G. (2010) Leather Structure Determination by Small Angle X-ray Scattering (SAXS): Cross Sections of Ovine and Bovine Leather. *Journal of Agricultural and Food Chemistry,* **58**(9), 5286-5291

Floden, E. W., Malak, S., **Basil-Jones, M. M.**, Negron, L., Fisher, J. N., Lun, S., Dempsey, S. G., Haverkamp, R. G., Ward, B. R., May, B. C. (2011) Biophysical Characterization of Ovine Forestomach Extracellular Matrix Biomaterials. *Journal of Biomedical Materials Research Part B,* **96B**(1), 67-75

Basil-Jones, M. M., Norris, G.E., Edmonds, R. L., Cooper, S. M., Haverkamp, R.G., (2011) Collagen Fibril Orientation in Ovine and Bovine Leather Affects Strength: A Small Angle X-ray Scattering (SAXS) Study. *Journal of Agricultural and Food Chemistry,* **59**(18), 9972-9979

Basil-Jones, M. M., Norris, G.E., Edmonds, R. L., Haverkamp, R.G. (2012) Collagen Fibril Alignment and Deformation during Tensile Strain of Leather: A SAXS Study. *Journal of Agricultural and Food Chemistry,* **60**(5), 1201-1208

Sizeland, K. H., **Basil-Jones, M. M.**, Edmonds, R. L., Cooper, S. M., Kirby, N., Hawley, A., Haverkamp, R. G. (2013) Collagen Orientation and Leather Strength for Selected Mammals. *Journal of Agricultural and Food Chemistry,* **61**(4), 887-892

Conference

Richard L. Edmonds, **Melissa M. Basil-Jones**, Richard G. Haverkamp "Understanding leather through understanding structure" 61st Annual LASRA conference, Napier, 26-27 August 2010

Melissa M. Basil-Jones, Richard G. Haverkamp "Fibrilar collagen structure determination of cross-sections of ovine leather using Small-Angle X-ray Scattering (SAXS)" Pacifichem 2010, Honolulu, 15-20 December 2010

Melissa M. Basil-Jones, Richard G. Haverkamp "The relationship between ovine leather structure and strength from an X-ray scattering sturdy" 62nd Annual LASRA conference, Palmerston North, 11-12 August 2011

Richard L. Edmonds, Timothy F. Allsop, Geoff Holmes, Sue M. Cooper, **Melissa M. Basil-Jones**, Richard G. Haverkamp "A novel low sulphide process for improved ovine leather quality", XXXI IULTCS Congress, Valencia, 27-30 September 2011

Richard G. Haverkamp, **Melissa M. Basil-Jones**, Richard L. Edmonds "A SAXS study of the relationship of collagen fibril orientation in leather with strength" NZIC conference, Hamilton, 27 November – 1 December 2011

Richard G. Haverkamp, **Melissa M. Basil-Jones**, Richard L. Edmonds, Gillian E. Norris "Alignment and Stretching of Collagen Fibrils in Leather" Australian Synchrotron Users Conference, Melbourne, 3-4 December 2011

Katie H. Sizeland, **Melissa M. Basil-Jones**, Richard L. Edmonds, Richard G. Haverkamp "SAXS of Leather Reveals a Structural Basis for Strength" Australian Synchrotron User Meeting, Melbourne, 29-30 December 2012

Richard G. Haverkamp, **Melissa M. Basil-Jones**, Katie H. Sizeland, Richard L. Edmonds "SAXS Structural Studies of Collagen Materials" Australian Synchrotron User Meeting, Melbourne, 29-30 December 2012

CHAPTER 1 INTRODUCTION

1.1 Outline of the Problem

Leather, produced by humans since prehistoric times, is one of the world's oldest products (Kroschwitz 1989) and was initially produced by treating animal skins with fats, smoke or bark. The process of preserving animal skins was developed independently in Europe, Africa, Asia and North America.

Leather is used in a range of industries with most prominent uses being in the footwear, upholstery and clothing industries. Approximately 65% of leather produced worldwide is used by the footwear industry which produces high-value products from the raw material. Leather has a number of desirable physical properties that make it suitable for use in footwear production. These include the balance of plastic and elastic properties that allow shoes to conform to the shape of an individual foot and maintain their shape, while withstanding the considerable external forces experienced during walking. Leather is also waterproof but is able to dispel the moisture produced by perspiration (Kroschwitz 1989).

The physical properties of leather vary greatly, depending on the type of animals skin used to produce it and the type of processing used (Kroschwitz 1989). The physical and aesthetic properties of leather determine both its profitability and end use. There are an estimated 6 million tonnes of bovine raw hide and 0.7 million tonnes of ovine and caprine raw skin produced worldwide each year (United Nations 2010) which produce approximately 18 million square meters of leather, 13 million square meters from bovine hides and 5 million square meters from ovine and caprine skins (United Nations 2010).

A lack of data makes it difficult to determine the amount of footwear that is produced from ovine and caprine skins, although the amount is thought to be insignificant when compared to the 4.7 billion pairs of shoes produced from bovine leather (United Nations 2010). Despite such large volumes of footwear being produced, the demand for leather exceeds its supply (Kroschwitz 1989). One of the most important mechanical properties of leather is its ability to resist tensile and tearing forces. Bovine leather is favoured for

footwear production, due to its superior strength. Ovine leather, which is not so strong, is predominately used in the garment industry. Demand in this industry is variable and the per unit value is lower than in the footwear industry. Ovine leather could be used in the footwear industry if a significant increase in its strength could be produced. This could significantly increase the revenue of the New Zealand leather industry, where leather production is primarily focused on ovine leather due to the large numbers of sheep skins produced locally. New Zealand produces 8% (by weight) of the worldwide production of sheep skins, with over 40% of the worldwide production of sheep raw skins being produced in Australasian region (United Nations 2010).

Despite significant advances in the production of leather since prehistoric times, its structure is still poorly understood. It is thought that a greater understanding of the structure of leather, and the factors that influence the physical properties of leather, would assist in designing leather processing stages that result in leather with desired physical properties.

However, leather is an extremely complex material and determining its composition and the structure of all of its components is beyond the scope of this project. It is therefore necessary that the focus of this project be further specified. Fibrillar collagen is a major structural component of a number of tissues and is the major protein in leather. It is thought to be related to the structural properties of a number of tissues. This work will focus on the fibrillar collagen structure of ovine leather, which will be investigated through the use of small angle X-ray scattering (SAXS). SAXS is a powerful X-ray diffraction technique that can be used to investigate macromolecular structures. It has been used to investigate the structure of a range of collagen-rich materials including tendon (Sasaki and Odajima 1996; Sasaki and Odajima 1996); bone (Cedola *et al.* 2006; Burger *et al.* 2008) and human articular cartilage (Mollenhauer *et al.* 2003).

Fibrillar collagen is found in a number of other materials where its organisation is also of interest. An example of this is its structure in decellularized extracellular matrixes (dECM) for wound repair. dECMs, implanted at a wound site, assist in wound healing by providing a framework for cell adhesion (Lun *et al.* 2010). These materials have been found to remain for 1-2 months after implantation (Lun *et al.* 2010) and during that time they provide structural support. The area of implantation can undergo significant stresses and, therefore, the material's response to strain is of importance.

1.2 Aims and Objectives

The aim of this research was to investigate the key relationships, if any, between the fibrillar collagen structure of ovine leather and its strength.

The objectives of this research were:

- To understand the basis for strength in leather,
- To understand the fibrillar collagen structure of leather and similar materials,
- To understand the difference in fibrillar collagen structure between strong and weak ovine and bovine leather, specifically;
    - Fibre orientation
    - Average amount of fibrillar collagen
    - Structure of individual collagen fibrils (in regards to *d* spacing)
- To understand the variation in fibrillar collagen structure for leather from different positions on the animal,
- To investigate how the stages of the leather production process affects the fibrillar collagen structure,
- To investigate the changes that occurs to the fibrillar collagen structure of ovine leather during uni-axial stretching,
- To investigate the fibrillar collagen structure of ovine forestomach material after preparation for grafting.

There are necessary limitations to this work. This work focuses on one component of leather and is focused predominantly on ovine leather. There are many proteins present in leather; the work of identifying these is the subject of a different PhD project operating in parallel with this study. This work also does not take into account changes resulting from variation in processing such as the presence of lubricants or cross-links; this also is the work of a separate PhD study following on from this study.

This work has produced a substantial contribution to the understanding of leather structure. The methods developed in this work are also widely applicable to other research designed to understand collagen-rich tissues.

CHAPTER 2 LITERATURE REVIEW

Leather is a product with an extremely complex structure and the relationship between this structure and its properties are still poorly understood. The properties of leather are thought to ultimately depend on a number of factors including the properties of the component fibres and their structure. This structure is dependent both on the structure of the raw skin and the production process used. Leather consists primarily of a network of collagen fibrils that are interlinked with natural and synthetic chemical bonds. The structure of other materials produced from tissue, such as biological scaffolds used in wound repair, is also of interest and can be affected by processing.

2.1 Collagen

The collagens are a group of proteins that are responsible for providing structure and desirable physical properties to a number of tissues in the body. Collagen is found in many area of the body including bone, tendon and ligaments, skin, dentin and cornea. There are currently 28 proteins in this group and, in mammals, collagen type I is the most plentiful of all proteins (Kadler *et al.* 2007).

The collagens exist in a number of different structures, from thick fibres to networks. All the protein molecules in the collagen group consist of three polypeptide chains, each containing a Gly-X-Y repeat, that form a triple helical structure (Bailey *et al.* 1998). These molecules then assemble to form the wide range of structures. These are illustrated in Figure 2.1.

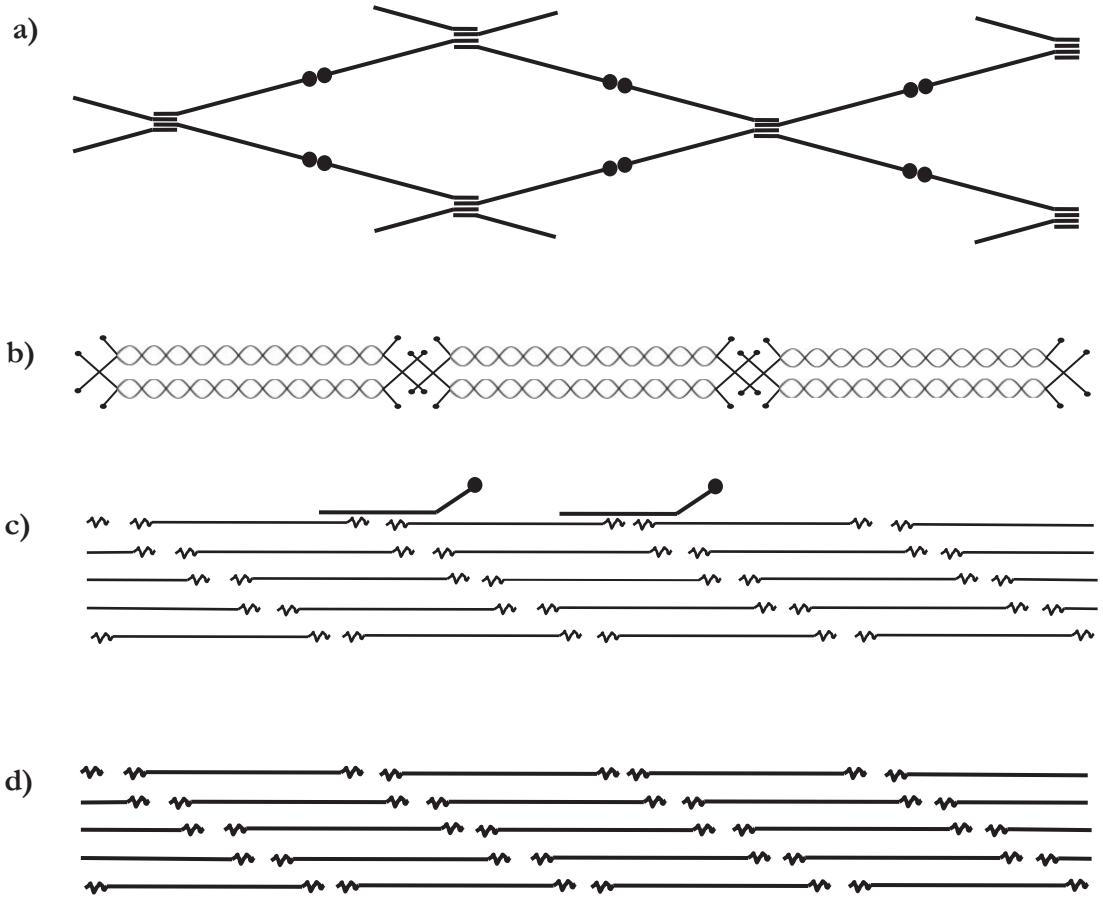

Figure 2.1: Diagram illustrating different forms of collagen a) network collagens, b) filamentous collagens, c) fibril associated collagens and d) fibrous collagens.

2.1.1 Network Collagens

Networks collagens form an open network structure and include collagen types IV, VIII and X. Type IV collagen molecules are 400 nm long and have irregularities in their triple helix sequence (Bailey *et al.* 1998). They interact via their amino and carboxyl terminal ends to form a 'chicken-wire' network. The large carboxyl terminal region of the molecule interacts with the same region of a neighbouring molecule. The amino terminal regions of the type IV collagen molecule also interact; four molecules align in an antiparallel fashion to produce a 110 nm long overlap region (Bailey *et al.* 1998). Through these interactions, networks are formed.

2.1.2 Filamentous Collagens

Type VI collagen molecules align in an end-to-end arrangement to form a filamentous structure with an axial repeat of 100 nm (Bailey *et al.* 1998). This structure is quite loosely packed.

2.1.3 Fibril Associated Collagens

Some collagens do not form a specific structure. Instead they interact with other types of fibre forming collagen. This group includes collagen types IX, XII, and XIV (Bailey *et al.* 1998).

2.1.4 Fibrous Collagens

The fibrous collagens are a sub-group of collagen proteins that form fibrils. Collagen fibrils are the main tensile stress-bearing component in connective tissue (Hulmes *et al.* 1995). The main proteins in this group are types I, II and III collagens. Types V and XI are part of this sub-group but they are found in lesser amounts in tissue (Burgeson 1988).

Fibrous collagen has a complex hierarchical structure (Sasaki and Odajima 1996). At the lowest level three left handed collagen helices wind around each other in a right handed manner to form a triple helix. These triple helixes arrange themselves in a parallel fashion to form collagen microfibrils. The different structural properties of various tissues are thought to be generated through variations in the structural arrangement of collagen molecules rather than significant chemical differences.

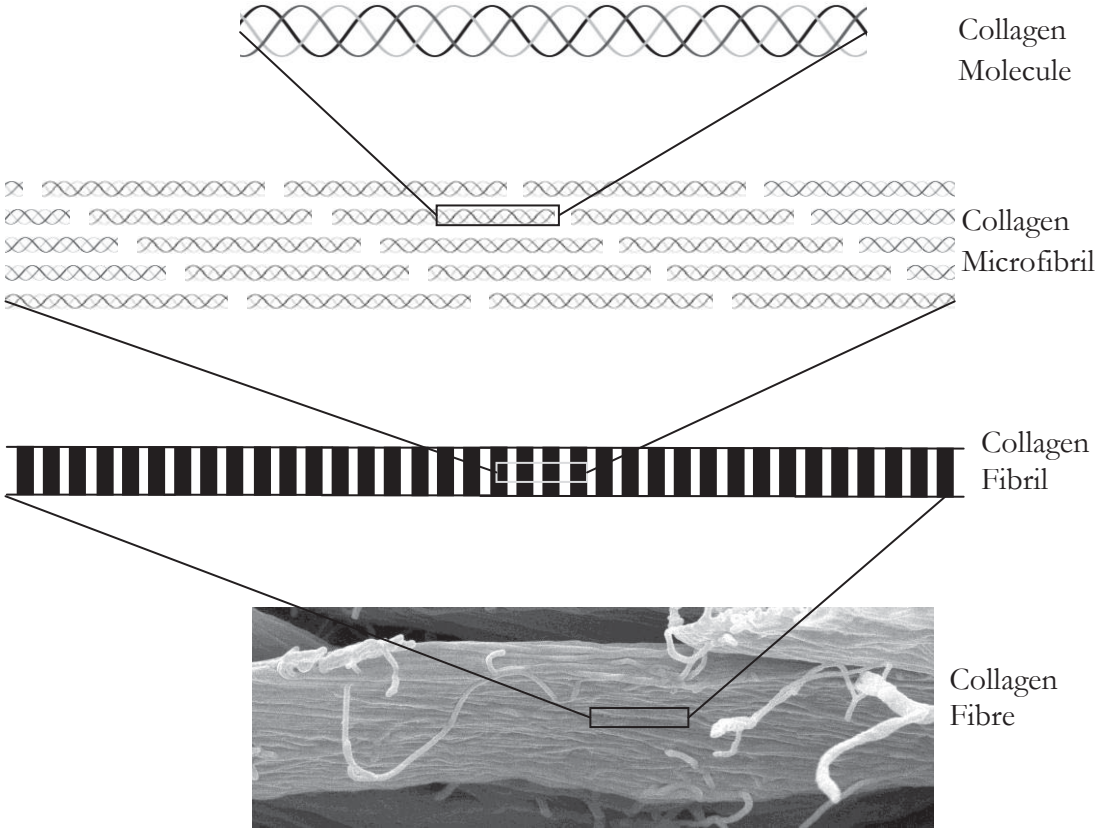

Figure 2.2: Diagram displaying the hierarchical organisation of fibrillar collagen.

2.1.4.1 Primary Structure

The primary structure of collagen consists of a repetitive central sequence of residues with non-repetitive sequences approximately 20 residues long at both the amino-terminal and carboxy-terminal ends. These short sequences are known as telopeptide segments. The most important part of the chain related to structure is the repetitive chain sequence, which is common to all collagens and is responsible for their characteristic triple helical structure.

This repetitive sequence is $(Gly\text{-}X\text{-}Y)_n$ where Gly is glycine, X and Y are any amino acid, and n is the number of repeats, usually 100-400 (Bailey and Paul 1999). Glycine, the simplest amino acid, has no sidechain. In the triple helical structure there is an absolute requirement for glycine in the centre of the triple helix. Amino acids with larger sidechains would not fit in the centre of the helix, due to sterical hindrance, disrupting the structure (Glanville and Kuhn 1979). The X and Y residue side chains point away from the helix axis and can interact with other sidechains from neighbouring helixes.

The incorporation of imino acids in the chain is another distinguishing feature of collagen. The imino acids proline and hydroxyproline combined occupy approximately 35% of the X and Y positions in the repetitive sequence (Fraser *et al.* 1979). Hydroxyproline is enzymically produced by the hydroxylation of proline residues after the protein has been synthesised (Woodhead-Galloway 1980). The side-chains of these imino acids reduce the flexibility about the peptide bond due to their cyclic nature contributing to the stability of the triple helix (Hulmes 2008). Hydroxyproline is found exclusively in the Y position due to the specificity of the hydroxylating enzyme (Fraser *et al.* 1979).

The distribution of other amino acids between the X and Y positions is also not uniform. Phenylalanine, leucine and glutamic acid are almost exclusively found in the X position while arginine is mainly found in the Y position. Evidence suggests that ionic interactions as well as hydrogen bonding and hydrophobic interactions are important in stabilizing the triple helix (Glanville and Kuhn 1979). It is thus logical that the distribution of peptides will have an effect on helix properties and is thought to be why the peptides have an uneven distribution.

2.1.4.2 The Triple Helix

The triple helix structure of collagen is composed of three polypeptide chains, known as α chains. The helix can be made-up of three identical chains or of up to three different chains depending on collagen type. An individual α chain is named α*n*(N) where N is the collagen type, in Roman numerals, and *n* is the α chain's number. The molecule's composition is then, for example, $[\alpha1(I)]_2\alpha2(I)$ for collagen I, which contains two α1 chains and one α2 chain, and $[\alpha1(II)]_3$ for collagen II, which contains three identical α chains.

Collagen polypeptide chains spontaneously combine to form a triple helix in the cell (Bailey and Paul 1999). The initial association between pro collagen chains is thought to be due to disulfide bonding (Wess *et al.* 1998; Bailey and Paul 1999). The resulting helix is rod-like, approximately 280 nm long and 1.5 nm in diameter and has a molecular weight of approximately 300 000 Da (Bailey *et al.* 1998; Diamant *et al.* 1972). Evidence shows that the individual helices twist or coil together to form a coiled coil with a pitch of approximately 90 Å (30 amino acid residues) (Diamant *et al.* 1972; Hulmes *et al.* 1973). The structure is stabilised by hydrogen bonding within the triple helix between the glycines of adjacent

polypeptide chains (Bailey and Paul 1999). Some of these hydrogen bonds are bridged by water (Suzuki *et al.* 1980).

2.1.4.3 Microfibril Structure

Tropocollagen molecules spontaneously self assemble with an axial stagger of 234 residues or 67 nm (a unit referred to as D), an arrangement thought to be due to the large hydrophobic and charged amino acid residues present along the collagen molecule (Mayne and Burgeson 1987; Bailey and Paul 1999). As a result, a total of five collagen molecules form a parallel but quarter-staggered array in each microfibril as shown in Figure 2.3 (Mayne and Burgeson 1987; Bailey and Paul 1999; Cuq *et al.* 2000; Orgel *et al.* 2006). Each molecule of collagen in the microfibril makes at least one intramicrofibril bond as well as at least two intermicrofibrillar bonds (Orgel *et al.* 2006). The microfibrils have a supertwist which helps to stabilises the collagen structure and protects the collagen molecule structure from small amounts of torsion (Orgel *et al.* 2006).

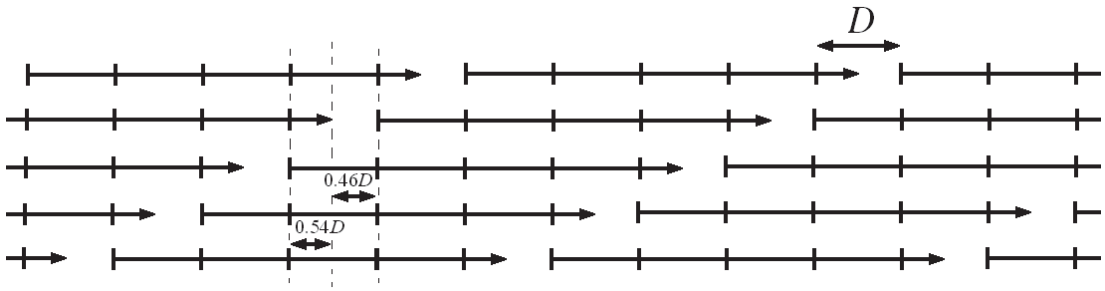

Figure 2.3: Illustration of the alignment of collagen molecules in a microfibril.

2.1.4.4 Collagen Banding

Due to the staggering of collagen molecules in microfibrils, fibrillar collagen has a characteristic banding pattern produced by regions of high and low density, known as the over-lap and gap regions, resulting in a characteristic pattern known as *d* spacing. The structure contains overlap regions that are 0.54*D* in length and gap regions of 0.46*D* in length (Gautieri *et al.* 2011). The molecular density of these gap regions is approximately 20% lower than that of the overlap regions (Misof *et al.* 1997) which means that molecules in the gap region have a greater flexibility (Misof *et al.* 1997) along with a higher degree of disorder (Orgel *et al.* 2006).

Collagen microfibrils appear to have a banding pattern with a period of approximately 67nm. This period can vary from 64nm in the dry state to 68nm in the wet state (Diamant *et al.* 1972) and is affected by the technique used to measure it. It is approximately 67 nm when measured by X-ray diffraction compared to 64 nm when measured using an electron microscope (Bailey *et al.* 1998). The collagen banding pattern period is also affected by the tissue type. Tendon collagen displays a *d* period of approximately 67 nm while skin collagen displays a *d* period of approximately 64 nm (Brodsky *et al.* 1980). This is thought to be due to the molecules in the fibril not being arranged parallel to the fibril direction but rather following a helical course around the fibril with, in the case of skin, a tilt of 18° (Gathercole *et al.* 1987). The observed *d* period is then $64 \approx 67.\cos(\alpha)$, where α is 17-18°.

2.1.4.5 Native Cross-Linking in Collagen Molecules

The mechanical properties of collagen have been shown to be greatly affected by cross-links. Increased numbers of native cross-links has been shown to increase material stiffness and brittleness, while collagen that is cross-link deficient has displayed a diminished fracture load (Puxkandl *et al.* 2002). The native cross-linking in collagen occurs by distinctly different mechanisms.

2.1.4.5.1 Enzymatic Cross-Linking

Enzymatic cross-links in collagen can be classified as either immature or mature cross-links. Immature cross-linking in collagen is usually telopeptide-to-helix and is catalysed by the enzyme lysyl oxidase which converts specific lysine and hydroxylysine residues in the telopeptide region of the collagen into aldehydes. These can then interact with other helical lysine or hydrolysine residues through the formation of a Schiff base to form dehydro-hydroxylysinonorleucine (dehydro-HLNL), a major cross-link in skin, or dehydro-dihydroxylysinonorleucine (dehydro-DHLNL) (Eyre and Wu 2005). The compound lysinonorleucine (LNL), produced by the reaction of lysine and lysine aldehyde, is only found in low concentrations in connective tissue.

Dehydro-DHLNL is reducible, undergoing an Amadori rearrangement to form the stable ketoimine hydroxylysino-5-ketonorleucine (HLKNL) (Eyre and Wu 2005). Dehydro-HLNL cannot, however, undergo this rearrangement which means that the cross-link remains labile and may be broken, for example at low pH (Light and Bailey 1979). The

relative proportions of these two cross-links, and the thermal stability of the tissue, is therefore dependent on the extent of the hydroxylation of the telopeptide lysines.

Mature cross-links form from reducible immature cross-links. Mature cross-links are stable and thought to be tri-functional. One such cross-link found is skin is histidino-hydroxylysinonorlucine (HHL), which is formed from the spontaneous reaction of dehydro-HLNL with a histidine (Bailey *et al.* 1998). Other mature cross-links, such as hydroxylysyl-pyridinoline (HL-Pyr) and lysyl-pyridinoline (L-Pry), have also been identified in tissues.

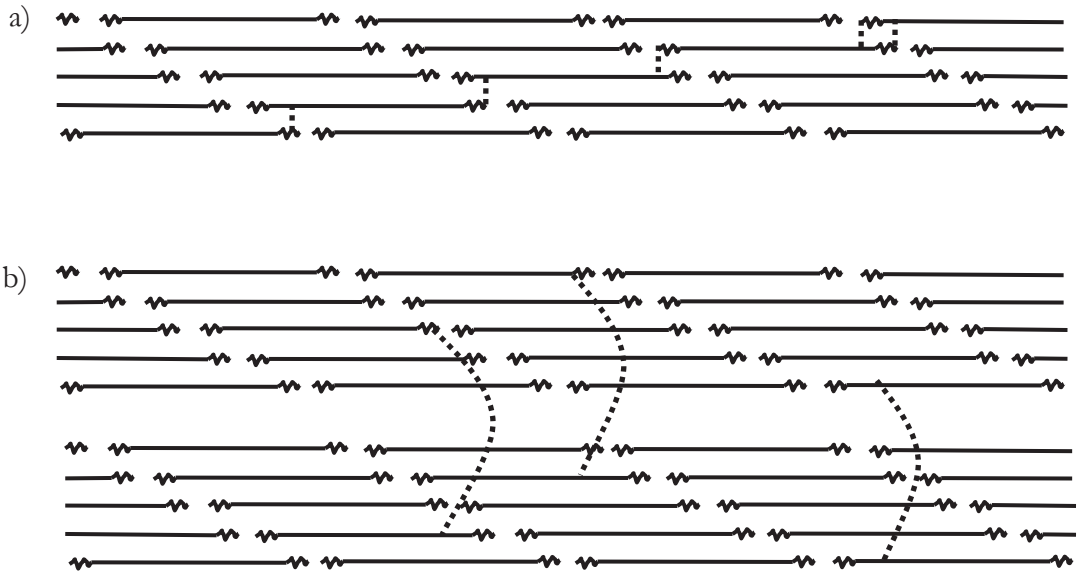

Figure 2.4: Diagram of the probable location of; a) immature and b) mature, enzymatic cross-links in fibrillar collagen.

2.1.4.5.2 Non-Enzymatic Cross-Linking

The non-enzymic process of cross-linking is called glycation and results from the spontaneous reaction of collagen with glucose. Because the reaction is spontaneous the quantities of this type of cross-link increases with tissue age. These cross-links are not advantageous and decrease the flexibility and permeability of tissues (Bailey *et al.* 1998).

The reaction occurs when glucose, in its open chain form, reacts with a free ε-amino group of a lysine in the collagen peptide chain. This reaction forms glycosyl-lysine that then spontaneously forms a ketoimide via Amadori rearrangement. The ketoimide next undergoes further reactions either with other amino acid residues or with metal ions that

induce oxidative breakdown. This results in the formation of advanced glycation end products (AGEs) (Bailey *et al.* 1998).

The variation of physical properties of tissues with age, such as reduced solubility, reduced flexibility and increased resistance to enzymes indicates that these cross-links occur between the triple helical regions of separate molecules as opposed to the telopeptide ends, as enzymic cross-links already exist in this region. Evidence also suggests that glycation occurs in the gap region of the fibre, and is thought to be due to this region being more accessible to glucose than the overlap regions (Bailey *et al.* 1998).

2.1.4.6 Fibril Structure

The exact arrangement of collagen microfibrils into fibrils is not known, although, it is obvious that in the axial direction, there is substantial long-range order (Hulmes *et al.* 1995). Fibrils are approximately cylindrical with diameters ranging from 10-500 nm depending on factors like tissue source and the composition of different collagen types (Hulmes *et al.* 1995).

It is thought that molecules are arranged within the fibril in a hexagonal or quasi-hexagonal type array (Fraser *et al.* 1983; Kajava 1991; Orgel *et al.* 2006) in the form of a relaxed, radially packed cylindrical structure (Hulmes *et al.* 1995). Experimental evidence indicates that, in some tissues, the lateral arrangement of molecules display only short range order (Fratzl *et al.* 1993) with significant azimuthal mobility. It has also been observed that fibril diameter increases in 8 nm increments (Craig and Parry 1981, Hulmes *et al.* 1995) and this is thought to be due to a cylindrical packing structure. It has been shown that the winding angle on the surface of fibrils is independent of diameter (Raspanti *et al.* 1989).

Fibril structure, to a certain extent, is related to tissue type and fibril diameter clearly affects the physical properties of the tissue. Fibrils with a large diameter, and therefore cross-sectional area, have a greater tensile strength (Parry and Craig 1984), related to the fact that there is the potential for a greater amount of intrafibrilar covalent cross-linking in large fibrils which helps the fibril to resist stress (Parry *et al.* 1979).

Interfibrillar binding is greater in smaller fibrils as it is dependent on surface area. Smaller fibrils are also more flexible. Such fibrils therefore have a higher ability to withstand creep,

and it has been suggested that they help tissue to return to its original shape after the removal of stress (Parry *et al.* 1979).

The type of network formed by the fibrils also affects the physical properties of the tissue. Alignment can vary from near complete alignment in one direction to a random three dimensional network. A random two-dimensional web has a maximum tensile strength that is 3/8 of a tissue where the fibrils are all aligned in one direction (for example tendon) (Wainwrigth *et al.* 1976).

The collagen fibril structure in tissue can often be separated into one of two classes. In the first class, fibrils are straight and parallel with a large variation in diameter (Ottani *et al.* 2001). It has been shown that fibrils can fail through tearing, which occurs when the tensile strength is exceeded, or creep, caused by fibrils sliding past each other. Having fibrils with both large and small diameters can help prevent the failure of tissue. This is because large fibrils provide the tissue with strength, due to a greater cross-sectional area which provides the potential for a greater amount of intrafibrilar covalent cross-linking, while small fibrils prevent creep due to a greater surface area to volume ratio allowing for a greater amount of interfibrillar binding (Parry *et al.* 1979). The second class has a more uniform fibril diameter, in the range of 25 to 100 nm, which are more widely spaced. These fibrils usually form three dimensional networks of small wavy bundles (Ottani *et al.* 2001).

Collagen fibres can have a crimped structure with repeat units that are approximately 10-100 μm long (Bailey *et al.* 1998). This structure is thought to allow stretching without damage to the overall collagen structure. However, individual collagen molecules have a moderately straight path due to the large repeat length of the crimp structure (Wess *et al.* 1998).

2.2 Skin

2.2.1 Skin Structure

Skin has several distinct layers. These are the epidermis, dermis, and subcutaneous tissue. The epidermis is comprised mainly of cells and serves as a barrier for chemicals. The subcutaneous tissue is a fatty layer that houses the blood vessels and attaches the dermis to the muscle (Kroschwitz 1989). The weakness of this layer allows skin to be mechanically removed from carcasses. The dermis provides much of the toughness of skin and is comprised mostly of collagen with elastin and some proteoglycans.

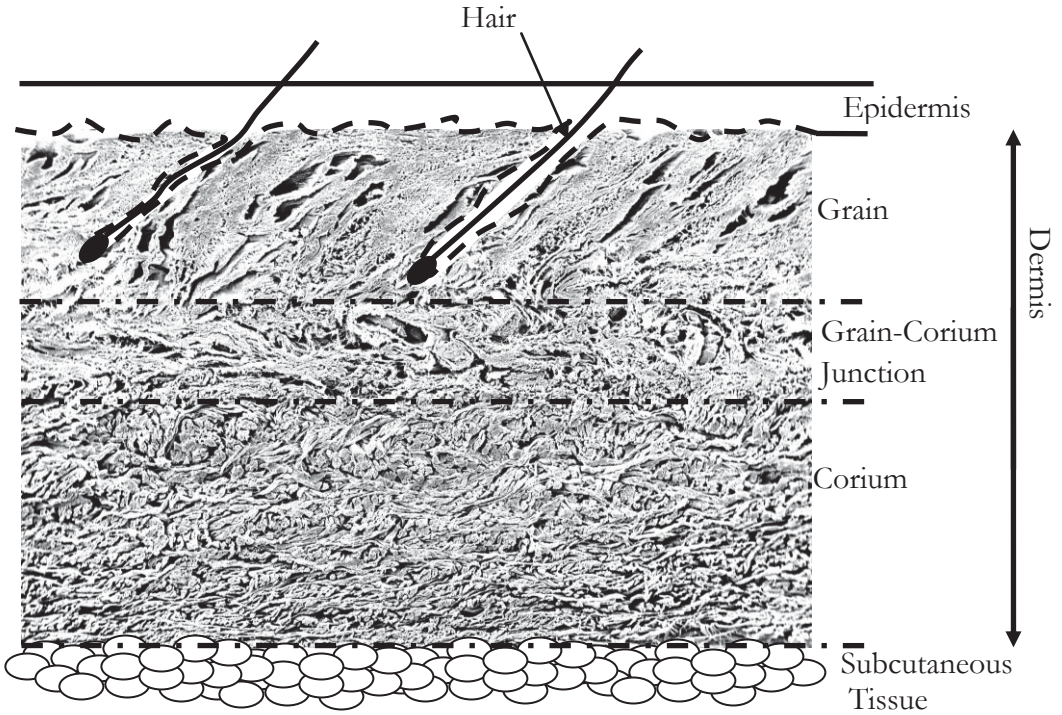

Figure 2.5: Diagram of the cross-sectional structure of skin.

2.2.1.1 Dermis Structure

The dermis can be further separated into two layers; the grain and the corium. The grain contains the entire length of the hair follicle as well as small blood vessels and capillaries (Kroschwitz 1989). This layer also contains a three dimensional network of thin collagen fibres and a network of thinner tissue fibres that are arranged parallel to the dermis surface (Kroschwitz 1989). These tissue fibres contain elastin which provides elasticity to the tissue (Deb Choudhury *et al.* 2006). The corium contains a three-dimensional network of randomly interwoven thick bundles of collagen fibres (Gathercole *et al.* 1987; Kroschwitz 1989; Purslow *et al.* 1998; Waller and Maibach 2006). There is a species variation in the angle of weave of these fibres in the direction perpendicular to the layer surface (Kroschwitz 1989), which is related to the physical properties of leather, especially with respect to strength (Kroschwitz 1989).

2.2.2 Skin Components

Chemical analysis of bovine skin shows it contains 65-70% water, 30-35% dry substance, and less than 1% ash. While collagen is the most common hide protein, it contains more

non-collagenous materials than some other tissues, for example tendon (Brodsky *et al.* 1980). Keratin is the second most common protein in skin, making up 6-10% of the total protein (Kroschwitz 1989; Deb Choudhury *et al.* 2006). Elastin is the third most common protein in skin overall, amounting to 2-5% of skin dry weight, and the second most common protein present in the grain layer, where it exists in a network parallel to the surface (Mithieux and Weiss 2005; Deb Choudhury *et al.* 2006). Proteoglycans are present in the corium in small quantities (Kroschwitz 1989; Keene *et al.* 1997). The skin also contains anionic glycosaminoglycans (GAGs) (Cameron *et al.* 2002). Lipids are found in both the corium and grain layers and account for approximately 9% of the dry substance in the grain and 1 to 11% in the corium (Kroschwitz 1989).

2.2.2.1 Collagen

Collagen makes up approximately 70-80% of the dry weight of the dermis (Waller and Maibach 2006). There are at least nine collagen types present in skin with types I, III and V being the most prominent (Keene *et al.* 1997). Types I and III collagen combine to form fibrillar structures (Cameron *et al.* 2002) with the ratio of type I to type III being 4:1 (Light and Bailey 1979). Type III collagen is thought to be distributed on the surface of the fibrils while type I collagen forms the bulk of the fibril (Cameron *et al.* 2002). In the embryonic dermis the amount of type III collagen is much higher, approximately 50%, but this decreases during post-natal growth (Bailey *et al.* 1998). Fibres containing exclusively type III collagen have a smaller diameter, and therefore a greater elasticity, compared to fibres containing exclusively type I collagen (Bailey *et al.* 1998).

Type IV collagen forms a highly flexible widespread network throughout the dermal layer (Kielty and Shuttleworth 1997). Although the precise function of this structure has not been determined, it has been suggested that it is responsible for organising the dermal matrix during production (Kielty and Shuttleworth 1997) and ensuring that the integrity and alignment of the dermal structure is maintained (Kielty and Shuttleworth 1997; Bailey and Paul 1999).

Type V collagen is also present in skin and is thought to be responsible for the regulation of collagen fibril diameter. The exact process is unknown but it is thought that it may be dependent on the amino-terminal domain of the molecule (Birk *et al.* 1990). Experimental evidence shows that the amino-terminal end of type V collagen molecule is present on the

surface of fibrils containing type I and V collagens, while at least a part of the helical region of the molecule is buried within the fibril (Linsenmayer *et al.* 1993). This indicates that the length of the helical region of the type V collagen molecule may have some influence on fibril diameter.

The collagen fibril diameter in skin is approximately 100 nm (Bailey *et al.* 1998) with reported values ranging from 60-80 nm (Wang *et al.* 2005) to 123 nm with a standard deviation of 20 nm (Deb Choudhury *et al.* 2007). These collagen fibres are arranged into a loosely interwoven random three-dimensional network, (Gathercole *et al.* 1987; Purslow *et al.* 1998; Waller and Maibach 2006) granting it a level of flexibility and strain resistance in all directions. Upon extension, the collagen fibre network reorganises and becomes increasingly aligned in the direction of the force (Purslow *et al.* 1998). The predominant cross-link in skin is HLNL (Light and Bailey 1979) with the turnover of collagen being several years (Bailey and Paul 1999).

Another important collagen in skin is type VI. Type VI monomers form a 105 nm long triple helix with a globular domain at each end resulting in a dumbbell-shape (Kielty and Shuttleworth 1997). The molecules arrange so that they overlap in an anti-parallel fashion and are stabilised by intermolecular disulfide bonds to form dimers and tetramers (Kielty and Shuttleworth 1997).

2.2.2.2 Keratin

The keratins are a group of proteins, the largest subgroup of the intermediate filament proteins, which have a high level of the thiol amino acid cysteine. These proteins form fibrous structures (Mier and Cotton 1976). Keratins form diamers with a 50 nm long α-helical coiled-coil structure, stabilised by interchain ionic associations. These align laterally in an end-to-end fashion to form filaments which are 10 nm in diameter. It has been suggested that the arrangement is as follows; keratin diamers align in a half staggered head-to-tail arrangement, with two of these strings aligning in an antiparallel fashion to produce a protofilament. The intertwinement of two protofilaments produces a protofibril and the intertwinement of four protofibrils produces a single kertin filament (Aebi *et al.* 1983)

Keratin is the main protein in the epidermis where its main function is to protect epidermal cells, from both mechanical and nonmechanical stresses, and so prevent cell death. It is found in two forms; soft keratin in the stratum corneum and hard keratin present as hair

and wool (Mier and Cotton 1976). Hard keratins are thought to have higher concentrations of cysteine and therefore greater levels of disulpide bonding between polypeptides.

2.2.2.3 Elastin

Elastin is essential for elasticity and resilience of tissues. Elastin is has an estimated half-life of 70 years resulting in no significant turnover in tissue (Sherratt 2009). In skin it forms highly ordered large diameter fibres that are arranged parallel to the skin surface (Sherratt 2009) and vertical in the upper grain (Allsop *et al.* 2006).

Elastin forms fibres with a number of macromolecules including fibrillin-1, fibrillin-2, and microfibril-associated glycoprotein-1 (MAGP-1) (Mithieux and Weiss 2005). Elastic fibres are comprised of a core of covalently cross-linked amorphous elastin molecules enclosed in a layer of fibrillin rich microfibrils. Tropoelastin molecules contain a high level of glycine and this is thought to contribute to the elasticity of the polypeptide (Debelle and Tamburro 1999).

2.2.2.4 Proteoglycans

Preteoglycans are proteins that consist of a protein core covalently linked to one or more glycosaminoglycan (GAG) chain. GAGs are a group of high molecular weight straight chain polysaccharides comprised of a repeating disaccharide unit (Mier and Cotton 1976). These, along with protein fibres, can be visualised by electron microscope (Thyberg *et al.* 1975, Scott 1980). Proteoglycans, such as decoran, are thought to interact with the extracellular matrix (Cameron *et al.* 2002) through strong ionic interactions (Deb Choudhury *et al.* 2007; Chan *et al.* 2009). These proteins are involved in a number of different processes in tissue and the function of specific proteoglycans varies but includes; the regulation of collagen fibrillogenesis, regulating cell growth and providing strength to tissue (Iozzo 1998; Prathiba and Gupta 2000; Reed and Iozzo 2003).

2.3 Leather

2.3.1 Leather Production

The process of leather production includes three main steps; hide preparation, tanning and finishing. The exact process depends on the tanning agent used. Commonly used tanning agents are metal salts (mainly chromium salts), organic aldehydes, and vegetable tannins. The most commonly used tanning agent is chrome, which is used for the majority of leather production (Kroschwitz 1989).

2.3.1.1 Skin Preparation

Skin is removed from carcass at the place of slaughter, usually an abattoir. The skin is carefully cut and then removed either by hand flaying or mechanical pulling. Damage to the skin can occur during this removal process (Daniels 2002). Skins are then usually sprayed with cold water to wash and decrease the temperature of the skin. If skins are not intended to be processed immediately they are covered in salt and stacked in piles. This preservation technique means that when skins are ready to be used they contain about 14% salt by weight and need to be soaked before further processing (Kroschwitz 1989). As well as removing salt, soaking removes water soluble proteins and any dirt.

2.3.1.2 Hair Removal and Liming

In the case of sheep skins the wool has value and therefore damage during the removal process is avoided. To achieve this, the flesh side of the skin is treated with an alkaline paste of lime and sodium sulfide. These reagents in combination dissolve the keratin of the hair follicle and allow the hair to be easily removed by mechanical action (Daniels 2002). Liming achieves several objectives: it removes the epidermis and any remaining hair; the alkali swells the skin which splits the collagen fibre bundle sheaths; it breaks down some compounds including complex sugars and non-structural proteins; and it results in the conversion via hydrolysis of some collagen side chains from amide to acid groups (Kroschwitz 1989; Daniels 2002).

Studies have found that *d* spacing is reduced by the process of liming (Maxwell *et al.* 2006). It has been suggested that this change could be caused by the high alkalinity of the lime

liquor resulting in hydrolysis of amino acid side chains, allowing collagen molecules to more easily slide past each other (Maxwell *et al.* 2006).

2.3.1.3 Deliming and Bating

Deliming and bating steps are usually carried out together. After liming the skin is washed to remove unwanted protein residues and soluble lime. The pH is lowered from 12.5 to 8-9, usually through the use of ammonium sulfate, which de-swells the skin. A bating enzyme, usually a protease, is added to break down non-collagenous proteins and helps relax the skin. This is known as the bating step, and is 1-4 hours long (Kroschwitz 1989; Daniels 2002).

2.3.1.4 Pickling

After deliming and bating the skins still have quite a high pH. If skins were tanned in this state the tanning agent would very quickly fix to the skin at the surface and would not penetrate through the skin thickness. To avoid this sulfuric and sometimes formic acid are added to decreases the pH to 1-2. Salt is also added in this step to prevent swelling (Daniels 2002; Fathima *et al.* 2010).

2.3.1.5 Tanning

In the case of chrome tanning, chromium sulfate is added to the pickled skin, which dissolves and propagates into the hide. After enough time has passed for the chrome to fully propagate the skin, the pH is slowly raised to 3.4-3.6 by the addition of sodium bicarbonate. At this pH range the chrome reacts with the collagen. The chrome continues to fix to the collagen for several days (Kroschwitz 1989).

Tanning results in an increase in the degree of cross-links between collagen molecules. This results in the contraction of collagen fibres and the shrinkage of the hide during treatment (Heidemann 1979). The type of cross-linking that occurs depends on the tanning agent.

During chrome tanning, binuclear chromium (III) complexes react with the ionised carboxylate sidechains of aspartic and glutamic acids in collagen (Reich 1999; Fennen 1999; Covington *et al.* 2001; Gayatri *et al.* 2001) linking tropocollagen molecules (Cuq *et al.* 2000).

Organic aldehydes react with the ε-amino group of the lysine side-chain forming a covalent bond. Vegetable tannins form intermolecular hydrogen-bonds and salt links (Kroschwitz 1989).

2.3.1.6 Retanning and Fat-liquoring

After tanning a variety of wet processing steps may be performed to improve the physical properties of the final product. Two such processes are retanning and fat-liquoring. Retanning involves adding materials such as; vegetable tannins, fillers, acrylic resins and synthetic tanning agents, normally in combination, to the neutralized leather. The addition of these materials improves the leather, with the final result depending on the materials used. Improvements can include increased softness, fullness and embossability and improved leather break (Daniels 2003). Fat-liquoring involves the addition of oils that will emulsify with water. These oils penetrate the leather and lubricate the fibres allowing fibres to more easily slide past one another in the dry product and thereby softening the final leather (Daniels 2003).

2.3.1.7 Drying and Finishing

Once wet processing is complete the skins are dried. The drying technique and finishing process used are dependent on the end-product that the leather will produce. A high rate of drying, high tension and high compression forces applied during drying produce harder and firmer leathers (Daniels 2003). Drying techniques include hang drying, toggle drying and vacuum drying.

2.3.2 Leather Structure

The strength and softness of leather are believed to be related to its internal structure (Russell 1985; Michel 2004) and aesthetic properties to the internal fibre looseness (Rabinovich 2001). Leather has a complex hierarchical structure with a number of distinct layers. The junction between the epidermis and dermis becomes the surface of leather, due to the removal of the epidermis during leather production. The grain layer is therefore found at the leather outer surface while the corium layer lies beneath. These layers have

visually different structures and impart different properties to the final product (Vera *et al.* 1993).

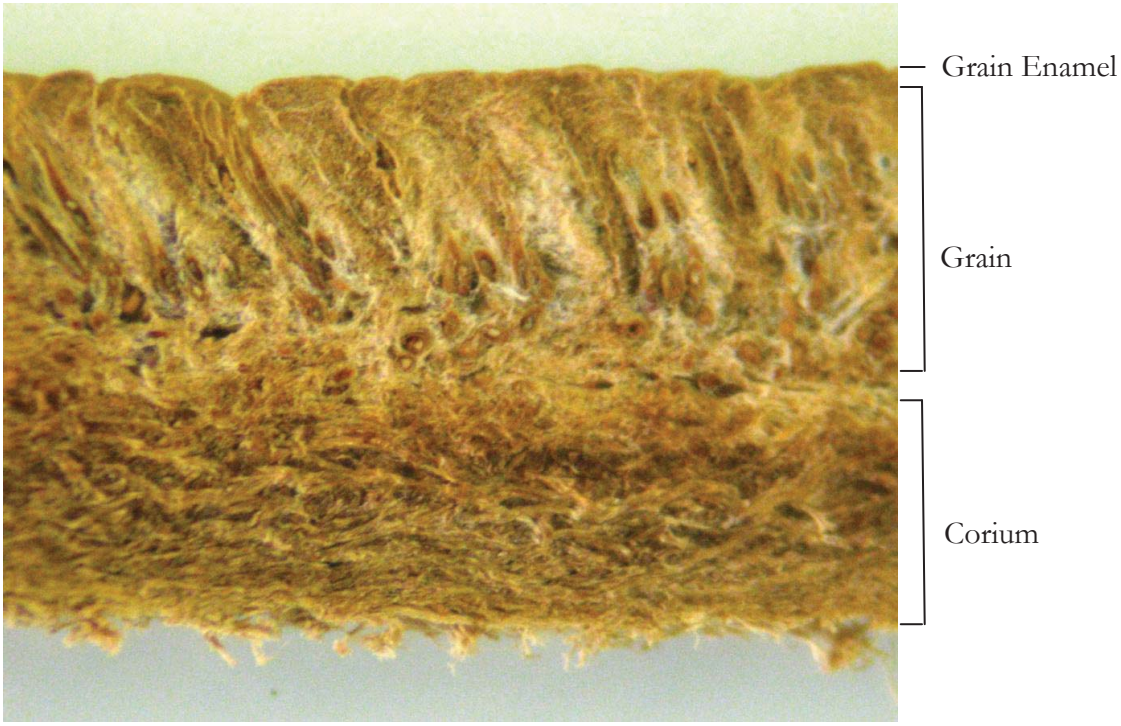

Figure 2.6: A photograph showing the different layers of leather. The thickness of this leather cross-section is approximately 2.2 mm.

The physical properties of those layers are strongly related to their fibre structure and the amount and type of cross-linking (Folkhard *et al.* 1987; Folkhard *et al.* 1987; Cuq *et al.* 2000; Chan *et al.* 2009). The fibres in the grain layer form layers which have only minor connections between them, while the corium has a more network like structure (Liu and McClintick 1999).

2.3.3 Leather Composition

The removal of many proteins and proteoglycans from the raw skin occurs during the pickling stage. After this process predominately collagens and elastins remain (Edmonds *et al.* 2008). Most of the remaining material is therefore collagen (Deb Choudhury *et al.* 2006). Once the proteins are removed, tanning agents, fats, dyes and filling substances are added to the skin to preserve the structure. Interestingly, leather contains 10 to 20% water (Heidemann 1979).

2.3.3.1 Collagen

It has been found that collagen fibres, containing type I and III collagen, remain intact for the first 24 hours of liming. After this time, however, the collagen begins to denature due to hydrolysis (Stephens *et al.* 1993; Menderes *et al.* 2000). Type I and type III collagen have also been found to be present after the pickling process (Stephens *et al.* 1993). Type VI collagen has also been found to remain intact during the liming, bating and pickling (Kronick *et al.* 1991). However type VII collagen is either mostly or completely removed by the liming process (Stephens *et al.* 1993) while, type XII collagen is partially lost during bating (Kronick *et al.* 1991).

The fibre structure of the corium has been found to be influenced by animal age at slaughter (Russell 1988). It was found that weaners had a dense network of fine fibre bundles in the corium region with extensive interweaving. Samples from 23 and 39-week old animals had fibres which were thicker and had less interweaving in the corium as well as a thicker grain layer (Russell 1988).

2.3.3.2 Effect on Leather Quality

The quality of finished leather depends on a number of factors. These are mainly the structure of the collagen matrix and the removal and retention of specific compounds in the raw hide (Deb Choudhury *et al.* 2006). As laminin forms a network that is independent of collagen IV its loss does not have an adverse effect on the grain enamel (Stephens *et al.* 1993). The removal of specific proteoglycans, such as decorin, may increase the quality of leather (Deb Choudhury *et al.* 2006) as it binds to type I collagen preventing the opening up of collagen fibres if it is not removed (Deb Choudhury *et al.* 2006). GAGs, such as hyaluronic acid, can also prevent the opening up of collagen fibres if not removed. Both hyaluronic acid and dermatan bind to collagen *via* electrostatic interactions and are found in the gap regions of collagen fibrils in skin. Dermatan is removed during the liming process while hyaluronic acid is removed simply by soaking skin in water (Deb Choudhury *et al.* 2006).

There is some argument as to whether elastin removal is desired for good quality leather. When elastin is treated with chrome it becomes brittle and inelastic when the leather is dried. However, elastin can improve the tensile strength of collagen fibres and its complete

removal often results in loose leather with low tensile and tear strengths (Deb Choudhury *et al.* 2006).

2.4 Physical Properties of Collagen Rich Materials

2.4.1 Rheology of Tendon

Stretching of tendon results in the production of a stress-strain curve with three distinct regions (Puxkandl *et al.* 2002). These are the toe, heel and linear regions.

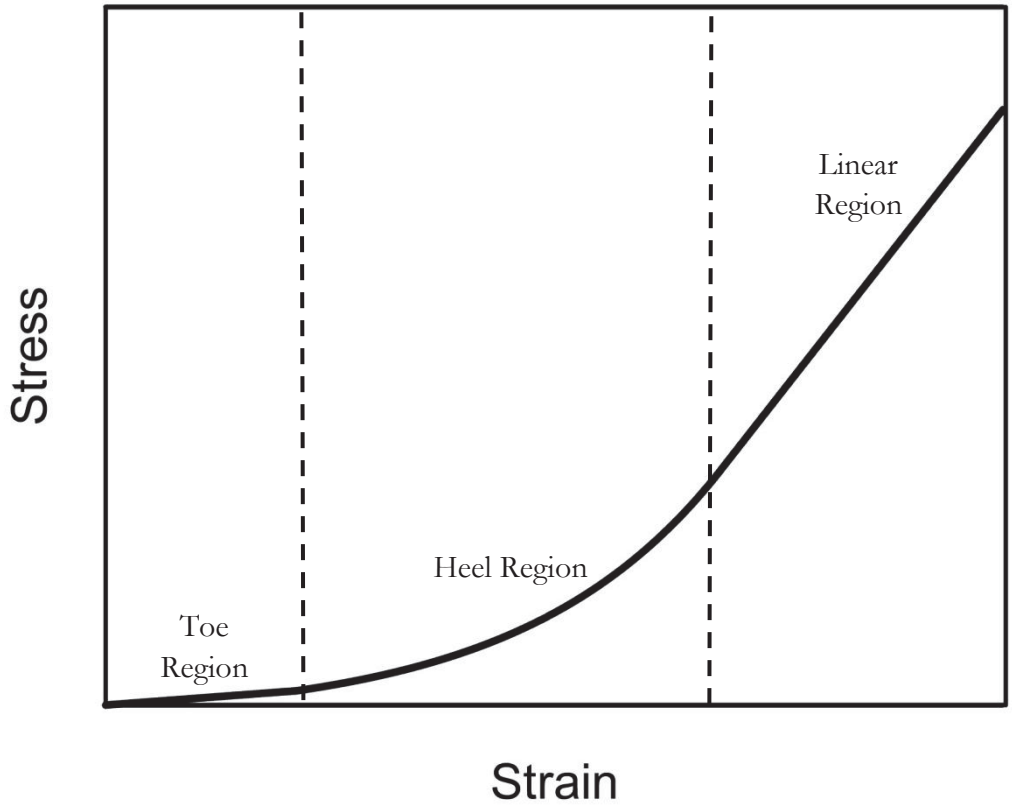

Figure 2.7: Diagram illustrating the general response of tendon to tensile deformation.

In the toe region very small stresses cause elongation of the tendon, due to the removal of macroscopic crimps in the collagen fibrils (Puxkandl *et al.* 2002) which have a period of 100 μm or less (Misof *et al.* 1997). These changes in the initial stages of stretching are visible via a light microscope, while those in the latter stages of stretching are not (Fratzl *et al.* 1997).

In the heel region, tendon stiffness increases (Fratzl *et al.* 1997). Elongation in this region is thought to result from a decrease in the disorder of lateral packed collagen fibrils. Strain is thought to straighten out the kinks that occur in the gap regions of the fibrils (Fratzl *et al.* 1997). Kinks are thought to form because of the lower density of collagen in the gap regions coupled with a greater flexibility of the collagen chains, due to reduced concentrations of proline and hydroxyproline (Fratzl *et al.* 1997).

In the linear region experimental evidence indicates that stretching increases the ratio between the lengths of the gap and overlap regions (Fratzl *et al.* 1997). There have been three suggested deformation mechanisms for this region of the stress-strain curve. These are (a) molecular elongation, (b) increase in the gap region between longitudinally adjoining molecules along the fibre axis and (c) relative slippage of laterally adjoining molecules along the fibre axis (Sasaki and Odajima 1996). Evidence has also indicated that the overlap region decreases in length (Mosler *et al.* 1985). This indicates that the sliding mechanism is, at least, in part responsible for the length increase. Sliding is limited by the extent to which the cross-linked telopeptides can be stretched. Further stretching results in permanent damage to the fibrillar structure (Folkhard *et al.* 1987).

2.4.2 Rheology of Leather

2.4.2.1 Tensile Testing

Tensile strength is measured as the maximum tensile load a sample can be subjected to before it fails. The tensile strength of leather samples is known to decrease with increasing animal slaughter age (Russell 1988). Leather tends to produce non-linear stress-strain curves in tensile tests, with stiffness increasing with increasing strain (Attenburrow 1993). This type of curve is also found for other collagen containing tissues including skin (Attenburrow 1993). There have been many different suggestions as to what causes the curvature. It has been suggested that this could occur due to initial strain resulting the alignment of fibres in the direction of strain instead of the stretching of the fibres themselves. Then as strain increases further the individual fibres stretch (Attenburrow 1993). Another explanation is that due to the variable tautness of the fibres in the network structure, initially only some of the fibres are under strain, but as strain increases more fibres come under strain (Attenburrow 1993).

Interestingly, load-extension curves of individual fibre bundles, both tanned and untanned, show a similar shape to stress-strain curves of leather (Attenburrow 1993). This is thought to be due to smaller structural elements of the fibre bundle initially aligning at low strain levels.

2.4.2.2 Tear Testing

For tear tests the force-elongation curve shows a zigzag pattern in the tearing region (Liu and McClintick 1999), thought to be due to the structural variation across the sample which results in variation in the resistance to tearing (Liu and McClintick 1999). An investigation of the fractured ends of chrome-tanned collagen fibrils indicates that the fracture mechanism is due to the splitting-up of fibres into smaller fibrils as opposed to the fracture occurring in a single plane perpendicular to the fibre axis (Arumugam *et al.* 1995).

2.4.2.3 Effect of Splitting

Leather can be mechanically sliced across the thickness to produce more than one sheet of leather, a process known as splitting. Split leather that has had the grain layer partially or completely removed is termed a flesh splits and is comprised predominantly of the corium layer. Grain splits are produced by the partial or complete removal of the corium.

Studies have shown that flesh splits have a greater tensile strength compared to grain splits in the thickness range of 0.9 to 2.0 mm (Russell 1988; Attenburrow 1993). The corium also has a higher breaking elongation compared to the grain layer (Liu and McClintick 1999). These results indicate that the grain layer of leather is weaker than that of the corium since the removal of the grain results in a reduction of tear strength that is less than that which results from the removal of the corium layer.

A factor thought to influence the strength of the grain layer is the presence of pores, generated by the removal of hair follicles during leather production (OLeary and Attenburrow 1996). These pores occupy 10% of the leather surface and have a mean surface diameter of 0.23 ± 0.08 mm (OLeary and Attenburrow 1996). Grain weakness has also been suggested to be due to the way in which the structure reforms and the amount of fibre pull out (OLeary and Attenburrow 1996). Although it has been suggested that grain weakness could be due to the collagen fibres of this region having a smaller diameter,

studies have found that fibres with a smaller diameter may actually be stronger than those with larger diameters (Attenburrow 1993).

2.5 Biological Scaffold Materials

Chronic wounds are a significant health problem, due partially to an aging population and an increase in the incidence of diabetes. There is, therefore, a huge potential for products that assist in the healing of chronic wounds. One such product is biological scaffold materials, which consist mainly of collagen and produced from selected mammalian tissues.

2.5.1 Tissue Sources

Biological scaffolds are produced from tissues harvested from a range of sources including bovine, porcine, equine, ovine and human. Currently, the types of tissues used to produce ECM scaffolds include; dermis, urinary bladder, pericardium, small intestine, blood vessels and heart valve (Badylak *et al.* 2009; Crapo *et al.* 2011).

2.5.2 Processing

Decellularised extracellular matrix scaffolds are produced from various tissue sources by decellularization which is required to avoid immune response from the host after implantation. Although processing is required for decellularization, changes to the native ECM structure can result in a decreased degradation rate of the ECM scaffold and cause an immune response after implantation (Badylak 2007; Badylak *et al.* 2009). Processing is therefore required to remove cells without significantly altering the ECM structure.

The processing techniques used depend on a number of factors associated with tissue type such as thickness, lipid content and density. A process that successfully decellularizes one tissue without damage may damage the ECM of other tissues (Badylak *et al.* 2009).

Initially the desired tissue must be separated mechanically from unwanted tissue. Tissue decellularization can then occur. The decellularization process varies but usually involves both physical and chemical methods. Physical processing include freezing and thawing, sonication and agitation (Badylak *et al.* 2009). Chemical decellularization includes treatment with acids, bases, detergents, alcohols, enzymes and chelating agents (Crapo *et al.* 2011).

ECM materials may then be dehydrated to make the material easier to handle, increase shelf life and limit the loss of specific biomolecules during storage. This is usually performed by freeze drying or vacuum pressing. The product is then sterilized to destroy the infectivity of any pathogens, including viral and bacterial, that may be present (Crapo *et al.* 2011).

2.5.3 Composition

The composition of ECM scaffolds is dependent on the tissue source (Badylak *et al.* 2009). Much of the research conducted on ECM materials has been on material produced from porcine small intestinal submucosa. The main component of this material is collagen, which makes up more than 90% of its dry weight. While it is predominantly type I collagen, types III, IV, V and VI are also present. Other components include glycosaminoglycans, fibronectin, laminin, decorin, glycoproteins and growth factors (Badylak *et al.* 2009).

2.5.4 Assistance in Healing

Biological scaffold materials assist in constructive tissue remodelling (Badylak *et al.* 2009) although the exact mechanism involved is unknown. The ECM scaffolds are thought to support host cell attachment, a process that is promoted by growth factors released during degradation of the scaffold. Growth factors are also thought to encourage cell division and the growth of blood vessels (Badylak 2007). In order to better understand how ECM scaffolds assist in wound healing it helps to understand the molecular processes occurring in the wound environment.

2.5.5 Introduction to the Biology of Wound Healing

2.5.5.1 Types of Wounds

A wound is an injury to the skin usually caused by the skin being torn, cut or punctured in some way. The healing response of a wound determines the type of wound. Although the response is somewhat of a spectrum, the type generally falls under one of two categories.

An acute wound is a wound that is of short duration and which has a normal healing response. In an acute wound there is a balance between the amount of tissue molecules, such as collagen, being degraded and produced.

A chronic wound is a wound that persists over a long period of time, generally greater than three months. These wounds may take many years to heal, if at all. The reasons why a wound becomes chronic are multifaceted. These wounds generally get stuck in one of the healing stages, such as inflammation, and have a greater rate of degradation than production of tissue molecules. Chronic wounds generally fall into one of three types; venous ulcers, diabetic ulcers or pressure ulcers.

2.5.5.2 Exudate Production

Tissue naturally contains moisture, some of which is stored in the extracellular matrix. This fluid is constantly supplied by blood circulation and removed through the lymphatic system. The volume of liquid is kept constant by interactions between the interstitial fluid pressure, the capillary filtration pressure and the rate of lymphatic drainage (Bishop *et al.* 2003). Fluid flows into the tissue from the blood capillaries, due to capillary filtration pressure, but skin integrity prevents free-swelling. In this way interstitial fluid pressure counteracts capillary filtration pressure and controls fluid inflow from the blood vessels. Also an increase in interstitial fluid pressure increases the rate of lymphatic drainage (Bishop *et al.* 2003).

In a wound, this balance is disturbed, and fluid influx is increased by a number of factors: disruption of the skin structure decreases its ability to maintain the interstitial fluid pressure, thus disturbing the fluid control system; inflammation makes the blood vessels more permeable to fluid outflow and; wound granulation tissue absorbs more fluid than normal skin tissue meaning it can absorb moisture from the surrounding tissue (Bishop *et al.* 2003). This increase of fluid results in the excess fluid being removed from the site as exudate. The rate of exudate production varies from wound to wound. In the case of chronic wounds, the exudate fluid is highly corrosive due to its high concentration of proteinases (Bishop *et al.* 2003). These enzymes are essential for natural healing processes but at high concentrations they can be detrimental to wound healing.

2.5.5.3 Normal Healing Process

In the normal healing process neutrophils, a type of white blood cell, act as a first defence against pathogens. In the event of inflammation, these cells which store enzymes that degrade and digest devitalised tissue and pathogens migrate to the wound site releasing their contents when required (Yager and Nwomeh 1999).

2.5.5.4 Proteinases

One group of enzymes stored by neutrophils are proteinases which are particularly important in wound healing. They are responsible for the degradation of the extracellular matrix and invading cells. Degradation of the extracellular matrix is required to allow cell migration and to remove damaged matrix components. However, high levels of these proteinases can result in the destruction of connective tissues and normal cells. An important group of these proteinases are matrix metalloproteinases (MMPs). These are a class of proteinases that collectively can degrade virtually all the protein components of the extracellular matrix, including collagen, fibronectin, laminin, proteoglycan and elastin (Trengove *et al.* 1999). A sub group of this class are the interstitial collagenases. This group of three MMPs (MMP-1, MMP-8, and MMP-13) are responsible for initiating the degradation of fibrillar collagens (Yager and Nwomeh 1999).

2.5.5.5 Proteinases in Chronic Wounds

MMP-1 is found in chronic wound fluid in levels up to 3 times higher than peak levels found in fluid from healing dermal wounds (Yager and Nwomeh 1999). Other MMPs have also been found to be at higher levels in chronic wound fluid, including MMP-2 and MMP-9, than in acute wound fluids (Wysocki *et al.* 1999). Elevated activity of neutrophil elastase has also been observed in chronic wound fluid (Yager and Nwomeh 1999). Neutrophil elastase is a serine proteinase that is capable of degrading nearly every component of the extracellular matrix. Other serine proteinases, such as cathepsin G and urokinase-type plasminogen activator (uPA), are also found in elevated levels in chronic wounds (Yager and Nwomeh 1999). These are thought to be responsible for the significant levels of degraded fibronectin, vitronectin and tenascin that have been found in chronic leg wounds. Most, if not all, proteinases found in elevated levels in chronic wounds are of neutrophil origin.

2.5.5.6 Proteinase Inhibitors

To prevent damage from proteinases mammals produce a range of proteinase inhibitors. These inhibiters are present in both plasma and interstitial fluids and regulate the activity of proteinases.

2.5.5.7 Inhibitors in Chronic Wounds

Tissue inhibitor of metalloproteinases (TIMP) are a group of small proteins that specifically inhibit MMPs. Of this group TIMP-1 and TIMP-2 are most important in the inhibition of MMPs (Barrick *et al.* 1999). TIMP-1 levels have been found to be lower in chronic wounds compared to peak levels in surgical wounds (Yager and Nwomeh 1999). α_2-macroglobulin is a non-specific protease inhibitor found in plasma. Evidence suggests that there is a decrease in the level of intact α_2-macroglobulin in chronic wounds (Yager and Nwomeh 1999). Another plasma proteinase inhibitor, α_1-antiprotease, forms a complex with neotrophil elastase thereby inhibiting it. Significantly increased levels of this complex have been found in chronic wound fluid (Yager and Nwomeh 1999).

There are several possible reasons for the reduction in proteinase inhibitor activity observed in chronic wounds. Firstly the high concentrations of proteinases, due to the influx of neutrophils, put these inhibiters under strain. Secondly the concentrations of endogenous protease inhibitors may be decreased by other proteinases. For example TIMP-1 can be degraded by neutrophil elastase, and α_1-antiprotease is a substrate for MMP-8. Also neutrophils produce hypochlorous acid and N-chloramines which oxidise both α_1-antiprotease and α_2-macroglobulin further decreasing the inhibitor levels.

2.6 Microstructure measurements

The collagen structure of leather can be investigated by a number of methods including; optical microscopy, FTIR-microscopy, confocal scanning optical microscopy, Transmission Electron Microscopy (TEM), Scanning Electron Microscopy (SEM), Atomic Force Microscopy (AFM), Small Angle X-ray Scattering (SAXS) and Extended X-ray Absorption Fine Structure (EXAFS) (Reich 1999).

Differences between fibre structures have been determined through the use of optical microscopy, scanning electron microscopy (SEM) (Barlow 1975; Dempsey 1984; Haines 1984; Kielty and Shuttleworth 1997; Deb Choudhury *et al.* 2007), and atomic force microscopy (AFM) (Reich *et al.* 1998; Deb Choudhury *et al.* 2007; Edmonds *et al.* 2008). Microscopic techniques generally give qualitative measurement of fibre organization but may also give quantitative measurement of fibre dimensions and *d* period.

2.6.1 Small Angle X-ray Scattering

X-ray diffraction is a powerful technique for investigating material structures. The study by X-ray diffraction techniques of long range structural order, with repeat distances in the order of 0.1 to 100 nm, is particularly useful for protein assemblages, such as collagen. Such measurements require small diffraction angles, θ, typically less than 10 degrees and are often referred to as Small Angle X-ray Scattering (SAXS). The scattering momentum q ($q = 4\pi sin\theta/\lambda$ where λ is the x-ray wavelength used) is generally used rather than θ in SAXS plots as it allows direct comparison of SAXS measured at different incident x-ray wavelengths.

SAXS can provide information on macromolecules either in solution or in solid materials (Tsutakawa *et al.* 2007; Bernado *et al.* 2007) and has been used to investigate the structure of collagen (Cameron *et al.* 2002) and collagenous materials such as tendon (Sasaki and Odajima 1996; Sasaki and Odajima 1996); bone (Cedola *et al.* 2006; Burger *et al.* 2008) and human articular cartilage (Mollenhauer *et al.* 2003). SAXS analysis can be used to sample a large area making the results statistically robust and does not require any special treatment of samples.

2.6.1.1 Theory of Small Angle X-ray Scattering

Small angle X-ray scattering is based on the theory of diffraction. Diffraction occurs when X-rays pass through a particle which is larger than half the wavelength of the X-rays. The electrons of the particle, which are the main scatters of the X-rays, resonate at the frequency of those incoming X-rays (Glatter and Kratky 1982) and then emit secondary waves. These X-rays interfere with each other to produce a scattering pattern. Since incoherent scattering is insignificant at low angles only coherent scattering needs to be considered.

Scattering angle is inversely proportional to particle size so that the larger the particle being studied the smaller the scattering angle that needs to be recorded (Glatter and Kratky 1982). This principle is visualised in Figure 2.8. There is no theoretical limit to how small the angle being studied is, but it is limited by the equipment used.

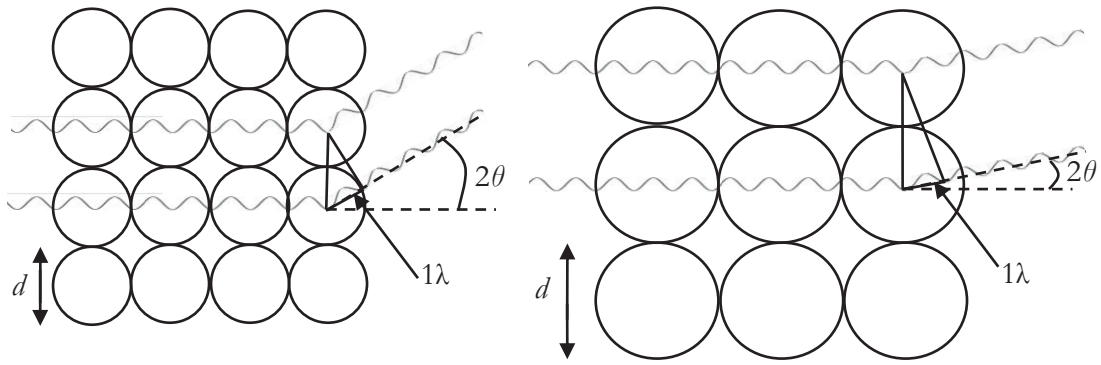

Figure 2.8: Diagram demonstrating the effect of particle size on scattering angle.

2.6.1.2 Bragg Scattering

When X-rays are scattered by a highly repetitive periodic array, such as a crystal lattice, constructive and destructive interference occurs. The regions of high intensity, due to constructive interference, are known as Bragg peaks and their location can be used to determine spacing between planes. This can be determined using Bragg's law:

$$n\lambda = 2d \sin\theta$$

Where n = an integer, the peak order

λ = wavelength of the incident wave (nm)

d = spacing between planes (nm)

θ = the angle between the incident ray and the scattering planes (degrees)

The regular gap and overlap regions of collagen fibrils are highly repetitive and, as a result, cause Bragg Scattering to occur. This means that the location of Bragg peaks can be used to determine the *d* spacing of collagen fibrils.

2.6.1.3 Small Angle X-ray Scattering of Fibrillar Collagen

Due to the sensitivity of SAXS to ordered arrays, when used on collagenous materials, the diffraction pattern is generally only influenced by the fibrillar collagen component of the

material (Fratzl 2008). SAXS patterns carry information on the packing of fibrils within samples, the lateral packing of molecules within fibrils and the distribution of residues along the fibril axis (Costa *et al.* 2009).

The X-ray diffraction pattern of collagen fibres consists of two main regions; equatorial scattering and meridional reflections. The scattering in the meridional direction gives information on the variation of electron distribution along the axis, while the equatorial scattering gives information on the packing and diameter of fibrils (Cameron *et al.* 2002).

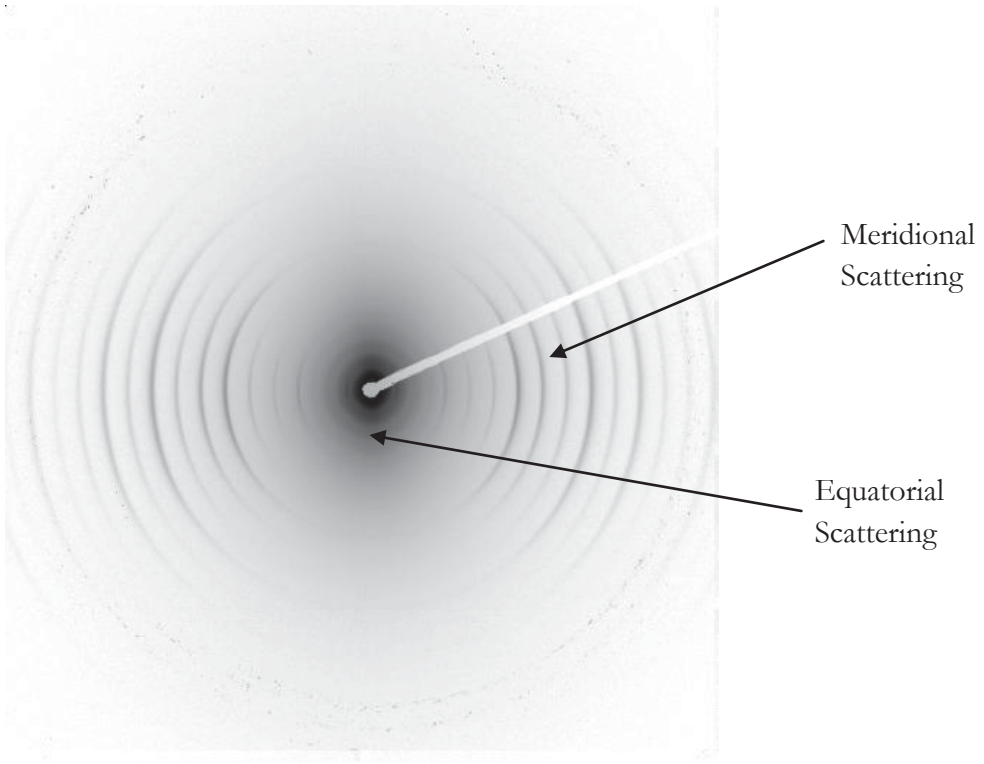

Figure 2.9: Sample SAXS diffraction pattern showing the locations of equatorial and meridional scattering.

The meridional scattering patterns of collagenous tissue are affected by the alignment of the collagen fibrils. A variation in the orientation of individual fibrils results in reflections appearing at different positions on an arc that corresponds to the spacing of the fibrils. The large sample size results in a smooth distribution of intensity across the arc. Therefore, if the orientation of collagen fibrils is completely random a uniform circle of diffraction intensity is produced. Preferred orientations results in arcs that are centred at the average orientation direction (Purslow *et al.* 1998).

2.6.1.4 Small Angle X-ray Scattering of Leather

Leather has previously been investigated using SAXS. Fibre orientation was identified in leather samples under strain (Boote *et al.* 2002; Sturrock *et al.* 2004) although in these studies the resolution appears to be rather limited with collagen *d* spacing Bragg peaks not easily observed in the diffraction patterns.

CHAPTER 3 EXPERIMENTAL METHODS

This chapter outlines the experimental methods used during this project. All concentrations in this chapter are expressed as weight per weight percentages unless otherwise stated.

3.1 Leather Sampling

Leather samples were provided by the New Zealand Leather and Shoe Research Association Inc.

3.1.1 Leather preparation

Leather samples from ovine and bovine skins were predominantly used throughout this work. The process used to prepare skins was systematically varied slightly so that skins with a larger range of tear strength could be produced, as shown in Figure 3.1. Samples from approximately 600 ovine leather skins were produced, with further analyses being carried out on a selection of skins which had a range of tear strengths. The processing method is outlined below.

Ovine skins were sourced from early season 5-months old lambs from "black-face" breeds, such as Suffolk, South Suffolk and Dorset Down. Bovine hides were obtained from a variety of breeds of 2 to 3-years-old cattle.

After the skins had been removed from the carcasses they were immediately cooled to 10°C using a cold water wash, then excess water removed by placing them in a tumbling device with perforations. The skins were then salted and stored as salted green skins until they were needed. Samples of salted green skin were removed from skins before they were soaked in water (10 kg of water for every 1 kg of skins) with agitation for 1 hour. The water was drained and the skins washed with running water and agitated for 4 hours before being drained.

The skins were then depilated using one of two methods; an overnight paint or a 2 hour quickpull paint. The overnight paint contained 140 g/L of sodium sulfide, 50 g/L hydrated

lime and 23 g/L of solvitose (AVEBE U.A., Netherlands) a pre-gelled starch thickener, in water. The 2 hour quickpull paint contained 200 g/L of sodium sulfide, 45 g/L of sodium hydroxide, 50 g/L of hydrated lime and 23 g/L of solvitose (AVEBE U.A., Netherlands) in water. These ingredients were mixed together and then painted on the flesh side of the skins at a thickness of 400g/m^2 which were then incubated at 20°C for 16 hours in the case of the overnight paint or for 2 hours in the case of the 2 hour quickpull paint. The wool was mechanically removed from the skins and depilated slat samples were removed at this point.

The depilated skins were placed in a slowly rotating drum with 800g of water for every 1 kg of skins for 1 hour after which time the sodium sulfide concentration was measured and increased to 0.8, 1.2, 1.6, or 2% using sodium sulfide. The temperature of the solution was maintained at either 16, 18, 20, 22 or 24°C and the skins were soaked in this solution for a period of 8, 10, 12, 14 or 16 hours depending on the batch. After this time the solution was drained from the skins which were then soaked in water at 20°C for 15 minutes, then drained. This washing procedure was repeated three times, with a soaking time of 20 minutes.

A solution of 2% ammonium chloride, 0.2% hydrogen peroxide and 0.025, 0.05, 0.075 or 0.01% bating enzyme, depending on batch, were then added to the wet skins and maintained at a temperature of 35°C. The bating enzyme was either a bacterial enzyme (Rohapon ANZ, Shamrock Ltd.) or pancreatic enzyme (Tanzyme, Tryptec Biochemicals Ltd.) depending on batch and the skins were left in the enzyme solution in a rotating drum for 75 minutes. After incubation the solution was drained from the skins which were again washed three times with water at 20°C for 20 minutes.

A solution of 20% sodium chloride at 20°C was added to the skins and left for 10 minutes before sulfuric acid was added to a final concentration of 2%. After 1.5 hours the sodium chloride concentration was checked to ensure it was between 11-13%, and the skins agitated for 3 hours before the solution was then drained, and pickled skin samples were removed at this point.

The skins were then soaked in a solution of 10% sodium chloride at 35°C for 10 minutes after which time an aqueous surfactant, Tetrapol LTN (Shamrock, New Zealand), and a pretanning agent, Zoldine ZE (Angus, USA) were added to final concentrations of 8 and 4% respectively. After 20 minutes sodium formate and sodium bicarbonate were added to a

concentration of 2% for each compound. After 20 minutes the same amount of sodium bicarbonate was added and after another 20 minutes half that amount was added again. The pH of the solution was then checked to ensure that it was between 7.5 and 8.0. Twice the volume of water was then added and the solution was left for a further 60 minutes at 45°C. The solution was then drained and the pretanned samples removed. A 0.67% solution of Tetrapol LTN (Shamrock, New Zealand) at 45°C was then added, left for 30 minutes then drained and the skins washed three times with water at 45°C soaking for 20 minutes each time.

The skins were soaked in a solution of 8% sodium chloride, 1% disodium phthalate (40% active, Feliderm DP, Clarient, UK) and 1% Formic acid for 10 minutes at 25°C before chromium sulfate powder (Chromosol B, Lanxess, Germany) was added to produce a concentration of 5%. After 30 minutes 0.6% magnesium oxide was added and the temperature was increased to 40°C and the skins left to soak overnight. The solution was drained and the skins rinsed with water at 25°C. Wet blue samples were removed at this point.

The skins were soaked in a solution of 0.067% Synthecol AC (Chemcolour, New Zealand) at 30°C for 10 minutes, then drained before being soaked in a solution of 1% sodium formate, 0.15% sodium bicarbonate and 1% Tanigan PAK-N (Bayer, Germany), a retanning agent, at 35°C for 60 minutes. The solution was drained and the skins soaked in water at 50°C for 15 minutes before being drained and soaked in a solution of 2% mimosa (Tanac, Brazil), a vegetable retanning agent, at 50°C for 5 minutes. Fat liquors were then added to a final concentration of 1% chromopol SG (TFG Ledertechnik GmbH, Germany), 1.5% chromopol UFB-W (TFG Ledertechnik GmbH, Germany), and 3.5% Coripol ZXK (TFG Ledertechnik GmbH, Germany). After 45 minutes formic acid was added to a final concentration of 0.5%. After 30 minutes the solution was drained and retanned samples removed. The skins were then soaked in water at 20°C for 15 minutes before being drained, dried and mechanically softened.

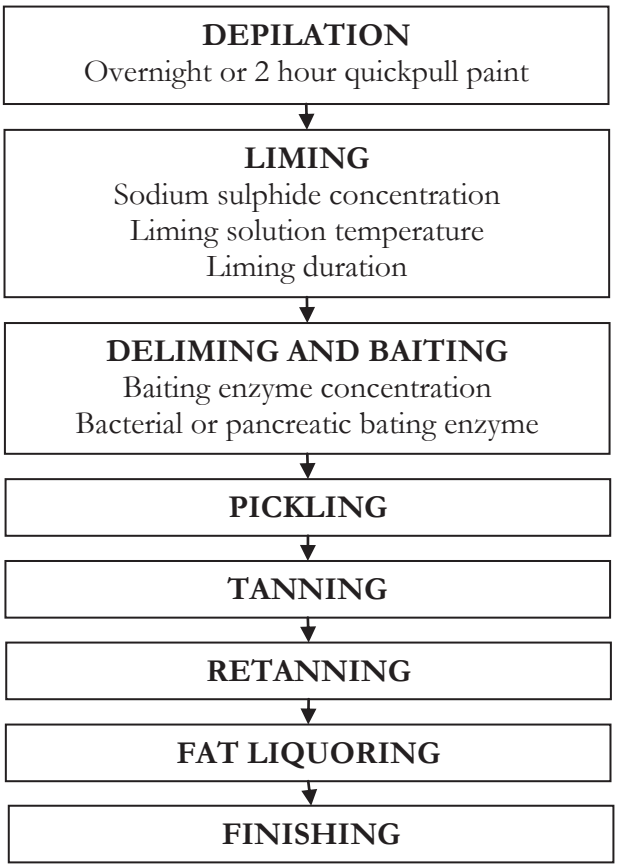

Figure 3.1: Flow diagram of the key stages of leather production illustrating the systematic variations in processing that took place to create a greater range of tear strengths.

3.1.2 Sample Selection

Ovine skins for further testing were selected based on the results of tear test measurements taken from the official sampling position (OSP). Skins were selected with tear strengths of approximately 20 N/mm and 40 N/mm, with the same number being selected for each group. The total number of ovine skins selected was 30.

Samples of leather were taken from four locations on the skin. These were termed the OSP, the neck, the belly and the butt. A schematic diagram of these positions on a skin is shown in Figure 3.2. They were selected as they were expected to give the largest variation in terms of structure, based on investigations of bovine hides, and were therefore considered to give a good representation of the variation expected across a skin.

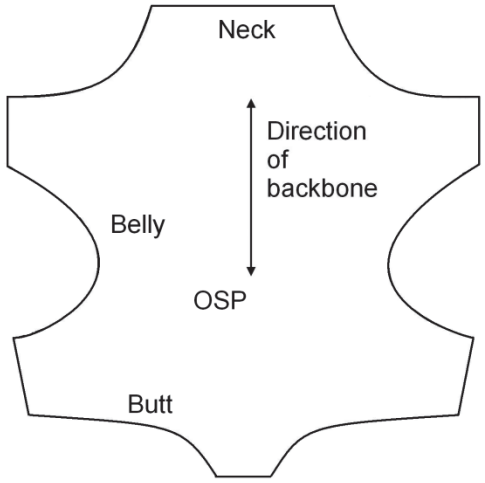

Figure 3.2: Diagram of sample locations on leather skin with direction of backbone indicated.

At each of these positions samples were cut in three different directions. These were cross-sections cut parallel to the backbone, cross-sections cut perpendicular to the backbone and flat samples cut parallel to the backbone. Flat samples were further separated into corium and grain samples.

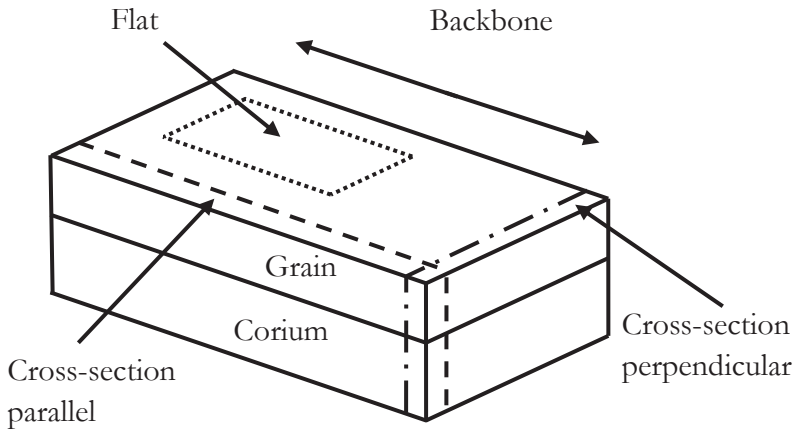

Figure 3.3: Diagram showing the direction of samples cut from leather skin in relation to the direction of the animal's backbone.

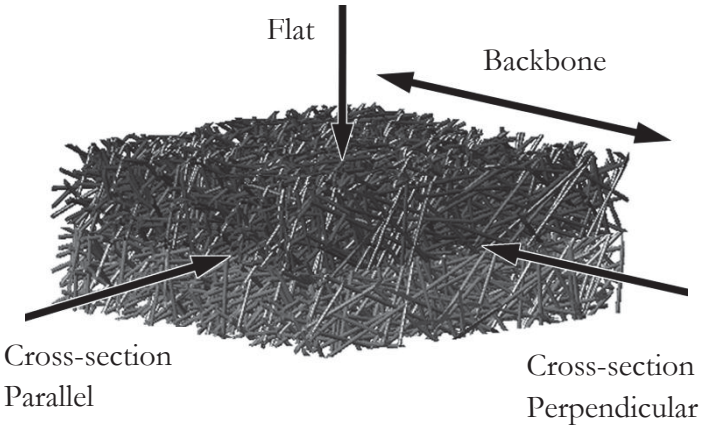

Figure 3.4: Directions of X-ray beam with descriptors used in the text shown relative to the direction of the animal's backbone (Basil-Jones *et al.* 2011).

The method of cutting samples is as follows. Skins were laid out flat and the selected location identified. The samples were then cut out using a sharp scalpel and ruler. Cross-sectional samples were 1 mm thick and 30mm or 50 mm long depending on whether the sample was to be unstrained or stretched respectively. Flat samples were 5 mm thick and 30 mm long. After being cut from the skin the sample was separated into grain and corium layers by visually identifying the grain-corium junction and cut using a scalpel and ruler.

This method of layer separation was selected over mechanical separation as it was thought that it would result in less damage to the structure of the samples, although it is thought that the method used may be less precise than mechanical separation. It is possible that the separation method employed could influence results, specifically those produced from stretching, but it is thought that this influence would not be considerable.

3.2 Decellularized Extracellular Matrix Sampling

Decellularized Extracellular Matrix samples were provided by Mesynthes Ltd.

3.2.1 Decellularized Extracellular Matrix Production

New Zealand sheep, less than 18 months of age, were slaughtered and their forestomach removed. The contents were removed and the forestomach was then cleaned with water before being stored at 4°C for 2-6 hours.

The forestomach was then turned inside out, filled with 4 M sodium chloride and sealed before being immersed in a solution of 0.1% ethylenediaminetetraacetic acid (EDTA), a chelating agent, and 0.028% Tritron X-200 (The Dow Chemical Company, USA), a ionic detergent at 4°C for 16 hours. The filled forestamach was then immersed in a solution of 0.1% sodium dodecyl sulfate (SDS), another ionic detergent, at 4°C for 4 hours.

The forestomach was drained and then the epithelium and muscle of the forestomach were mechanically removed. The remaining material was washed in water at ambient temperature for 30 minutes and then transferred to a solution of 0.1% peracetic acid, 5% ethanol and 1 M sodium chloride for 60 minutes. After this time it was removed from the solution, drained and then immersed in a solution of phosphate buffered saline (PBS) pH 7.2 for 60 minutes. It was then soaked in sterile water for 15 minutes, followed by PBS for 15 minutes. This process was repeated once more before the material was lyophillised. Samples measuring approximately 50 mm x 10 mm were then cut from the material for testing.

3.3 Tear Strength Measurement

Tear strengths were measured using international standard methods (BS EN ISO 3377-2:2002(E), BS EN ISO 2418:2002(E), BS EN ISO 2419:2012(E)). Tear strengths were measured using a double edge tear strength method. Briefly, two samples were cut from the leather skin from each of the positions being tested. These samples were 50 x 25 mm rectangles with a hole in the middle. A diagram of this sample shape is shown in Figure 3.5. The direction of the test was determined in relation to the backbone with parallel test samples being cut with the long sample edge perpendicular to the direction of the backbone and perpendicular test samples being cut with the long sample edge parallel to the direction of the backbone. The samples were stored in an incubator at 20°C for 24 hours. The relative humidity of the incubator was maintained at 65% by the inclusion of a container of saturated magnesium nitrate solution in the incubator.

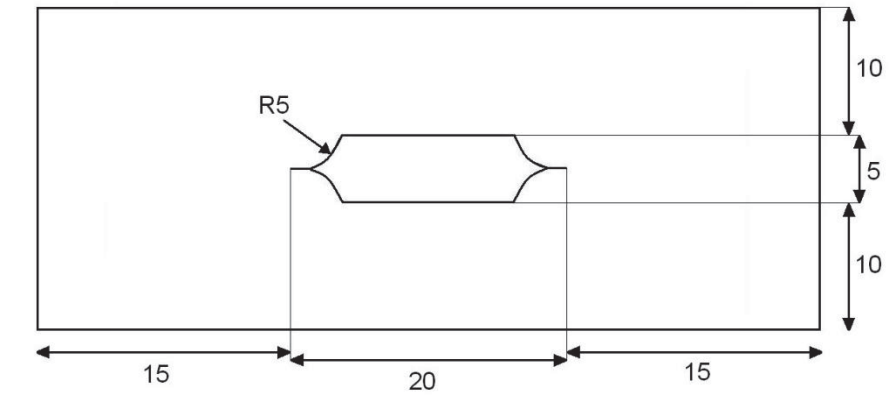

Figure 3.5: Diagram and photograph of tear strength sample. Units in diagram are in mm.

Samples were removed from the incubator and the thickness of the sample measured using a Bray leather substance gauge (Bray Leather Instruments) with an uncertainty of ± 0.02 mm. The sample was then placed in an Instron 4467 (Instron, Massachusetts, U.S.A) strength testing device with tear strength hook attachments attached as shown in Figure 3.6a. These attachments were separated at a rate of 100 mm/min until the samples has completely torn. The maximum load recorded by the instrument was recorded. This value was termed the absolute tear strength. The normalised tear strength was calculated by dividing the absolute tear strength by the sample thickness.

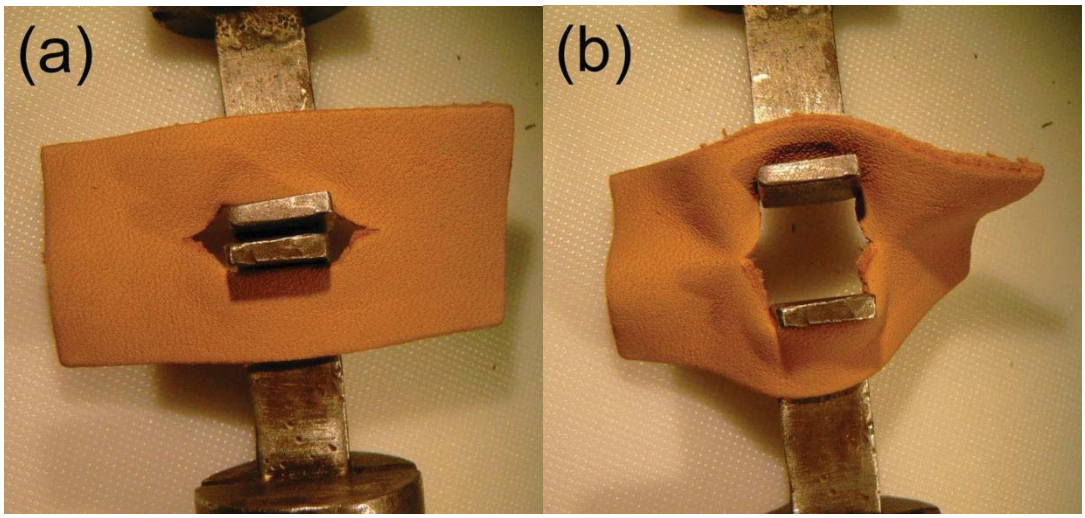

Figure 3.6: Photograph of a tear test on a leather sample a) placement of sample in the Instron device and b) part way through the tear testing process (Sizeland *et al.* 2012).

3.4 Small Angle X-ray Scattering

As discussed in the previous chapter Small Angle X-ray Scattering (SAXS) is a technique used to determine parameters relating to the structure of samples in the macromolecular size range.

3.4.1 Sample Preparation

One of the advantages of the SAXS technique is that no specialized sample preparation is required for SAXS experiments. This means that samples can be investigated in their native state. However, the thickness of the sample needs to be suitable; thicker samples result in more scattering material being exposed to the X-ray beam but also result in a greater level of X-ray absorption. Samples were analysed either as unstrained samples or to investigate the change in structure under increasing strain.

Due to the destructive nature of strength testing and the difference in required sample size, the samples analysed by SAXS where not the same as those used to determine strength values. However, the samples used for SAXS were taken from an area of skin as close as possible to the position of that used for the strength tests.

3.4.1.1 Unstrained Samples

Sample plates were produced from a sheet of stainless steel into which 36 (4 x 9 grid) or 132 (12 x 11 grid) circular holes, with 2 cm and 1 cm diameters respectively, were stamped. A sample was attached horizontally and without tension across each of the holes in the sample plate using adhesive tape. The loaded plate was then attached to a remotely controlled sample stage in the Small-Angle X-ray Scattering (SAXS) beamline at the Australian Synchrotron. The ability to move the stage to place different samples in the X-ray beam meant that a large number of samples could be analysed without having to constantly enter the beamline hutch to change or position samples.

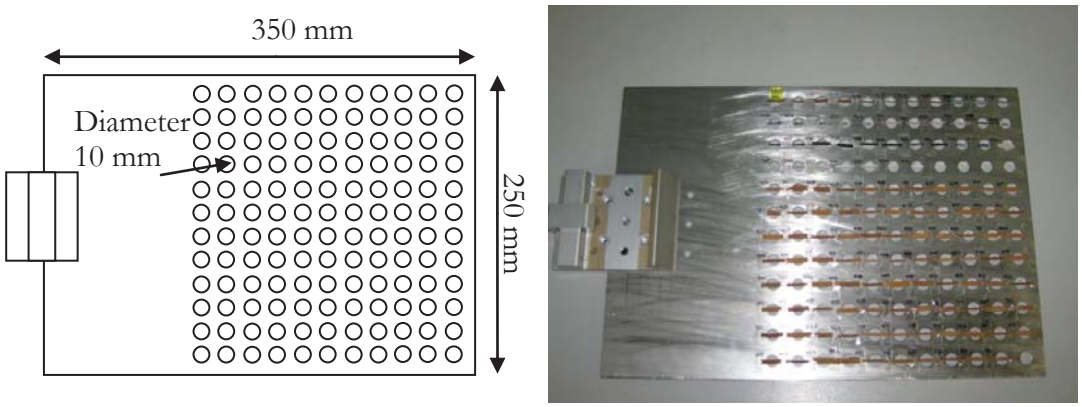

Figure 3.7: Diagram and photograph of unstrained sample plate (12 x 11 grid).

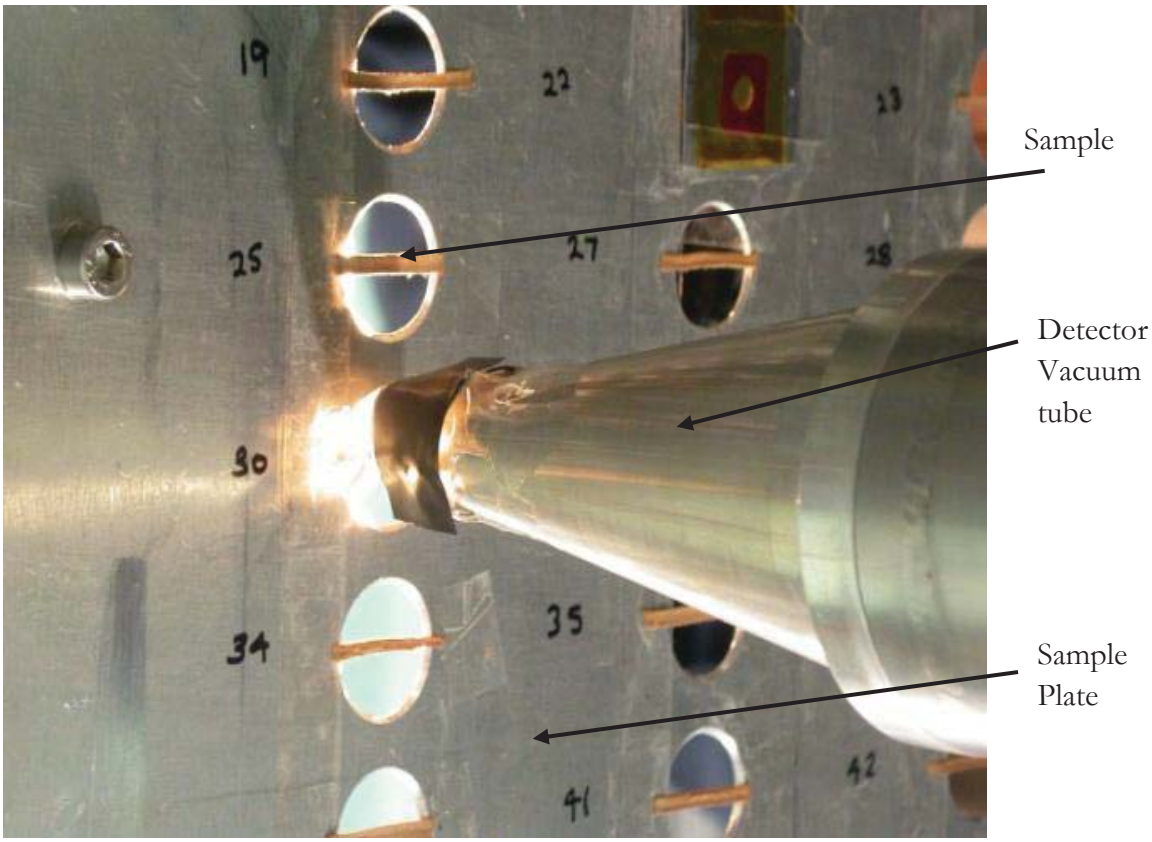

Figure 3.8: Photograph of position of sample plate in relation to X –ray beam (Basil-Jones *et al.* 2010).

3.4.1.2 Stretched Samples

In order to stretch samples in the beamline a stretching apparatus had to be constructed. This device consisted of a linear motor (Linmot PS01-48x240/3x180-C, NTI AG, Switzerland), which was attached to a purpose built frame. A custom-made clamp, designed not to put a sharp point load on the sample, was attached to the end of the slider. A second clamp was attached to the other end of the frame via a L6D Aluminum Alloy OIML single-point loadcell (Hangzhou Wanto Precision Technology Co., Zhejiang, China). Samples were horizontally attached between the clamps, without tension. The set-up, which was attached to the sample stage, was then moved so that the sample was in the path of the X-ray beam.

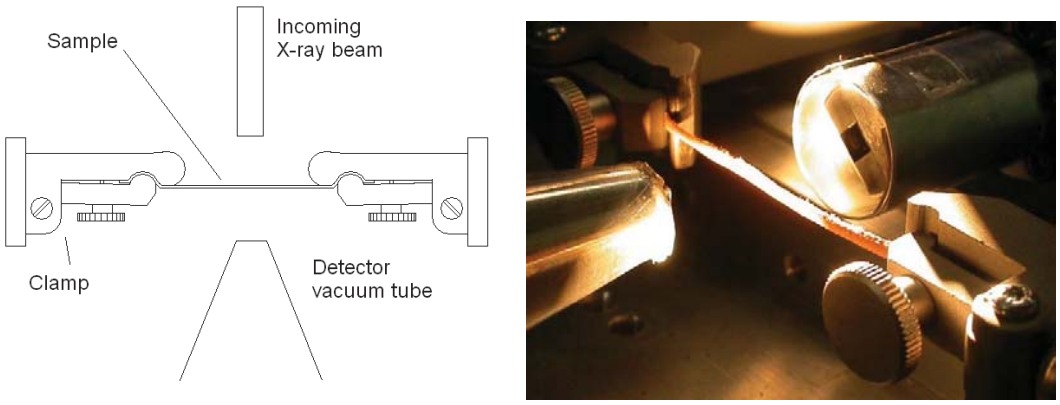

Figure 3.9: Diagram (Basil-Jones *et al.* 2012) and photograph of the position of the sample in the stretching device during SAXS measurements.

The sample was stretched, in 1 mm increments, until a force was recorded on the loadcell. The tension was removed by moving the slider back 1 mm and diffraction patterns of the sample were recorded. The sample was stretched in 1 mm increments, with the sample being left to stabilise for 1 minute before patterns were recorded. Force and extension data was also recorded and the stretching process was repeated until sample failure.

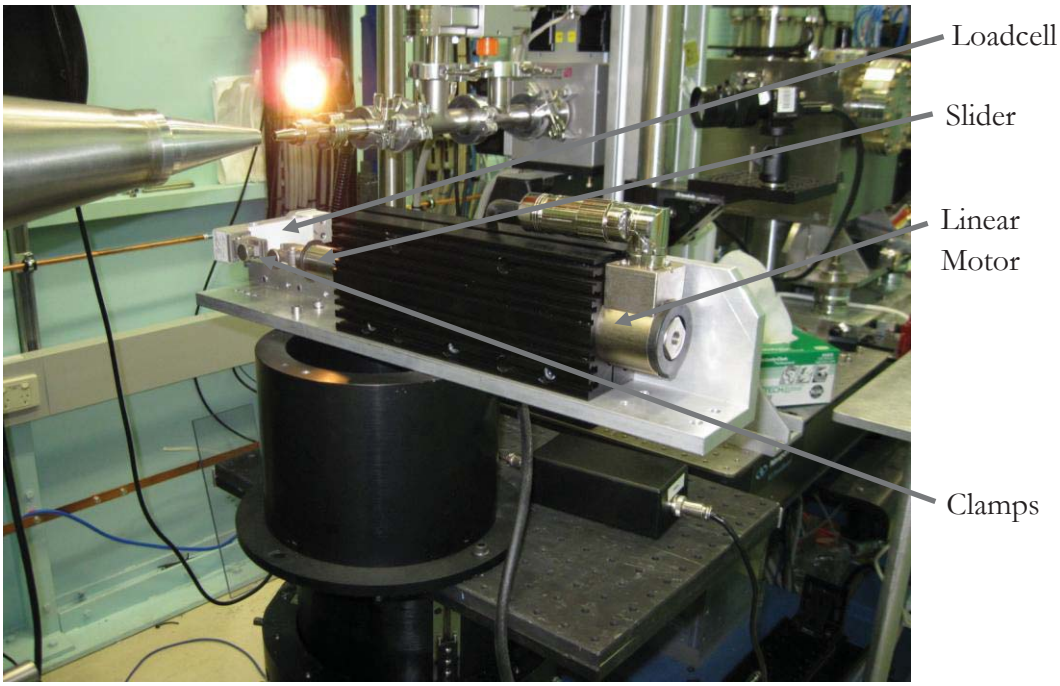

Figure 3.10: Photograph of stretching device installed in the SAXS/WAXS beamline.

3.4.2 SAXS Experimental Set-up

Small Angle X-ray Scattering diffraction patterns were recorded at the SAXS/WAXS beamline at the Australian Synchrotron. The X-rays are generated by an undulator in the storage beam with a length of 3 m, a period of 22 mm and a K_{max} of 1.56. The X-ray beam at the sample was approximately 250 x 80 μm in size and consisted of approximately 2 x 10^{12} photons per second. A sample to detector distance of 3371 mm was used and patterns were recorded on a Pilatus 1 M detector with an active area of 170 x 170 mm.

The absorption edge of zinc, at 9.659 keV, was used to calibrate the monochromator energy. Experiments were performed at a photon energy of 11 keV, with an accuracy of less than 5 eV. The image length was scaled using the diffraction peak of silver behenate. This allowed values of θ, and therefore *q*, to be determined using trigonometry.

Samples were placed in the path of the incoming X-ray beam and an appropriate location on the sample was selected. Cameras in the experimental hutch meant that the exact location of the X-ray beam on the sample could be determined. Patterns were recorded towards the centre of the sample, so that interference from the sample holder would be minimised. An exposure time was 1 s was used to generate patterns.

For unstrained cross-sectional samples diffraction patterns were recorded every 0.25 mm starting at the grain edge and progressing through to the corium and then this scan was repeated at a different location on the sample. This resulted in approximately 10 patterns per scan and 20 patterns per sample. For stretched cross-sectional samples a single scan from grain to corium was performed recording every 0.10 mm. For flat samples four patterns were recorded for each sample in a 1 mm square grid.

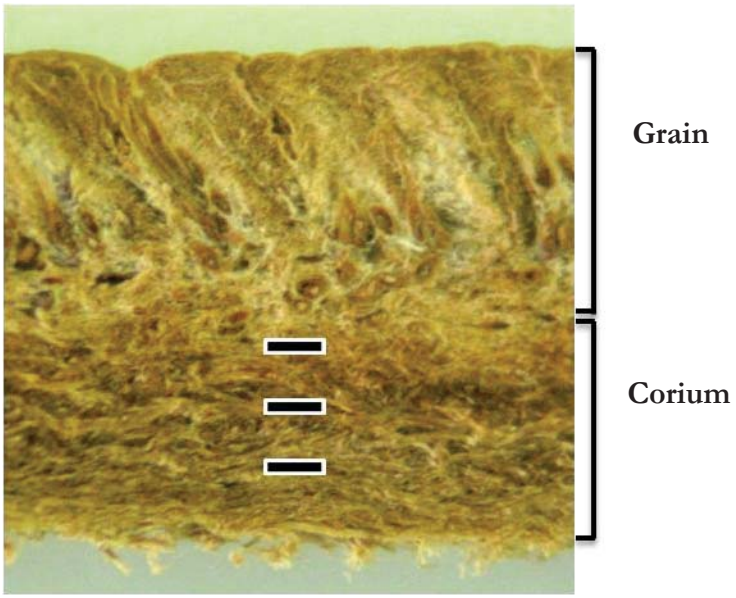

Figure 3.11: Optical image of a cross-section of ovine leather as seen by the SAXS X-ray beam. The height (leather thickness) of the section shown is 2.2 mm, but varies between samples. The rectangles indicate the size of the beam used to probe the sample and the spacing between sampling positions for unstrained cross-sections (Basil-Jones *et al.* 2011).

No normalization was performed on beam intensity as the sample was not in any kind of container or solution meaning that there was no interference from these sources. Blank diffraction patterns were recorded with the intention of using them to remove any scattering due to air. However, as it was found that the effect of air on the scattering pattern was negligible, no normalisation was required.

3.4.3 SAXS Diffraction Patterns

The raw results of SAXS analysis are two dimensional scattering images, as is shown in Figure 3.12. The meridional and equatorial scattering regions can be clearly seen in this image. Bragg's peaks produced by the collagen banding can be clearly seen in the meridional area of the pattern.

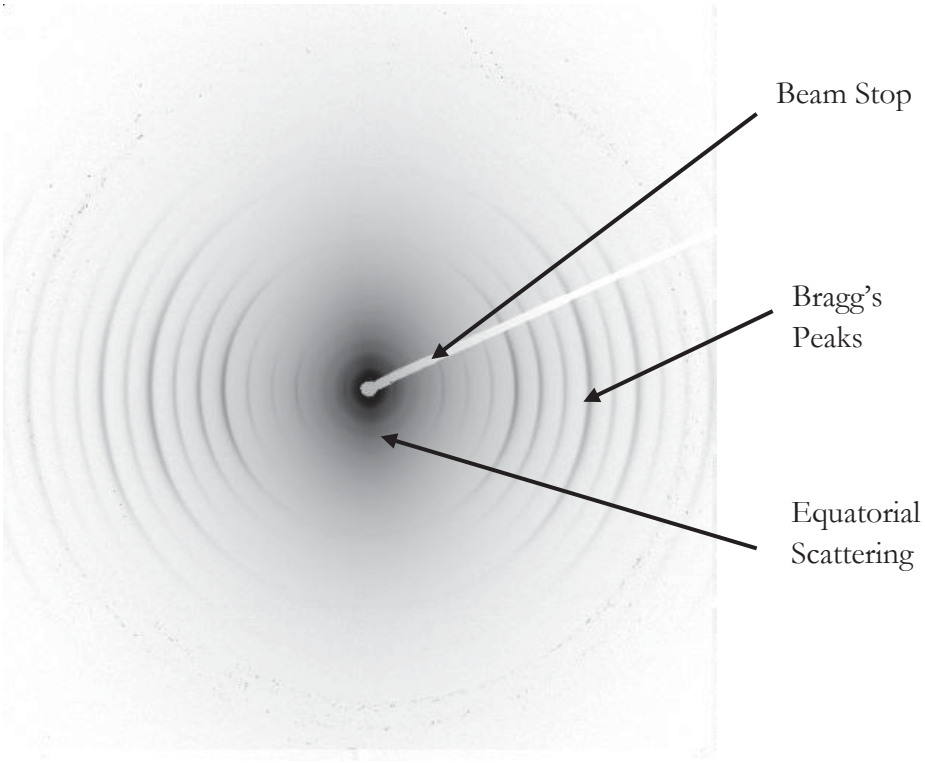

Figure 3.12: Example of SAXS diffraction pattern generated from leather (Basil-Jones *et al.* 2012).

The scattering image can be integrated to produce a plot of intensity versus *q*.

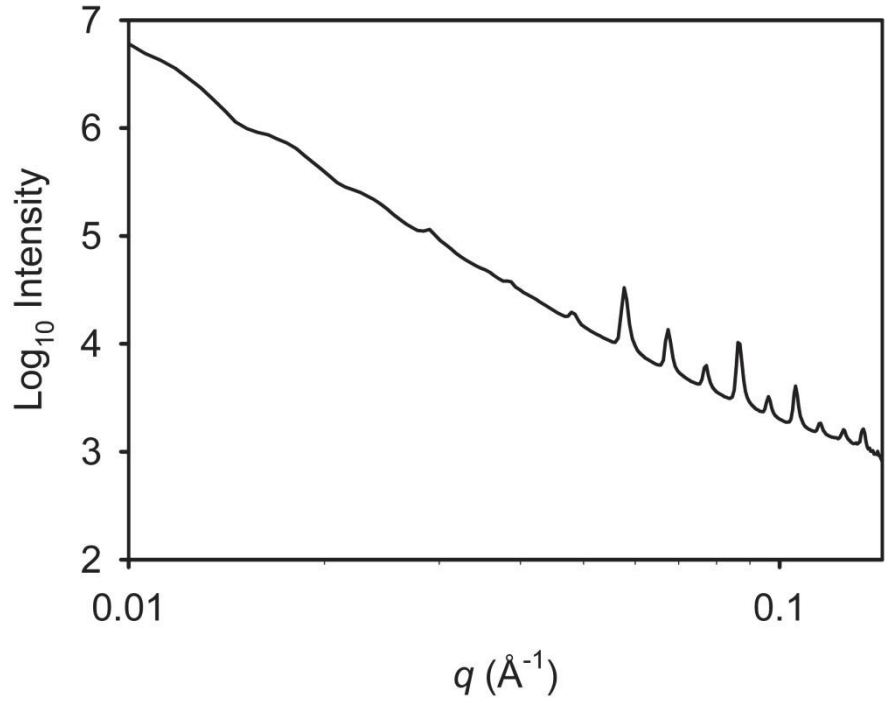

Figure 3.13: Plot of intensity versus *q* for a SAXS pattern of leather (Basil-Jones *et al.* 2012).

3.4.4 Analysis of SAXS Diffraction Patterns

Analysis of SAXS patterns focused on the Bragg's peaks located in the higher *q* regions of the patterns. Three values were calculated from the data obtained; the amount of crystalline collagen, the *d* spacing of the collagen fibrils and the orientation of the collagen fibrils. Data were processed using SAXS15ID and Excel software.

3.4.4.1 Collagen *d* Spacing

The 2-D diffraction pattern was converted to a plot of intensity versus scattering vector, *q*, as shown in Figure 3.12, using SAXS15ID software where;

$$q = \frac{4\pi \sin\theta}{\lambda}$$

A peak fitting function within this program was then used to determine the Bragg peak location. Peak fitting was carried out on the 5th to 9th Bragg peaks and the scattering momentum converted to a *d* value using Bragg's law;

$$2d \sin\theta = n\lambda$$

Therefore;

$$d = \frac{n2\pi}{q}$$

Where; *d* = *d* spacing and n = Bragg peak order.

The values obtained were averaged to give a *d* spacing value for each pattern.

3.4.4.2 Amount of Crystalline Collagen

The amount of collagen was calculated using the sixth-order collagen peak. First, each SAXS pattern was integrated between the *q* values of 0.05 and 0.067 Å^{-1} using the SAXS15ID software. This produced a file that contained a table of intensity values recorded across the range of *q* values, at approximately 0.003 increments, and azimuthal angles, in 5° increments.

The intensity values were then transferred into an excel worksheet and values between 0.05-0.056 and 0.062-0.067 *q* summed over the azimuthal range. These intensity values and *q* values were then logged and a least squares method used to determine a linear relationship between the resulting values. The resulting equation could then be used to give the baseline intensity at any *q* value.

The intensity at each *q* value between 0.056 and 0.062, summed over the azimuthal range, was calculated, and the baseline intensity subtracted to give the intensity of the peak above the baseline. This value was then multiplied by half the difference between the *q* value preceding and following the *q* value at which the intensity value was located. The values calculated across the *q* range of 0.056 to 0.062 were summed. The *q* value corresponding to the maximum peak intensity was identified and the baseline intensity at this point was calculated. The summed area value was then divided by the baseline intensity at the peak and multiplied by 100 to give a measure of the concentration of crystalline collagen.

3.4.4.3 Collagen Fibril Orientation

The orientation of collagen fibrils was measured using a value called the Orientation Index (OI). This is a measure of the spread of the fibrils. A value of 0 indicates no preferred alignment and a value of 1 indicates that all microfibrils are aligned with each other and with the sample surface in the case of cross-sectional samples, or the direction of the backbone in flat samples. The OI is calculated from the most intense Bragg peak, which was located at a *q* value of approximately 0.059 $Å^{-1}$.

To generate an OI value, a SAXS pattern was first integrated between the *q* values of 0.05 and 0.067 $Å^{-1}$ using the SAXS15ID software, producing a file that contained a table of intensity values recorded across the range of *q* values and azimuthal angles. These intensity values were then transferred into an excel worksheet. The values were logged and a linear best fit was produced for the baseline values for each azimuthal angle. The peak intensity at each azimuthal angle was determined and the baseline value at this *q* subtracted. The intensity of the peak above the baseline was summed between 90° and 270°. In order to determine the minimum azimuthal range centred at 180° that contains 50% of the microfibrils, the intensity of peaks above the baseline was incrementally summed in both directions from the values at 180° and divided by the sum of intensities calculated between

90° and 270°. When this value reached 0.5, the angle range was defined as the OA. The orientation index (OI) was then calculated using;

$$\mathrm{OI} = \frac{90° - \mathrm{OA}}{90°}$$

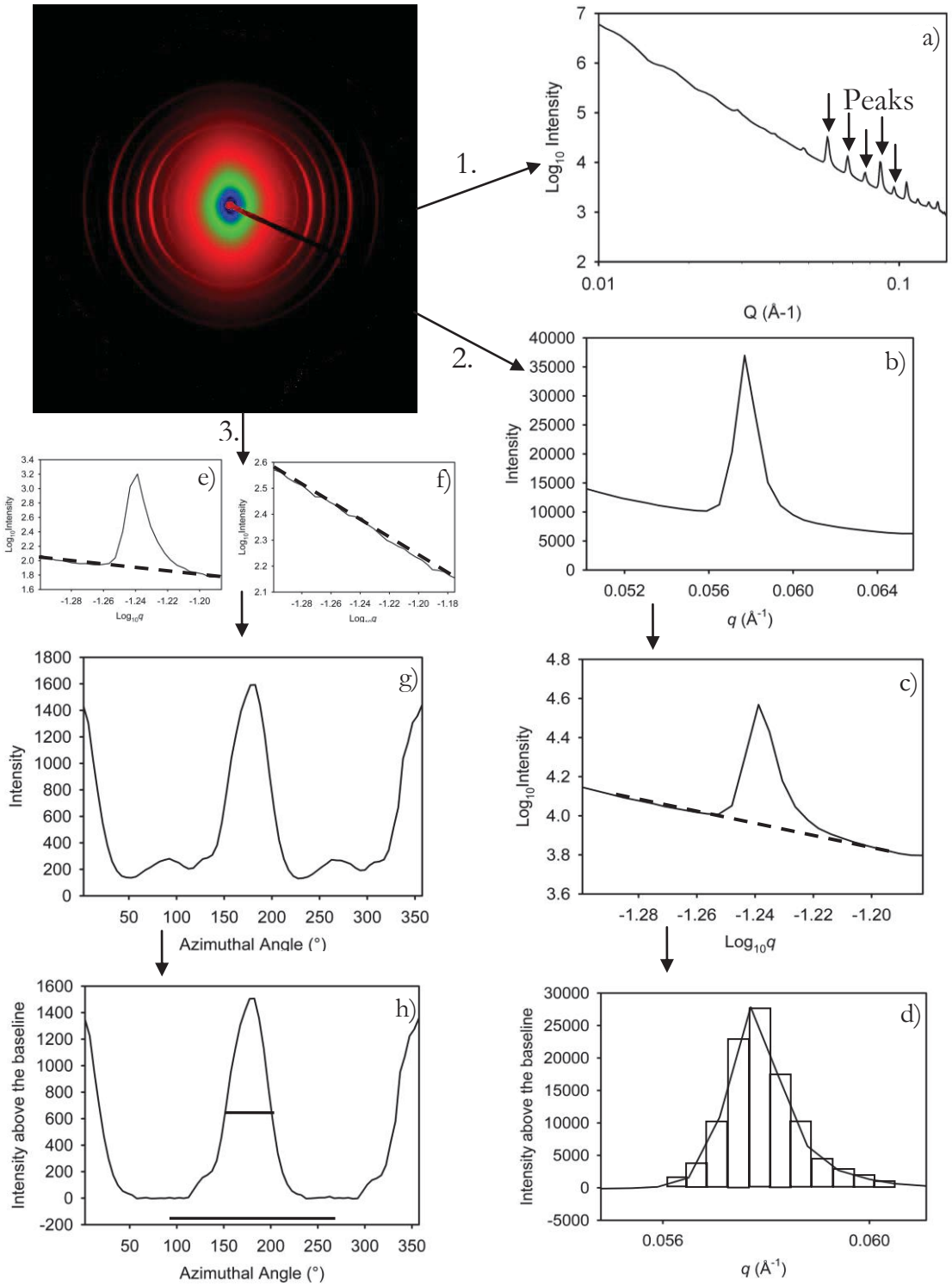

Figure 3.14: Diagram of data treatments used to calculate; 1. collagen *d* spacing, 2. amount of crystalline collagen, and 3. collagen fibril orientation a) graph of intensity versus *q* showing the location of Bragg peaks, b) graph of summed intensity versus *q*, c) graph of log summed intensity versus log *q* used to determine the baseline, d) graph of intensity above the baseline versus *q* used to determine the amount of collagen, e) graph of log summed intensity versus log *q* used to determine the baseline at 180°, f) graph of log summed intensity versus log *q* used to determine the baseline at 90°, g) graph of intensity versus azimuthal angle, and h) graph of intensity above the baseline versus azimuthal angle used to determine OI.

3.5 Scanning Electron Microscopy

3.5.1 Sample Preparation

Thin cross-sections of leather taken parallel to the backbone were cut using a clean new razor blade. These samples were attached to a scanning electron microscope (SEM) stub using double sided tape and conductive silver paint. Samples were then splutter coated with gold.

3.5.2 Image Recording

SEM was undertaken at the Manawatu Microscopy and Imaging Centre. SEM images were viewed using a FEI Quanta 200 Environmental Scanning electron microscope (FEI Electron Optics, Eindhoven, The Netherlands) at an acceleration voltage of 20KV and a pressure of 4.75×10^{-4} Pa. Digital images were recorded at a range of magnifications.

CHAPTER 4 VARIATION OF FIBRILLAR COLLAGEN STRUCTURE OF LEATHER SAMPLES WITH STRENGTH

4.1 Introduction

Some investigation of qualitative relationships between collagen fibre orientation and physical properties in bovine leather has been undertaken previously (Ward and Brooks 1965; Kanagy 1967; Tancous and Schmitt 1967; Tancous *et al.* 1967). Very little research, however, has been undertaken to determine the relationship between fibrillar collagen structure and strength in ovine leather. Better understanding of fibrillar collagen structure and how it relates to physical properties would mean that processes could be developed to produce ovine leather with desired characteristics. Therefore, an investigation into the fibrillar collagen structure of ovine leather and how that relates to strength is of interest. With this purpose in mind, initial research investigated samples of varying strengths that were not under any strain.

It was decided that initially the difference between skins would be investigated by analysing samples taken from the same position on the skin. This would indicate whether there was any identifiable difference between samples of different strength when not under strain. Structural differences are more easily identified when samples are unstrained.

A small group of bovine samples were also analysed. Bovine leather is stronger than ovine produced under the same processing conditions, with bovine leather having approximately twice the normalised tear strength of ovine leather. Increasing the strength of ovine leather to be comparable to that of bovine leather would greatly increase the value of leather produced from ovine skins. Therefore an indication of how the fibrillar collagen structure of bovine leather varies from ovine would be helpful. An investigation was undertaken to explore the relationship between the structure of fibrillar collagen in both ovine and bovine leather samples and their physical properties. To achieve this, samples of ovine and bovine leather of varying strength were analysed using SAXS which resulted in the determination of relevant structural parameters that could be correlated to physical properties of leather.

Samples of leather in all three directions were taken from the official sampling position of 30 ovine skins of varying strength and 10 bovine hides. SAXS patterns were recorded at the SAXS/WAXS beamline at the Australian Synchrotron. The number of patterns recorded depended on sample type with 4 patterns in a grid pattern 1 x 1 mm recorded for flat samples, and 2 scans 1 mm apart across cross-sections with spacing between patterns of 0.25 mm. A more detailed description of the experimental method used can be found in chapter 3.

4.2 Results

As discussed in the previous chapter, SAXS patterns were analysed in the high *q* region. This region provides information on the axial structure of collagen fibrils due to the production of Bragg peaks. Information about the fibrillar structure of collagen was determined from each pattern including; the amount of crystalline collagen, the orientation of collagen fibrils and the *d* spacing of collagen fibrils. These values were related to the strength measurements made on skins. Four physical properties were measured; absolute tear strength, normalised tear strength, tensile strength and tensile extension. Interestingly, significant relationships were only consistently found between the structural measurements and normalised tear strength. Therefore the results presented in this chapter are in relation to normalised tear strength. Results of the comparison of the measured fibrillar collagen structure to the other physical properties measured are provided in Appendix IV.

4.2.1 Amount of Crystalline Collagen

The amount of crystalline collagen was determined from the intensity of the Bragg's peak above the baseline scattering, as, the greater the amount of fibrillar collagen present the greater the resulting scattering intensity. The units of this measurement are arbitrary, as without the analysis of standard controls an absolute value of the amount of crystalline collagen present cannot be calculated. None the less, values obtained for different samples can be compared to give an indication of the variation between samples and be related to physical properties measured.

The distribution of crystalline collagen was found to not be uniform across profiles of cross-sectional samples as can be seen in Figure 4.1. There was a consistently higher concentration of collagen in the corium region, compared to the grain region, with two to

three times more crystalline collagen in the cross-sectional direction. This result was consistent in both the directions measured.

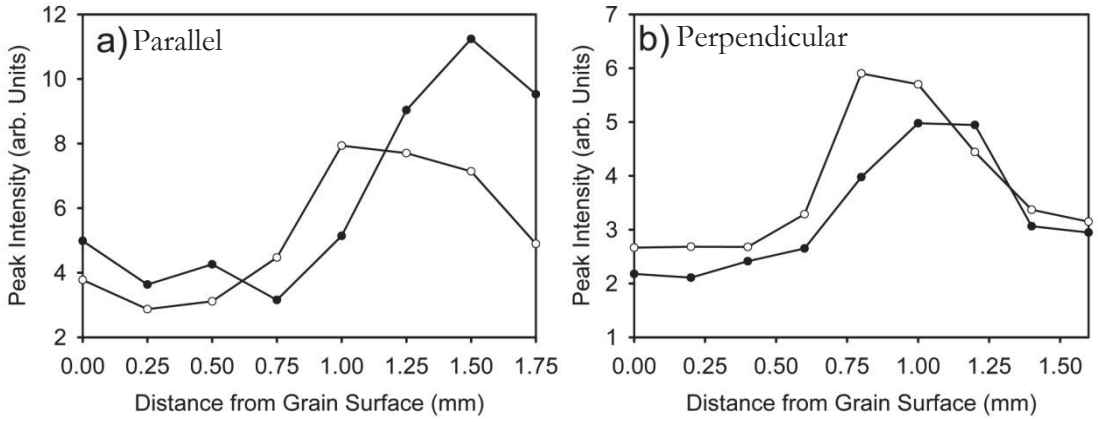

Figure 4.1: Amount of fibrillar collagen through the thickness of ovine leather cross-sections (averages of 12 samples each) cut a) parallel to the backbone, and b) perpendicular to the backbone. Weak leather - solid circles, and strong leather - open circles (Basil-Jones *et al.* 2011).

It is interesting to note that, in the direction parallel to the backbone, leather samples considered to be weak appeared to have a higher maximum concentration of crystalline collagen in the corium than stronger samples. In contrast, the stronger ovine samples appeared to have a larger region of high normalised intensity, indicating a thicker corium region. This is consistent with earlier finding which indicate the relative importance of corium content in determining strength (Russell 1988; Attenburrow 1993; Liu and McClintick 1999).

As the SAXS technique does not measure fibrils in line with the incident X-ray beam, the measurement of amount of collagen in one direction does not accurately demonstrate the amount of collagen present. The amount of collagen detected in all three directions was, therefore, averaged to give a better indication of the total amount of crystalline collagen present in each sample.

There was found to be no relationship between the average amount of crystalline collagen and the tear strength of the leather samples, as shown in Figure 4.2. The ovine leather samples were selected so that they could be split into two groups; weak samples with an average tear strength of 19.9 N/mm, and strong samples with an average tear strength of 39.5 N/mm. The relative average amount of collagen in these samples was calculated to be

8.8 for weak ovine samples, 8.5 for strong ovine samples and 7.1 for bovine samples. Student t-test results show that there is no significant difference between the amount of crystalline collagen in weak and strong ovine samples, or between strong ovine and bovine samples. A regression analysis of the data gave an r-squared value of 0.04 indicating that the relative amount of collagen is not related to tear strength in the tear strength range studied.

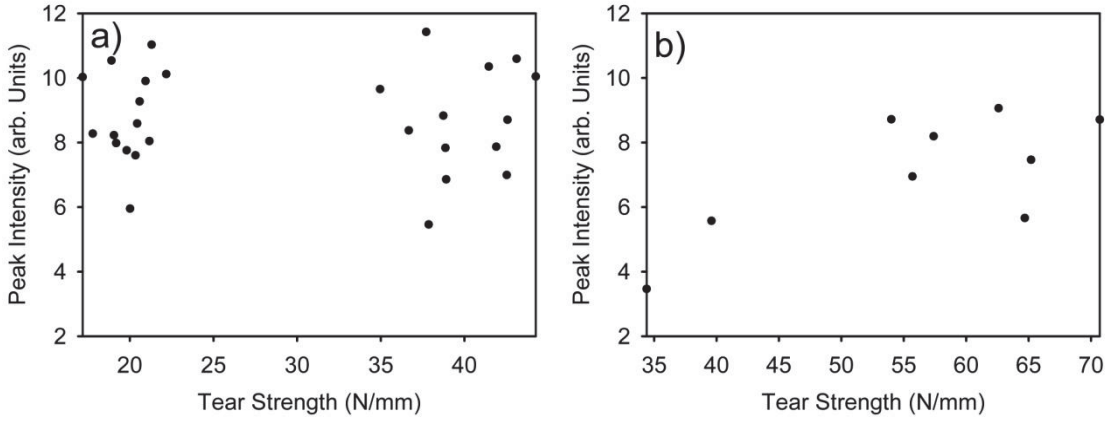

Figure 4.2: Amount of collagen determined from the intensity of the sixth-order collagen *d* spacing peak (at around 0.059–0.060 $Å^{-1}$) versus tear strength for: a) ovine leather; b) bovine leather (Basil-Jones *et al.* 2011).

The amount of crystalline collagen was found to be greater in the corium than in the grain. Because data was collected from different cross-sections, the peak intensity could be averaged over specific regions. This combined with the flat samples being divided into corium and grain regions means that the average peak intensity of the grain and corium regions could be calculated. A student t-test found that the corium region contained a significantly greater amount of crystalline collagen than grain region ($|t\text{-stat}| = 12.34$, t-crit = 2.03, $P = 6.52 \times 10^{-14}$). There was also a relationship between the amount of crystalline collagen in the corium and tear strength with a regression analysis producing a slope of -2.40 mm. Arb. Units/N, $r^2 = 0.20$ and $P = 7.42 \times 10^{-3}$. There was however, no statistically significant relationship between the amount of crystalline collagen in the grain and tear strength. These results are shown in Figure 4.3.

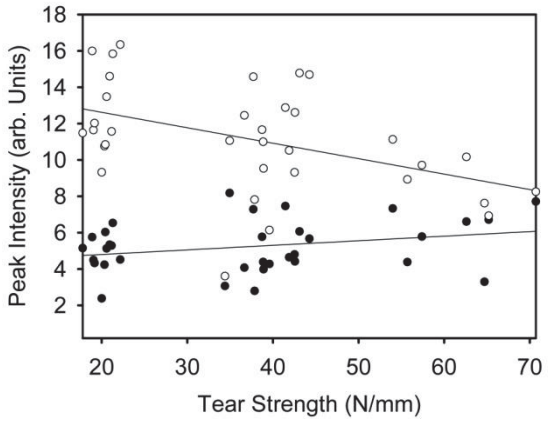

Figure 4.3: Amount of collagen, determined from the intensity of the sixth-order collagen *d* spacing peak (at around 0.059–0.060 $Å^{-1}$), in the corium - open circle, and the grain - closed circle, versus tear strength for both ovine and bovine samples.

4.2.2 Orientation of Collagen Fibrils

Collagen fibril orientation was measured using orientation index, with details of how this value was calculated provided in chapter 3. It should be noted that the implication of this value varies slightly between cross-sectional and flat samples. For cross-sectional samples this value indicates the extent to which collagen fibrils align with the leather surface while for flat samples this value indicate the extent of preferred alignment with the direction of the backbone.

The orientation index (OI) of collagen fibrils varies depending on the direction in which the measurements are made, as seen in Figure 4.4. The OI was lowest in the flat samples and highest in the cross-sectional samples taken perpendicular to the backbone. There were found to be statistically significant differences between the OI of strong and weak leather samples.

In cross-sectional samples the OI was lower for weak ovine samples than for strong ovine samples. For cross-sectional samples of ovine leather cut parallel to the backbone the average OI was found to be 0.422 (with a standard deviation of 0.063) for low strength samples and 0.452 (0.070) for high strength samples (Figure 4.4 a)). A student t-test showed that the difference was statistically significant ($|t\text{-stat}| = 2.06$, t-crit = 2.00, $P = 0.044$). For cross-sectional samples of ovine leather cut perpendicular to the backbone the average OI was found to be 0.578 (0.106) for low strength samples and 0.630 (0.065) for

high strength samples (Figure 4.4 e)). This difference was also found to be significant (|t-stat| = 3.21, t-crit = 2.01, P = 0.0023).

There is no trend visible in the cross-sectional bovine data (Figure 4.4 b) and f)). This may be due to the limited number of samples analysed. Strong bovine leather was found to have a significantly higher OI (0.493 (0.126)) than strong ovine leather in the cross-sectional direction parallel to the backbone (|t-stat| = 2.20, t-crit = 2.01, P = 0.03).

There was found to be a significant difference between the OIs of the cross-sections measured parallel and perpendicular to the backbone of ovine leather samples (|t-stat| = 15.77, t-crit = 2.01, P = 1.86×10^{-21}). This difference is also found in the bovine samples (|t-stat| = 2.12, t-crit = 2.12, P = 0.05), although the relationship is not as significant, possibly due to the smaller sample size.

From Figure 4.4 it can be seen that although OI has a significant effect on tear strength other factors are also important. This can be seen by the scatter present in the figures. Regression analysis for ovine leather samples produced a slope of 1.79×10^{-3} mm/N, r^2 = 0.08 and P = 0.04 for cross-sections cut parallel to the backbone and a slope of 2.60×10^{-3} mm/N, r^2 = 0.16 and P = 3.40×10^{-3} for cross-sections cut perpendicular to the backbone.

For flat samples the OI was found to be higher in the corium than in the grain. The OI was 0.248 for the grain and 0.329 for the corium of ovine leather (Figure 4.4 c)). The difference between the OI of the corium and grain in ovine leather was found to be significant (|t-stat| = 3.7, t-crit = 2.1, P = 0.001). The difference in OI for the corium and grain was also found to be significant for bovine samples with the grain having an OI of 0.184 and the corium 0.364 (|t-stat| = 4.7, t-crit = 2.45, P = 0. 003) (Figure 4.4 d)). There was no significant difference between the OI of strong and weak samples in the corium or the grain of flat samples.

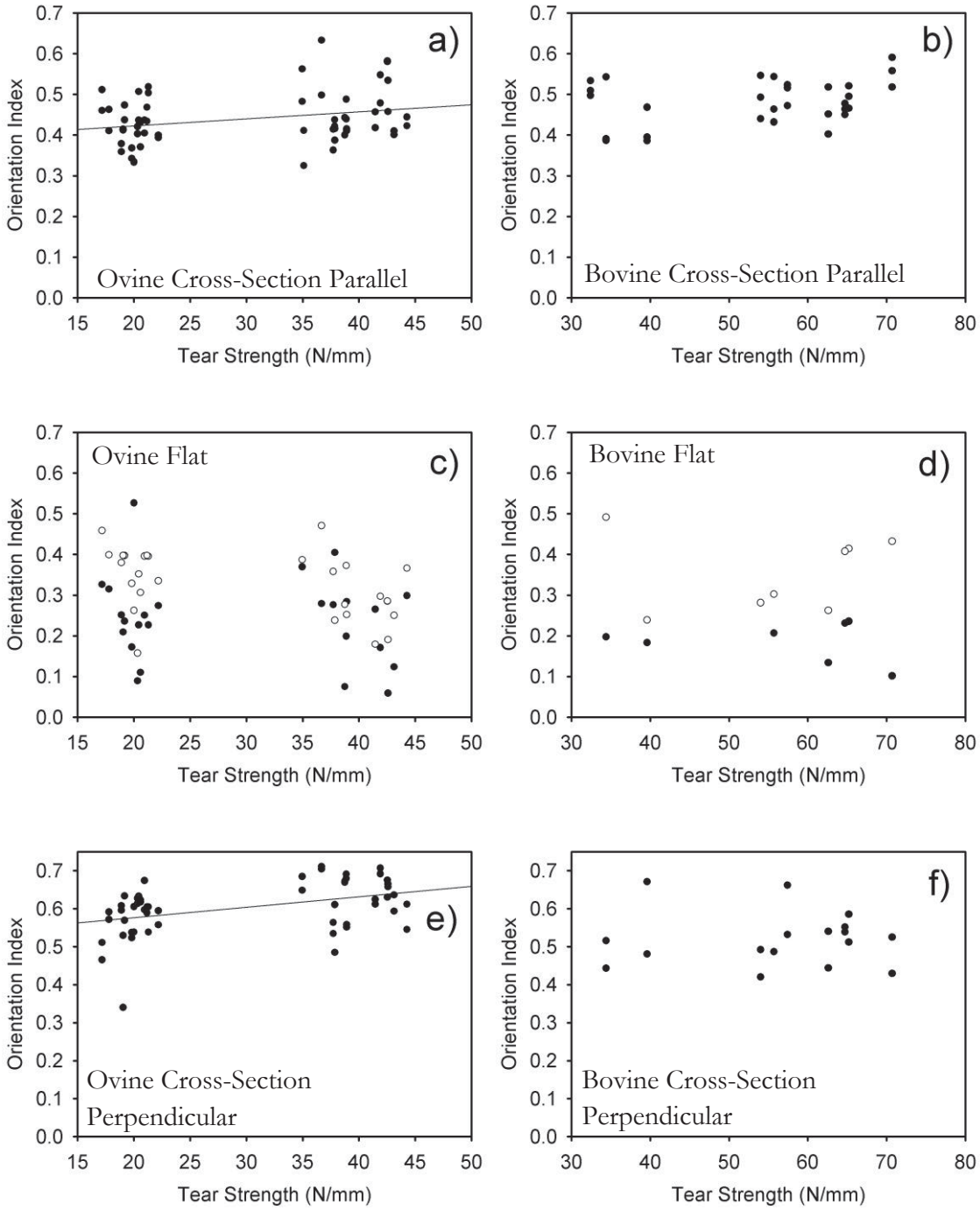

Figure 4.4: Orientation index versus tear strength for OSP samples of leather for a) ovine cross-sections cut parallel to backbone; b) bovine cross-sections cut parallel to backbone; c) flat ovine samples, grain- closed circle and corium - open circle,; d) flat bovine samples, grain - closed circle and corium - open circle,; e) ovine cross-sections cut perpendicular to backbone; f) bovine cross-sections cut perpendicular to backbone. A higher OI indicates a greater degree of fibre alignment (Basil-Jones *et al.* 2011).

As several diffraction patterns at different positions were taken for the cross-sectional samples, the change in OI across the sample could be analysed. Averages of these profiles

are shown in Figure 4.5. The profiles of both the cross-sections parallel and perpendicular to the backbone are similar, with the corium having a higher OI than the grain and the minimum OI found to be in the grain-corium junction region. The cross-sections perpendicular to the backbone tended to have a higher OI across their entire thickness, especially in the grain. From Figure 4.5 c) and d) it can be seen that stronger samples generally had higher OI's across their entire thickness and they had the OI minimum, associated with the grain-corium junction, closer to the grain edge indicating that the stronger samples have a thicker corium layer.

For ovine leather cross-sections cut parallel to the backbone, Figure 4.5 a) show that the average OI in the grain layer varies between approximately 0.29 and 0.41 and in the corium between 0.50 and 0.61. A t-test was performed to determine if there was a difference between the OI at 0.25 and 1.5 mm through ovine leather samples. These values were chosen as they were considered to be near the middle of the grain and corium regions respectively. It was found that the average OI at 0.25 mm from the grain surface was 0.33 and the average OI at 1.50 mm from the grain surface was 0.61. There was found to be a significant difference between the groups ($|t\text{-stat}| = 13.7$, t-crit = 2.05, $P = 1.1 \times 10^{-13}$).

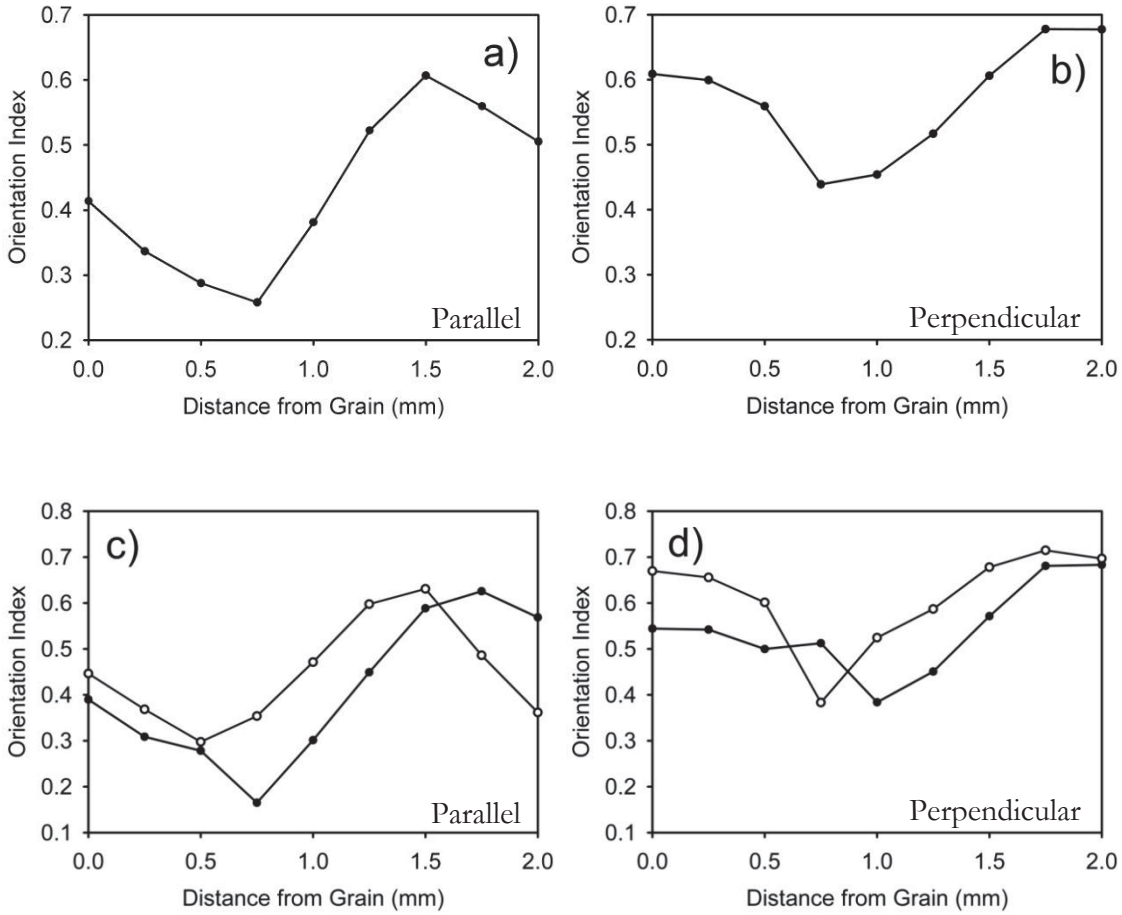

Figure 4.5: Average orientation index across the thickness of ovine leather measured a) all samples cut parallel to the backbone (Basil-Jones *et al.* 2011); b) all samples cut perpendicular to the backbone; c) weak - closed circle and strong - open circle, cut parallel to the backbone; and d) weak - closed circle and strong - open circle, cut perpendicular to the backbone. Graphs are of an average of 28 leather samples for all samples and 14 leather samples for weak and strong samples.

Results indicate that the relationship between OI and tear strength is continued through different species. Figure 4.6 shows the average OI value for cross-sections of each of the different leather types studied; weak ovine (15 samples, 228 analysis points), strong ovine (14 samples, 249 analysis points) and strong bovine (10 samples, 167 analysis points), versus the average tear strength for the group. A regression line was fitted to the data and it was found that the line had a slope of 1.708×10^{-3} mm/N, $r^2 = 0.20$ and $P = 4.45 \times 10^{-5}$. This result confirms that there is a significant relationship between OI and tear strength when analysing data from more than one species.

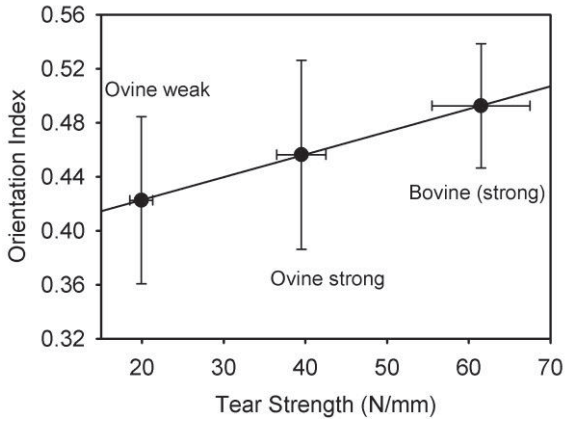

Figure 4.6: Orientation index versus tear strength for the averages of each of the leather types measured through cross-sections cut parallel to the backbone. Error bars are one standard deviation (Basil-Jones *et al.* 2011).

Collagen fibres have been observed to have a wavy structure with a repeat distance of several micrometers, which is known as crimp. It was thought that the presence of this might affect the OI measurements recorded using SAXS.

Crimp could increase the average OI measurement calculated. This is because the wavy crimp structure of collagen fibres would result in the direction of the fibrils and microfibrils being that of the crimp at that point in the fibre, as opposed to aligning with the fibre axis. Therefore, the measured OI for a fibre with crimp would be greater than that for a fibre without crimp. For this reason samples of ovine and bovine leathers were investigated using Scanning Electron Microscopy (SEM) (Figure 4.7). No crimp was visible in either the strong or weak ovine leather samples. Some crimp was found, however, in the bovine sample but since the bovine samples had the highest OI, it was concluded that the presence of crimp did not distort the OI measurements determined from the SAXS patterns. Additional SEM images, taken at a larger scale, are provided in Appendix IV.

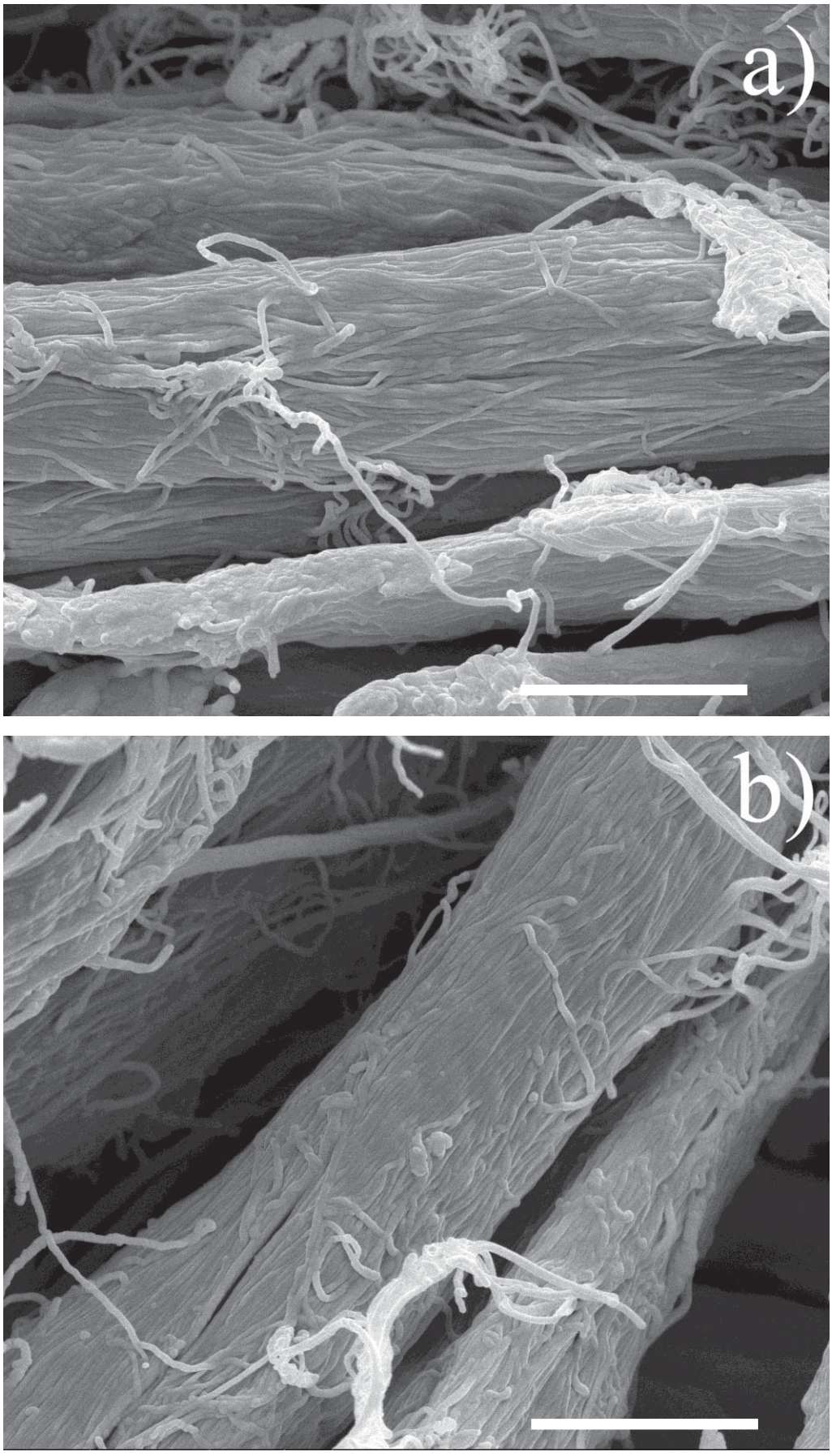

(caption over page)

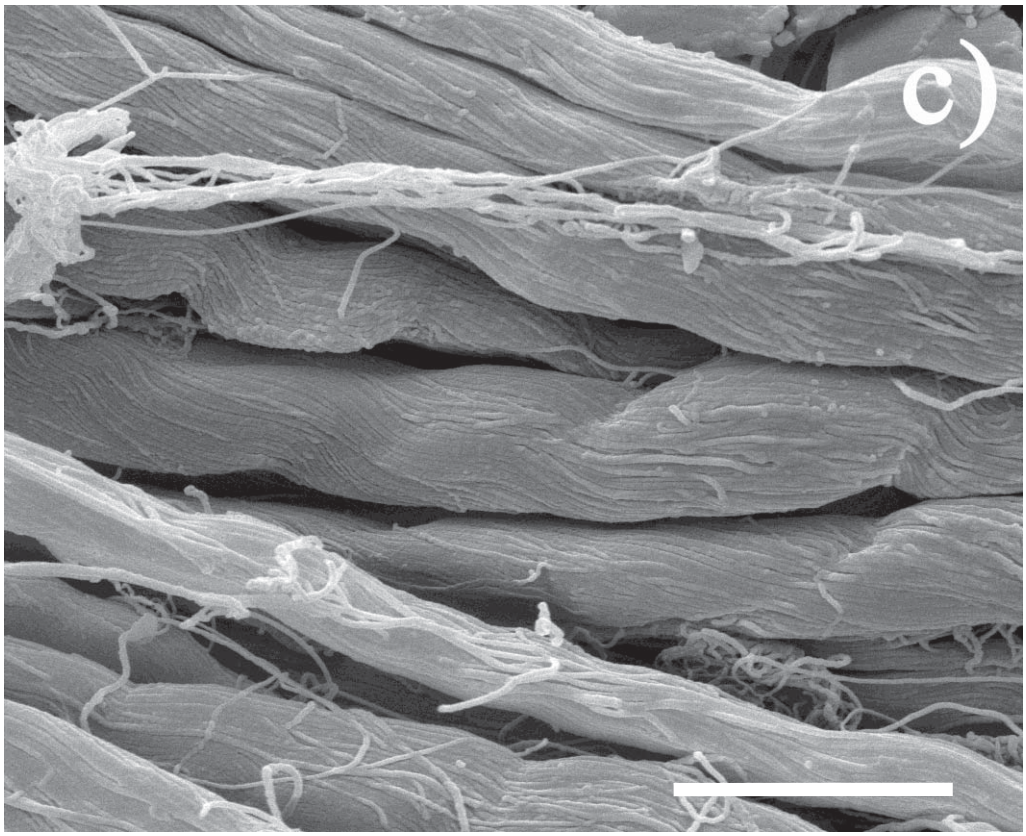

Figure 4.7: Representative SEM images of cross-sections of leather observed parallel to the backbone for a) weak ovine; b) strong ovine and c) strong bovine. Scale bars 10 μm (Basil-Jones *et al.* 2011).

4.2.3 *d* Spacing

The *d* spacing of ovine and bovine leather cross-sections cut parallel to the backbone were found to be significantly different ($|t\text{-stat}| = 11.58$, t-crit = 2.04, $P = 1.34 \times 10^{-12}$). The average *d* spacing of ovine leather was 64.3 (0.2) nm while that for bovine leather was 63.5 (0.2) nm in cross-sectional samples cut parallel to the backbone (Figure 4.8 a) and b)). In cross-sections cut perpendicular to the backbone the difference was also significant with an average *d* spacing of 64.2 (0.6) for ovine and 63.7 (0.3) for bovine samples ($|t\text{-stat}| = 4.52$, t-crit = 2.00, $P = 3.34 \times 10^{-5}$) (Figure 4.8 e) and f)). The variation of *d* spacing of cross-sections with sample direction was not statistically significant in either the ovine or bovine samples. However, the *d* spacing of the bovine samples was consistently lower than that of the ovine samples.

There was found to be no correlation between the *d* spacing and tear strength for samples of ovine or bovine leather cut on the cross-section perpendicular to the backbone. There was, however, a relationship between the tear strength and *d* spacing of sample of bovine

leather cross-sections cut parallel to the backbone, where the *d* spacing increased with increasing tear strength (least squares fit slope = 0.014 nm. mm/N, $r^2 = 0.53$, $P = 2.98 \times 10^{-4}$) (Figure 4.8 b)).

There is a significant difference between the *d* spacing of the corium and the grain of weak flat ovine samples (|t-stat| = 5.08, t-crit = 2.06, $P = 2.75 \times 10^{-5}$). The average *d* spacing of the corium was found to be 64.1 (0.2) nm and that for the grain was 64.4 (0.1) nm for weak samples. However, in strong ovine samples the difference between the *d* spacing of the corium and grain was found to be insignificant, with an average *d* spacing of 64.3 nm for both (Figure 4.8 c)). There was also no significant difference between the *d* spacing of the grain of the weak and strong ovine flat samples (Figure 4.8 c). There was, however, a significant difference between the *d* spacing of the corium of weak, 64.1 (0.2) nm, and strong, 64.3 (0.2) nm, ovine flat samples (|t-stat| = 3.11, t-crit = 2.06, P = 0.005).

In contrast, the *d* spacing of flat bovine samples was larger in the corium, 63.9 (0.3) nm, than in the grain which had an average *d* spacing of 63.0 (0.3) nm (|t-stat| = 6.91, t-crit = 2.12, $P = 3.49 \times 10^{-6}$). From Figure 4.8 d) it appears that the *d* spacing of the corium and grain also increased with increasing tear strength. However regression analysis indicates that these relationships may not be significant with the following least squares fits being produced; for corium; slope = 0.015 nm.mm/N, $r^2 = 0.40$ and P = 0.07, and, for the grain; slope = 0.013 nm.mm/N, $r^2 = 0.25$ and P = 0.17.

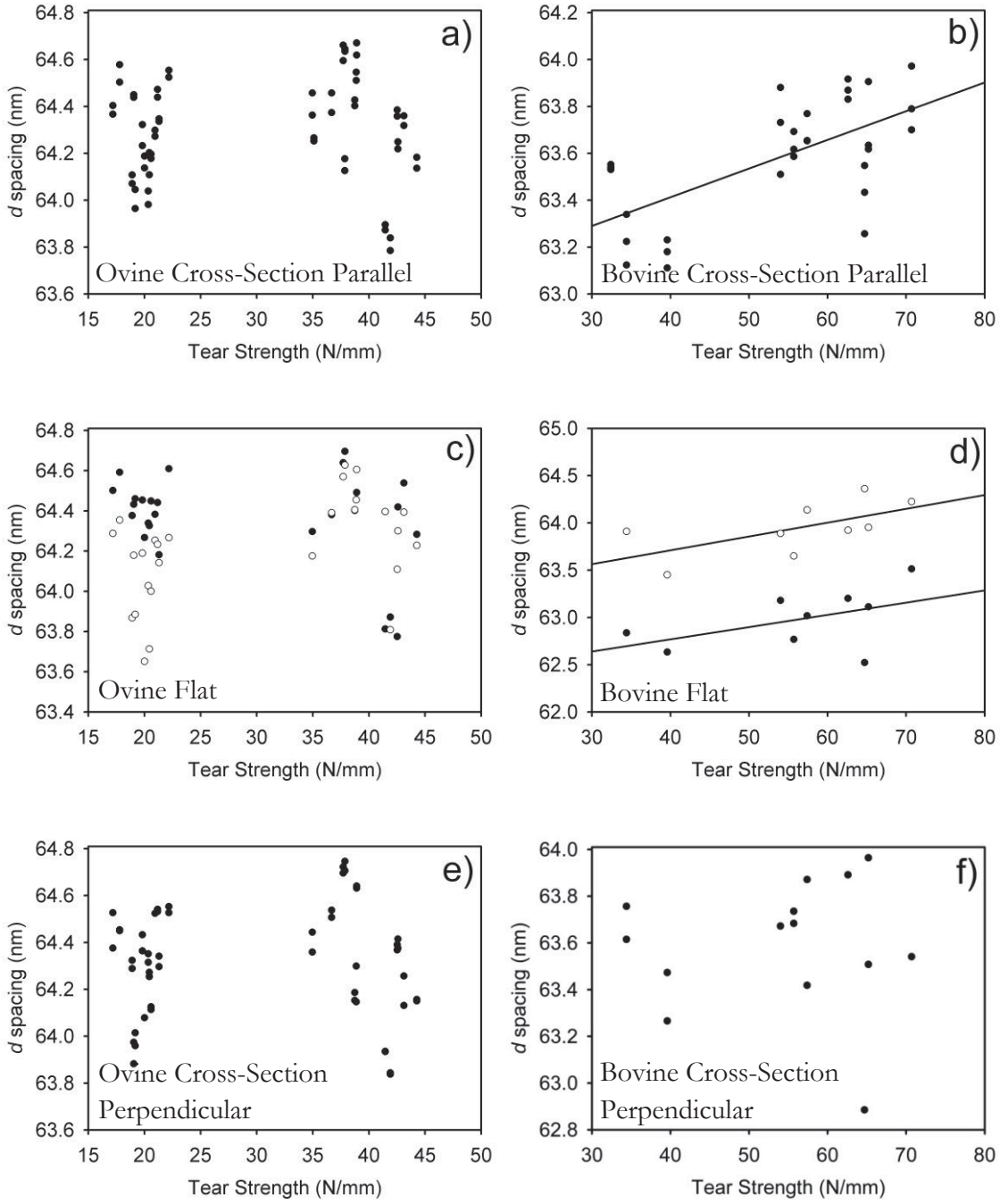

Figure 4.8: *d* spacing versus tear strength for a) ovine cross-sections cut parallel to backbone; b) bovine cross-sections cut parallel to backbone; c) flat ovine samples, grain- closed circle and corium - open circle, ; d) flat bovine samples, grain - closed circle and corium - open circle, ; e) ovine cross-sections cut perpendicular to backbone; f) bovine cross-sections cut perpendicular to backbone (Basil-Jones *et al.* 2011).

Profiles of *d* spacing across the thickness of cross-sectional samples were produced. The profiles of the leather samples were found to be different but the difference between weak ovine, strong ovine and bovine was fairly consistent. An example of profiles of weak ovine,

strong ovine and bovine is shown in Figure 4.9. As can be seen, the weak ovine sample has the least variation in *d* spacing across the sample, while the strong bovine sample had a significant dip in the middle of the sample. It is possible that this dip may explain the variation in average *d* spacing between ovine and bovine samples. This is because the *d* spacing value at the grain surface was similar for ovine and bovine samples. Therefore the larger dip found in bovine samples, in both extent and length, could lower the average value across the thickness for these samples.

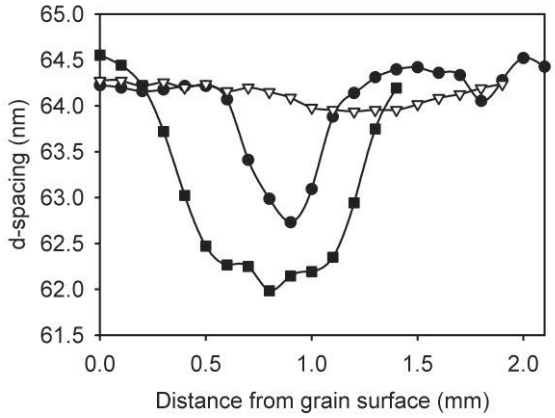

Figure 4.9: Variation in *d* spacing through representative samples of weak ovine - open triangle, strong ovine - closed circle, and bovine - closed square, leathers (Basil-Jones *et al.* 2011).

4.3 Discussion

4.3.1 Amount of Crystalline Collagen

The amount of crystalline collagen was found to be higher in the corium than in the grain region. Previous studies have shown that the collagen structure of the corium and the grain are significantly different (Vera *et al.* 1993; Liu and McClintick 1999). The grain region of skin contains hair filaments and blood vessels, and these are removed during leather processing resulting in gaps in the structure (Kroschwitz 1989). The structure of collagen fibres is also different, with fibres in the corium being thicker than those in the grain. These differences are visualised in Figure 4.10, where large gaps in the grain layer are clearly visible.

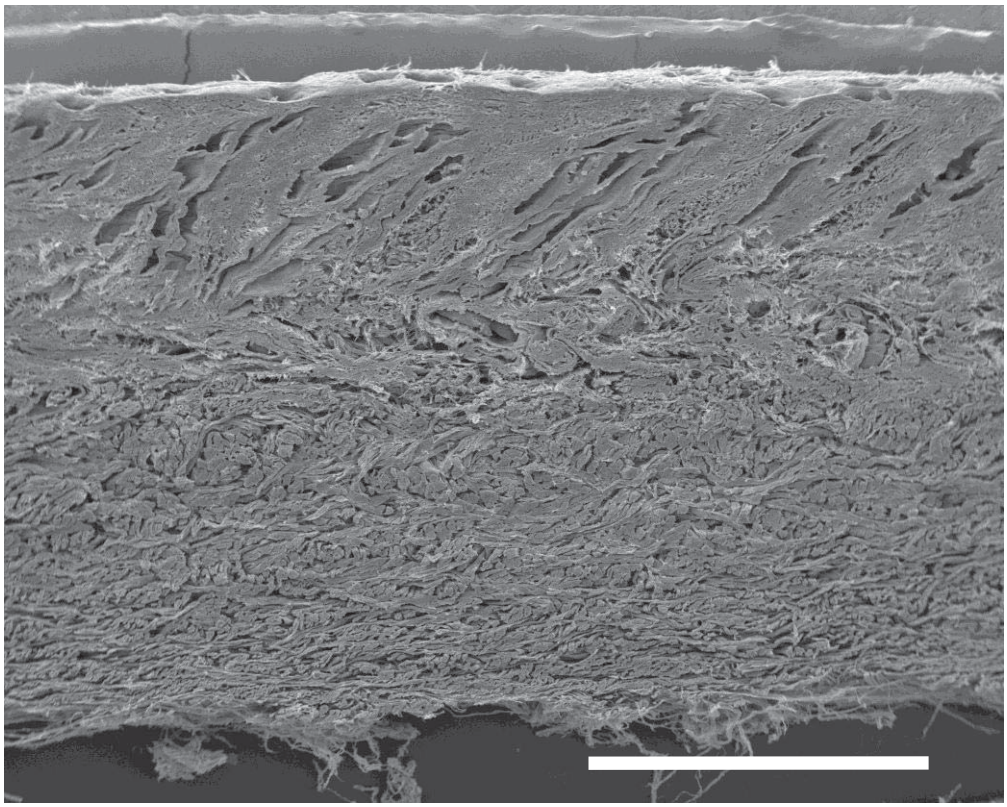

Figure 4.10: SEM image of a cross-section of strong ovine leather. Scale bar 1 mm.

There was found to be no correlation between the total average amount of crystalline collagen and tear strength. This finding is further supported by there being no significant difference in the average amount of crystalline collagen between ovine and bovine samples. There must be a lower limit to this lack of correlation as a material that did not contain collagen would have no strength. However, there was found to be a relationship between the amount of collagen in the corium and the tear strength of samples studied.

Literature indicates that the physical properties of leather samples are dictated by the corium structure (Russell 1988; Attenburrow 1993) and that collagen is a major structural protein responsible for strength in tissues. Therefore, greater concentrations of collagen should result in a higher strength sample, especially in the corium. However, the results of this experiment indicate that this is not that case.

4.3.2 Orientation of Collagen Fibrils

The analysis of the orientation data shows that stronger ovine leather has a higher OI in samples cut on the cross-section than weak ovine leather. Although there is no obvious

trend in the bovine data (thought to be due to the small number of samples) bovine samples were found to have a significantly higher OI than strong ovine cross-sections cut parallel to the backbone. These results show that fibril orientation is related to the tear strength of leather. Stronger leather has more collagen microfibrils that are parallel to the leather surface and fewer crossing over between the layers of the leather. Figure 4.11 provides a visualisation of what samples with a high and low OI measured in the cross-sectional direction would look like.

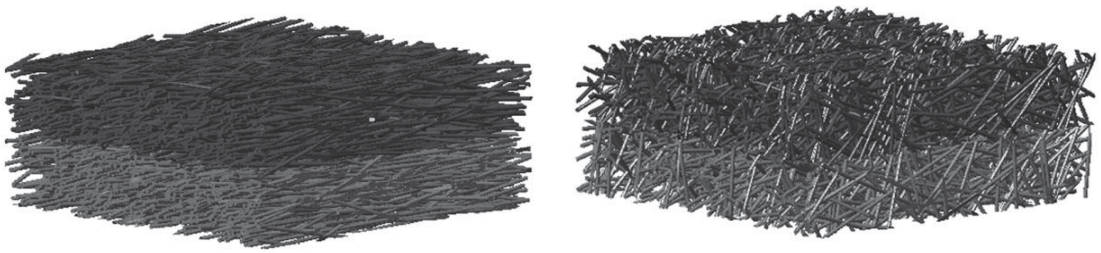

Figure 4.11: Sketch of fibre orientation in a) leather highly aligned in two directions and b) leather with no proffered alignment. The orientation change is exaggerated to better illustrate the difference (Basil-Jones *et al.* 2011).

These results also show that the relationship found for ovine leather, that tear strength is related to OI, extends to bovine leather. This finding indicates that this relationship could extend to other species. It is proposed that there is an upper limit to this relationship, as if all fibrils were aligned in one direction there would be no connection between the layers. It is possible that the OI calculated could be overemphasised due to variations in the amount of collagen present.

From the SEM results it was found that there was no visible crimp in either strong or weak ovine samples, showing that the OI measured was a measurement of the fibre alignment and was not affected by crimp. The presence of crimp may, however, contribute to the greater strength observed for bovine leather as it could allow greater levels of stretching of leather samples before damage to the collagen structure occurs.

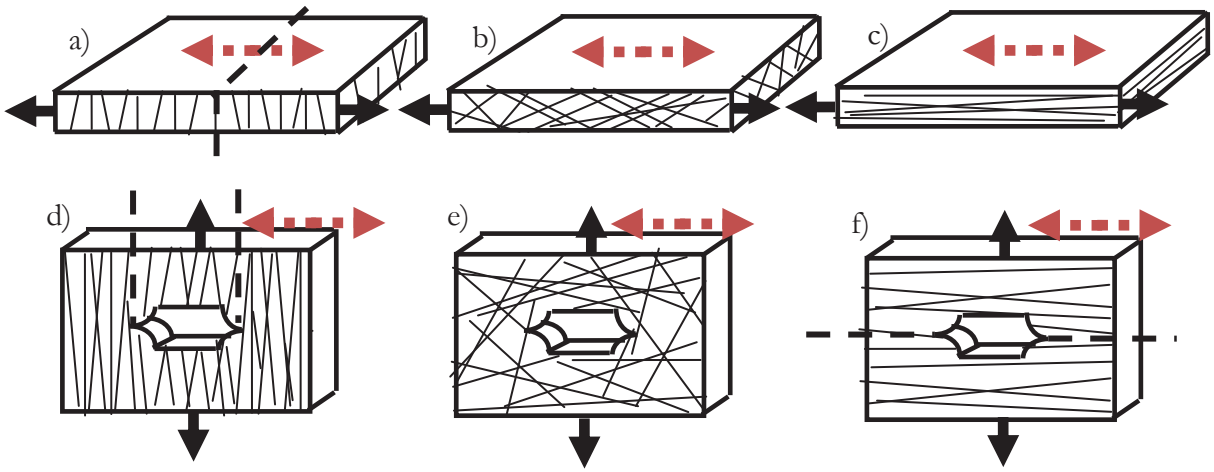

Figure 4.12: Diagram illustrating the relationship between collagen fibre alignment and OI in leather. a) Cross-section with high negative OI, b) cross-section with low OI, c) cross-section with high OI, d) flat sample with high negative OI, e) flat sample with low OI, and f) flat sample with high OI. Black arrows indicate the direction of applied stress in tear strength measurements. Dotted lines represent probable lines of failure. Red arrows indicate the direction of the backbone.

The illustrations in Figure 4.12 provide a visualisation of the alignment of fibres in samples with high and low OI measurements. The relationship between orientation index and tear strength is thought to be due to the mechanism of failure in tear tests. Failure follows the path of least resistance, with tearing occurring either by separating fibres, attached by a degree of entanglement, or by causing the failure of individual fibres. When fibrils are aligned with the direction of tear (low cross-sectional OI), tearing would occur by the process of fibre separation. But if fibrils were aligned perpendicular to the direction of tearing (high cross-sectional OI) failure must occur by tearing individual fibres, a process that requires significantly more force. In this way a greater force would be required to tear samples with a high OI in the cross-sectional direction. It is also possible that a high OI influences tear strength by providing a greater opportunity for fibre recruitment.

4.3.3 *d* Spacing

d spacing does not appear to be correlated with tear strength in ovine leather cross-sections. However, the *d* spacing of flat corium samples was found to be significantly lower than that of the grain in weak samples. The structure of the collagen fibres in the corium

and grain are distinctly different and it is reasonable to expect that a variation in structure may result in a variation in *d* spacing

The relationship between tear strength and *d* spacing in bovine samples may be due to the variations in age in the samples. While the ovine samples were all produced from 5-month old skins, the bovine samples were produced from hides of cows aged between 2- and 3-years. It has been shown that the *d* spacing of fibrillar collagen changes with tissue age (James *et al.* 1991) and that the strength of skin samples is also affected by age (Nimni *et al.* 1966). Therefore, the relationship observed between tear strength and *d* spacing of bovine samples may be due to both of these parameters varying with the age of the skin at slaughter.

This difference in animal age between ovine and bovine samples could be a reason for the variation in the *d* spacing observed between ovine and bovine samples. These are, however, average values so it is also possible the difference may be due to the large dip in *d* spacing that occurs at the grain-corium junction of bovine samples (Figure 4.9). This decrease is significant and would decrease the average *d* spacing value for bovine samples.

Collagen *d* spacing is determined by both the length of collagen molecules and the distance between two end-aligned molecules. The value is also dependant on the angle at which the collagen molecules align with the collagen microfibril axis. Therefore it is believed that variation in *d* spacing could be due to three main factors; changes in the length of the collagen molecules that make up the microfibril (due to different collagen type or due to differences in the collagen molecule because of source species), a change in the distance between end-aligned molecules, or a change in the extent of coiling of the collagen molecules in the collagen microfibril. It is unlikely that crimp would affect *d* spacing as the repeat distance of the crimp observed in bovine samples was significantly larger than the *d* spacing period.

The leather making process appears to decrease the *d* spacing values of skins. The average *d* spacing value for ovine leather samples was found to be 64.3 nm in contrast to values reported in literature which indicates that the *d* spacing for lamb skin is approximately 65.2 nm (Fratzl 2008). This value is fairly consistent with those recorded for salted skins in our experiments where the average *d* spacing was found to be 65.0 nm.

4.4 Conclusions

The relationships between the fibrillar collagen structure of ovine leather and the physical properties of the material were explored using SAXS. Most significantly, the orientation index of the fibrils correlates strongly with the normalised tear strength in cross-sectional samples both within ovine leather and when bovine leather is included. This means that stronger leather has collagen fibrils aligned mostly parallel to the plane of the leather surface (high orientation index) while weaker leather has more collagen fibrils out of this plane (low orientation index).

The other parameters measured, the amount of collagen and the collagen *d* spacing, were found to be less related to the strength of the sample. There was however a relationship between the tear strength and both the *d* spacing and amount of collagen in the corium. This indicates that the collagen structure of the corium plays a role in the strength of ovine leather.

CHAPTER 5 VARIATION IN COLLAGEN STRUCTURE FROM DIFFERENT POSITIONS ON THE ANIMAL FOR OVINE LEATHER

5.1 Introduction

Leather is a natural product and as such is subject to a certain amount of variation, both across skins and between skins. In the previous chapter variations in the organisation of fibrillar collagen between skins was investigated. There were significant variations between the fibrillar collagen structure of skins and some of that variation could be related to tear strength. In this chapter variations in the fibrillar collagen structure across ovine skins will be investigated.

There are many reasons why studying the consistency of the collagen structure across skins is of interest. To determine if a skin meets the specifications for use in a particular application, tests of the skin need to be undertaken. These tests are often destructive and therefore small samples are used. By determining the variation in properties across the skin, the importance of sampling position can be better understood, as some applications require large leather pieces which are consistent across their entirety.

There are many tests used to determine the strength of leather samples, including tensile and tear tests. Tongue-tear tests involve a square sample that is cut from the middle of one side through to the centre of the sample. This produces two 'tongues' which are pulled in opposite directions, causing failure to occur along a single tear. Stitch-tear testing is used to determine the susceptibility of a material to tearing at a stitched seam. It involves cutting small holes, usually one or two, in one side of a sample and threading a metal wire through them. This wire and the side of the material opposite the holes are then clamped and pulled in opposite directions. Tearing does not necessarily propagate from the site of the holes in stitch tear testing.

Variation of physical properties of leather across cattle hides (Mann *et al.* 1951; Kanagy *et al.* 1952; Kanagy *et al.* 1952; Randall *et al.* 1952; Maeser 1960; Menkart *et al.* 1962), as well as kangaroo (Stephens and Peters 1989), mink and fox skins (Mantysalo *et al.* 1991) have

previously been investigated. These studies found significant variation in tensile strength, tear strength and elongation according to sample location and direction of measurement. Tongue-tear and stitch-tear strengths of bovine hides were found to vary with position, with strengths being lower in the butt and backbone areas and higher in the belly and shoulder regions (Kanagy *et al.* 1952; Kanagy *et al.* 1952; Randall *et al.* 1952). Tensile strength was found to be greatest in the belly region (Kanagy *et al.* 1952) and tensile strength measurements taken parallel to the backbone were found to be approximately 20% higher than those taken in the perpendicular direction (Randall *et al.* 1952).

Previous studies have investigated the variation in collagen fibre orientation across bovine leather hides (Osaki 1999), however, this study investigated the orientation only in the direction parallel to the surface, which has not been found to relate to strength (Basil-Jones *et al.* 2011). The aim of this chapter is to investigate if there is variation in the fibrillar collagen structure across ovine leather skins and how this relates to tear strength.

To investigate this variation four positions across the skin were selected, the belly, butt, neck and OSP positions. An illustration of the location of these positions on the skin is provided in chapter 3. Skins were selected based on their tear strength at the OSP so that a range of strengths were represented.

Samples of cross-sections from 29 ovine skins were cut from 4 different positions; the belly, butt, OSP and neck. The belly and neck cross-sections were cut parallel to the backbone while the butt cross-sections were cut perpendicular to the backbone. OSP samples were cut in both directions. In addition samples in all directions; flat and cross-sections, were cut from each position on four skins. Samples were analysed using the methods and sample directions outlined in chapter 3.

5.2 Results

5.2.1 Thickness

The thickness of samples from all positions sampled was measured, with the results shown in Figure 5.1. The neck position was found to be thickest with an average thickness of 1.85 (with a standard deviation of 0.42) mm. The belly was the thinnest position with a thickness of 1.08 (0.20) mm. The average thickness of the OSP was found to be 1.29 (0.22) mm for samples cut perpendicular to the backbone and 1.36 (0.24) mm for samples cut

parallel. The butt was found to have an average thickness of 1.57(0.39) mm, making it the second thickest position.

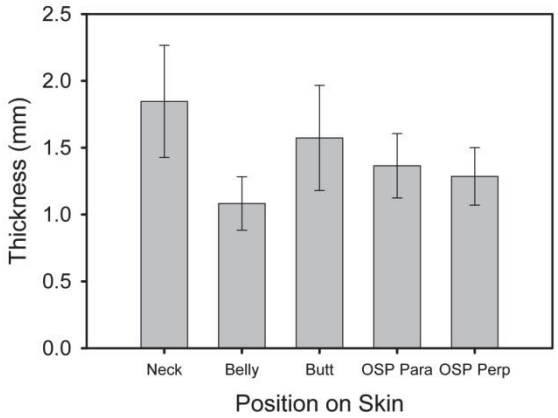

Figure 5.1: Thickness of leather taken from different positions on the ovine skin.

Statistical analysis found significant differences between the thicknesses of some of the different positions on the skin. The results of this statistical analysis are shown in Table 5.1. The neck was found to be significantly thicker than all other positions measured except the butt where the difference was not significant. The belly was found to be significantly thinner than all other positions measured except the OSP measured perpendicular to the backbone where the difference was not significant. The butt was also found to be significantly thicker than the OSP measured perpendicular to the backbone.

Table 5.1: The statistical significance of differences between the thicknesses of leather samples from different positions on the skin as determined by Tukey test.

Position	Neck Perpendicular	Belly Perpendicular	Butt Perpendicular	OSP Perpendicular	OSP Parallel
Neck Perpendicular		Significant	Not Significant	Significant	Significant
Belly Perpendicular			Significant	Not Significant	Significant
Butt Perpendicular				Significant	Not Significant
OSP Perpendicular					Not Significant
OSP Parallel					

5.2.2 Tear Strength

The tear strength of all positions sampled was measured. The average absolute tear strength was found to be highest for the neck with an average value of 50.7 (11.7) N. The OSP measured perpendicular to the backbone was found to have the lowest average tear strength with an average value of 35.5 (8.9) N. The belly position had a similar average absolute tear strength with a value of 35.6 (10.5) N. The butt and OSP measured parallel to the backbone had similar average tear strengths with average values of 43.6 (11.8) N and 42.1 (10.5) N respectively (Figure 5.2 a)).

In contrast, the average normalised tear strength was highest in the belly with an average value of 33.6 (9.7) N/mm. The second highest average normalised tear strength value was 31.3 (7.8) N/mm for the OSP measured parallel to the backbone. The remaining three positions had similar normalised tear strength with an average value of 28.1 (6.4) N/mm for the neck, 28.5 (7.2) N/mm for the butt and 28.2 (7.7) N/mm for the OSP measured perpendicular to the backbone (Figure 5.2 b)).

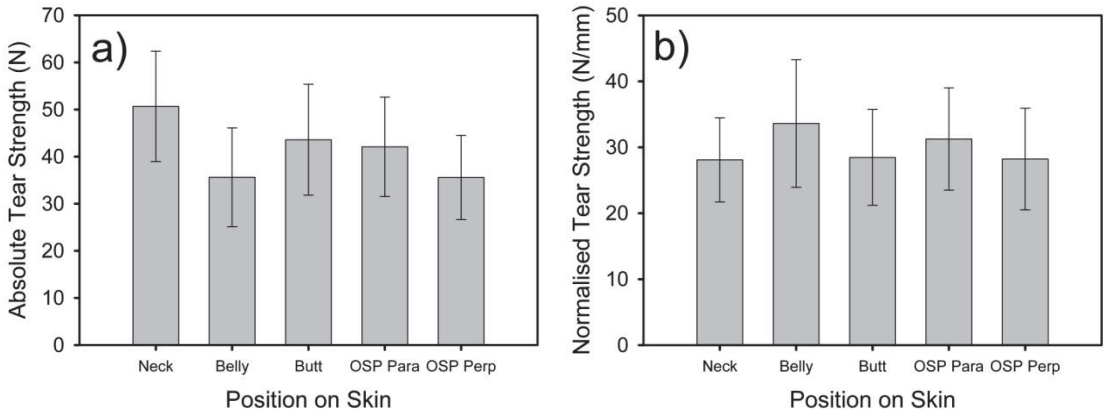

Figure 5.2: a) absolute tear strength and b) normalised tear strength of leather taken from different positions on the ovine skin.

Statistical analysis found significant differences between the absolute tear strengths of most of the positions measured. Results of this analysis are shown in Table 5.2. The only positions that did not have significant differences between their absolute tear strengths were: the belly and OSP cut perpendicular to the backbone; the neck and OSP cut parallel to the backbone; and the butt and OSP cut parallel to the backbone.

A Friedman test found that the normalised tear strength of skin from belly position samples was significantly higher than that of skin from all other positions except the OSP measured parallel to the backbone where the difference was not significant. There was also a significant difference between the normalised tear strength of OSP samples measured in the different directions, with normalised tear strength being greater when measured parallel to the backbone.

Table 5.2: The statistical significance of differences between the tear strength's of leather samples from different positions of the skin as determined by Tukey tests. Bottom left side absolute tear strength and top right side normalised tear strength.

Position	Neck Perpendicular	Belly Perpendicular	Butt Perpendicular	OSP Perpendicular	OSP Parallel
Neck Perpendicular		Significant	Not Significant	Not Significant	Not Significant
Belly Perpendicular	Significant		Significant	Significant	Not Significant
Butt Perpendicular	Significant	Significant		Not Significant	Not Significant
OSP Perpendicular	Significant	Not Significant	Significant		Significant
OSP Parallel	Not Significant	Significant	Not Significant	Significant	

Plots of the normalised tear strength of each position versus the average normalised tear strength of a skin were produced and are shown in Figure 5.3. Skins with a high average tear strength value were found to be consistently strong in all positions measured. This means that skins with a high average normalised tear strength are consistently strong in all positions sampled, as opposed to strong at some positions and weak at others. Trend lines were fitted to these plots with results provided in Table 5.3. These results indicated that the relationship was significant for all positions studied.

Table 5.3: Parameters for fitted regression lines of normalised tear strength of each position versus the average normalised tear strength of a skin data for each position sampled.

	Slope	r^2	P-value (slope)
Neck	0.74	0.62	3.74×10^{-7}
Belly	1.31	0.83	4.7×10^{-12}
OSP	1.04	0.84	2.7×10^{-12}
Butt	0.91	0.72	7.11×10^{-9}

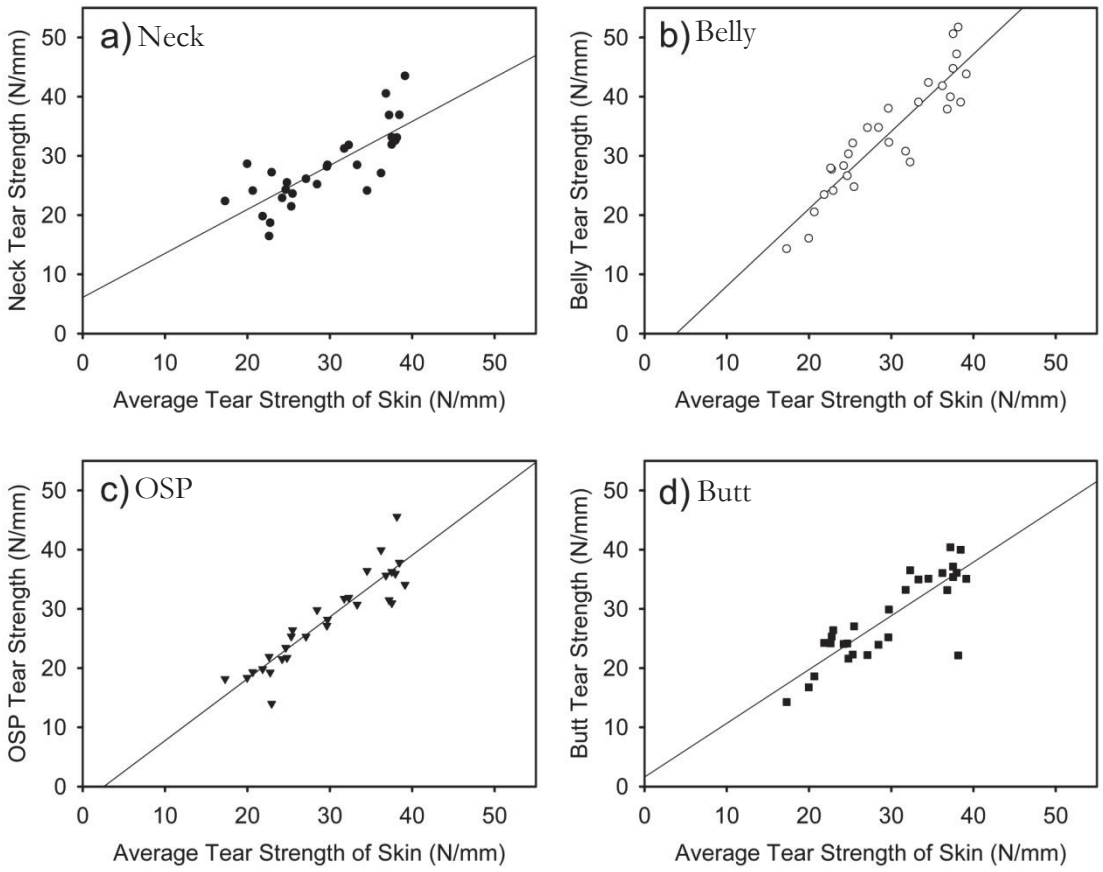

Figure 5.3: Normalised tear strength of position versus the average normalised tear strength of the entire skin for; a) neck, b) belly, c) OSP and d) butt.

5.2.3 Directionality of Normalised Tear Strength

Tear strength measurements were recorded for all four positions in both the parallel and perpendicular to the backbone direction for four skins with a range of tear strengths. The results are shown Figure 5.4. There was found to be a relationship between tear strengths measured parallel to the backbone and those measured perpendicular to the backbone for all positions measured, with tear strength measured in the parallel direction increasing linearly with that measured in the perpendicular direction.

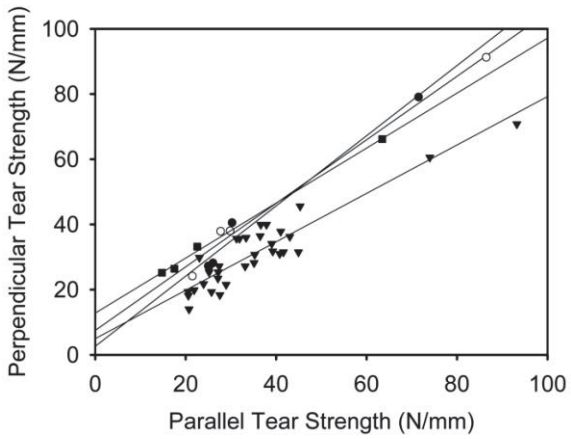

Figure 5.4: Perpendicular versus parallel tear strengths for neck - closed circle; belly - open circle; OSP - closed triangle; and butt - closed square, positions.

Regression analysis was performed on data from each position with results provided in Table 5.4. These results indicated that the relationship was significant for all positions studied.

Table 5.4: Parameters for fitted regression lines of perpendicular versus parallel tear strength data for each position sampled.

	Slope	r^2	P-value (slope)
Neck	1.08	0.97	0.011
Belly	0.97	0.98	6.1×10^{-3}
Butt	0.84	1.00	1.4×10^{-3}
OSP	0.74	0.84	1.1×10^{-14}

The tear strength at all the positions measured, except the OSP, was not significantly affected by whether the measurement was taken parallel or perpendicular to the backbone. The OSP was, however, affected by the direction of the measurement, with the tear strength values measured being lower when measured in the perpendicular direction.

5.2.4 Visual Variation in Structure across Cross-Sections

In order to allow greater understanding of how profiles of measured parameters across sample thicknesses relate to the SEM images of skin cross-sections, a SEM image of an

ovine leather cross-section is shown in Figure 5.4. As can be seen from this image, the grain-corium junction is located near the middle of the sample.

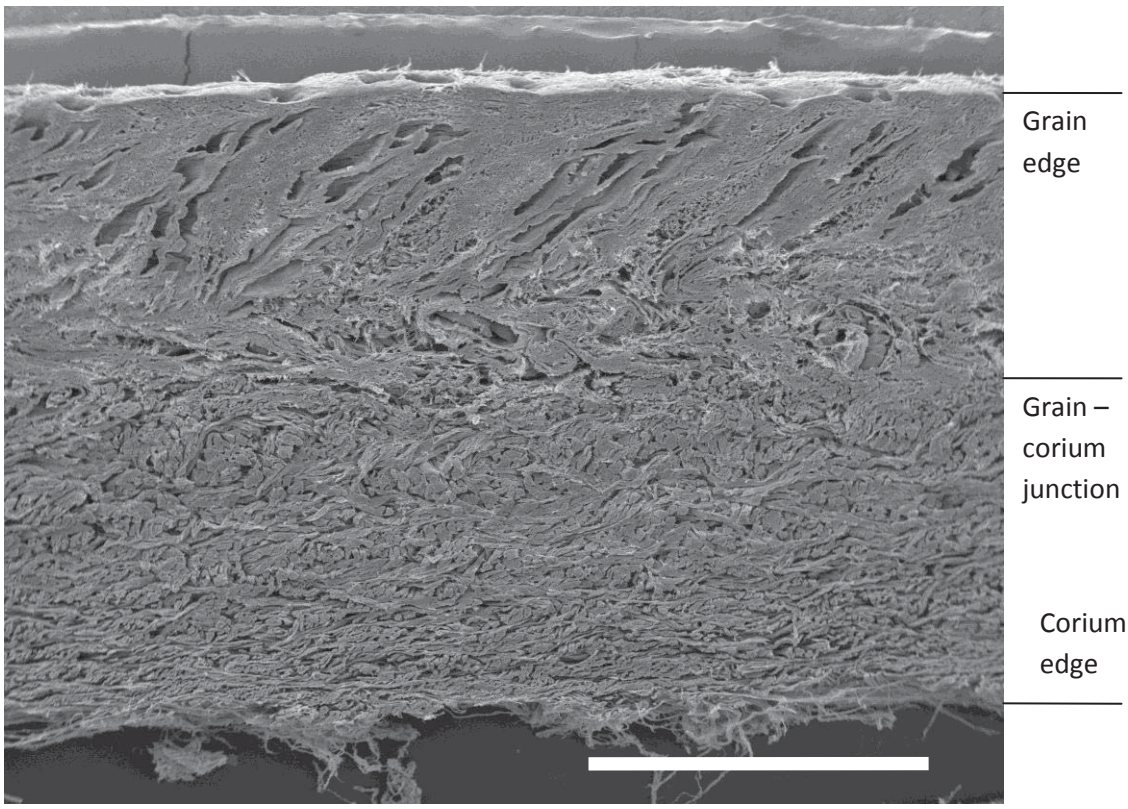

Figure 5.5: SEM image of a cross-section of ovine leather showing the approximate location of the grain-corium junction. Scale bar 1 mm.

5.2.5 Amount of Fibrillar Collagen

The amount of crystalline collagen was found to vary throughout the thickness of all samples of ovine leather as shown in Figure 5.6. All sampled positions have the same general profile, with higher concentrations of fibrillar collagen in the corium region than in the grain. It is known that corium is stronger than the grain and that fibrous collagen is the primary contributor to strength, therefore this finding supports this understanding.

The average profile does, however, differ between the positions. The profiles of the OSP cut parallel to the backbone and belly cross-sections are quite similar; the slight difference can be explained by the OSP having a greater thickness. This is understandable as the belly and OSP are quite close to each other. The cross-sections from the butt also have a similar profile to that seen for the belly and the OSP cut parallel to the backbone.

The OSP profile appears to vary significantly with sample direction, when cut perpendicular to the backbone lower concentrations of fibrillar collagen across the entire

profile are observed. The neck samples, which appear to have the greatest concentration of collagen in the corium and the thickest grain layer of all positions sampled, show the largest differences in profile compared to other positions.

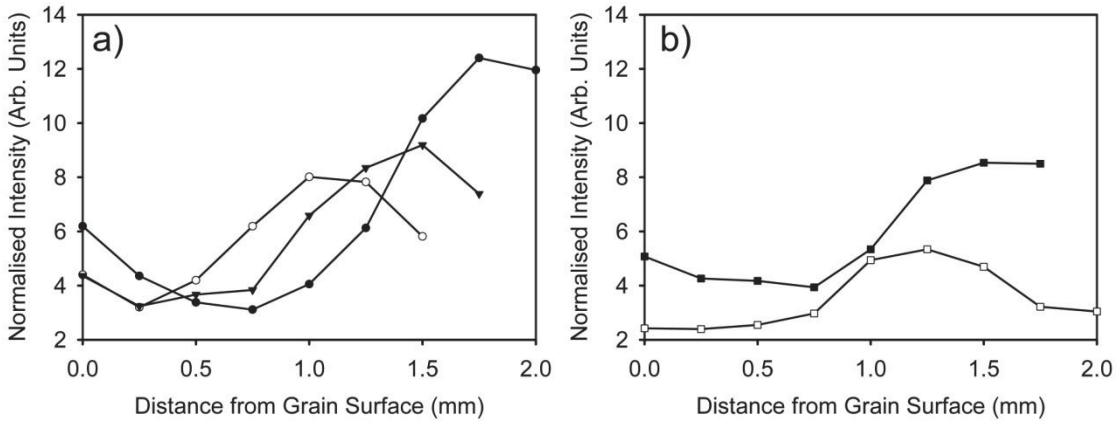

Figure 5.6: Profiles of amount of crystalline collagen across sample thicknesses a) cut parallel to the backbone from the: neck - closed circle; belly - open circle; OSP - triangle, and b) cut perpendicular to the backbone from the: butt - closed square; OSP- open square.

Figure 5.7 shows the average amount of collagen versus tear strength for samples from different positions for four skins. Statistical analysis found that there was no significant difference between the average amounts of fibrillar collagen in samples taken from different sample positions on the skin, despite obvious differences in cross-sectional profiles. Although the data appears to have a downwards trend, there was found to be no significant relationship between the amount of crystalline collagen and tear strength. A regression line fitted to all the data gave a slope of -0.035 arb. units.mm/N, r^2 value of 0.13 and P-value of 0.09. This finding is consistent with that found in chapter 4 for samples from the OSP position. Similarly, regression analysis of samples of skin from different positions found there was no significant relationship between the amount of crystalline collagen and the tear strength in any of the positions studied.

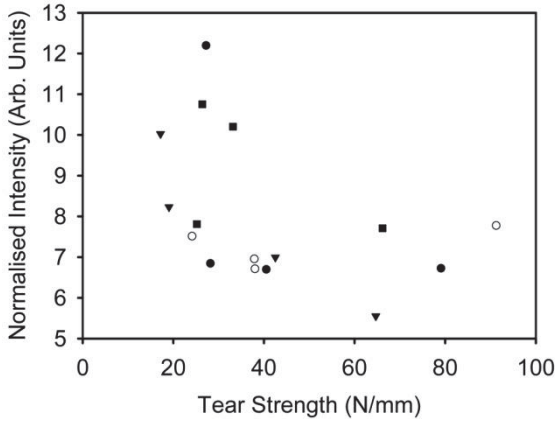

Figure 5.7: Average amount of crystalline collagen versus tear strength for the: neck - closed circle; belly - open circle; OSP - closed triangle; and butt - open triangle.

5.2.6 *d* spacing

Ovine leather cross-sections display a characteristic *d* spacing profile with a dip in *d* spacing near the middle of the cross-section. The graphs in Figure 5.8 show that skin samples from the positions sampled all display this profile. As can be seen, the depth of the dip in *d* spacing varies between sample positions, with samples having a higher average thickness displaying a larger dip. The dip is most significant in the neck position, which is the thickest of all positions sampled. In contrast the dip is only very slight in the belly and butt positions. The profiles for the OSP cut parallel and perpendicular to the backbone are quite similar, indicating that *d* spacing profile is independent of the direction of measurement.

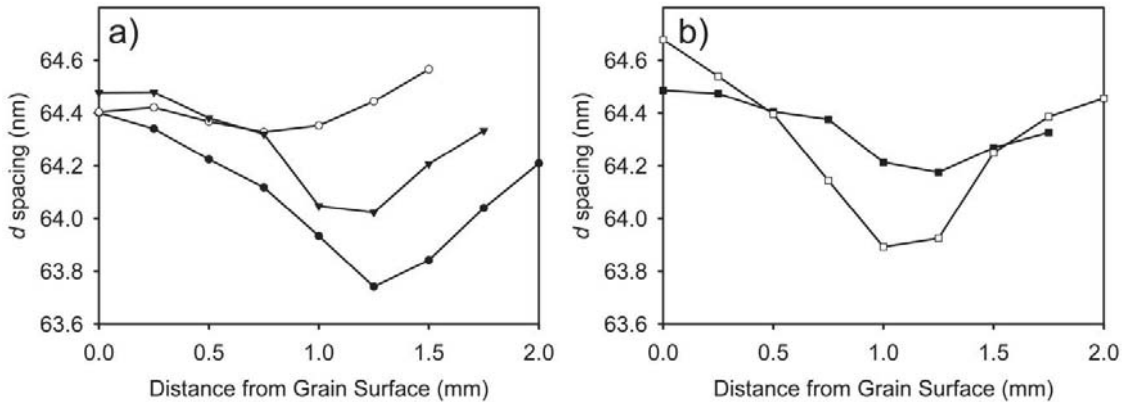

Figure 5.8: Profiles of *d* spacing across sample thicknesses a) cut parallel to the backbone from the: neck - closed circle; belly - open circle; OSP - triangle; and b) cut perpendicular to the backbone from the: butt - closed square; OSP - open square.

Tear strength and *d* spacing were shown not to be related in any of the positions studied. Figure 5.9 shows the average *d* spacing for cross-sections of ovine leather from the different positions. It can be seen from this figure that there is no correlation between tear strength and *d* spacing. This is consistent with the findings in chapter 4. There are, however, differences between the average *d* spacing of the different positions.

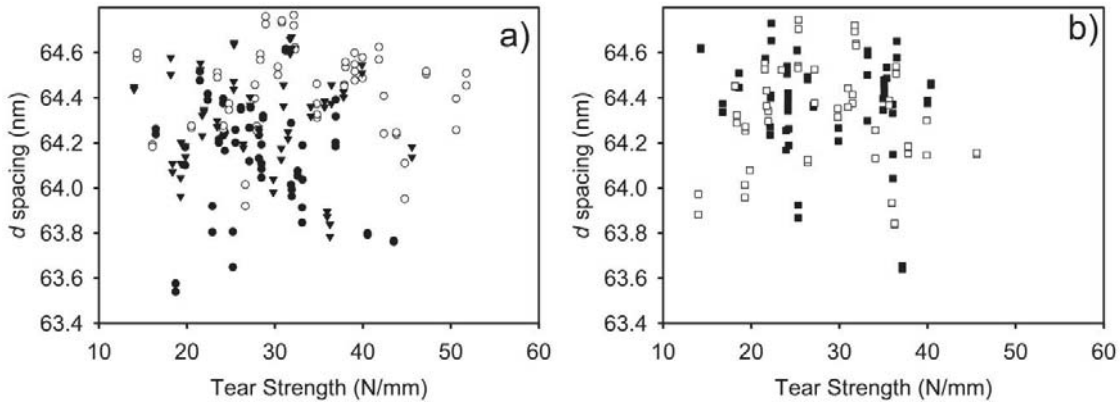

Figure 5.9: Average *d* spacing versus tear strength for samples a) cut parallel to the backbone from the: neck - closed circle; belly - open circle; OSP - triangle; and b) cut perpendicular to the backbone from the: belly - closed square; OSP - open square.

Butt samples were cut perpendicular to the backbone while the other samples were cut parallel to the backbone. The analysis of the OSP position revealed that there is no significant difference ($|t\text{-stat}| = 0.94$, t-crit = 2.01, P = 0.35) between the *d* spacing of cross-sections cut parallel and perpendicular to the backbone and it was assumed that this trend is consistent across the entire skin. Analysis of the samples from different positions and analysed in both directions support this assumption ($|t\text{-stat}| = 1.86$, t-crit = 2.05, P = 0.07), although the sample size was quite small. It was therefore concluded that the results from samples cut perpendicular to the backbone could be compared with those cut in the parallel direction.

A Tukey test found that the neck had a significant lower average *d* spacing than that of all other positions measured. The only other significant difference in *d* spacing was between the belly and OSP cut perpendicular to the backbone (Table 5.5), with the average *d* spacing being higher in the belly. These differences could be explained by the variation in the *d* spacing profile with position. The average *d* spacing value was lowest (64.20 (0.25) nm) for the neck position which had both the largest variation in *d* spacing across its profile and the greatest thickness. The average *d* spacing value was highest for the belly

and butt positions (64.43 (0.20) nm and 64.38 (0.23) nm respectively) and showed the lowest variation in *d* spacing across its profile. The average value for the OSP was 64.31(0.22) nm in the parallel direction and 64.23 (0.62) nm in the perpendicular direction.

Table 5.5: The statistical significance of differences between the *d* spacing's of leather samples from different positions on the skin as determined by Tukey test.

Position	Neck Parallel	Belly Parallel	Butt Perpendicular	OSP Parallel	OSP Perpendicular
Neck Parallel		Significant	Significant	Significant	Significant
Belly Parallel			Not Significant	Not Significant	Significant
Butt Perpendicular				Not Significant	Not Significant
OSP Parallel					Not Significant
OSP Perpendicular					

To investigate whether the variations in average *d* spacing with position was due to the extent of the variation in *d* spacing across cross-sectional thicknesses the variation in *d* spacing across the profile was calculated. The variation in *d* spacing across the profile of each sample was calculated by subtracting the minimum *d* spacing value recorded from the maximum *d* spacing value recorded and was used to approximate the extent of dip in the *d* spacing profile. The variation in *d* spacing was highest for neck samples with an average value of 1.12 nm. The variation in *d* spacing was lowest for the belly and butt samples with average values of 0.49 nm and 0.66 nm respectively. The average value for the OSP was 0.74 nm in the cross-sectional direction parallel to the backbone and 1.04 nm in the cross-sectional direction perpendicular to the backbone.

The variation in *d* spacing of the neck was found to be significantly higher than that of all other positions except the OSP cut perpendicular to the backbone where the difference was not significant (Table 5.6). There were also other statistically significant differences in the variation in *d* spacing with the value of the belly being lower than that of the OSP cut

in both directions and the value of the butt being lower than that of the OSP cut perpendicular to the backbone.

Table 5.6: The statistical significance of differences between the variation in *d* spacing across profiles of leather samples from different positions on the skin as determined by Tukey test.

Position	Neck Parallel	Belly Parallel	Butt Perpendicular	OSP Parallel	OSP Perpendicular
Neck Parallel		Significant	Significant	Significant	Not Significant
Belly Parallel			Not Significant	Significant	Significant
Butt Perpendicular				Not Significant	Significant
OSP Parallel					Not Significant
OSP Perpendicular					

Results indicate that there was no significant difference between the *d* spacing of samples from the different positions on the skin in any of the cross-sectional or flat directions and statistical analysis confirmed this. The results shown in Figure 5.10 are for four skins, three ovine and one bovine. Bovine samples had higher tear strengths and consistently displayed lower *d* spacing values than the ovine samples. This is consistent with the results of chapter 4.

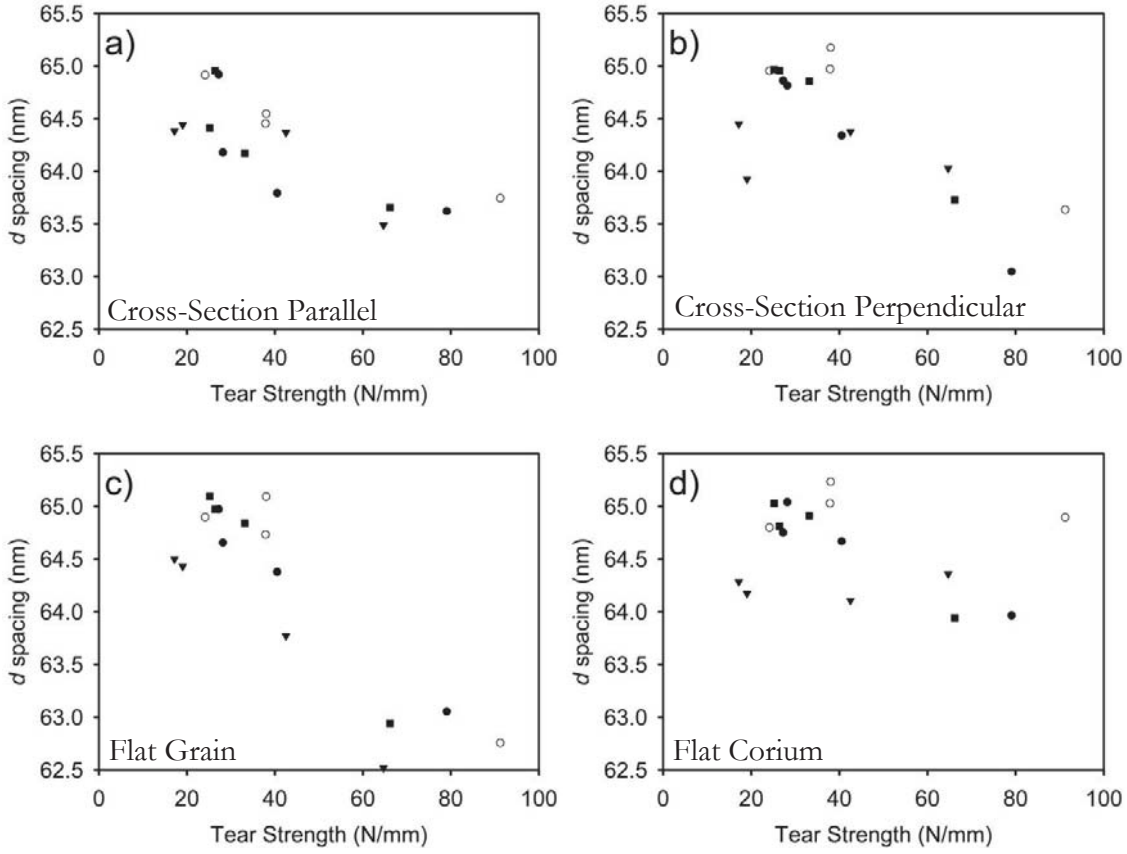

Figure 5.10: Average *d* spacing versus tear strength for: neck - closed circle; belly - open circle; OSP - closed triangle; and butt - open triangle, for: a) cross-sections cut parallel to the backbone, b) cross-sections cut perpendicular to the backbone, c) flat samples of the grain, and d) flat samples of the corium.

5.2.7 Orientation

All samples display a characteristic ovine leather profile with a dip in the OI at the grain-corium junction as shown in Figure 5.11. The orientation profile is consistent for all three positions for samples cut parallel to the backbone. The OSP and belly samples have a slightly higher OI in the corium than the neck samples. The belly samples have a slightly higher OI in the grain than the neck and OSP samples. In contrast, there is a difference between the profiles of the butt and OSP positions cut perpendicular to the backbone.

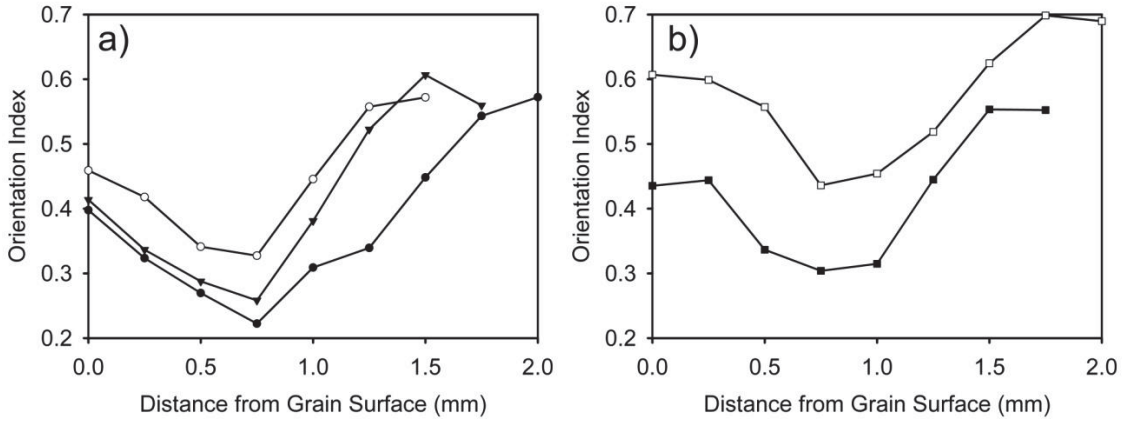

Figure 5.11: Profiles of orientation index across sample thicknesses a) cut parallel to the backbone from the: neck - closed circle; belly - open circle; OSP - triangle; and b) cut perpendicular to the backbone from the: butt - closed square; OSP - open square.

The relationship between orientation index and tear strength, identified in chapter 4, was found to exist in all positions studied. It can be seen from Figure 5.12 that as orientation index in the cross-sectional direction increases, the tear strength of samples also increases. These results further support the finding that tear strength and collagen fibril orientation in cross-sectional samples are related.

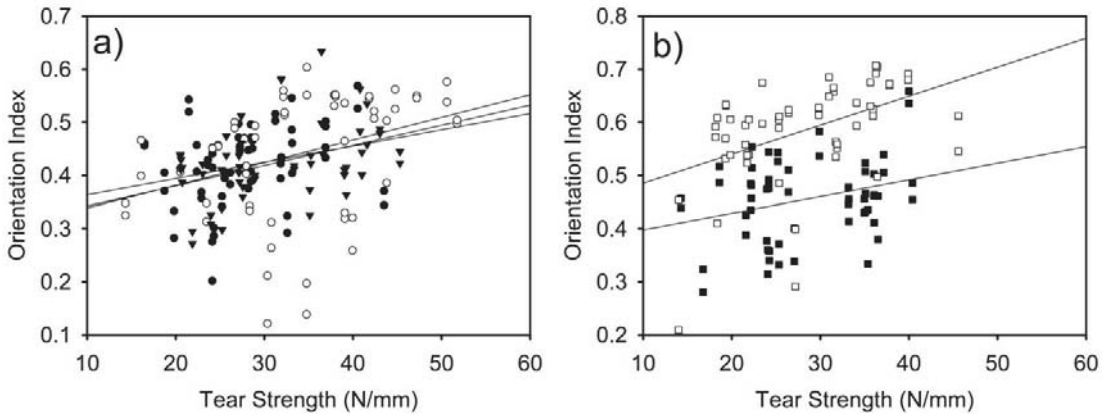

Figure 5.12: Average orientation index versus tear strength, with lines of best fit for each sample set, for cross-sectional ovine leather samples a) cut parallel to the backbone from the: neck - closed circle; belly - open circle; OSP - triangle; and b) cut perpendicular to the backbone from the: butt - closed square; OSP - open square.

Regression lines fitted to the data shows that the relationship between orientation index and tear strength is significant at all positions studied. The slope was fairly consistent, ranging from 3.1 x 10^{-3} to 5.5 x 10^{-3}, the r^2 value ranged from 0.09 to 0.2 and the P-values

ranged from 0.026 to 6.2 x 10^{-4}. A table of these values for each position is shown in Table 5.7. There is no significant difference in the relationship between orientation index and tear strength for samples from the neck, belly and OSP cut parallel to the backbone.

Table 5.7: Parameters for fitted regression lines of orientation index versus tear strength data for each position sampled.

	Slope	Y-intercept	r^2	P-value (slope)
Neck	$3.93x10^{-3}$	0.31	0.10	0.018
Belly	$4.26x10^{-3}$	0.30	0.13	$6.5x10^{-3}$
Butt	$3.13x10^{-3}$	0.37	0.09	0.026
OSP (parallel)	$3.52x10^{-3}$	0.33	0.14	$3.4x10^{-3}$
OSP (perpendicular)	$5.46x10^{-3}$	0.43	0.20	$6.2x10^{-4}$

Statistical analysis found that the average orientation index of OSP samples cut perpendicular to the backbone were lower than that of all other positions studied (Table 5.8). These results further indicate a difference in the relationship between OI and tear strength in OSP samples cut perpendicular to the backbone to that of the other positions studied. There was no significant difference between the OI of the other positions.

Table 5.8: The statistical significance of differences between the orientation indexes of leather samples from different positions on the skin as determined by Dunn's method.

Position	Neck Parallel	Belly Parallel	Butt Perpendicular	OSP Parallel	OSP Perpendicular
Neck Parallel		Not Significant	Not Significant	Not Significant	Significant
Belly Parallel			Not Significant	Not Significant	Significant
Butt Perpendicular				Not Significant	Significant
OSP Parallel					Significant
OSP Perpendicular					

The average orientation index, for both cross-sectional and flat samples, versus tear strength is shown in Figure 5.13. Results indicate there are no significant changes in orientation of collagen fibres between all areas of ovine skin studied. The trend seen in Figure 5.12 and Figure 4.6 of the orientation index increasing with tear strength in cross-sectional samples is not seen in Figure 5.13. This is thought to be due to the small sample size for this data set. It is thought that the other data sets are more reliable as the number of samples studied was significantly greater.

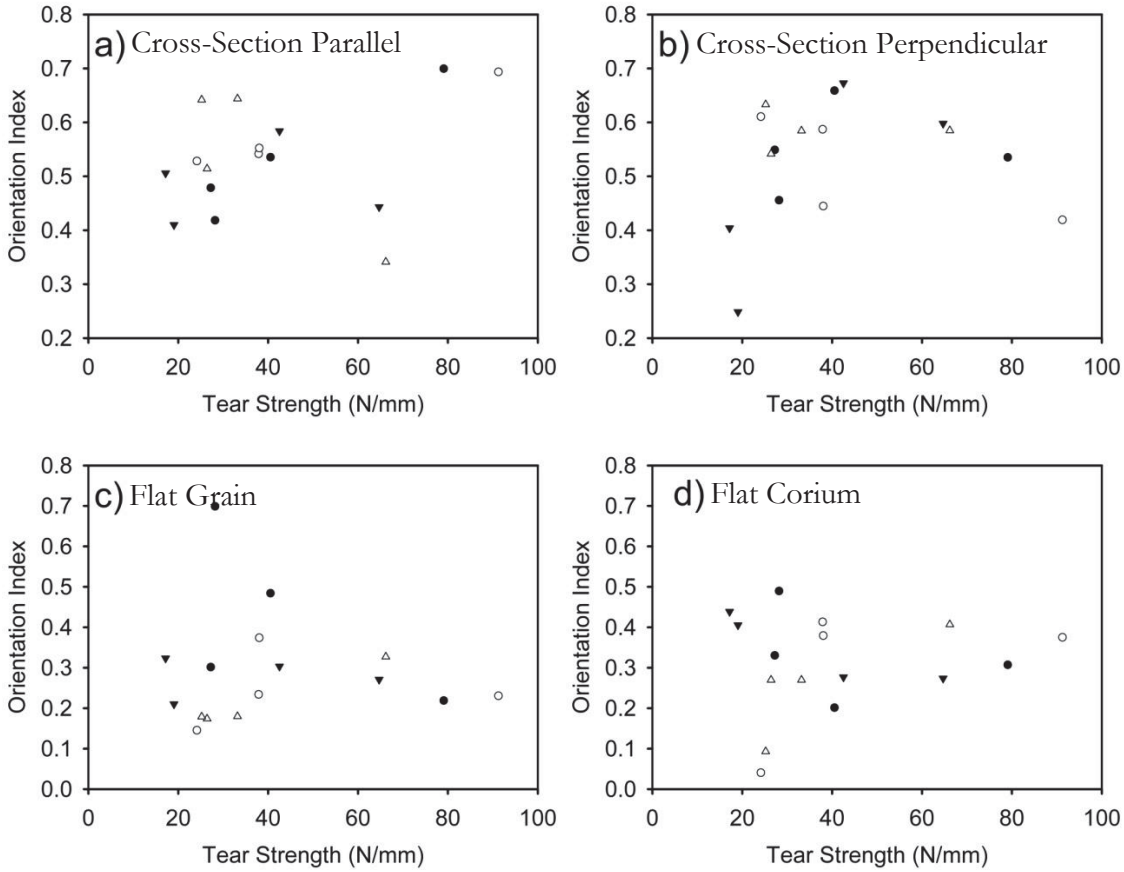

Figure 5.13: Average orientation index versus tear strength for samples from: neck - closed circle; belly - open circle; OSP - closed triangle; and butt - open triangle; for a) cross-sections cut parallel to the backbone, b) cross-sections cut perpendicular to the backbone, c) flat samples of the grain, and d) flat samples of the corium.

5.3 Discussion

5.3.1 Thickness

The thickness of samples was found to vary between different positions across ovine leather skins. Samples of the neck were found to have the greatest thickness and were significantly thicker than most of the other positions sampled. The belly was also found to have a significantly different thickness to most other positions sampled in that the skin appeared to be thinnest in this position. This variation in leather thickness was not unexpected based on anecdotal evidence from the leather industry.

5.3.2 Absolute Tear Strength

For leather produced from ovine skins the absolute tear strength was found to vary significantly with the position of the sample. There was a significant difference between the absolute tear strengths of most of the positions measured. Not surprisingly, absolute tear strength could be related to sample thickness. The absolute tear strength was found to be highest in neck samples which had the greatest thickness, while samples from the belly position, which were thinnest, had nearly the lowest average absolute tear strength.

5.3.3 Normalised Tear Strength

The relationship between the average normalised tear strength of a skin and the normalised tear strength at a selected position was found to be significant for all positions studied. This indicates that skins are strong or weak across an entire skin as opposed to being strong in some positions and weak in others. This also indicates that a sample from any of the positions studied can be used to determine the approximate tear strength of the entire skin, although r^2 values were highest for the OSP and belly indicating that these positions are the most accurate for determining tear strength.

The average normalised tear strength, from the skin samples tested, was similar for the neck, butt and OSP positions. A Friedman test found that the normalised tear strength of leather from belly position was significantly greater to that of all other positions except the OSP measured parallel to the backbone. These results appear to be consistent with those

for bovine leather. Tongue-tear and stitch-tear strengths of bovine hides were found to vary with position, with strengths being lower in the butt and backbone areas and higher in the belly region (Kanagy *et al.* 1952; Kanagy *et al.* 1952; Randall *et al.* 1952).

Although the normalised tear strength of leather from the belly position was quite high, the absolute tear strengths of these samples was actually quite low, similar to those from the OSP and lower than those for leather produced from all other positions sampled. The higher relative tear strength values for the belly are therefore due to the thickness of the leather samples, with the belly samples being the thinnest samples from all the positions studied. The reason that the relative tear strength values for the belly position are so high is possibly due to the stresses that the skin in this area would be suspected to undergo on a regular basis. As an animal eats and digests food its stomach expands and contracts putting stress on the skin in the belly region.

The tear strength of leather produced from all positions, excluding the OSP, appears to be independent of the direction it is measured with tear strengths measured parallel to the backbone being consistent with those measured perpendicular to the backbone. The OSP, however, is affected by the direction of the measurement, with the tear strength being lower for samples cut perpendicular to the backbone. This variation of the OSP tear strength with sample direction is confirmed by there being a significant difference between the normalised tear strength of the OSP measured in the different directions.

Previous investigations of the dependence of tear strength on sampling direction in bovine hides have been inconsistent. Tongue tear strengths have been found to be independent of sample direction (Kanagy *et al.* 1952; Randall *et al.* 1952) or greater when tear propagation occurred in the direction perpendicular to the backbone (Kanagy *et al.* 1952). Kangaroo skins were found to have a greater tear strength when the tear propagated in the perpendicular direction (Stephens and Peters 1989). The results observed are therefore considered comparable with those for other leather types as parallel tear tests result in tear propagation in the perpendicular direction.

The dependence of tear strength on sampling direction at the OSP is not surprising, however it is surprising that this dependence appears to be present at this one position and there is no obvious explanation for this.

5.3.4 Amount of Crystalline Collagen

Profiles of the amount of fibrillar collagen measured in samples cut on the cross-section indicate that the distribution of fibrillar collagen may vary with the position on the hide but there appeared to be no difference in the average amount of fibrillar collagen between positions. This indicates that although there might be some variation in the directional distribution of collagen fibrils the total amount of fibrillar collagen does not vary across the skin. No relationship was found between the amount of fibrillar collagen and tear strength in any of the positions sampled. There must be a lower limit to this lack of correlation as a material that did not contain collagen would have no strength

5.3.5 *d* Spacing

All positions sampled displayed a reduction in *d* spacing values near the centre of the cross-sectional profiles with the size of the dip varying with position. The dip was found to be most prominent in samples taken from the neck and least noticeable in samples taken from the belly. The reason for this is unknown, but given its location it may be indicative of a variation in the collagen structure around the grain-corium junction.

The cross-sectional profiles of samples taken from all positions, except the belly, showed the highest *d* spacing at the grain surface and *d* spacing values in this region were similar for all samples, with a value of approximately 64.5 nm. In fact the *d* spacing throughout the grain layer appears to be similar for all positions sampled, with variations occurring in the grain-corium junction and the corium region itself.

The neck position was found to have a significantly lower average *d* spacing compared to all the other positions measured, perhaps indicating that the collagen structure of the skin in the neck is different to that of other positions. Given the cross-sectional *d* spacing profile of leather from the neck sample, which had the largest dip of all the positions measured, it is not surprising that the average *d* spacing of the position is lower. The significant difference of the variation of *d* spacing between the neck and most other positions measured further supports the supposition that the lower *d* spacing is due to this dip.

There was no apparent relationship between *d* spacing and tear strength in any of the positions sampled. This is consistent with the findings of chapter 4, where *d* spacing was found not to be related to tear strength in ovine leather cross-sections.

5.3.6 Orientation

The relationship between orientation index and tear strength identified in the previous chapter is significant in all the positions studied. In all the leather samples tested, those which were stronger had a higher measured orientation index than weaker ones. The apparent relationship between tear strength and fibrillar collagen orientation reported in chapter 4 is further supported by these findings.

The relationship between orientation index and tear strength was consistent in all positions tested except for the OSP cut perpendicular to the backbone as shown by a similar slope of the regression lines. For the OSP cut perpendicular to the backbone, the intercept was higher. The relationship between orientation index and tear strength has an r^2 value of 0.1-0.2 for all positions measured which strongly indicated that there are other parameters significantly affecting tear strength. It is therefore highly likely that it is a variation in one of these parameters is responsible for the variation in the relationship between tear strength and orientation index at the OSP.

5.3.7 Variation of Tear Strength and Collagen Orientation with Direction of Measurement in the OSP

The inconsistency of the OSP in terms of variation with sample direction in both tear strength and orientation index is highly surprising. Despite the significant difference of the orientation index of the OSP measured perpendicular to the backbone from all other positions measured, the position does not vary consistently in any of the other parameters measured. The reason for this variation is unknown.

5.4 Conclusions

The fibrillar collagen structure across the animal skin is fairly consistent in ovine leather, despite some small variations. This is encouraging as it indicates that the location on the skin chosen in manufacturing for ovine leather may be less important than for bovine and some other hides. There were some significant differences between the properties measured at different positions but only two positions had a consistent variation to the other positions in any of the properties investigated.

The neck had a significantly lower average *d* spacing to that of all other positions measured. This property appeared not to be related to strength but rather indicates a difference in collagen structure. This variation is thought to be due to a significant dip in *d* spacing at the grain-corium junction, which may be greatest in the neck skin due to its thickness. The belly was found to have a greater normalised tear strength than the other positions sampled. Samples from the belly did not have a significantly higher absolute tear strength indicating that differences observed are probably due to the thinness of the sample.

The relationship between tear strength and orientation was found to be significant at all positions measured across the skin, which further supports the hypothesis that fibrillar collagen orientation is related to tear strength. However, the relationship between orientation index and tear strength was different in OSP cross-sections cut perpendicular to the backbone to all other positions studied.

CHAPTER 6 CHANGES IN FIBRILLAR COLLAGEN STRUCTURE DURING PROCESSING OF OVINE LEATHER

6.1 Introduction

The process of leather production is, in part, a way of preserving skins to stop decomposition. In order for this to occur significant changes in structure need to take place. Changes that occur during leather production include the removal of some skin components and the addition of compounds such as cross-linking agents. The addition and removal of these compounds could result in changes to the fibrillar collagen structure of the material.

By understanding the changes that occur to the fibrillar collagen structure of skins during leather processing, it is possible that the properties of leathers may be determined from the initial skin structure. This would allow skins the be graded on some quantifiable properties and those not fit for leather production removed before the initiation of processing, or that processes could be varied to produce targeted products.

The aim of this chapter is to investigate the changes that occur to the fibrillar collagen structure and physical properties of skin during the leather production process. For this purpose samples were removed from the same skins during several stages of processing. Salted green skin samples, raw skin that had been cooled and stored with salt to dehydrate the skin and thereby preserve it, were the first samples removed. Depilated pelts were the next samples removed, taken from skins that had undergone initial processing and liming to remove wool. Pickled pelt samples were taken after skins had undergone the pickling process. Pretanned samples were removed after the addition of pretanning compounds but before the addition of chrome tanning agents. Wet blue samples were removed after chrome tanning and retanned samples were removed after the addition of retanning and fatliqoring agents. Dry crust samples were taken at the end of processing after drying but before finishing processes such as shaving.

Samples were cut from the skin parallel to the backbone and as close together as possible and kept below 4°C until analysis to prevent microbial degradation. Three cross-sectional unstrained samples from the same skin were analysed using SAXS at each selected processing stage. They were attached to the sample holder and then sealed in mylar film to prevent them drying out during analysis. A more detailed description of experimental methodology can be found in chapter 3. Tear tests and thickness measurements were performed on wet samples from 10 different skins. The results were averaged to produce an average value for each stage.

6.2 Results

Diffraction patterns of cross-sectional samples were analysed to determine the average orientation index and *d* spacing. Samples taken during processing were also tested to determine thickness and tear strength values.

6.2.1 Orientation Index

The orientation index was shown to progressively increase through all processing stages except between the salted green skin and pickled pelt samples, ranging from 0.53 in the pickled pelt to 0.68 in the retanned state (Figure 6.1). These results indicate that processing results in the collagen becoming more aligned in the direction parallel to the leather surface. Because only three samples were analysed at each processing stage a large standard deviation resulted.

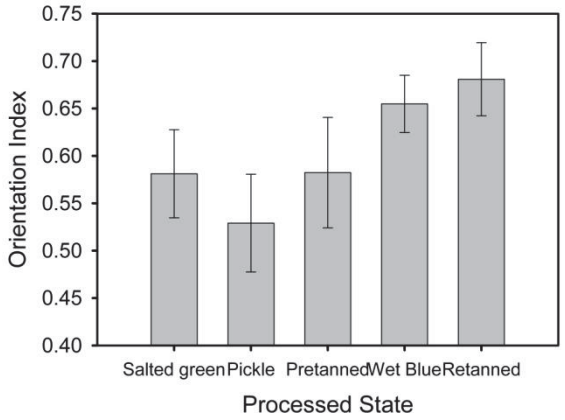

Figure 6.1: Orientation index at various stages of processing.

Statistical analysis found that there was a significant difference between the orientation index of all groups except; salted green skin and pretanned samples, and retanned and wet blue samples. Table 6.1 shows the results of this statistical analysis. These results indicate that significant changes in fibrillar collagen orientation occur during leather processing.

Table 6.1: The significance of differences between the orientation indexes of partially processed leather samples as determined by the Holm-Sidak Method

Processing Stage	Salted Green	Pickled Pelt	Pretanned	Wet Blue	Retanned
Salted Green		Significant	Not Significant	Significant	Significant
Pickled Pelt			Significant	Significant	Significant
Pretanned				Significant	Significant
Wet Blue					Not Significant
Retanned					

6.2.2 *d* Spacing

There was an obvious variation in the *d* spacing of skin samples taken at different stages of leather processing (Figure 6.2). Although the average *d* spacing value varied between 64.0 nm and 65.3 nm, there was no visible trend in the results. The *d* spacing obtained from salted green skin was 65 nm, which is comparable to the value of 65.2 nm for ovine skin which has previously been determined using SAXS (Brodsky and Eikenberry 1982).

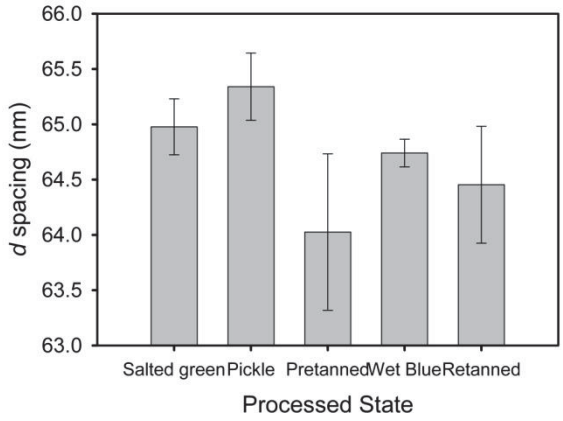

Figure 6.2: *d* spacing at various stages of processing.

A Friedman test found that there was a significant difference between the *d* spacing of pickle and pretanned and retanned skins. There was also a significant difference between the *d* spacing of salted green skin and pretanned skin. The results of the statistical analysis are shown in Table 6.2. There was no significant difference between the average *d* spacing at the other stages analysed.

Table 6.2: The significance of differences between the *d* spacing's of partially processed leather samples as determined by Tukey Test.

Processing Stage	Salted Green	Pickled Pelt	Pretanned	Wet Blue	Retanned
Salted Green		Not Significant	Significant	Not Significant	Not Significant
Pickled Pelt			Significant	Not Significant	Significant
Pretanned				Not Significant	Not Significant
Wet Blue					Not Significant
Retanned					

When plotted against the pH the skins were exposed to during processing, it is apparent there is relationship between *d* spacing and pH, the *d* spacing increases with decreasing pH in a non-linear fashion. This relationship can be seen in Figure 6.3.

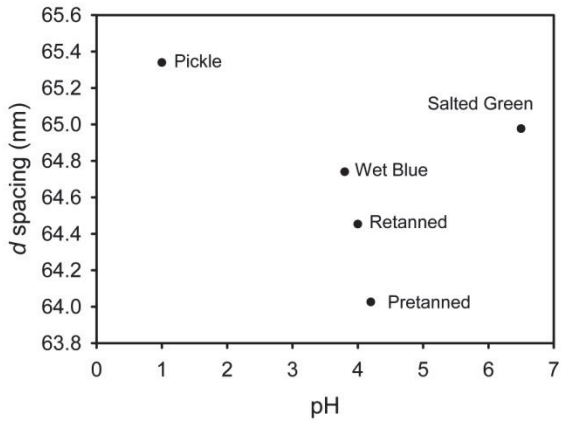

Figure 6.3: *d* spacing of fibrillar collagen versus the pH of processing fluid at various stages of processing.

6.2.3 Thickness

The thicknesses of samples throughout leather processing were also measured. These results are shown in Figure 6.4. Not surprisingly, the thickness appears to decrease during processing with the most significant changes occurring between the depilated slat and pickled pelt stages and the retanned and dry crust stages.

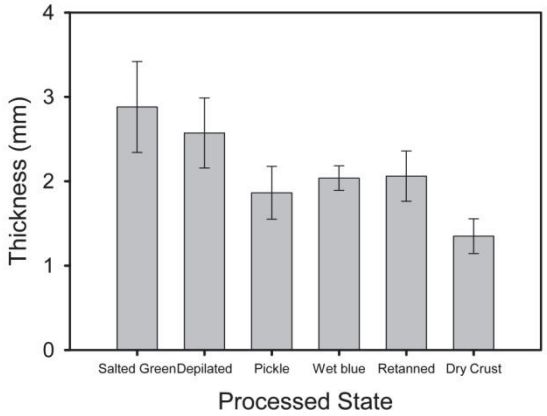

Figure 6.4: Thickness at various stages of processing.

This was confirmed by Tukey Test, which found there was no significant difference between the thickness of pickled pelt, wet blue and retanned samples and no difference between raw skin and depilated slat samples. There was, however, a significant difference between the thicknesses of samples in all other stages as indicated by Table 6.3.

Table 6.3: The significance of differences between the thicknesses of partially processed leather samples as determined by Tukey Test.

Processing Stage	Salted Green Skin	Depilated Slat	Pickled Pelt	Wet Blue	Retanned	Dry Crust
Salted Green Skin		Not Significant	Significant	Significant	Significant	Significant
Depilated Slat			Significant	Significant	Significant	Significant
Pickled Pelt				Not Significant	Not Significant	Not Significant
Wet Blue					Not Significant	Significant
Retanned						Significant
Dry Crust						

6.2.4 Tear Strength

The absolute and relative tear strengths were also found to vary with processing stage, which can be seen in Figure 6.5. Absolute tear strength varied between 32.0 N in the pickled pelt stage to 48.5 N in the dry crust stage. The relative tear strength varied between 14.4 N/mm in the salted green and 36.3 N/mm in dry crust samples. Dry crust was found to have both the highest absolute and relative tear strength.

The absolute tear strength appears to decrease between the depilated and pickling stages and then steadily increase through the remaining processing stages. In contrast, the normalised tear strength did not appear to vary significantly until the final stages of processing. This was confirmed by statistical analysis that found there was no significant difference between the relative tear strengths of early stage samples (see Table 6.4). Only dry crust and retanned samples displayed significantly different normalised tear strengths to those of other processing stages.

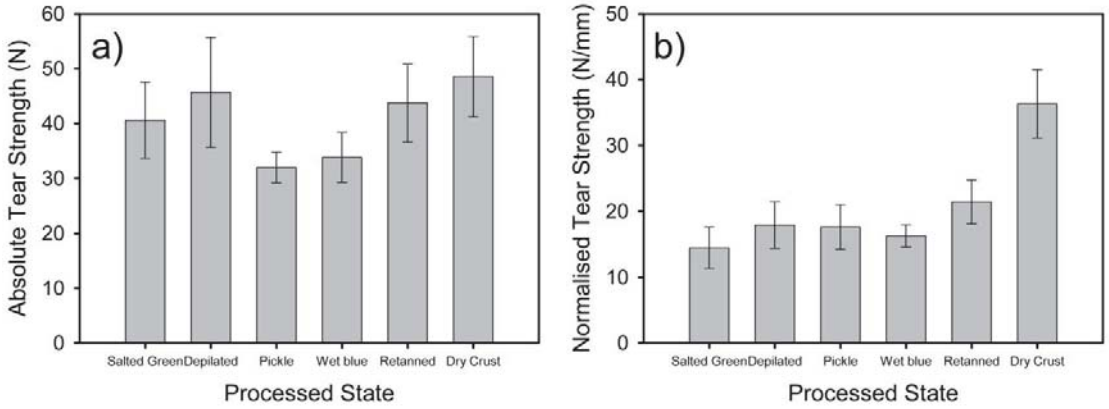

Figure 6.5: Measured a) absolute tear strength and b) normalised tear strength at various process stages.

Statistical analysis found that the absolute tear strength of pickled pelt and wet blue samples were significantly lower to that of all other processing stages except each other. There was no significant difference between the absolute tear strengths of the other four processing stages. The results of this analysis are shown in Table 6.4.

Table 6.4: The significance of differences between the tear strength's of partially processed leather samples as determined by Tukey Tests. Bottom left side absolute tear strength and top right side normalised tear strength.

Processing Stage	Salted Green Skin	Depilated Slat	Pickled Pelt	Wet Blue	Retanned	Dry Crust
Salted Green Skin		Not Significant	Not Significant	Not Significant	Significant	Significant
Depilated Slat	Not Significant		Not Significant	Not Significant	Not Significant	Significant
Pickled Pelt	Significant	Significant		Not Significant	Not Significant	Significant
Wet Blue	Significant	Significant	Not Significant		Significant	Significant
Retanned	Not Significant	Not Significant	Significant	Significant		Not Significant
Dry Crust	Not Significant	Not Significant	Significant	Significant	Not Significant	

From Figure 6.6 it can be seen that the relationship between orientation index and relative tear strength observed previously does not appear to apply to partially processed samples. This is not surprising since components of leather that are also thought to contribute to leather strength, such as cross-linking agents, are present in varying amounts during processing.

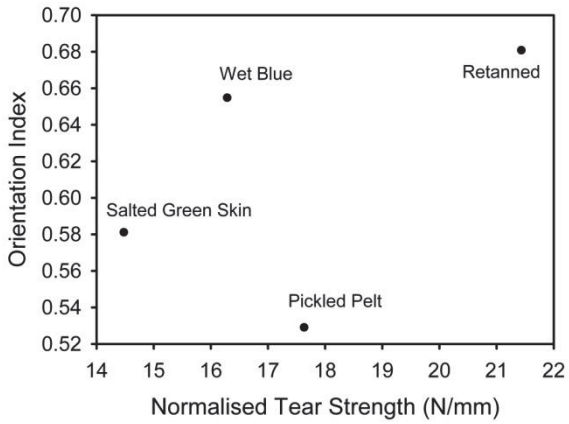

Figure 6.6: Orientation index versus relative tear strength of processing stages.

6.3 Discussion

6.3.1 Orientation Index

Results show that the orientation of collagen fibrils decreases between the salted green skin and pickled skin and then increases steadily during the remainder of processing.

A decrease in orientation index was observed between the processing stages of salted green and pickled skin. This may be due to the removal of several components of the skin during the initial stages of processing including non-collagenous proteins such as glycosaminoglycans (GAGs) which interact with collagen fibres (Deb Choudhury *et al.* 2007; Edmonds *et al.* 2008). In addition, initial processing causes the skin to 'swell' opening up the collagen structure, and probably affecting the orientation of collagen fibrils.

Orientation index increased during the remainder of the process. Cross-linking agents, added to the material between the remaining stages of pretanned, wet blue and retanned, link collagen fibrils and could be responsible for the increase in collagen fibril alignment.

The changes that occur to orientation index during processing are significant. This is evident from the differences between the orientation indexes of all processing stages being statistically significant except for two. The absence of a significant difference between the salted green skin and pretanned is not surprising given the average value for both groups were 0.58. These stages are not successive indicating that the similarity in orientation index is a coincidence.

There is no significant difference between the orientation index of wet blue and retanned samples. If the main cause of increasing orientation index during processing is the addition of cross-linking agents then this result is not surprising. Wet blue samples have been chrome tanned so that the fibrous collagen structure is largely fixed. The addition of further cross-linking agents between the wet blue and retanned stages is not likely to have as significant an effect on the structure.

6.3.2 *d* Spacing

The collagen *d* spacing did not progressively change with processing. However, there were significant changes in the *d* spacing between some process stages; pickle and pretanned, pickle and retanned skins and also between salted green skin and pretanned skin.

There appears be a non-linear relationship between the *d* spacing of collagen fibrils and the pH of processing fluid, thought to be due to the swelling of collagen fibres. Extremes of pH will alter the charges on carboxyl and amino groups of proteins, and can even result in deamidation of asparagine and glutamine, changing a charged sidechain into a polar residue. The triple helix molecule is thought to be stabilised by $N\text{-}H_{(Gly/Y)}\cdots O{=}C_{(X/Gly)}$ hydrogen bonds (Shoulders and Raines 2009). Changes in the charges of these groups would affect the stability of these bonds and the interaction of the molecule with water. The alignment of collagen molecules it thought to be due, in part, to the charge and hydrophobic nature of amino acid side chains, so these changes could also affect the alignment of adjacent collagen molecules. This would affect the *d* spacing of collagen fibrils.

6.3.3 Thickness

Not surprisingly, the thickness of samples decreased during processing. Statistical analysis determined that there was no significant difference between the thickness of pickled pelt, wet blue and retanned samples and no difference between raw skin and depilated slat. Significant changes in thickness are therefore thought to occur between the depilated slat and pickled pelt stages and the retanned and dry crust stages.

Between the depilated slat and pickled pelt stages most of the proteins of the skin, excluding collagen and elastin, are removed (Deb Choudhury *et al.* 2006). This would significantly decrease the amount of dry substance in the skin and would therefore be expected to decrease the pelts thickness. Between the retanned and dry crust stages the most significant alteration is the removal of significant amounts of water. It is thought that this removal is responsible for the decrease in thickness that occurs during these two processing stages.

6.3.4 Tear Strength

Absolute tear strength is significantly lower in the pickle and wet blue samples than in the other samples measured. The low absolute tear strength of the pickle state is not very surprising since at this stage natural cross-linking agents have been removed and have not yet been replaced. The low absolute tear strength of the wet blue stage is more surprising but may be due to the absence of lubricating agents at this stage.

Lubricating agents such as fat-liquors are added during retanning and allow collagen fibres to slide past one another (Daniels 2003). In the next chapter the changes that occur to the collagen fibril structure during leather stretching are investigated. This investigation found that fibril reorientation was one of the main mechanisms that occurred during leather stretching. The absence of lubrication may restrict the amount of reorientation that can occur and so decrease the strength of wet blue samples.

No significant changes occur to the normalised tear strength of the skin during initial processing. Only the dry crust, and less significantly retanned samples, shows a variation in normalised tear strength. The greater normalised tear strength of the dry crust may be due to the decrease in sample thickness due to the removal of water.

6.4 Conclusions

Significant changes to the collagen structure of skins occur during leather production. The orientation index decreases during pickling and then increases during the remaining processing stages, probably due to the addition of cross-linking agents. The *d* spacing also changes during processing, possibly due to changes in the pH.

Changes to the physical properties of the skin also occur. Not surprisingly the thickness of the skin decreases, due to the removal of skin components and water. Changes to the tear strength of the skins do occur but are less significant. The absolute tear strength of skins decreases during pickling and then increases again after retanning. The normalised tear strength did not change significantly during processing but did increase significantly after drying.

These results show that significant changes occur to skins during leather processing. The changes that occur are not just localised to the addition and removal of specific compound but also result in changes to the arrangement and structure of collagen fibrils.

CHAPTER 7 THE EFFECT OF STRAIN ON THE FIBRILLAR COLLAGEN STRUCTURE OF LEATHER

7.1 Introduction

To assist in the understanding of the relationship between collagen structure and the physical properties of ovine leather, the response of the fibrillar collagen structure to strain is of importance. Understanding the mechanisms that occur as a result of strain and how these mechanisms vary between different types of leather assists in our understanding of the basis for leather strength.

In previous chapters investigation into how collagen structure is related to the strength of unstrained leather samples was undertaken, with results indicating that leather samples of higher strength have more collagen fibrils aligned parallel to the plane of the leather surface than weaker leathers. It is possible, however, that differences in the mechanisms for the response of leather samples to strain, as well as the initial structure of the sample, may contribute to the strength of samples.

SAXS requires samples of a suitable thickness; thicker samples result in more scattering material being exposed to the X-ray beam but also result in a greater level of X-ray absorption. This means that full thickness leather samples are too thick to be analysed by this method and therefore, many of the standard strength tests available are inappropriate for combination with SAXS measurements.

There are many different tests such as tensile strength, tear strength or burst strength that can be used to determine the strength of samples under different types of strain. The mechanisms for failure and the distribution of forces on the material during these tests can vary. Some types of strength measurement are also more relevant to the stresses experienced by leather than others. With this information in mind it was decided that the effect of uni-axial strain on the fibrillar collagen structure of leather would be investigated.

The use of uni-axial stretching in combination with SAXS presents some restrictions to the stretching method that can be used due the thin sample size needed for SAXS. It is possible that the thinness of samples disrupts the continuity of fibres and therefore has an

effect on the response to strain. It is thought that, if there is an effect of sample thickness on fibre continuity, this would be more evident in cross-sectional samples than in the flat samples. This is because there is very little crossover of fibres between the grain and corium layer and flat samples had a greater thickness in the cross-sectional direction. The effect of thickness on fibre continuity is not thought to be substantial and due to the requirements of SAXS it is not possible to avoid it. The experiment is also not optimised for the determination of stretching properties because the sample cannot be stretched continuously until failure but instead must be stretched in increments.

The aim of this chapter is to investigate the changes that occur to the fibrillar collagen structure of ovine leather under uni-axial strain. The response of both cross-sectional and flat samples, cut parallel to the backbone, to strain was studied. Our previous results have shown that there is a relationship between the orientation of collagen fibrils in the cross-sectional direction and tear strength so the changes that occur in this direction during strain are thought to be of importance. Information on how fibrillar collagen structure changes in the flat direction when samples are under strain will also add to the overall understanding of how leather responds to strain.

Samples of varying strengths were stretched at regular increments and the SAXS patterns produced by the samples recorded. This meant that reorganisation of the fibrillar collagen structure at increasing strain levels could be determined. Analysis was carried out on cross-sections of leather, 1 x 50 mm, which were cut from the official sampling position parallel to the backbone. Flat samples of the corium and grain, 5 x 50 mm, from the same position were also used. The average thickness of these samples was 1.3 mm. Samples were stretched and analysed using the methods described in chapter 3.

7.2 Results

Tear strength values for a number of skins were used to classify skin samples as either strong or weak. Samples in the weak group had tear strengths of approximately 20 N/mm while strong samples had tear strengths of around 40 N/mm. A small number of these skins considered representative of their group were then stretched to investigate their response to strain.

7.2.1 Stress-Strain Curves

From the force-extension data collected, stress-strain curves could be produced, these are shown in Figure 7.1. The experimental method was not optimised for the determination of stretching properties such as Young's modulus or breaking strength. However general information about the stress-strain characteristics of the leather samples can be determined.

The general curve shape is similar for both the strong and weak ovine leathers. For the ovine leather samples the slope of the stress-strain curve increases with increasing strain but becomes somewhat constant above a strain value of 0.2. This is consistent with other investigations of the response of leather to strain (Attenburrow 1993). However the bovine leather sample does not display this trend, but instead displays a somewhat constant slope.

From the slope of the curves in Figure 7.1 the range of the modulus of elasticity of the leather samples could be calculated. It was found to be 2–25 N/mm^2 for weak ovine; 5–39 N/mm^2 for stronger ovine; and 17 N/mm^2 (but only up to 0.20 strain) for strong bovine. The modulus of elasticity at 0.20 strain was found to be 8 N/mm^2 for weak ovine; 30 N/mm^2 for strong ovine; and 15 N/mm^2 for strong bovine.

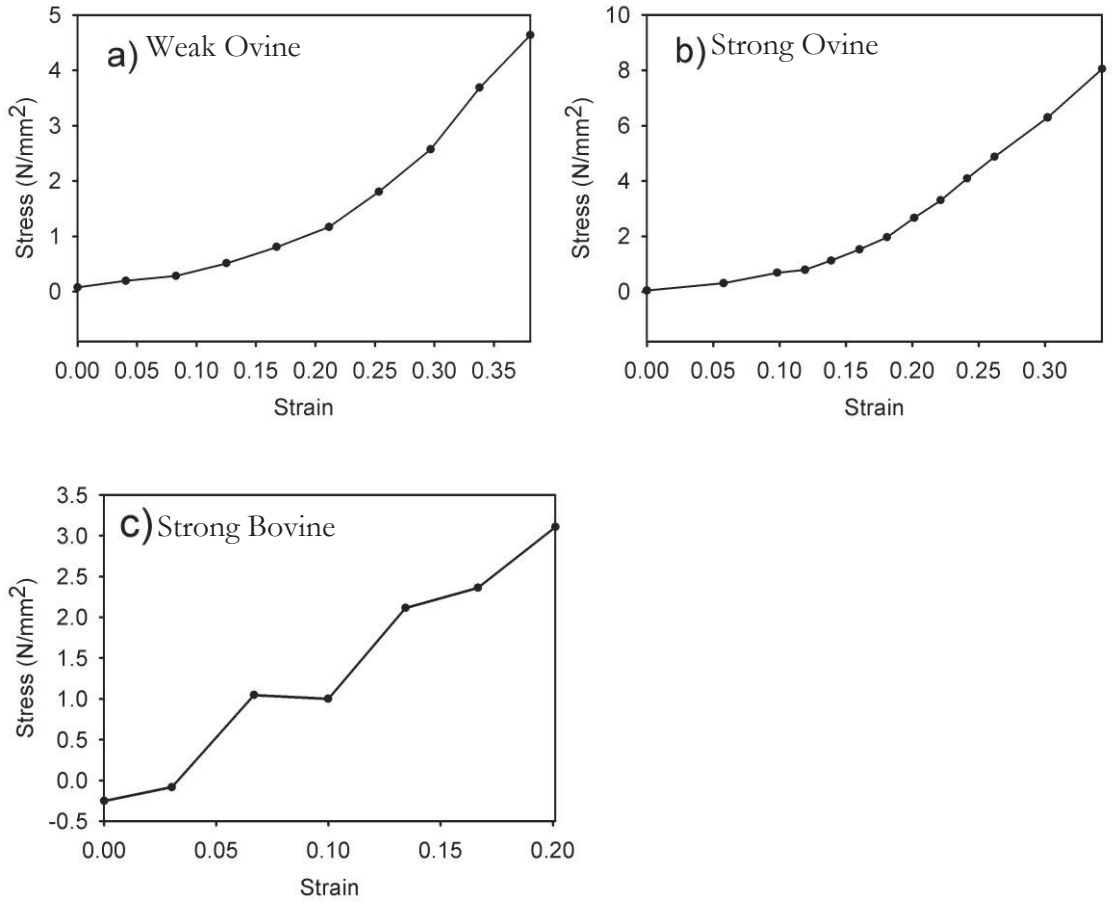

Figure 7.1: Graphs of stress versus strain for a) weak ovine, b) strong ovine and c) strong bovine (Basil-Jones *et al.* 2012).

Stress-strain plots were produced for flat grain and corium samples and are shown in Figure 7.2. The graphs for flat grain samples show an approximate linear slope. For flat corium samples the response is similar to that of ovine leather cross-sections with the slope increasing with increasing strain.

From the slope of the curves in Figure 7.2 the range of the modulus of elasticity of the flat leather samples could be calculated for each sample. These values were found to vary between grain and corium and also between strong and weak samples. For weak ovine grain the modulus of elasticity was 4-5 N/mm^2; for weak ovine corium 8-22 N/mm^2; for strong ovine grain 7-10 N/mm^2 and for strong ovine corium 8-18 N/mm^2. The modulus of elasticity at 0.20 strain was found to be; 5 N/mm^2 for weak ovine grain, 11 N/mm^2 for weak ovine corium, 7 N/mm^2 for strong ovine grain and 14 N/mm^2 for strong ovine corium.

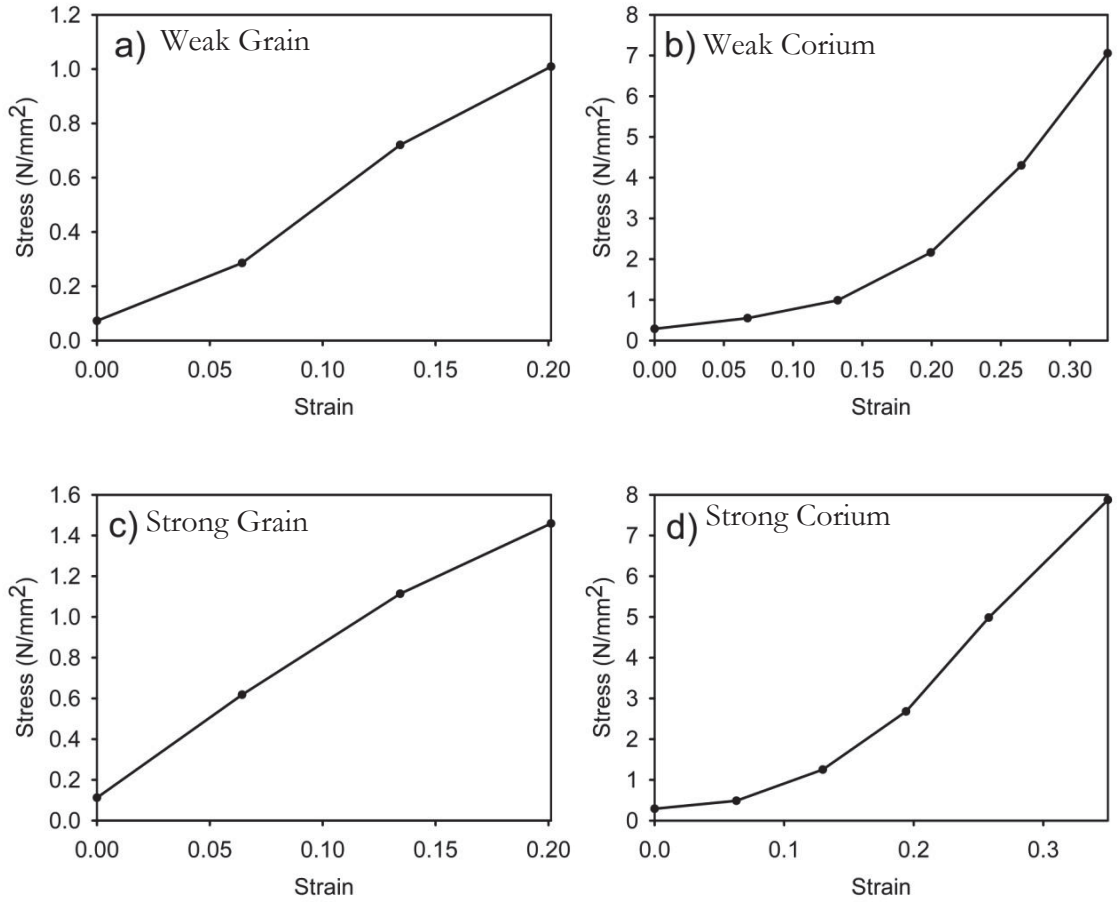

Figure 7.2: Graphs of stress versus strain for a) weak ovine grain, b) weak ovine corium, c) strong ovine grain and d) strong ovine corium.

7.2.2 Variation of *d* Spacing and Fibril Orientation with Strain

The orientation index (OI) and *d* spacing were plotted against strain for both cross-sectional and flat samples, to allow a visual comparison of how these parameters changed as the strain on the sample increased.

The graphs in Figure 7.3 show there was a substantial change in fibril orientation across the cross-sectional samples during stretching. The OI changes from 0.56 to 0.72 in the ovine samples and from 0.53 to 0.62 in the bovine leather sample. These results indicate a significant rearrangement of fibres in the leather to become more aligned with the direction of the strain.

There were also found to be significant changes in the *d* spacing of collagen fibrils. For the weak ovine skin sample the *d* spacing increased from 64.12 to 64.48 nm equating to a fibril extension of 0.56%, while for the strong ovine skin the change was from 64.34 to 64.67 nm equating to an extension of 0.51%.

Initially strain resulted in a reorientation of the fibrils with no changes in *d* spacing. However, once the strain rose above 0.05-0.08 the rate of reorientation of the fibrils decreased significantly. The *d* spacing remained fairly constant at levels of strain less than 0.10-0.13. Above this level it began to sharply increase.

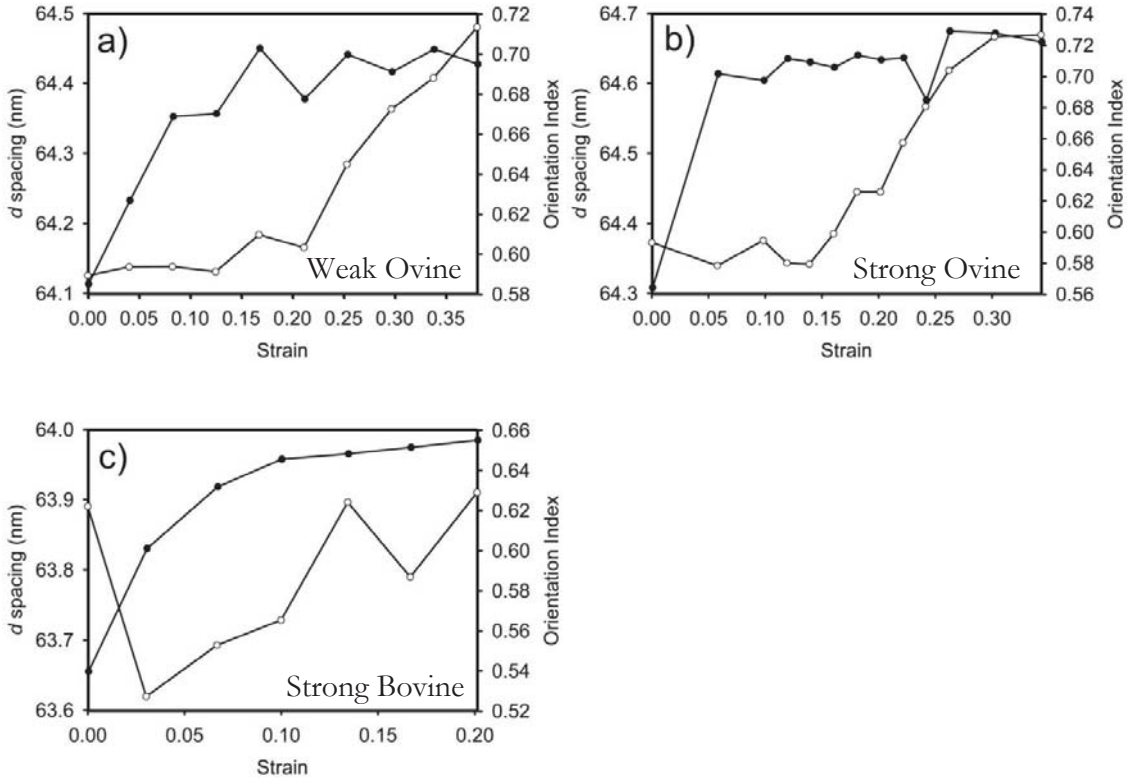

Figure 7.3: *d* spacing and orientation index versus strain measured edge on parallel to the backbone. *d* spacing - open circle; OI - closed circle. a) weak ovine, 19 N/mm tear strength; b) stronger ovine, 39 N/mm; c) strong bovine, 71 N/mm (Basil-Jones *et al.* 2012).

Flat grain and corium stretching measurements were made for strong and weak ovine samples only. Initially, the OI's were lower than those measured for the cross-sectional samples and these of the grain samples were lower than those for the corium. It can be seen from Figure 7.4 that the OI changed significantly under strain, going from 0.20 to 0.51 in the grain and 0.34 to 0.74 in the corium of weak ovine leather, and 0.44 to 0.79 in the corium of strong ovine leather.

The changes in the *d* spacing were significant in the corium of both the weak and strong ovine leathers. In the corium of the weak ovine leather the *d* spacing changed from 64.25 to 65.10 nm which equates to a 1.3% extension, while for strong leather it changed from 64.27 to 65.65 nm, a 2.1% extension. In contrast, the change in the *d* spacing of the

collagen in the grain of both samples was very small, 64.42 to 64.52 nm for weak and 64.29 to 64.19 nm for strong. Interestingly, for the strong sample the *d* spacing actually decreased.

The response to strain varied between grain and corium samples. For samples from the grain the increase in OI with strain was almost linear, especially in the weak sample, and there was no significant increase in *d* spacing. In corium samples the rate of change in the OI decreased as strain was increased, then did not change significantly at high levels of strain. The changes in *d* spacing observed were significant in the corium and the rate of change in the *d* spacing of collagen fibres increased as strain was increased.

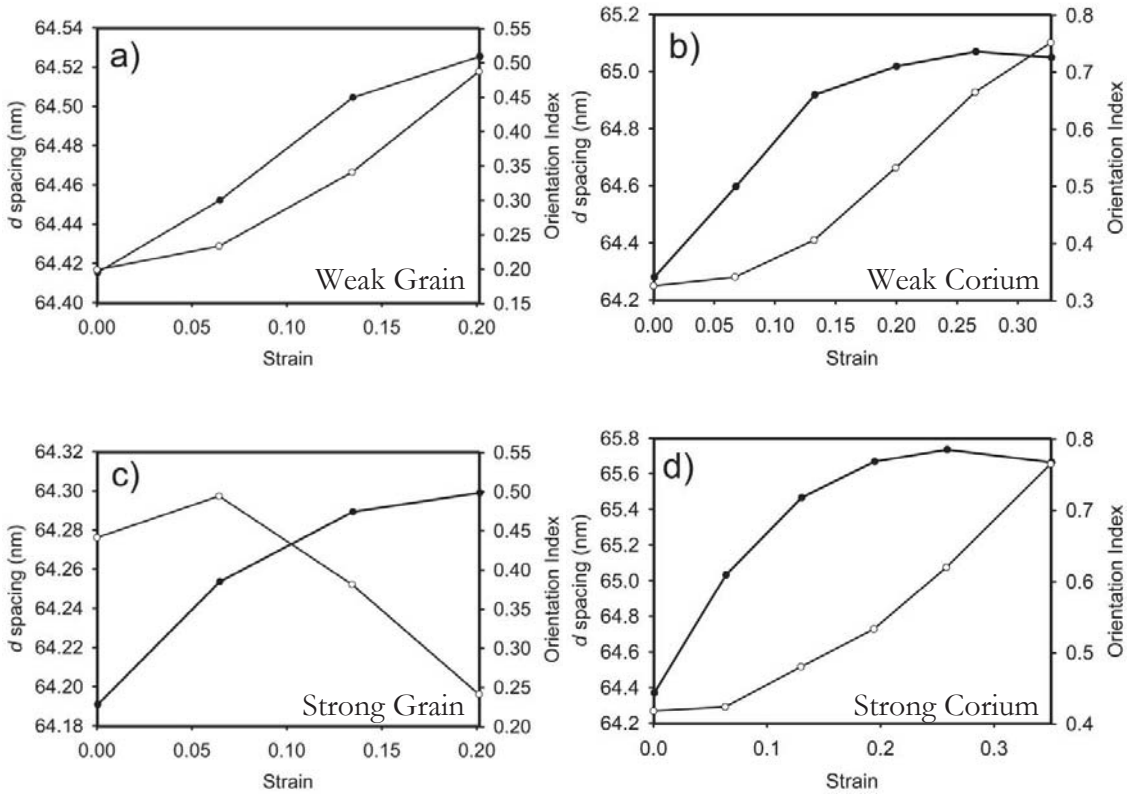

Figure 7.4: *d* spacing and orientation index versus strain measured for flat samples. *d* spacing - open circle; OI - closed circle. a) weak ovine (21 N/mm tear strength) grain; b) weak ovine, corium; c) stronger ovine (44 N/mm) grain; d) stronger ovine, corium (Basil-Jones *et al.* 2012).

7.2.3 Variation of *d* Spacing and Fibril Orientation with Stress

Graphs were also produced of change in *d* spacing and OI versus stress. These figures show how the structural changes in the skin samples are related to stress. Changes in the orientation index of cross-sectional samples subjected to stress occur rapidly, with most

reorientation occurring before stress levels reach 0.5 N/mm^2. Significant changes in *d* spacing are not observed, however, until stress levels of approximately 1.0 N/mm^2 are reached. Figure 7.5 shows that as stress increases above this level, the rate of change in *d* spacing of collagen fibrils decreases, and for ovine leather samples the OI decreases slightly prior to sample failure.

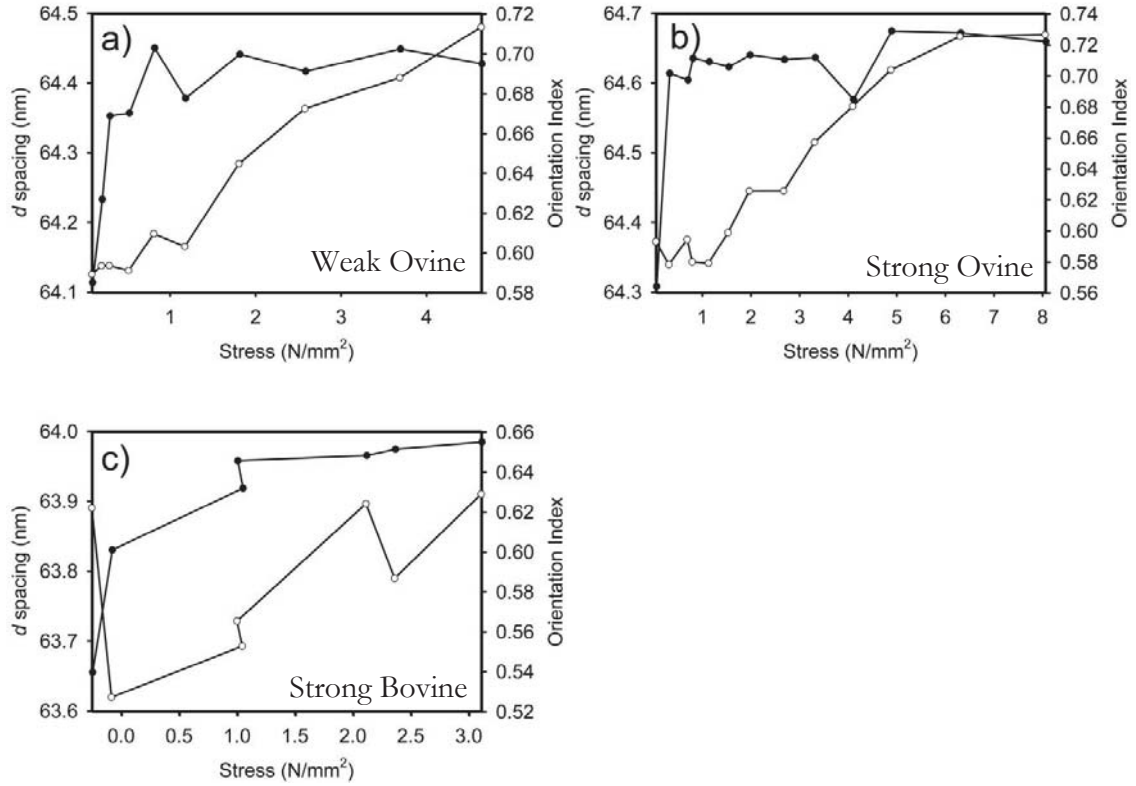

Figure 7.5: *d* spacing and orientation index versus stress measured edge on parallel to the backbone. *d* spacing - open circle; OI - closed circle a) weak ovine, 19 N/mm tear strength; b) stronger ovine, 39 N/mm; c)strong bovine, 71 N/mm (Basil-Jones *et al.* 2012).

The *d* spacing of both corium and weak grain samples increased almost linearly as the stress on the sample was increased. In contrast, the rate of change of orientation index varied between grain and corium samples (Figure 7.6). In grain samples the OI increased somewhat linearly with stress, whereas for the corium samples the relationship was not linear, with the rate of change of orientation index decreasing under higher stress. Most of the change in the OI for corium samples occurred before a stress level of 1.0 N/mm^2 had been reached as well as decreasing slightly before failure, which did not occur in grain samples.

Corium samples consistently withstood higher stress before sample failure compared to grain samples. The flat grain samples failed at stress values of approximately 1.1 N/mm^2 for weak ovine and 1.6 N/mm^2 for strong ovine skins, while the flat corium samples failed at stress values of 7.9 N/mm^2 for weak ovine and 8.9 N/mm^2 for strong ovine skins.

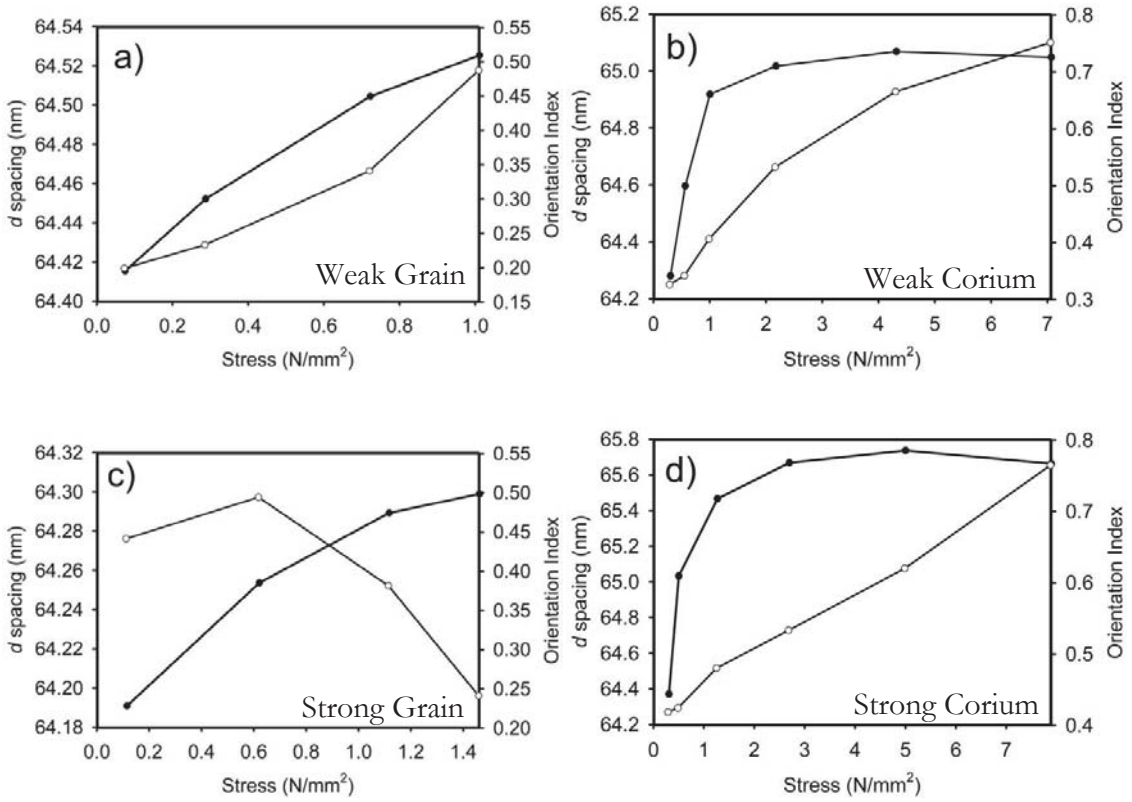

Figure 7.6: *d* spacing and orientation index versus stress measured flat parallel to the backbone. *d* spacing - open circle; OI - closed circle. a) weak ovine (21 N/mm tear strength) grain; b) weak ovine, corium; c) stronger ovine (44 N/mm) grain; d) stronger ovine, corium (Basil-Jones *et al.* 2012).

7.2.4 Variation of *d* Spacing across Sample Thickness

Because cross-sectional leather samples were analysed, profiles of *d* spacing across the leather thickness could be produced, to give a visual analysis of how stress affects the fibrillar collagen structure through the leather thickness.

The *d* spacing profile of weak ovine leather was quite even when not under tension, displaying only a slight variation of 0.3 nm across the thickness, with the *d* spacing decreasing in the corium region (Figure 7.7 a)). One of the stronger ovine leather samples also showed a rather flat profile with a variation of only 0.6 nm (Figure 7.7 b)).

The bovine leather and other strong ovine leather samples had a different *d* spacing profile when not under tension, displaying a significant decrease in *d* spacing in the region of the corium-grain junction; 1.8 nm for the strong ovine leather and 2.2 nm for the strong bovine sample leather.

When tension was applied to samples of strong ovine and bovine leathers, the *d* spacing profiles retained the same basic shape throughout the stretching process. However the weak ovine leather *d* spacing profile changed significantly under tension. The strain on the fibrils was not uniformly distributed through the leather cross-section; rather it was concentrated in regions of the grain surface and the bulk of the corium with little stress being transferred to the fibrils in the middle section of the sample.

d spacing increases of up to 1 nm were observed for the weak ovine sample, much higher than those observed for the stronger samples. At high tensions, the *d* spacing profile of the weaker samples somewhat resembles that of the stronger samples, with a significant dip in the middle of each sample. This dip in *d* spacing of 0.7 nm is still, however, much less than those observed in the strong samples.

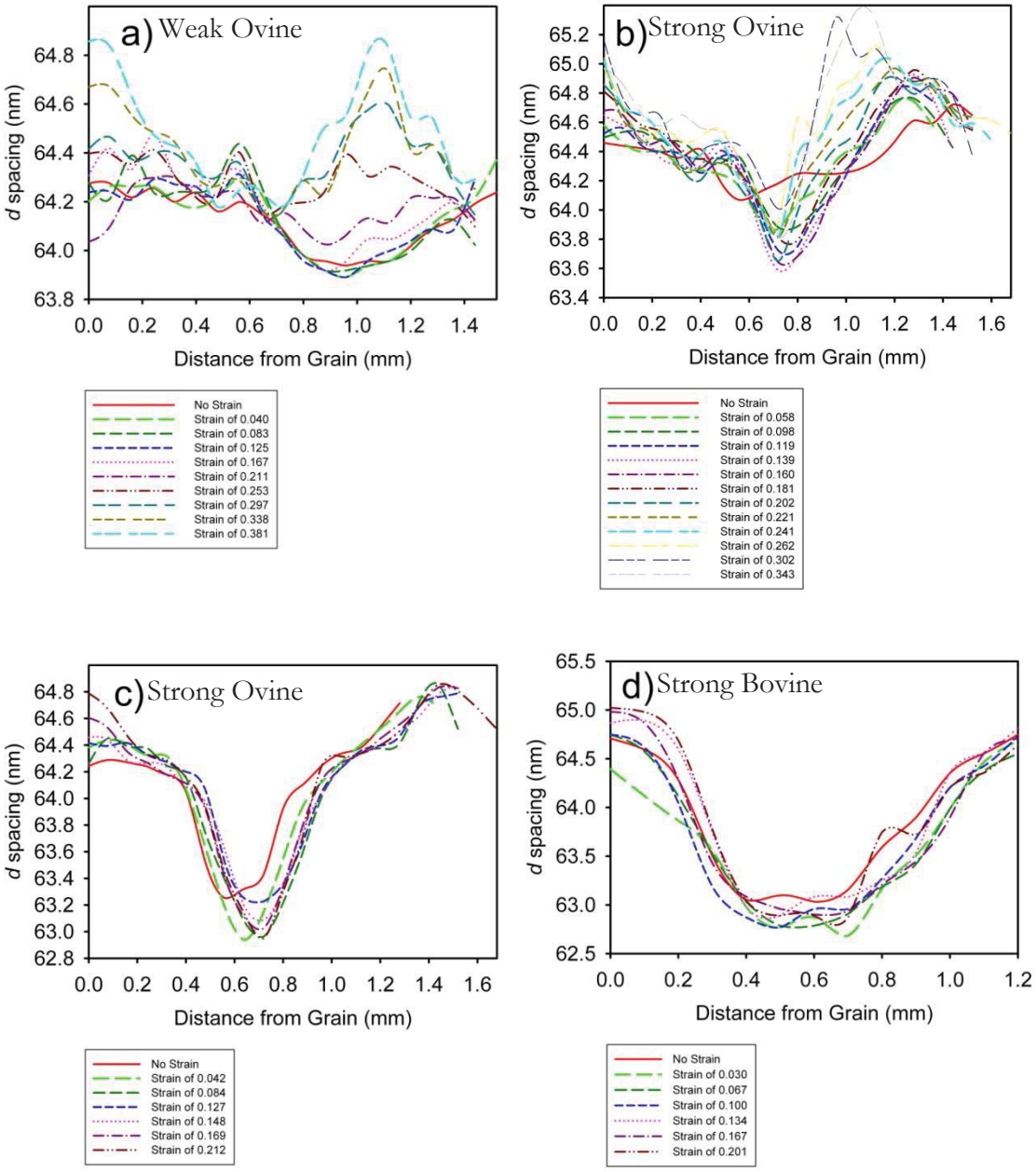

Figure 7.7: *d* spacing profiles through the thickness of the leather and change in *d* spacing as a consequence of increasing strain, for cross-sectional samples cut parallel to the backbone. a) weak ovine, 19 N/mm tear strength; b) stronger ovine, 39 N/mm; c) second strong ovine leather with a tear strength of 42 N/mm; d) strong bovine, 71 N/mm (Basil-Jones *et al.* 2012).

7.2.5 Variation of Fibril Orientation across Sample Thickness

Profiles of the change in orientation index across the sample thickness were also produced. This provides information about how strain affects the orientation of collagen fibrils at different regions across the thickness of the cross-section.

The profiles of fibrillar collagen orientation show that the orientation is fairly constant across most of the thickness of the ovine leather samples as seen in Figure 7.8. There is, however, a less aligned region near the grain-corium boundary in ovine samples. This region is more prominent in the weaker sample. In the bovine samples this lack of alignment is not seen. Instead, the sample has significantly less alignment in the corium region of the sample.

The response to strain varies slightly between strong and weak samples. During the first one or two increments of stress the greatest change in the OI occurs. This change is most noticeable in the weaker samples. The OI profile also changes in weaker samples, with the OI in the low OI regions increasing to become comparable to the values of the rest of the sample. These changes are less noticeable in the stronger samples.

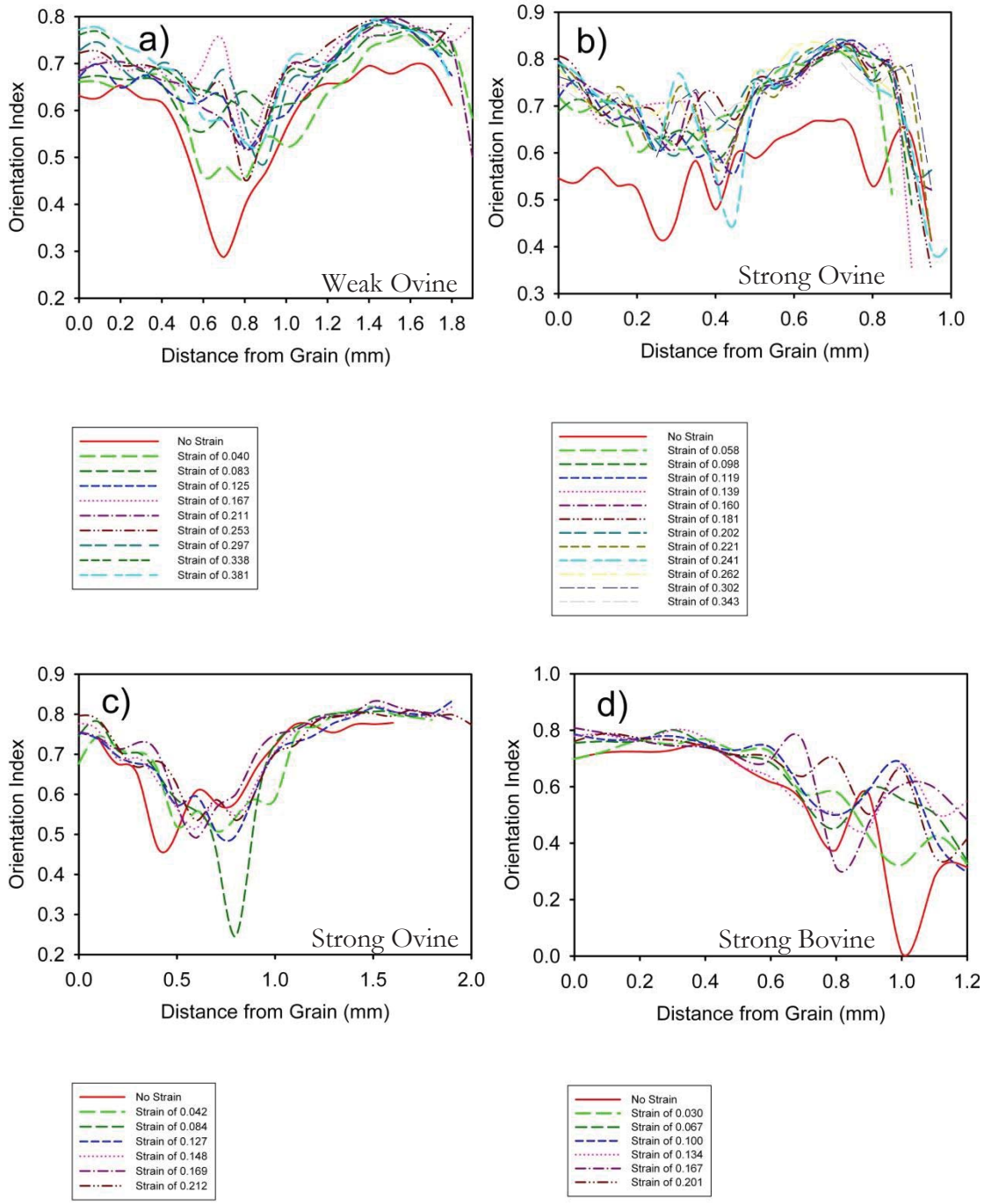

Figure 7.8: Orientation index through the thickness of the leather versus strain and change in orientation as a consequence of increasing strain for cross-sectional samples cut parallel to the backbone. a) weak ovine, 19 N/mm tear strength; b) stronger ovine, 39 N/mm; c) second strong ovine leather with a tear strength of 42 N/mm; d) strong bovine, 71 N/mm (Basil-Jones *et al.* 2012).

7.3 Discussion

7.3.1 Cross-Sectional Samples

The non-linear stress-strain response of ovine leather cross-sections is consistent with those recorded in literature (Attenburrow 1993). At low strain levels the stiffness is low but as strain increases the stiffness of the leather also increases. This type of stress-strain curve is known as a 'J' curve and is the type of curve recorded for a number of collagenous tissues including skin (Attenburrow 1993) and tendon (Fratzl *et al.* 1997).

In cross-sectional samples, application of strain initially resulted in a rapid reorientation of fibres in the direction of the applied force. As the strain increased above 0.05-0.08, which equates to a stress of 0.3-0.5 N/mm^2, the rate at which the OI increased significantly decreased. At around 0.10-0.13 strain (1.0 N/mm^2 stress) the *d* spacing, which had remained fairly constant below this strain level, began to sharply increase. The fibrils stretched by up to 0.6% before they begin to fail. Samples were not analysed after strain had been removed and therefore whether the changes that occurred were elastic or not cannot be determined.

The initial stretching of the leather resulted in the reorientation of fibres in the direction of the strain. However, as strain increased the capability for reorientation decreased. Reorientation of collgen fibrils on stretching was earlier suggested by Attenburrow in 1993 as an explanation for the 'J' stress-strain curve characteristic of leather.

The changes in *d* spacing indicate that the strain is being experienced by individual fibres. It is thought to result from four possible mechanisms; either the individual collagen molecules stretching (due to the stretching of chemical bonds), the collagen molecules sliding past one another, the uncoiling of the coiled structure of the microfibril or the straightening out of individual collagen molecules (largely in the gap region where lower packing density results in a higher degree of disorder).

There is an interval between when the orientation index stops increasing and the increase in *d* spacing starts, indicative of the occurrence of an intermediate mechanism in response to strain between those of fibre reorientation and fibril stretching. This mechanism cannot be identified by the measurement methods employed in this study.

It is possible that this intermediate process is a result of the fibres sliding past one another. Once collagen fibres had aligned with direction of strain it is possible that they could be

pulled and shifted in relation to other fibres in the sample. This response would eventually be limited by the entanglement and cross-linking which connect collagen fibres.

A model of leather stretching has been developed based on the response of cross-sections of leather to strain. Initially, the strain is taken up by the reorientation of the fibres. As the ability of fibre to reorient decreases fibres or fibrils begin to slide past one another. Eventually cross-links or entanglement limit this response and the fibrils begin to be individually stretched, as indicated by increases in *d* spacing.

These changes assist in the understanding of the stress-strain curves produced. When the fibres are reorienting the stiffness is relatively low, as the process requires relatively low force. As the mechanism of strain absorption changes from fibre reorientation to fibril stretching, the stiffness begins to increases. These changes in response assist in understanding the changes that occur to the elastic modulus during stretching.

The variation of *d* spacing and OI across cross-sections of leather (Figure 7.7 and Figure 7.8) show that these parameters vary across the sample thickness. These profiles provide a great deal of information on the variation in the response to strain in different regions.

When not under tension, the *d* spacing and OI vary across sample thickness. The *d* spacing is fairly consistent across the sample thickness of weak samples, with the *d* spacing being slightly lower in the corium, but there is a significant dip in *d* spacing around the grain-corium junction of strong samples. In the weak ovine sample the OI is highest in the grain surface and in the corium, while in the strong ovine sample the OI is highest in the corium. In both samples the OI is lowest in the area around the grain-corium junction in the middle of the sample, with this dip being greater for weaker samples.

It is curious that the weaker samples show the greatest change in their OI profile when under strain; with significant changes in OI across the entire profile, especially in areas with low OI initially. In stronger samples the change in OI across the profile is less noticeable but a change in OI in areas with low initial OI is still observed.

The greatest difference between the weak and strong samples is associated with the changes in the *d* spacing profile in response to strain. In weak samples the change in *d* spacing is not uniform; with significant changes occurring in areas that had initially high OI values. However, in stronger samples the change in *d* spacing is relatively uniform across the profile.

These results indicate that in weak samples strain initially results in reorientation across the sample while in strong samples this initial reorientation is more focused in areas of lower fibril orientation. Because the reorientation is not focused in weak samples, areas that initially had high OIs quickly reach an optimum orientation and in these areas, further strain results in fibril stretching. It is likely that fibrils in these areas quickly reach their maximum extension and fail, quickly followed by complete sample failure.

In stronger samples strain is initially focused on areas of low OI and reorientation occurs almost exclusively in these areas. Once an optimum orientation is achieved fibril stretching begins uniformly across the whole sample profile.

In strong leather the strain is initially distributed unevenly to the fibrils across the sample thickness, focusing initially on areas with low orientation. In weak leathers the strain is much more evenly distributed. These results indicate that in strong samples strain can more easily be transferred between fibres compared to weak samples, which makes sense. Tears occur across a path of least resistance and these results show that samples classified as weak are more likely to contain areas characterised by high strain levels on individual fibrils.

7.3.2 Flat Samples

The initial OI, of 0.34 in weak ovine and 0.44 in strong ovine leather samples, is much lower in the flat corium samples than the cross-sectional samples. This is consistent with the findings discussed in chapter 4. The initial OI of 0.20 measured in the grain samples was significantly lower than those recorded in cross-sectional and flat corium samples and the final value recorded, 0.52, was also lower. The final average OI for the flat corium samples is, however, comparable to those of the cross-sectional samples, with final OI values of 0.74 for weak and 0.79 for strong ovine leather samples. This indicates that an optimal OI value is reached for both flat corium and cross-sectional samples. Due to the low initial OI values for flat corium samples, the overall change in OI during stretching was found to be greater in flat corium samples than in cross-sectional samples.

The rate of change of orientation index varied between grain and corium samples. In grain samples the orientation index increased somewhat linearly with stress. The relationship was not linear for the corium samples. Rather the rate of change in the orientation index decreased at greater stress levels, with most of the change occurring before stress levels of

1.0 N/mm^2 had been reached. The OI of corium samples also decreased slightly before failure which, in contrast, did not occur in grain samples.

Flat corium samples showed a decrease in average OI at the final point before rupture. This also occurs in ovine leather cross-sections and is thought to be due to the failure mechanism of the sample. It is unlikely that all fibrils would fail at once. It is more likely that the weaker fibres (or fibres under greater stress) would fail first and as strain increased more and more fibres fail. Once a fibre fails, it no longer has to align with the direction of strain, so as the number of failed fibres increases the OI decreases.

The changes in the *d* spacing in response to strain were significant in the corium of both weak and strong ovine leathers, occurring at strain levels of 0.6 in flat corium samples and at all stress levels. This value is lower than that observed for the cross-sectional samples, indicating that in the flat samples the strain is transferred earlier to the fibres. The *d* spacing of both corium and weak grain samples increased linearly with stress.

In the corium of weak ovine leather the *d* spacing changed from 64.25 to 65.10 nm which equates to a 1.3% extension. In the strong leather the *d* spacing of the corium changed from 64.27 to 65.65 nm which equals a 2.1% extension. In contrast, the change in *d* spacing of the grain for both samples was very small, 64.42 to 64.52 nm for the weak and 64.29 to 64.19 nm for the strong sample. For the strong sample the *d* spacing actually decreased by a small amount. It is thought that the changes in *d* spacing recorded for flat grain samples are simply due to small variations in the samples, as opposed to a change in the *d* spacing due to strain on fibres.

The overall response to strain is different for the flat corium samples to that observed in the cross-sectional samples. In the flat corium samples the *d* spacing begins to increase at lower strain values, well before the mechanism of collagen fibre reorientation is completed. There is no indication that any mechanism other than fibril reorientation and fibril stretching occurs.

The flat grain samples failed at much lower stress values than flat corium samples. The grain has been found to be weaker than the corium (Russell 1988; Attenburrow 1993) and these results may help clarify the mechanism for this. The mechanism of stretching appears to be different to that in the flat corium samples, with the final OI values being much lower in the grain than the corium and there being no significant change in the *d* spacing in grain samples. The constant stiffness of the flat grain samples and the fact that *d* spacing

does not change significantly indicates that the second mechanism of strain transfer, that of extension of collagen fibrils, does not occur significantly in the grain.

There is a difference in collagen fibre structure between the grain and corium. Collagen fibres are thicker in the corium than in the grain relating to a higher breaking strength of the fibres (Kroschwitz 1989). The arrangement of fibres is also different, with the corium having more of a network structure (Gathercole *et al.* 1987; Kroschwitz 1989; Waller and Maibach 2006). This means that strain could be more readily transferred between collagen fibres in the corium compared to the grain. Such differences in the structure of the different regions of the skin help to explain observed differences in response to extension and in strength.

From the results recorded it does not appear that the thickness of samples has an effect on their response to strain. This is thought to be due to the thin layer of samples being perpendicular to the direction of stain. This means that if the thinness of samples did affect fibre continuity it would be of those that are not significantly involved in the strain response. However, this is not possible to confirm this without investigating the response to strain of thicker samples, which is impossible using SAXS.

7.4 Conclusions

From the results of this study it can be seen that when leather samples are placed under strain the initial response is for fibres to undergo reorientation and become more aligned. At higher strain levels the rate of reorientation decreases and instead strain is transferred to individual fibres.

The results also show that stress on individual fibres is more evenly spread across cross-sections in stronger samples than in weaker samples, showing that weak leather samples are unable to spread applied stress across the sample. Instead it is concentrated at certain sites which results in samples failing at a lower stress.

CHAPTER 8 FIBRILLAR COLLAGEN STRUCTURE IN DECELLULARIZED EXTRACELLULAR MATRIX PRODUCED FROM OVINE FORESTOMACH

8.1 Introduction

Leather is only one of many products derived from collagen-rich tissues where an understanding of collagen structure could be advantageous. It is therefore of interest if the methods and results of this investigation are applicable to other collagen-rich products. For this reason the collagen structure of another collagen-rich product, ovine forestomach matrix, was investigated using SAXS.

Decellularized extracellular matrix (dECM) biomaterials are used for the treatment of wounds by allowing a platform on which host cell colonization can occur. These materials are produced from a number of different tissues including; dermis, urinary bladder, pericardium, small intestine and heart valve (Crapo *et al.* 2011) which are processed prior to implantation to remove cellular material. dECM materials have been found to be present for 1-2 months after implantation (Badylak 2007; Lun *et al.* 2010). During that time, among other functions, they provide structural support (Badylak *et al.* 2009). The area of implantation can undergo significant stresses and therefore it is important that these materials can resist strain without fracturing. Therefore, the materials response to stain is of importance.

One dECM product, known as ovine forestomach matrix (OFM), is produced from the propria subsucosa of ovine forestomach tissue (Floden *et al.* 2011). This material is produced for the treatment of chronic wounds such as pressure, venous and diabetic ulcers. The main component of the material is fibrillar collagen although other components such as elastin, fibronectin, and glycosoaminoglycans are also present (Floden *et al.* 2011).

In order to study the material both unstrained and stretched sample analyses were performed. SAXS analysis of OFM was only performed in the flat direction. This material has an average thickness of 0.25 mm and, as such, it was impractical to perform analysis in

the cross-sectional direction. Details of the experimental methods used are provided in chapter 3.

8.2 Results

Initial analysis of the OFM material found that Bragg's scattering consistent with that of fibrillar collagen occurred. The collagen was found to have a preferred orientation, although the strength of the preference varied with sample. The orientation index's measured varied between 0.2 and 0.8 with an average value of 0.54 (with a standard deviation of 0.28) indicating that there is a large variation in structure between samples. However, the *d* spacing was fairly consistent at an average value of 63.8 (0.2) nm.

A stress-strain curve was produced from the force-extension data collected from sample stretching and is shown in Figure 8.1. As mentioned in chapter 7, the experimental method was not optimised for the determination of stretching properties such as Young's modulus or breaking strength. However general information about the stress-strain characteristics of the OFM sample can be determined. Necking was not observed to occur during sample stretching and there is no indication of its occurrence from the results in Figure 8.1.

Stretching of OFM showed that the relationship between stress and strain was approximately linear, indicating a constant elasticity. From the slope of the curve the modulus of elasticity was calculated to be approximately 38 N/mm^2. This is comparable to that provided in literature of 44 N/mm^2 (Floden *et al.* 2011).

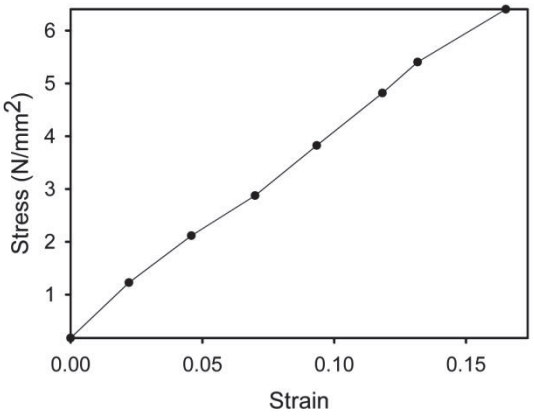

Figure 8.1: Graph of stress versus strain for a sample of OFM.

During uni-axial stretching there were changes to both the orientation index and *d* spacing of the sample, as seen in Figure 8.2. There was a substantial increase in the orientation index of the sample, increasing from an initial value of 0.24 to 0.51 prior to failure. Similarly the increase in *d* spacing was also substantial, increasing from 63.5 to 68.0 nm during stretching, which equated to an extension of 7%.

Initially, application of strain resulted in an increase in the orientation index of the sample with only slight changes in the *d* spacing being recorded. Increased strain resulted in significant changes occurring to the *d* spacing, while changes in the orientation index became less significant. The orientation index increased significantly before strain levels of 0.07, stress of 2.9 N/mm^2, after which the orientation index continued to increase but at a slower rate. The *d* spacing gradually increased following the application of strain, with significant increases occurring above strain levels of around 0.09 (stress of 3.8 N/mm^2).

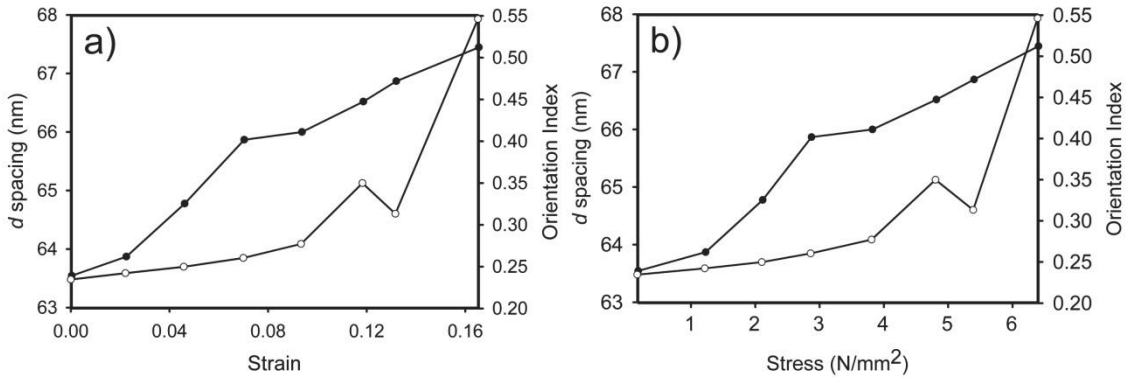

Figure 8.2: *d* spacing and orientation versus a) strain and b) stress for a sample of OFM. *d* spacing: open circle; OI: closed circle.

8.3 Discussion

Unstrained OFM samples displayed a large variation in the measured orientation index. This indicates that there is a large variability in material, presumably due to natural variation in the source material as opposed to changes caused during processing. This is probably due to the variation in the magnitude and direction of forces experienced by the material in different areas of the stomach.

The *d* spacing of unstrained OFM is significantly lower than those recorded for ovine leather samples. This is not unexpected as different tissues have different *d* spacing values. Although both products are produced from ovine tissue, OFM is produced from

forestomach while leather is produced from skin. Despite this, the *d* spacing for OFM is quite similar to that recorded for bovine leather.

The OFM sampled exhibited a linear stress-strain relationship. This relationship is different to those of most of the leather samples analysed, excluding flat grain samples, and is also different from those reported in literature for OFM, where samples displayed a 'J' type curve (Floden *et al.* 2011).

The response of OFM to strain is similar to that of flat leather samples rather than cross-sectional leather samples. This is expected, as this was the same relative dimension analysed as the flat leather samples. The initial and final orientation index values are also similar to those measured for flat grain samples. The orientation index continued to increase throughout the stretching process in a manner similar to that of the flat leather samples. Similarly, the *d* spacing began to increase at relatively low strain rates, around 0.05.

There was a substantial increase in *d* spacing during stretching of the OFM material (approximately 4.5 nm), equating to an extension of 7%. This extension is much greater than that recorded for leather samples under strain, indicating that the collagen fibres in OFM can withstand greater levels of extension prior to failure. This is not surprising as large forces would naturally occur to the stomach.

8.4 Conclusion

The response of OFM to uni-axial strain is similar to that of leather. When strain was first applied, the collagen fibrils reoriented to become more aligned in the direction of the strain with very little extension of the collagen fibrils themselves. As strain increased the rate of reorientation decreased, with more strain being taken up by the extension of individual collagen fibrils.

CHAPTER 9 CONCLUSIONS

9.1 Research Overview

The purpose of this investigation was to gain a better understanding of the relationship between the fibrillar collagen structure and strength of ovine leather. Fibrillar collagen is a major component of leather and it has been suggested that the physical properties of leather may be related to its structure. Advances in SAXS detection have allowed the fibrillar collagen structure of leather to be investigated in greater detail than has been previously possible. The investigation and quantification of the fibrillar collagen structure of leather and its relationship to strength has therefore been the subject of this work.

The most significant finding of this work is the discovery of a linear relationship between the orientation of collagen fibrils and tear strength of leather samples. This work shows that in stronger leather the collagen fibrils are aligned mostly parallel to the plane of the leather surface (high orientation index) while weaker leather has more collagen fibrils out of this plane (low orientation index). Most significantly, the orientation index was found to correlate with the normalised tear strength of cross-sectional samples, not only of ovine leather but also when bovine leather samples were included in the data set. This relationship was also found to be significant at all positions measured across the skin.

It is thought that the relationship between orientation index and tear strength is due to the mechanism of failure in tear tests. Failure follows the path of least resistance, with tearing occurring either by separating fibres, attached by a degree of cross-linking and entanglement, or by causing the failure of individual fibres. When fibrils are aligned with the direction of tear (low cross-sectional OI), tearing would occur by the process of fibre separation. But if fibrils were aligned perpendicular to the direction of tearing (high cross-sectional OI) failure must occur by tearing individual fibres, a process that requires significantly more force. In this way a greater force would be required to tear samples with a high OI in the cross-sectional direction.

While this finding is obviously significant for leather manufacturing, it could also be important to other products derived from tissue that maintain their native fibrillar collagen

structure, if this relationship extends to other tissues. For example, methods could be developed to increase the strength of ECM products without the addition of cross-linking agents.

Tear strength was found to not correlate with the average amount of collagen in the samples or the orientation of collagen fibrils in the direction of the leather surface. These findings are also important for leather processing as it means that the affect of processing on these properties, or the initial state of these properties in the raw skin, will not affect the tear strength of the finished leather.

This work showed that the structure of ovine leather is reasonably consistent across the skin of the animal. This is encouraging as it indicates that the location on the skin chosen in manufacturing for ovine leather may be less important than for bovine and some other hides.

Significant changes occur to ovine skins during leather processing. The changes that occur are not just localised to the addition and removal of specific compound but also result in changes to the arrangement and structure of collagen fibrils. Results show that significant changes to the orientation index occur, with a decrease being measured during pickling followed by an increase during the remaining processing stages. Interestingly, the *d* spacing also changed during processing. An understanding of the changes that occur to the fibrillar collagen structure of the skin during processing are important. By understanding the changes that occur at each stage, stages that have an important affect on the final leather structure can be identified and investigated in more detail.

Investigations into the changes that occur to the fibrillar collagen structure of leather during stretching provided information on the response of leather to strain. When leather is initially placed under strain the fibres undergo reorientation and become more aligned. At higher strain levels the rate of reorientation decreases and instead strain is transferred to individual fibres. Stress is more evenly spread to individual fibrils across cross-sections in stronger samples than in weaker samples. This indicates that weak leather samples are unable to spread stress uniformly across the leather thickness, resulting instead in concentrations of stress at certain sites, which results in samples failing at lower strain levels.

The response of a different processed collagen-rich material, OFM, to uni-axial strain was found to be similar to that of leather. Initial strain resulted in the reorientation of collagen

fibrils, to be more aligned in the direction of the strain, with very little extension of the collagen fibrils themselves. As stress increased the rate of reorientation decreased, instead greater stress levels resulted in the extension of individual collagen fibrils. This response shows that the mechanisms that occur as a response to stretching in leather also occur in other processed collagen-rich material.

Many of the aims of this research, outlined in chapter 1, have been achieved. However, some have not been fully realised, in particular the aim to understand the basis for strength in leather. The relationship between structure and strength in leather has been investigated, resulting in a greater understanding of this relationship but there are still obviously other factors affecting strength that were not identified in this work.

9.2 Directions for Future Research

While this work has increased the understanding of the relationship between fibrillar collagen structure and tear strength in ovine leather there are still many areas where more investigation is required. Given the broad nature of this investigation there were areas of research where more detailed research would be advantageous. This study also produced results that would benefit from further investigation. Suggested areas of further research include;

- SAXS patterns were analysed in the region of high *q* to determine information about the fibrillar collagen structure of the samples. SAXS patterns also include a great deal of information about collagen structure in the low *q* region including information about collagen fibre diameter. It is thought that the analysis of this information would increase the understanding of the relationship between fibrillar collagen structure and tear strength in ovine leather.
- Analysis showed that the tear strength of the OSP was affected by sampling direction and that the relationship between orientation index and tear strength was different in OSP cross-sections cut perpendicular to the backbone to all other positions studied. Greater investigation into the structure at this position is needed. If samples were taken at a range of angles in relation to the backbone at this position the variation of structure and strength with direction in this position could be investigated in more detail.

- Despite there being no strong relationships between *d* spacing and amount of collagen with tear strength, there was found to be a variation in both the *d* spacing and amount of collagen in the corium between weak and strong ovine leather samples. Therefore a more detailed investigation into the structure of the corium may increase understanding of the relationship between fibrillar collagen structure and tear strength in ovine leather.
- An investigation into how samples taken at different stages of leather processing respond to strain would provide more information on how changes in structure affect the response of collagen-rich material to strain. Variation in the response to strain at different stages of processing would assist in identifying the effect of the presence of compound such as cross-linking agent and fat liquors.
- An investigation into how variations in processing steps during leather production affect fibrillar collagen structure and the response to strain would be beneficial. For example; how variation in the concentration and type of cross-linking agents and variation of fat liquoring levels affects the collagen structure and how it affect the materials response to strain.
- An investigation into the changes that occur to the relative distribution of the meridional intensities of SAXS patterns produced by samples under stain is recommended. This could help to identify the mechanism responsible for the changes in *d* spacing that was found to occur to samples under strain. Constant intensity distribution during strain would indicate that all the bonds in the helix were being extended, while the sliding of molecules would result in changes in these relative intensities.

Some of these suggestions are expected to be taken up by the PhD project that is following on from this work.

CHAPTER 10 APPENDICIES

10.1 Appendix I: Publications

This appendix contains copies of publications based on my work. These works are listed below.

10.1.1 Journal Articles

Sizeland, K. H., Basil-Jones, M. M., Edmonds, R. L., Cooper, S. M., Kirby, N., Hawley, A., Haverkamp, R. G. (2013) Collagen Orientation and Leather Strength for Selected Mammals. *Journal of Agricultural and Food Chemistry,* **61**(4), 887-892

Basil-Jones, M. M., Norris, G.E., Edmonds, R. L., Haverkamp, R.G. (2012) Collagen Fibril Alignment and Deformation during Tensile Strain of Leather: A SAXS Study. *Journal of Agricultural and Food Chemistry,* **60**(5), 1201-1208

Basil-Jones, M. M., Norris, G.E., Edmonds, R. L., Cooper, S. M., Haverkamp, R.G., (2011) Collagen Fibril Orientation in Ovine and Bovine Leather Affects Strength: A Small Angle X-ray Scattering (SAXS) Study. *Journal of Agricultural and Food Chemistry,* **59**(18), 9972-9979

Floden, E. W., Malak, S., Basil-Jones, M. M., Negron, L., Fisher, M., Lun, S., Dempsey, S. G., Haverkamp, R. G., Ward, B. R., May, B. C. (2011) Biophysical Characterization of Ovine Forestomach Extracellular Matrix Biomaterials. *Journal of Biomedical Materials Research Part B,* **96B**(1), 67-75

Basil-Jones, M. M., Edmonds, R. L., Allsop, T. F., Cooper, S. M., Holmes, G., Norris, G. E., Cookson, D. J., Kirby, N., Haverkamp, R. G. (2010) Leather Structure Determination by Small Angle X-ray Scattering (SAXS): Cross Sections of Ovine and Bovine Leather. *Journal of Agricultural and Food Chemistry,* **58**(9), 5286-5291

10.1.2 Conference

Richard G. Haverkamp, Melissa M. Basil-Jones, Katie H. Sizeland, Richard L. Edmonds "SAXS Structural Studies of Collagen Materials" Australian Synchrotron User Meeting, Melbourne, 29-30 December 2012

Katie H. Sizeland, Melissa M. Basil-Jones, Richard L. Edmonds, Richard G. Haverkamp "SAXS of Leather Reveals a Structural Basis for Strength" Australian Synchrotron User Meeting, Melbourne, 29-30 December 2012

Richard G. Haverkamp, Melissa M. Basil-Jones, Richard L. Edmonds, Gillian E. Norris "Alignment and Stretching of Collagen Fibrils in Leather" Australian Synchrotron Users Conference, Melbourne, 3-4 December 2011

Richard G. Haverkamp, Melissa M. Basil-Jones, Richard L. Edmonds "A SAXS study of the relationship of collagen fibril orientation in leather with strength" NZIC conference, Hamilton, 27 November – 1 December 2011

Richard L. Edmonds, Timothy F. Allsop, Geoff Holmes, Sue M. Cooper, Melissa M. Basil-Jones, Richard G. Haverkamp "A novel low sulphide process for improved ovine leather quality", XXXI IULTCS Congress, Valencia, 27-30 September 2011

Melissa M. Basil-Jones, Richard G. Haverkamp, "The relationship between ovine leather structure and strength from an X-ray scattering sturdy" 62nd Annual LASRA conference, Palmerston North, 11-12 August 2011

Richard G. Haverkamp, Melissa M. Basil-Jones, "Fibrilar collagen structure determination of cross-sections of ovine leather using Small-Angle X-ray Scattering (SAXS)" Pacifichem 2010, Honolulu, 15-20 December 2010

Richard L. Edmonds, Melissa M. Basil-Jones, Richard G. Haverkamp "Understanding leather through understanding structure" 61st Annual LASRA conference, Napier, 26-27 August 2010

JOURNAL OF AGRICULTURAL AND FOOD CHEMISTRY

Article

pubs.acs.org/JAFC

Collagen Orientation and Leather Strength for Selected Mammals

Katie H. Sizeland,[†] Melissa M. Basil-Jones,[†] Richard L. Edmonds,[‡] Sue M. Cooper,[‡] Nigel Kirby,[§] Adrian Hawley,[§] and Richard G. Haverkamp*[,†]

[†]School of Engineering and Advanced Technology, Massey University, Private Bag 11222, Palmerston North, New Zealand 4442

[‡]Leather and Shoe Research Association of New Zealand, P.O. Box 8094, Palmerston North, New Zealand 4446

[§]Australian Synchrotron, Melbourne, Australia

ABSTRACT: Collagen is the main structural component of leather, skin, and some other applications such as medical scaffolds. All of these materials have a mechanical function, so the manner in which collagen provides them with their strength is of fundamental importance and was investigated here. This study shows that the tear strength of leather across seven species of mammals depends on the degree to which collagen fibrils are aligned in the plane of the tissue. Tear-resistant material has the fibrils contained within parallel planes with little crossover between the top and bottom surfaces. The fibril orientation is observed using small-angle X-ray scattering in leather, produced from skin, with tear strengths (normalized for thickness) of 20−110 N/mm. The orientation index, 0.420−0.633, is linearly related to tear strength such that greater alignment within the plane of the tissue results in stronger material. The statistical confidence and diversity of animals suggest that this is a fundamental determinant of strength in tissue. This insight is valuable in understanding the performance of leather and skin in biological and industrial applications.

KEYWORDS: *collagen, orientation, alignment, leather, strength, SAXS*

INTRODUCTION

The strength of collagen materials is of crucial importance in both medical and industrial contexts. Collagen is the main structural component of skin,[1] leather, and some medical scaffolds.[2] Medical conditions can arise when tissues do not have the required mechanical strength, such as in aneurysms,[3] cervical insufficiency,[4] osteoarthritis,[5] and damaged articular cartilage.[6] In addition, bone is a composite material in which the structure of collagen is considered to be important for bone toughness.[7,8] Strength is also a requirement for collagen-based medical materials such as extracellular matrix scaffolds[2] and processed pericardium for heart valve repair.[9] Leather, which is processed skin consisting mostly of collagen, is produced on a large scale for shoes, clothing, and upholstery,[10] with high strength being a primary requirement for high-value applications.

Factors that have previously been considered as possibly contributing to the strength of collagenous materials include the amount of collagen present, the molecular structure of the collagen (D-spacing, collagen type), the nature of the cross-linking between collagen,[11] collagen bundle size, and collagen orientation. Of these, much attention has been given to collagen orientation. Most collagen tissues are anisotropic, and it is understood that this is a result of the nonuniform requirements for mechanical performance and the consequence of the growth in volume of the animal. Collagen orientation has therefore been investigated in the cornea,[12,13] heart valve tissue,[14] pericardium,[15] bladder tissue,[16] skin,[17] and aorta.[18]

Crimp, the sinuous arrangement of fiber bundles, has been associated with high strength in tendons[19] as well as in heart valves,[20] with high crimp resulting in high strength. However, in studies of skin (leather) of various strengths, crimp was not observed.[21]

Collagen orientation has been measured by reflection anisotropy,[22] atomic force microscopy,[23] small-angle light scattering,[24] confocal laser scattering,[25] Raman polarization,[26] anisotropic Raman scattering,[27] multiphoton microscopy,[28] and small-angle X-ray scattering (SAXS).[21,29,30]

Our recent study of ovine and bovine leathers of differing strengths[21] found a statistically significant relationship between tear strength and edge-on orientation, and we speculated that this trend may be of a more general nature. We have now measured fibril orientation in seven species of mammals to see if this relationship is found more widely. We used SAXS at a modern synchrotron facility, which allows analysis of a small area (250 × 80 μm), and therefore easy measurement of fibril orientation edge-on in tissues that are of limited thickness;[21] such measurements are difficult to make quantitatively by other methods.

EXPERIMENTAL PROCEDURES

Skins were processed to produce leather by the following procedure. After mechanical removal of adhering fat and flesh, conventional lime sulfide paint, comprising 140 g/L sodium sulfide, 50 g/L hydrated lime, and 23 g/L pre-gelled starch thickener, was applied to the flesh side of the skin at 400 g/m^2. The skin was incubated at 20 °C for 16 h and the keratinaceous material manually removed. The skin was then washed to remove the lime, and the pH was lowered to 8 with ammonium sulfate, followed by the addition of 0.1% (w/v) Tanzyme (a commercial bate enzyme). After 75 min at 35 °C, the treated skin was washed and then pickled (20% w/v sodium chloride and 2% w/v sulfuric acid). Pickled pelts were degreased (4% nonionic surfactant; Tetrapol LTN,

Received: October 31, 2012
Revised: December 23, 2012
Accepted: January 8, 2013
Published: January 8, 2013

Shamrock, New Zealand) at 35 °C for 90 min and then washed. The skins were neutralized in 8% NaCl, 1% disodium phthalate solution (40% active; Feliderm DP, Clariant, UK), and 1% formic acid for 10 min. The running solution was then made up to 5% chrome sulfate (Chromosal B, Lanxess, Germany) and processed for 30 min followed by 0.6% magnesium oxide addition, based on the weight of the skins, to fix the chrome, and processed overnight at 40 °C. These wet-blue pelts were neutralized in 1% sodium formate and 0.15% sodium bicarbonate for 1 h and then washed, followed by retanning with 2% synthetic retanning agent (Tanicor PW, Clariant, Germany) and 3% vegetable tanning (mimosa; Tanac, Brazil). Six percent mixed fatliquors were added and the leathers maintained at 50 °C for 45 min, followed by fixing with 0.5% formic acid for 30 min and washing in cold water.

Tear strengths were measured for all samples using standard methods.[31] Samples were cut from the leather at the official sampling position (OSP).[32] The samples were then conditioned at a constant temperature and humidity (20 °C and 65% relative humidity) for 24 h and then tested on an Instron 4467 (Figure 1).

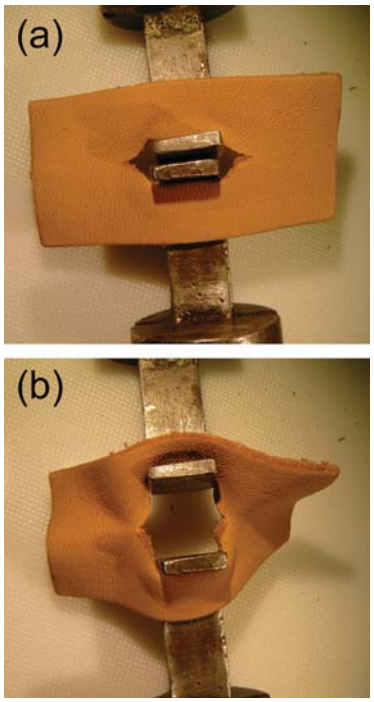

Figure 1. Tear test on a leather sample: (a) at start of test; (b) part way through test.

Samples were prepared for SAXS analysis by cutting strips of leather of 1 × 30 mm from the OSP.[32] Each sample was mounted, without tension, in the X-ray beam to obtain scattering patterns for two orthogonal directions through the leather. For the edge-on analyses measurements were made every 0.25 mm with the samples analyzed from the grain to the corium. For when the beam was directed flat-on (normal to) the surface of the leather, standard samples were cut parallel to the surface, producing a grain sample and a corium sample. These were mounted with the uncut face of the leather directed toward the X-ray beam, and four measurements were made per sample, in a rectangular grid. Diffraction patterns were recorded on the Australian Synchrotron SAXS/WAXS beamline, using a high-intensity undulator source. Energy resolution of 10^{-4} was obtained from a cryocooled Si(111) double-crystal monochromator, and the beam size (fwhm focused at the sample) was 250 × 80 μm, with a total photon flux of about 2×10^{12} ph/s. Diffraction patterns were recorded with an X-ray energy of 8 keV using a Pilatus 1 M detector with an active area of 170 × 170 mm and a sample-to-detector distance of 3371 mm. Exposure time for the diffraction patterns was 1 s, and data processing was carried out using SAXS15ID software.[33]

The orientation index (OI) is defined as (90° − OA)/90°, where OA is the minimum azimuthal angle range, centered at 180°, that contains 50% of the microfibrils.[34,35] OI provides a measure of the spread of microfibril orientation. In the limit, an OI approaching 1 indicates that the microfibrils are parallel to each other and the leather surface, whereas an OI of 0 indicates the microfibrils are randomly oriented. We have calculated the OI from the spread in azimuthal angle of the D-spacing peak, which occurs at around 0.059−0.060 Å^{-1}. Each OI value presented here represents the average of 14−36 measurements of one sample. For edge-on mounted samples these measurements were taken at 0.25 mm intervals from the corium to the grain so that the whole thickness of the sample was covered. For flat-on measurements these were taken on a number of points in a grid pattern. For the sheep and cattle samples the averages are derived from 228, 249, and 167 measurements from 15, 14, and 10 samples, respectively, and have been reported previously.[21]

It is not necessary that the samples are highly representative of the particular animal species for general strength−structure relationships to be studied; that there is a range of skins with different strengths is important, although the observed strengths for each species are within industry norms.

The D-spacing was determined for each pattern by taking the central position of several of the collagen peaks, dividing these by the peak order (usually from n = 5 to n = 10), and averaging the resulting values.

RESULTS

The SAXS patterns display rings representing the collagen fibril repeating structure (Figure 2a). The integrated intensity of the whole pattern enables the position of these peaks to be clearly identified (Figure 2b), and from these the D-spacing is

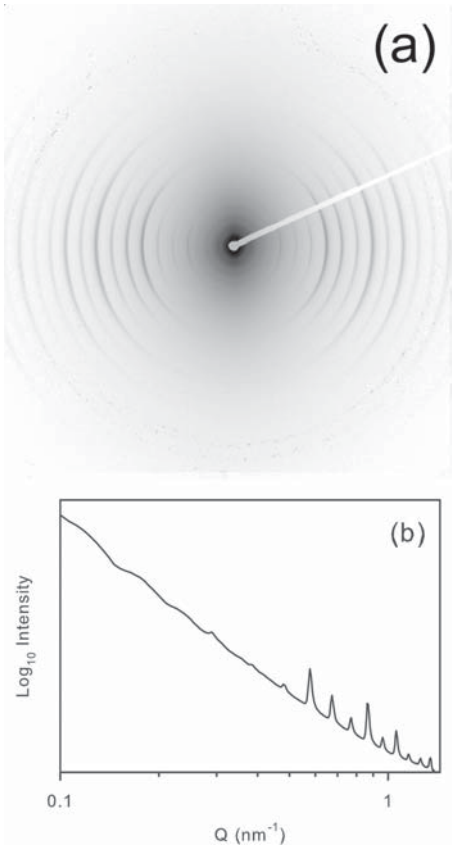

Figure 2. SAXS analysis of leather: (a) raw SAXS pattern; (b) integrated intensity of a whole pattern.

dx.doi.org/10.1021/jf3043067 | J. Agric. Food Chem. 2013, 61, 887−892

determined. The D-spacing varied from 0.628 to 0.653 nm (Figure 3), but there is no significant correlation between D-spacing and strength.

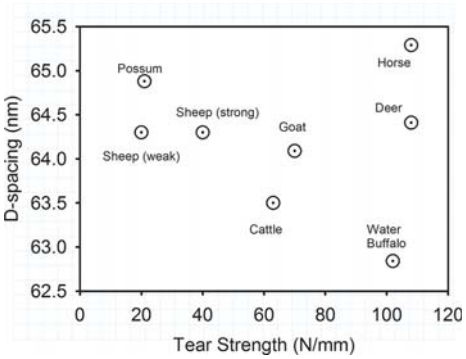

Figure 3. Collagen D-spacing and tear strength for leather from different animals.

For any of the rings visible in the SAXS pattern, which correspond to a peak in the meridional angle, the variation in intensity with azimuthal angle can be plotted (Figure 4), which gives a quantitative measure of fibril orientation, represented here as an OI.

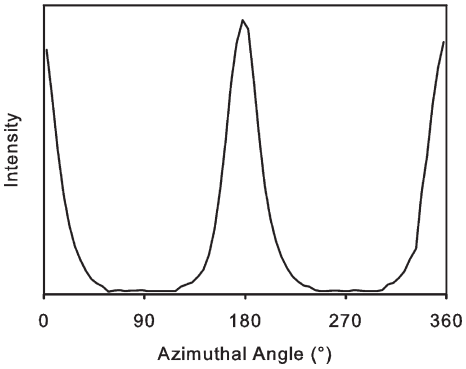

Figure 4. Azimuthal variation in intensity at one value of Q (one collagen peak).

There is a large difference in OI between the measurements taken normal to the leather surface and measurements taken edge-on to the leather. The OI normal to the surface is in the range 0.18−0.35, with the exception of horse leather (Figure 5a), whereas for the edge-on measurements the range is 0.41−0.63 (Figure 5b). Therefore, the major component of fibril alignment is planar.

We find that there is a strong correlation between tear strength and OI (Table 1; Figure 5b) for the edge-on measurements, with a least-squares fitted slope of 0.0024 mm/N ($n = 8$, $r^2 = 0.98$, $P < 0.0001$). This is a remarkably good correlation. Edge-on analysis provides a measure of fibril orientation not frequently accessed. It conveys the degree to which the collagen fibrils are organized in parallel planes as opposed to crossing between the top and bottom surfaces of the skin.

For the measurements on the flat, if we exclude horse leather as an outlier, then there is little correlation between tear strength and OI (Figure 5a) with a least-squares fitted slope of 0.0003 mm/N ($n = 7$, $r^2 = 0.06$, $P = 0.60$), suggesting the slight possibility of a negative correlation. This is the more widely used direction of analysis for collagen fibril orientation measurements.

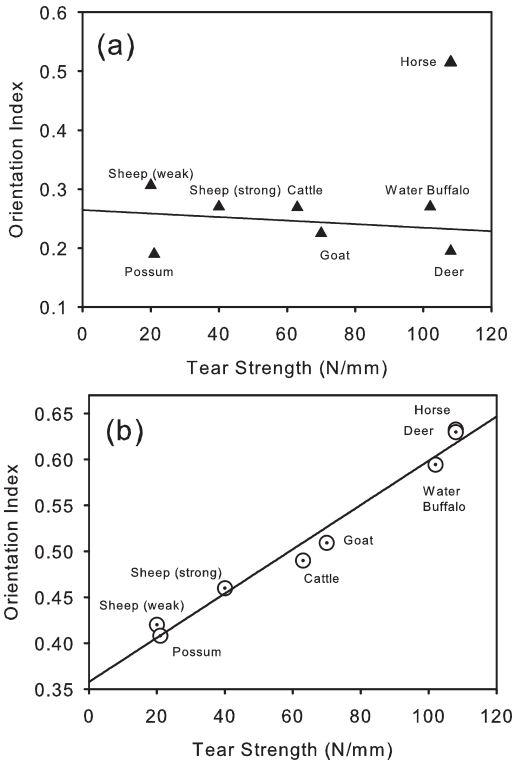

Figure 5. Collagen fibril orientation and tear strength for leather from different animals: (a) measured flat-on; (b) measured edge-on.

Table 1. Leather Tear Strength Compared with Orientation Index (OI) of Collagen Fibrils[a]

animal		tear strength normalized for thickness (N/mm)	OI measured edge-on (average through thickness)
sheep (selected weak)	*Ovis aries*	20	0.420
possum	*Trichosurus vulpecula*	21	0.408
sheep (selected strong)	*Ovis aries*	40	0.460
cattle	*Bos primigenius taurus*	63	0.490
goat	*Capra aegagrus hircus*	70	0.509
water buffalo	*Bubalus bubalis*	102	0.595
deer	*Cervus elaphus*	108	0.630
horse	*Equus ferus caballus*	108	0.633

[a]OI values are the average taken across the thickness of one sample (about 5−10 points) except for sheep and cattle, where these are an average of 6−10 leather samples with 5−10 analysis points for each.

DISCUSSION

D-Spacing. The D-spacing of collagen is known to vary with age,[36] but it has not, to the knowledge of the authors, been linked with mechanical strength. We also do not find a link with strength, therefore supporting the current understanding, although we find a large variation in D-spacing across a large range of strength (Figure 3).

Orientation and Strength. Collagen orientation shows a strong correlation with tear strength when measured edge-on, and this relationship is represented in part by existing models. A relationship between fiber alignment and tensile strength has

dx.doi.org/10.1021/jf3043067 | J. Agric. Food Chem. 2013, 61, 887−892

been modeled previously, where strength is due to the sum of the components of the fibrils that lie in the direction of force in addition to a component due to the other matrix materials.[37] This relationship is represented by eq 1

$$E_z = E_f v_f \int_0^{2\pi} \int_0^{\pi/2} \cos^4 \theta F(\theta, \phi)\, d\theta\, d\phi + (1 - v_f) E_m \quad (1)$$

where E_z is the composite Young's modulus of the material in direction z, E_f and E_m are the Young's moduli of the fibers and matrix, respectively, v_f is the volume fraction of the fibers, and $F(\theta,\phi)$ is the angular distribution function, where θ and ϕ are orthogonal.

This model has been applied to just the measured fibrous collagen, neglecting the contribution from matrix materials, to give an OI, which here we will call OI′ to distinguish it from the differently formulated OI[29,38] (eq 2).

$$OI' = \frac{\int_0^{2\pi} \int_0^{\pi/2} \cos^4 \theta F(\theta, \phi)\, d\theta\, d\phi}{\int_0^{2\pi} \int_0^{\pi/2} F(\theta, \phi)\, d\theta\, d\phi} \quad (2)$$

OI, calculated here from the angle range representing half of the fibrils, can be converted to the integral of $\cos^4\theta$ by numerical methods (where we assume a Gaussian form to the intensity distribution). The OI data plotted for the two orthogonal directions shown in Figure 5 can then be represented as OI′, where, if the model described above is applicable to this system, it should be proportional to the tensile strength. This results in a plot that also correlates with the tear strength data; however, the correlation is poorer than that obtained with the edge-on OI measurements (Figure 6). The fit that includes all data is reasonable ($n = 8$, $r^2 = 0.55$, $P = 0.06$), and this fit improves if the horse data point is removed ($n = 7$, $r^2 = 0.82$, $P = 0.02$). We do not know why horse leather should be an outlier, and this may warrant further investigation. These compare unfavorably with the r^2 of 0.98 for just the OI data edge-on. The reason that this three-dimensional model is a poorer fit than that of the edge-on OI data is considered below.

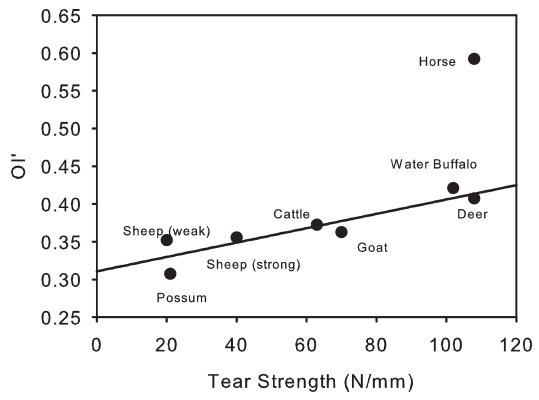

Figure 6. Three-dimensional modeled OI′ based on normalized integral of $\cos^4\theta$.

Alignment and Tear Strength: A More Complex Relationship. Tear strength and tensile strength are related but not identical measures of strength, and it is important to understand the difference between these two measures to be able to relate the model in ref 37 to the tear strength. The basic assumption of the model outlined in ref 37 is that the strength of collagen is along the axis of the fibrils themselves and that the total strength is the simple sum of these fibrils in the direction of tensile force. This is a good model for tensile strength; however, the more useful measure of strength for practical applications of leather is the tear strength, and this does not directly correlate with tensile strength. Tear strength is perhaps analogous to "toughness" in materials.

The ability of leather to resist tear also depends to some extent on the strength perpendicular to the fibril axis, which depends on the strength of the cross-links[11] or the degree of entanglement, and that strength will be less than the strength of the collagen fibrils. However, this appears to be of rather secondary importance compared with fibril alignment. The main component of tear strength for the work presented here is seen to be related to the planar alignment of collagen fibrils. Fibril alignment in the plane has a very strong correlation with tear strength. When the fibrils are not aligned in the plane but instead are perpendicular to the plane (Figure 7a), then any tearing force will need to just separate fibers, pulling in the weakest direction. This arrangement is known as vertical fiber defect and occurs sometimes in Hereford cattle.[38,39] No samples of this type were included in this study.

When the fibrils are rather anisotropic in alignment when measured edge-on (Figure 7b), then the tear strength is likely to be greater than would be found in the vertical fiber defect structure because now there are fibrils running in the direction of the applied force, and maximum strength is obtained when there is a high degree of alignment in this plane (Figure 7c). This trend, depicted in Figure 7 from image a to image c, is what we observe for SAXS measurements over a factor of nearly 5 in strength (Figure 7b), which is a much larger range than has been reported by any other studies.

The reason tear strength does not directly relate to collagen alignment considered in three dimensions (as in eqs 1 and 2) is that tearing is associated with point stresses. To prevent tearing, these point stresses must be resisted. Tearing is used as the industry standard for leather strength because it relates more closely with actual in-service performance than tensile strength. When the tearing process is viewed (Figure 1), looking flat onto

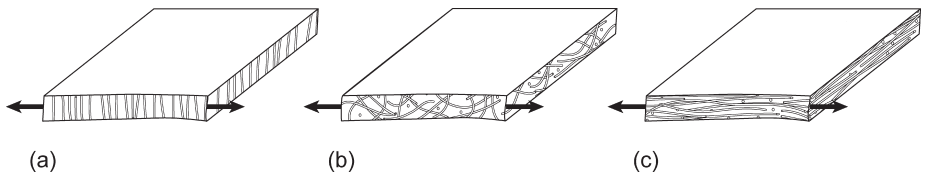

Figure 7. Relationship between collagen orientation index (OI) and strength of skin. OI measured edge-on with orientation that results in leather that is (a) very weak (vertical fiber defect), (b) medium strength (low OI), or (c) strong (high OI). Arrow indicates direction of applied stress in tear measurements.

dx.doi.org/10.1021/jf3043067 | J. Agric. Food Chem. 2013, 61, 887−892

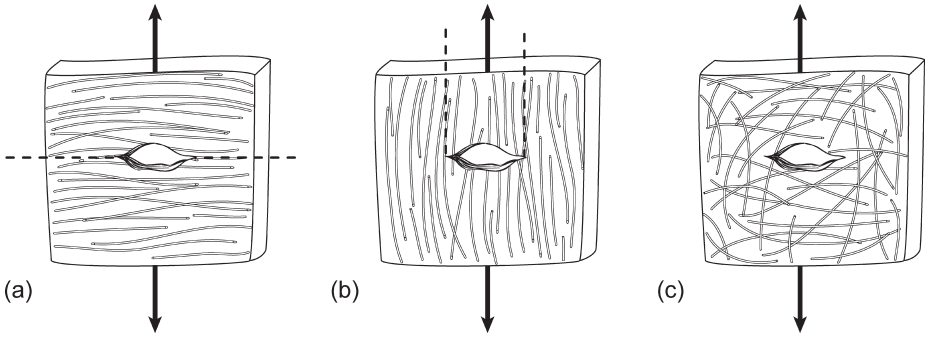

Figure 8. Relationship between collagen orientation index (OI) and strength of skin. OI measured on the flat with orientation that results in leather that is (a) weak (high OI), (b) fairly weak (high OI), (c) strong in all directions. Arrow indicates direction of applied stress in tear measurements. Dashed lines represent probable lines of failure.

the leather, the points where the tearing will occur are at the two ends of the linear cut hole. The fibers that run at right angles to the two edges to the hole (viewed on the flat) resist the tearing process (Figure 8a). However, if all of the fibers run in this direction, then strength may be low due to failure along shear lines (Figure 8b). Therefore, it might be expected that the optimum strength will be associated with a fiber arrangement somewhere between these two extremes, with skin that has a low OI measured in this direction (Figure 8c). Hence, this correlation is one where OI is inversely related to strength, which is what is weakly observed for these leathers (Figure 5a).

Therefore the existing model for strength, where strength depends on the degree of fibril orientation in the direction of stress considering the three-dimensional structure, does not provide an optimal description of the behavior of these materials. It does not take into account the fact that, in practice, a tearing process will follow the weakest part of the structure. The consequence of this is that the direction of the tear front is not well-defined and a degree of anisotropy when viewed flat-on is preferable. The anisotropy, as viewed flat-on, enhances the ability to resist point stresses.

These simplified sketches illustrate the mechanism behind the structure–strength relationship that has been measured for the range of animal skins reported here. What is remarkable is that the relationship between tear strength and edge-on orientation is so quantitative. The strength range across which this relationship holds is much greater than has previously been demonstrated. The correlation also extends across a wide range of mammals.

There is additional information contained in the SAXS patterns that we have not yet analyzed such as the collagen bundle size, which is contained in the low Q region of the pattern. We intend to address this in future work. We are also extending the study to a range of animals from other classes and to other tissue types. We hope, through this work, to build a more complete picture of the structural arrangement of collagen materials and the way in which nature constructs these materials for different applications to provide optimum function. We hope this will lead to an enhanced understanding of the basis of the hierarchical structure of skin and the reasons for the variations between skin from different positions on one animal, between skin of different species, animal classes, and different tissue types. From this study we have found a structural motif that is clearly of primary importance in mammals, but we have not yet demonstrated the generalization of this structural motif to other classes or other tissues.

The work is also being extended to develop an understanding of the changes to the collagen fibrils that take place during the processing of leather. Processing can affect the collagen structure, including both the D-period and the fibril orientation. To understand leather as an industrial material, it is desirable to understand the structural changes that take place as a result of chemical and physical treatments from skin to finished product.

In summary, we have investigated the structure of leather from different mammals to attempt to develop a generalized understanding of structure–strength relationships. We have shown that the tear strength of leather is correlated with collagen fibril orientation parallel to the surface of the leather over a large (factor of 5) range of strengths across seven species of mammals. This has been explained as being due to the strength of the collagen fibrils in their longitudinal axis when suitably arranged to resist the tearing process. This clear demonstration of the structural relationship and consequent insight enables research into other tissues to be better targeted by applying a greater focus to the collagen alignment in plane. We expect that this highly correlated structure–strength relationship extends to tissues other than those studied here.

AUTHOR INFORMATION

Corresponding Author

*E-mail: r.haverkamp@massey.ac.nz.

Funding

This work was supported by the Ministry of Business, Innovation and Employment, New Zealand (Grant LSRX0801). The Australian Synchrotron provided travel funding and accommodation.

Notes

The authors declare no competing financial interest.

ACKNOWLEDGMENTS

This research was undertaken on the SAXS/WAXS beamline at the Australian Synchrotron, Victoria, Australia. David Cookson and Stephen Mudie at the Australian Synchrotron assisted with data collection and processing. Sue Hallas, of Nelson, assisted with editing the manuscript.

REFERENCES

(1) Fratzl, P. *Collagen: Structure and Mechanics*; SpringerScience +Business Media: New York, 2008; Vol. Collagen: Structure and mechanics.

(2) Floden, E. W.; Malak, S.; Basil-Jones, M. M.; Negron, L.; Fisher, J. N.; Byrne, M.; Lun, S.; Dempsey, S. G.; Haverkamp, R. G.; Anderson, I.;

Ward, B. R.; May, B. C. H. Biophysical characterization of ovine forestomach extracellular matrix biomaterials. *J. Biomed. Mater. Res. B* **2010**, *96B*, 67−75.

(3) Lindeman, J. H. N.; Ashcroft, B. A.; Beenakker, J. W. M.; van Es, M.; Koekkoek, N. B. R.; Prins, F. A.; Tielemans, J. F.; Abdul-Hussien, H.; Bank, R. A.; Oosterkamp, T. H. Distinct defects in collagen microarchitecture underlie vessel-wall failure in advanced abdominal aneurysms and aneurysms in Marfan syndrome. *Proc. Natl. Acad. Sci. U.S.A.* **2010**, *107*, 862−865.

(4) Oxlund, B. S.; Ortoft, G.; Bruel, A.; Danielsen, C. C.; Oxlund, H.; Uldbjerg, N. Cervical collagen and biomechanical strength in non-pregnant women with a history of cervical insufficiency. *Reprod. Biol. Endocrin.* **2010**, *8*, 92.

(5) Narhi, T.; Siitonen, U.; Lehto, L. J.; Hyttinen, M. M.; Arokoski, J. P. A.; Brama, P. A.; Jurvelin, J. S.; Helminen, H. J.; Julkunen, P. Minor influence of lifelong voluntary exercise on composition, structure, and incidence of osteoarthritis in tibial articular cartilage of mice compared with major effects caused by growth, maturation, and aging. *Connect. Tissue Res.* **2011**, *52*, 380−392.

(6) Stok, K.; Oloyede, A. A qualitative analysis of crack propagation in articular cartilage at varying rates of tensile loading. *Connect. Tissue Res.* **2003**, *44*, 109−120.

(7) Zimmermann, E. A.; Schaible, E.; Bale, H.; Barth, H. D.; Tang, S. Y.; Reichert, P.; Busse, B.; Alliston, T.; Ager, J. W.; Ritchie, R. O. Age-related changes in the plasticity and toughness of human cortical bone at multiple length scales. *Proc. Natl. Acad. Sci. U.S.A.* **2011**, *108*, 14416−14421.

(8) Skedros, J. G.; Dayton, M. R.; Sybrowsky, C. L.; Bloebaum, R. D.; Bachus, K. N. The influence of collagen fiber orientation and other histocompositional characteristics on the mechanical properties of equine cortical bone. *J. Exp. Biol.* **2006**, *209*, 3025−3042.

(9) Jobsis, P. D.; Ashikaga, H.; Wen, H.; Rothstein, E. C.; Horvath, K. A.; McVeigh, E. R.; Balaban, R. S. The visceral pericardium: macromolecular structure and contribution to passive mechanical properties of the left ventricle. *Am. J. Physiol.−Heart C* **2007**, *293*, H3379−H3387.

(10) Commodities and Trade Division, FAO, United Nations. *World Statistical Compendium for Raw Hides and Skins, Leather and Leather Footwear 1990−2009*; Rome, Italy, 2010.

(11) Chan, Y.; Cox, G. M.; Haverkamp, R. G.; Hill, J. M. Mechanical model for a collagen fibril pair in extracellular matrix. *Eur. Biophys. J.* **2009**, *38*, 487−493.

(12) Boote, C.; Kamma-Lorger, C. S.; Hayes, S.; Harris, J.; Burghammer, M.; Hiller, J.; Terrill, N. J.; Meek, K. M. Quantification of collagen organization in the peripheral human cornea at micron-scale resolution. *Biophys. J.* **2011**, *101*, 33−42.

(13) Kamma-Lorger, C. S.; Boote, C.; Hayes, S.; Moger, J.; Burghammer, M.; Knupp, C.; Quantock, A. J.; Sorensen, T.; Di Cola, E.; White, N.; Young, R. D.; Meek, K. M. Collagen and mature elastic fibre organisation as a function of depth in the human cornea and limbus. *J. Struct. Biol.* **2010**, *169*, 424−430.

(14) Sellaro, T. L.; Hildebrand, D.; Lu, Q. J.; Vyavahare, N.; Scott, M.; Sacks, M. S. Effects of collagen fiber orientation on the response of biologically derived soft tissue biomaterials to cyclic loading. *J. Biomed. Mater. Res. B* **2007**, *80A*, 194−205.

(15) Liao, J.; Yang, L.; Grashow, J.; Sacks, M. S. Molecular orientation of collagen in intact planar connective tissues under biaxial stretch. *Acta Biomater.* **2005**, *1*, 45−54.

(16) Gilbert, T. W.; Wognum, S.; Joyce, E. M.; Freytes, D. O.; Sacks, M. S.; Badylak, S. F. Collagen fiber alignment and biaxial mechanical behavior of porcine urinary bladder derived extracellular matrix. *Biomaterials* **2008**, *29*, 4775−4782.

(17) Purslow, P. P.; Wess, T. J.; Hukins, D. W. L. Collagen orientation and molecular spacing during creep and stress-relaxation in soft connective tissues. *J. Exp. Biol.* **1998**, *201*, 135−142.

(18) Gasser, T. C. An irreversible constitutive model for fibrous soft biological tissue: a 3-D microfiber approach with demonstrative application to abdominal aortic aneurysms. *Acta Biomater.* **2011**, *7*, 2457−2466.

(19) Franchi, M.; Trire, A.; Quaranta, M.; Orsini, E.; Ottani, V. Collagen structure of tendon relates to function. *Sci. World J.* **2007**, *7*, 404−420.

(20) Joyce, E. M.; Liao, J.; Schoen, F. J.; Mayer, J. E.; Sacks, M. S. Functional collagen fiber architecture of the pulmonary heart valve cusp. *Ann. Thorac. Surg.* **2009**, *87*, 1240−1249.

(21) Basil-Jones, M. M.; Edmonds, R. L.; Cooper, S. M.; Haverkamp, R. G. Collagen fibril orientation in ovine and bovine leather affects strength: a small angle X-ray scattering (SAXS) study. *J. Agric. Food Chem.* **2011**, *59*, 9972−9979.

(22) Schofield, A. L.; Smith, C. I.; Kearns, V. R.; Martin, D. S.; Farrell, T.; Weightman, P.; Williams, R. L. The use of reflection anisotropy spectroscopy to assess the alignment of collagen. *J. Phys. D: Appl. Phys.* **2011**, 44.

(23) Friedrichs, J.; Taubenberger, A.; Franz, C. M.; Muller, D. J. Cellular remodelling of individual collagen fibrils visualized by time-lapse AFM. *J. Mol. Biol.* **2007**, *372*, 594−607.

(24) Billiar, K. L.; Sacks, M. S. A method to quantify the fiber kinematics of planar tissues under biaxial stretch. *J. Biomech.* **1997**, *30*, 753−756.

(25) Jor, J. W. Y.; Nielsen, P. M. F.; Nash, M. P.; Hunter, P. J. Modelling collagen fibre orientation in porcine skin based upon confocal laser scanning microscopy. *Skin Res. Technol.* **2011**, *17*, 149−159.

(26) Falgayrac, G.; Facq, S.; Leroy, G.; Cortet, B.; Penel, G. New method for Raman investigation of the orientation of collagen fibrils and crystallites in the Haversian system of bone. *Appl. Spectrosc.* **2010**, *64*, 775−780.

(27) Janko, M.; Davydovskaya, P.; Bauer, M.; Zink, A.; Stark, R. W. Anisotropic Raman scattering in collagen bundles. *Opt. Lett.* **2010**, *35*, 2765−2767.

(28) Lilledahl, M. B.; Pierce, D. M.; Ricken, T.; Holzapfel, G. A.; Davies, C. D. Structural analysis of articular cartilage using multiphoton microscopy: input for biomechanical modeling. *IEEE Trans. Med. Imaging* **2011**, *30*, 1635−1648.

(29) Kronick, P. L.; Buechler, P. R. Fiber orientation in calfskin by laser-light scattering or X-ray-diffraction and quantitative relation to mechanical-properties. *J. Am. Leather Chem. Assoc.* **1986**, *81*, 221−230.

(30) Basil-Jones, M. M.; Edmonds, R. L.; Norris, G. E.; Haverkamp, R. G. Collagen fibril alignment and deformation during tensile strain of leather: a SAXS study. *J. Agric. Food Chem.* **2012**, *60*, 1201−1208.

(31) Williams, J. M. V. IULTCS (IUP) test methods − measurement of tear load-double edge tear. *J. Soc. Leather Technol. Chem.* **2000**, *84*, 327−329.

(32) Williams, J. M. V. IULTCS (IUP) test methods − sampling. *J. Soc. Leather Technol. Chem.* **2000**, *84*, 303−309.

(33) Cookson, D.; Kirby, N.; Knott, R.; Lee, M.; Schultz, D. Strategies for data collection and calibration with a pinhole-geometry SAXS instrument on a synchrotron beamline. *J. Synchrotron Radiat.* **2006**, *13*, 440−444.

(34) Sacks, M. S.; Smith, D. B.; Hiester, E. D. A small angle light scattering device for planar connective tissue microstructural analysis. *Ann. Biomed. Eng.* **1997**, *25*, 678−689.

(35) Basil-Jones, M. M.; Edmonds, R. L.; Allsop, T. F.; Cooper, S. M.; Holmes, G.; Norris, G. E.; Cookson, D. J.; Kirby, N.; Haverkamp, R. G. Leather structure determination by small angle X-ray scattering (SAXS): cross sections of ovine and bovine leather. *J. Agric. Food Chem.* **2010**, *58*, 5286−5291.

(36) Scott, J. E.; Orford, C. R.; Hughes, E. W. Proteoglycan-collagen arrangements in developing rat tail tendon − an electron-microscopical and biochemical investigation. *Biochem. J.* **1981**, *195*, 573−584.

(37) Bigi, A.; Ripamonti, A.; Roveri, N.; Jeronimidis, G.; Purslow, P. P. Collagen orientation by X-ray pole figures and mechanical-properties of media carotid wall. *J. Mater. Sci.* **1981**, *16*, 2557−2562.

(38) Kronick, P. L.; Sacks, M. S. Quantification of vertical-fiber defect in cattle hide by small-angle light-scattering. *Connect. Tissue Res.* **1991**, *27*, 1−13.

(39) Amos, G. L. Vertical fibre in relation to the properties of chrome side leather. *J. Soc. Leather Technol. Chem.* **1958**, *42*, 79−90.

JOURNAL OF AGRICULTURAL AND FOOD CHEMISTRY

Article

pubs.acs.org/JAFC

Collagen Fibril Alignment and Deformation during Tensile Strain of Leather: A Small-Angle X-ray Scattering Study

Melissa M. Basil-Jones,[†] Richard L. Edmonds,[‡] Gillian E. Norris,[§] and Richard G. Haverkamp*[,†]

[†]School of Engineering and Advanced Technology, and [§]Institute of Molecular Biosciences, Massey University, Palmerston North 4442, New Zealand

[‡]Leather and Shoe Research Association, Palmerston North 4442, New Zealand

ABSTRACT: The distribution and effect of applied strain on the collagen fibrils that make up leather may have an important bearing on the ultimate strength and other physical properties of the material. While sections of ovine and bovine leather were being subjected to tensile strain up to rupture, synchrotron-based small-angle X-ray scattering (SAXS) spectra were recorded edge-on to the leather at points from the corium to the grain. Measurements of both fibril orientation and collagen *d* spacing showed that, initially, the fibers reorient under strain, becoming more aligned. As the strain increases (5−10% strain), further fibril reorientation diminishes until, at 37% strain, the *d* spacing increases by up to 0.56%, indicating that significant tensile forces are being transmitted to individual fibrils. These changes, however, are not uniform through the cross-section of leather and differ between leathers of different strengths. The stresses are taken up more evenly through the leather cross-section in stronger leathers in comparison to weaker leathers, where stresses tended to be concentrated during strain. These observations contribute to our understanding of the internal strains and structural changes that take place in leather under stress.

KEYWORDS: *Collagen, SAXS, tissue, skin, synchrotron*

INTRODUCTION

Leather is a remarkable biomaterial that exhibits strength, wear, and aesthetic properties that are hard to match with synthetic materials.[1] It is composed mostly of collagen fibrils that are arranged in a way that confers strength to the material. As a treated form of animal skin, leather is structurally similar to the skin of animals and humans in its natural state[2] and to some other tissues in animals, such as pericardium, cartilage, and tendon. Processed biomaterials, such as the extracellular matrix of ovine forestomach used for tissue regeneration, also have a similar structure.[3]

Ovine leather is weaker than bovine leather of the same thickness, typically half of the strength, making ovine leather a low-value product relative to bovine leather. Previously, we showed how small-angle X-ray scattering (SAXS) investigations of leather can provide detailed structural information on the amount of fibrous collagen, the microfibril orientation, and the *d* spacing.[4] We then showed that there is a correlation between the tear strength in ovine and bovine leather and the orientation of collagen microfibrils in those leathers. Stronger leather is found to have more fibrils aligned with the surface of the leather, with less crossover between layers, than weak leather (i.e., strong leather had a lower angle of weave).[5]

Previous studies have also used SAXS to investigate the structure of collagenous materials, such as those found in tendons,[6,7] bone,[8,9] ligaments,[10] human articular cartilages,[11] breast tissue,[12] mitral valve leaflets,[13] and materials for tissue regeneration scaffolds.[3]

SAXS has also been used to study collagenous materials under tension where changes in *d* spacing[7,14] and orientation[15] have been observed. The building blocks of collagen are pro-collagen molecules, with each one a repeating sequence of $(\text{glycine–X–Y})_n$, where X and Y can be any amino acid and *n* is the number of repeats (usually 100−400). Three pro-collagen molecules arrange in a coiled coil to form a collagen molecule. Several collagen molecules aligned in a quarter-staggered array form a collagen microfibril, which has overlap and gap regions, giving rise to a banding pattern visible by scanning electron microscopy (SEM) or atomic force microscopy (AFM). The distance between these bands is referred to as the *d* spacing and may be obtained from the diffraction pattern.

Leather has been subjected to biaxial stretching and monitored with wide-angle X-ray scattering (WAXS)[16] to observe changes to the fiber orientation measured both normal to the surface and normal to the edge. This study showed an increase in fibril orientation measured normal to the edge during stretching. Another technique, small-angle light scattering, has been used to monitor the effects of collagen fiber orientation during the stretching of bovine pericardium tissue, demonstrating increased fiber alignment when tissue is stretched in parallel to the dominant fiber direction.[17]

In this work, we investigate the changes that take place in the microstructure of leather as a strain is applied, particularly in the direction edge-on to the leather. The objectives of the study are to obtain physical data that can be related to the deformation and failure mechanism of the material. The results will identify physical differences between weak and strong leather and between ovine and bovine leather. They will thus inform the development of new processes to modify ovine leather to better accommodate strain and, therefore, to increase the tear strength to improve the value of the material.

Received: September 29, 2011
Revised: January 5, 2012
Accepted: January 10, 2012
Published: January 10, 2012

dx.doi.org/10.1021/jf2039586 | *J. Agric.Food Chem.* 2012, 60, 1201−1208

EXPERIMENTAL SECTION

Ovine pelts were from 5-month-old, early season lambs of breeds with "black face" lambs, which may include Suffolk, South Suffolk, and Dorset Down. The bovine hides were from 2−3-year-old cattle of a variety of breeds.

Leathers were generated with a variety of properties using a range of processing parameters during both the conventional beamhouse process and then the conventional tanning of the pelts. Specifically, the pelts were depilated using a caustic treatment comprising sodium sulfide (ranging from a slow-acting paint containing 160 g/L flake sodium sulfide to a quick-acting paint containing 200 g/L sodium sulfide) and a saturated solution of calcium hydroxide. Depilated slats were then processed to remove the residual wool in a solution of sodium sulfide ranging in concentration from 0.8 to 2.4% for 8−16 h at temperatures ranging from 16 to 24 °C. After this treatment, the pelts were washed and treated with a proteolytic enzyme, either a bacterial enzyme (Tanzyme, Tryptec Biochemicals, Ltd.) or a pancreatic enzyme (Rohapon ANZ, Shamrock, Ltd.), at concentrations ranging from 0.025 to 0.1%, followed by pickling in a 2% sulfuric acid and 10% sodium chloride solution. The pickled pelts were then pretanned using oxazolidine, degreased with an aqueous surfactant, and then tanned using chromium sulfate. The resulting "wet blue" was then retanned using a mimosa vegetable extract and impregnated with lubricating oil prior to drying and mechanical softening.

Tear strengths of the crust leathers were tested using standard methods.[18] In brief, samples (strips 1 × 50 mm) were cut from the leather at the official sampling positions (OSPs),[19] parallel to the backbone. The bovine leather was shaved, resulting in samples approximately 1.3 mm thick, consisting, on average, of 34% grain and 66% corium. All samples were then conditioned by storing them at a constant temperature and humidity (20 °C and 65% relative humidity, respectively) for 24 h, after which time they were tested on an Instron strength-testing device.

A stretching apparatus was built as follows. A linear motor, Linmot PS01, 48 × 240/30 × 180-C (NTI AG, Switzerland), was mounted on a purpose-built frame with a custom-made clamp fitted to the end of the slider. The clamp was designed not to put a sharp point load on the leather (Figure 1). A L6D aluminum alloy OIML single-point loadcell (Hangzhou Wanto Precision Technology Co., Zhejiang, China) was attached to a second clamp that would hold the other end of the sample and was attached to the frame.

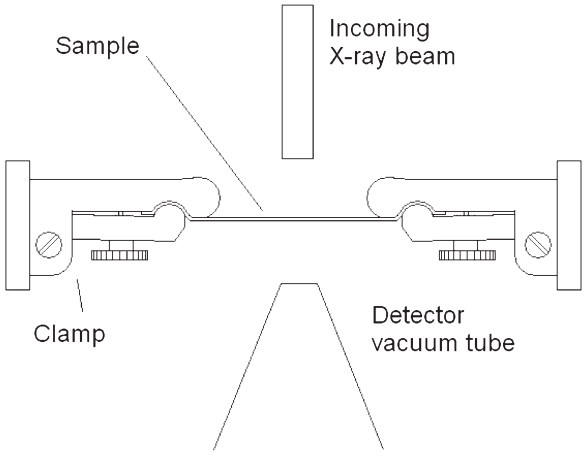

Figure 1. Sketch of the leather-stretching apparatus used for SAXS measurements.

Each leather sample was mounted horizontally between the clamps without tension and then moved into the X-ray beam. The sample was stretched in 1 mm increments until a force was registered by the loadcell. The slider was then moved back 1 mm, so that the sample was again not under tension, and spectra were recorded, with the sample being analyzed edge-on, parallel to the backbone, to allow the load to be correlated with tear strength.[5] Measurements were made, depending upon the mounted orientation of the leather, either normal to the leather surface (flat) in a 0.5 mm grid of four points or edge-on at 0.10 mm intervals across the sample from the grain to the corium. The sample was again stretched 1 mm and maintained at this extension for 1 min to stabilize, before SAXS spectra, the extension, and the force information was recorded. This process was repeated until the sample failed. Note that the flat samples were physically split into two layers, grain and corium, to produce two samples from each piece of leather, before diffraction patterns were recorded.

Diffraction patterns were recorded on the Australian Synchrotron SAXS/WAXS beamline, using a high-intensity undulator source. Energy resolution of 10^{-4} is obtained from a cryo-cooled Si (111) double-crystal monochromator, and the beam size [full width at half maximum (fwhm) focused at the sample] was 250 × 80 μm, with a total photon flux of about 2×10^{12} photons s^{-1}. All diffraction patterns were recorded with an X-ray energy of 11 keV using a Pilatus 1 M detector with an active area of 170 × 170 mm and a sample−detector distance of 3371 mm. Energy calibration used the absorption edge of zinc at 9.659 keV to set the zero angle of the monochromator. This results in energy calibration across the energy range used better than 5 eV and typically better than 2 eV. A diffraction peak of silver behenate is used to scale the camera length. The correct value of q is then calculated by trigonometry for each pixel in each diffraction image. Exposure time for diffraction patterns was 1 s, and data processing was carried out using the SAXS15ID software.[20] No normalization was performed for changes in beam intensity.

Orientation index (OI) is defined as (90° − OA)/90°, where OA is the minimum azimuthal angle range that contains 50% of the microfibrils centered at 180°. OI is used to give a measure of the spread of microfibril orientation (an OI of 1 indicates that the microfibrils are completely parallel to each other, and an OI of 0 indicates that the microfibrils are completely randomly oriented). The OI is calculated from the spread in azimuthal angle of the most intense d-spacing peak (at around 0.059−0.060 $Å^{-1}$).[5]

The d spacing was determined for each spectrum from Bragg's law by averaging the central values of several collagen peaks (usually from n = 5 to 10).

RESULTS

We present here a selection of the data recorded that is representative of the behavior observed in the weak ovine leather (19 or 21 N/mm, normalized for leather cross-section[5]), the stronger ovine leather (39 or 44 N/mm), and in the bovine leather that is stronger still (71 N/mm). An example of a SAXS pattern and the intensity profile are shown in Figure 2. Further details of the data processing may be found in ref 4.

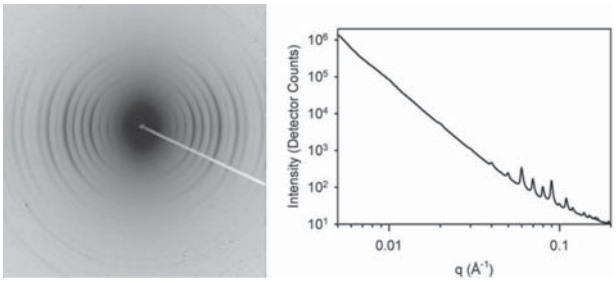

Figure 2. Example of a SAXS pattern of leather (left) and the corresponding intensity profile (right).

Mechanical Properties. Stress response to the applied strain was recorded while the leather samples were mounted edge-on in the SAXS beamline, and strain was applied as

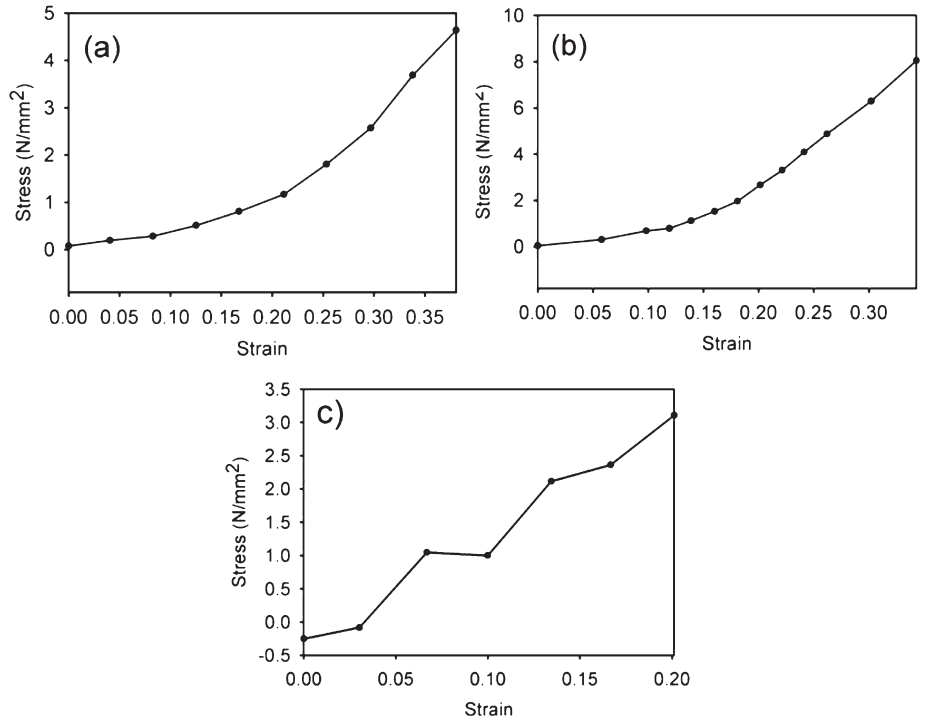

Figure 3. Stress (normalized for the leather cross-section) versus strain (fraction of total unstressed length) curves of leather obtained while SAXS data were collected: (a) weak ovine, 19 N/mm tear strength; (b) stronger ovine, 39 N/mm tear strength; and (c) strong bovine, 71 N/mm tear strength.

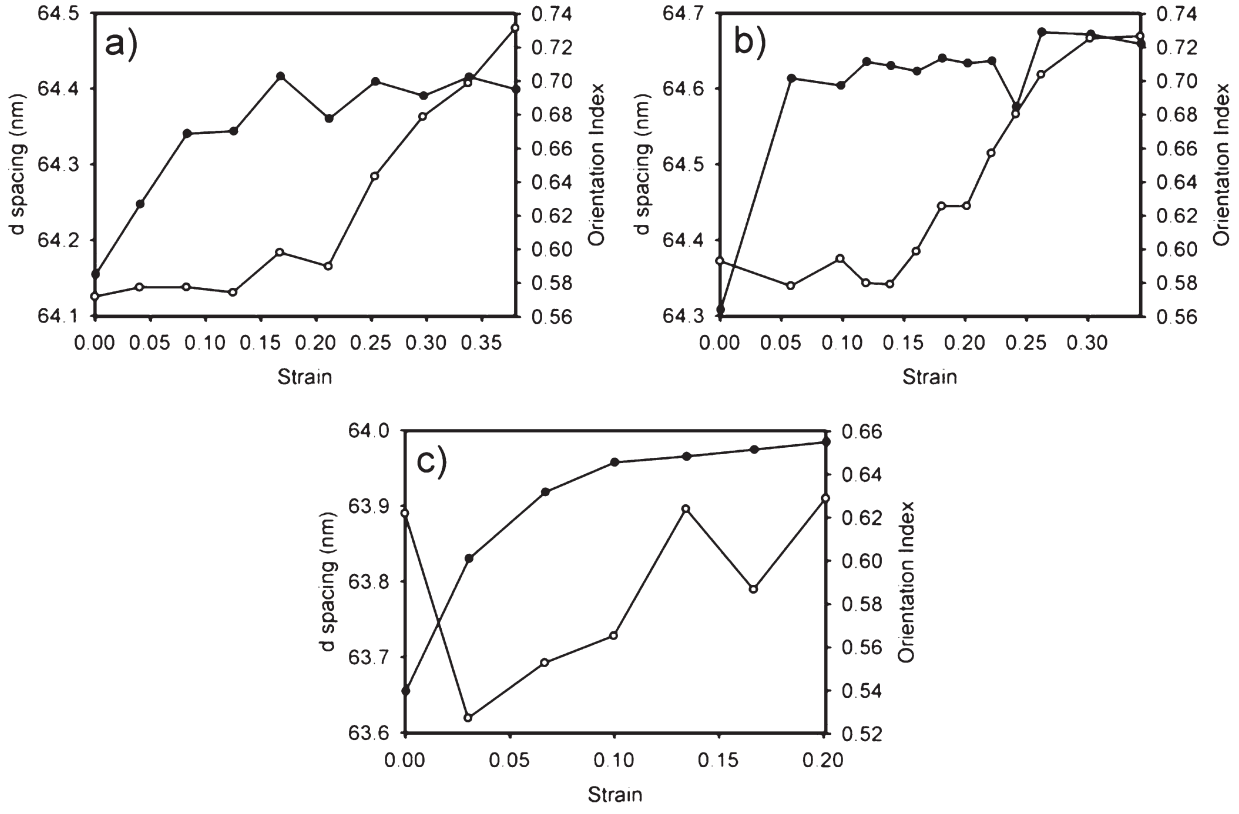

Figure 4. *d* spacing and orientation versus strain measured edge-on, parallel to the backbone: (○) *d* spacing and (●) OI (parallel, OSP) for (a) weak ovine, 19 N/mm tear strength; (b) stronger ovine, 39 N/mm tear strength; and (c) strong bovine, 71 N/mm tear strength.

dx.doi.org/10.1021/jf2039586 | *J. Agric.Food Chem.* 2012, 60, 1201−1208

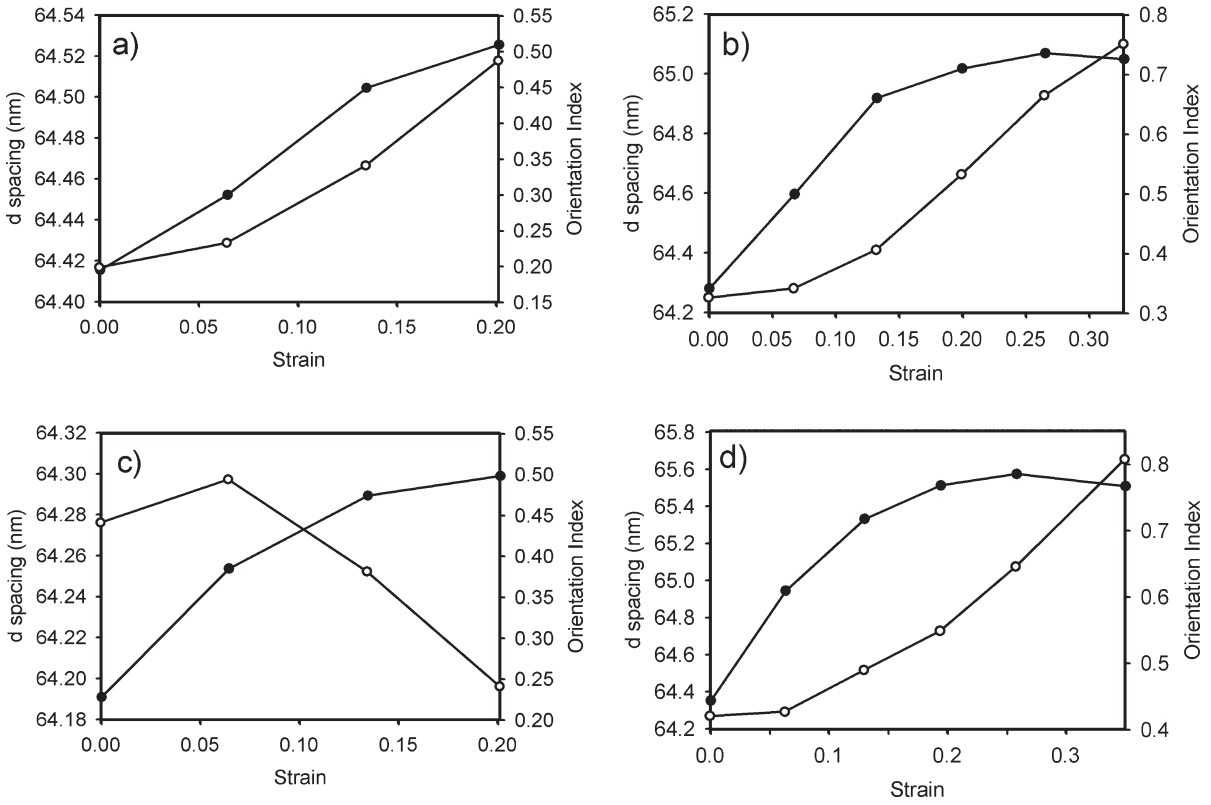

Figure 5. *d* spacing and orientation versus strain measured flat: (○) *d* spacing and (●) OI (parallel, OSP) for (a) weak ovine (21 N/mm tear strength), grain; (b) weak ovine, corium; (c) stronger ovine (44 N/mm tear strength), grain; and (d) stronger ovine, corium.

described in the Experimental Section. The ovine leather became progressively stiffer with stretching, with the slope of the stress strain curve increasing with strain (panels a and b of Figure 3). Qualitatively, the behavior was similar in both weak and stronger ovine leathers. Strong bovine leather did not have such an obvious change in stiffness (Figure 3c), although in the example presented, the strain extended to only 20% (note that strain is dimensionless).

Although the experimental arrangement was not optimized for determining the modulus of elasticity (stiffness) of the leather, it can be obtained from the slope of these plots. The range of the modulus of elasticity was calculated as 2−25 mm^2/N for weak ovine, 5−39 mm^2/N for stronger ovine, and 17 mm^2/N (but only up to 0.20 strain) for strong bovine (panels a, b, and c of Figure 3, respectively). For these leathers, the modulus of elasticity at 0.20 strain was 8, 30, and 15 mm^2/N for weak ovine, stronger ovine, and strong bovine, respectively. These measurements are the tensile stress of very small strips and differ substantially from the tear-strength measurements[18] that are used to determine whether the leather is considered "strong" or "weak".

Fiber Reorientation and Strain. The OI and *d* spacing were plotted as a function of both strain (Figures 4 and 5) and stress (Figures 6 and 7) to better illustrate the observed structural changes and the causes of these changes.

It is clear that there were complementary changes in the orientation and the *d* spacing. With increasing strain, in the edge-on measured samples, OI increased rapidly at first (i.e., with small strain) and then more slowly at larger strain (above about 0.05−0.08 strain). In contrast, the *d* spacing was almost constant at first before increasing steadily above a threshold of about 0.15−0.20 strain (Figure 4). This strain threshold for *d* spacing increase is similar to that reported for gluteraldehyde-treated bovine pericardium tissue.[15]

With measurement on the flat, the OI was much lower initially than when measured edge-on, but it then increased by a large amount as the leather was stretched (Figure 5). These flat measurements have been shown previously not to be correlated strongly with strength,[5] in contrast to edge-on measurements. However, this direction of measurement has been used in other studies of tissue and leather and, therefore, is included here for comparison, although data for only weak and strong ovine were available. With measurement on the flat, the two-stage process observed in the edge-on samples, where the OI changes with increasing strain first, followed later by a *d*-spacing change, was not as apparent, although there was a larger OI change.

In terms of the stress that the leather experienced, the threshold for OI changes measured edge-on occurred between 0.29 and 0.31 N/mm^2, while significant *d*-spacing changes began at approximately 1.2 N/mm^2 (Figure 6). Within the limitations of the data obtained, stress appears to give a more consistent measure of the thresholds at which changes in structure occur. Although it was expected that the *d* spacing would be a good indicator of structural change with increasing strain, it was less obvious that changes in OI could also predict structural differences.

These changes can be interpreted by the strain initially being taken up by reorientation of the fibrils and fibers, followed by fibril stretching (with less reorientation at this stage). The change in OI gives a quantitative measurement of the rearrangement of the fibers, in this case, with the data indicating that the fibers became more aligned. The change

dx.doi.org/10.1021/jf2039586 | J. Agric.Food Chem. 2012, 60, 1201−1208

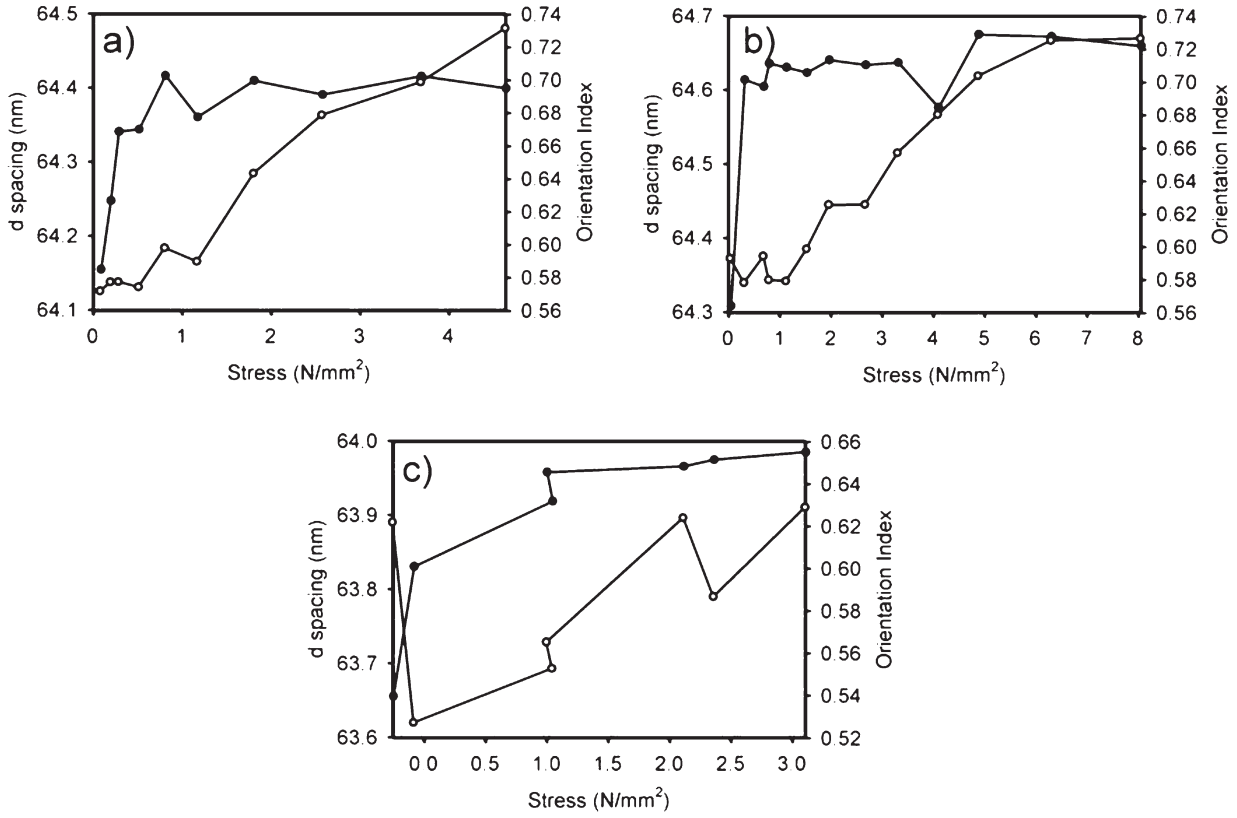

Figure 6. *d* spacing and orientation versus stress measured edge-on parallel to the backbone: (○) *d* spacing and (●) OI (parallel, OSP) for (a) weak ovine, 19 N/mm tear strength; (b) stronger ovine, 39 N/mm tear strength; and (c) strong bovine, 71 N/mm tear strength.

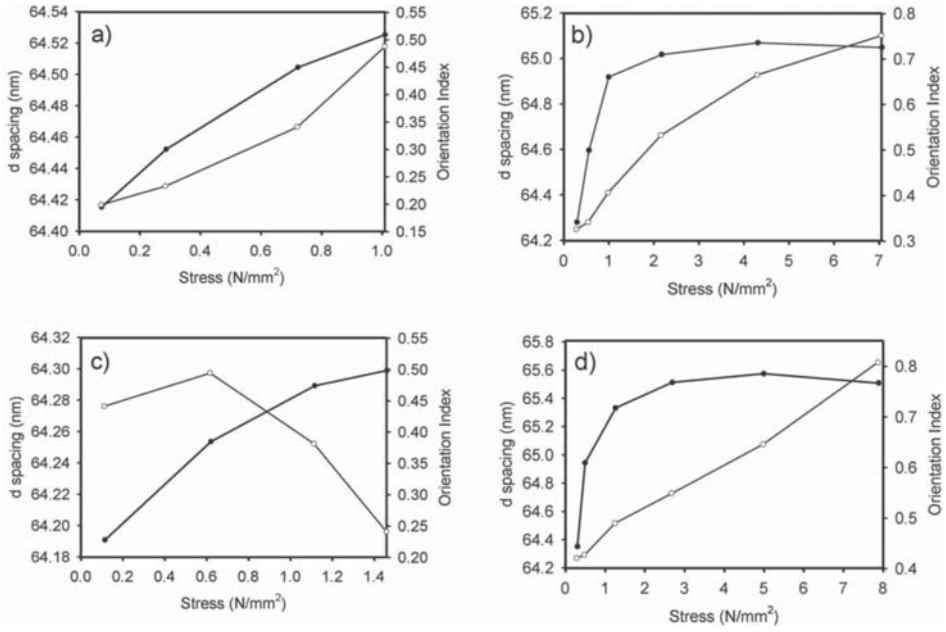

Figure 7. *d* spacing and orientation versus strain measured flat: (○) *d* spacing and (●) OI (parallel, OSP) for (a) weak ovine (21 N/mm tear strength), grain; (b) weak ovine, corium; (c) stronger ovine (44 N/mm tear strength), grain; and (d) stronger ovine, corium.

in *d* spacing is indicative of the strain experienced by individual fibrils as the leather was placed under tension. The decrease in orientation change occurred before the *d* spacing began to significantly increase, indicating that there may be an additional mechanism by which the strain is being distributed to the cross-links that is not apparent from these measurements.[21]

With measurement edge-on, the change observed for OI was very substantial, going from 0.56 to 0.72 for ovine leather and

dx.doi.org/10.1021/jf2039586 | *J. Agric.Food Chem.* 2012, 60, 1201−1208

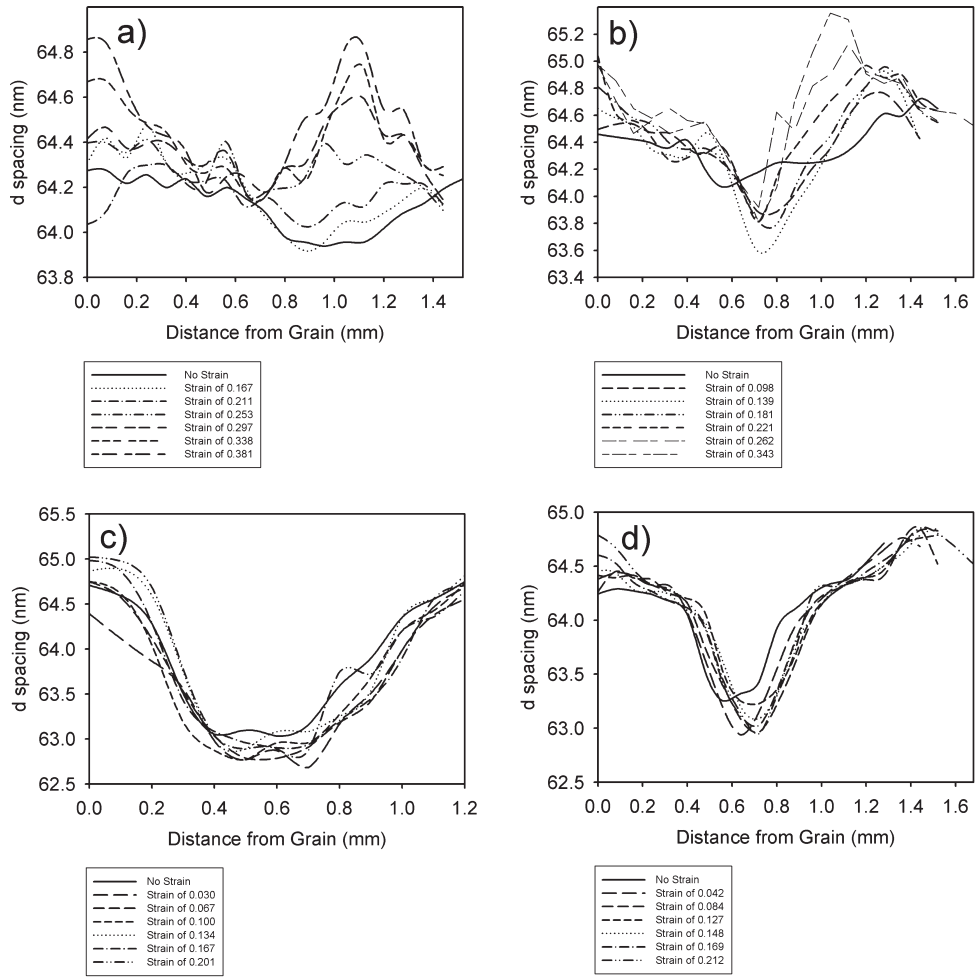

Figure 8. *d* spacing through the thickness of the leather and change in *d* spacing as a consequence of increasing strain, measured edge-on parallel to the backbone for (a) weak ovine, 19 N/mm tear strength; (b) stronger ovine, 39 N/mm tear strength; and (c) strong bovine, 71 N/mm tear strength. Panel d is an example of a second strong ovine leather with a tear strength of 42 N/mm.

from 0.53 to 0.62 for bovine leather (Figure 4). These changes represent a major rearrangement of fibers in the leather. The changes in the *d* spacing were also considerable, with values going from 64.12 to 64.48 nm (or 0.56% extension, with up to 4.6 N/mm^2 stress) for weak ovine skin and from 64.34 to 64.67 nm (or 0.51% extension, with up to 8 N/mm^2 stress) for stronger ovine skin. The *d* spacing continued to change as long as the stress continued to increase.

With measurement on the flat, OI started much lower and underwent a greater change, going from about 0.20 to 0.51 in the grain (panels a and c of Figure 5), from 0.34 to 0.74 in the corium of weak leather (Figure 5b), and from 0.44 to 0.79 in the corium of strong leather (Figure 5d). These changes also represent a major rearrangement of fibers in the leather, although there is not a strong correlation in this direction between strength and orientation.[5] The changes in the *d* spacing are likewise large, with values going from 64.25 to 65.10 nm (or 1.3% extension, with up to 7 N/mm^2 stress) for the corium of weak ovine leather and from 64.27 to 65.65 nm (or 2.1% extension, with up to 7.9 N/mm^2 stress) for the corium of stronger ovine leather. In contrast, in the grain, the increase in *d* spacing was smaller or was reversed (panels a and c of Figure 5).

While the changes in orientation and *d* spacing observed on the flat were greater than those observed edge-on, we believe that the edge-on measurements are of greater significance. It is the extent to which the fibrils are in parallel planes in the leather that determines the strength of the leather (it is the structure measured edge-on that has the most bearing on leather strength); therefore, the change in this structure under tension is of most interest. The quantification of fiber reorientation and stretching in leather during stress is important for developing a model of leather strength.

Cross-sections. SAXS spectra were recorded across the thickness of the leather taken from the OSP and in a direction that was parallel to the direction of the backbone. Previous work has shown that measurements of OI made along this direction are good indicators of strength.[5] The plots of *d* spacing and OI cross-sections (Figures 8 and 9) represent a large number of SAXS spectra and reveal that these parameters vary widely across the thickness of the leather samples and between samples.

For weak ovine leather, the *d*-spacing profile is rather flat when not under tension (Figure 8a), varying by only 0.3 nm and decreasing in the region of the corium. One of the strong ovine leathers showed a similar, fairly flat profile that varied

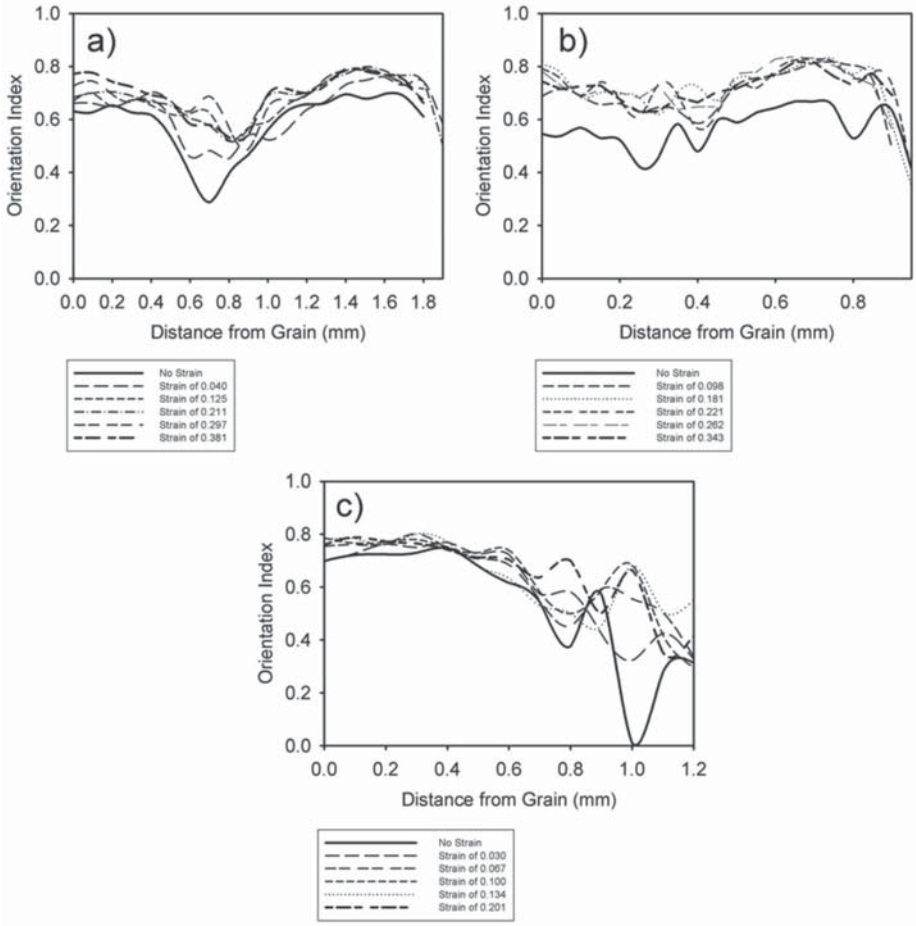

Figure 9. Orientation through the thickness of the leather versus strain and change in orientation as a consequence of increasing strain, measured edge-on parallel to the backbone for (a) weak ovine, 19 N/mm tear strength; (b) stronger ovine, 39 N/mm tear strength; and (c) strong bovine, 71 N/mm tear strength.

only by 0.6 nm at rest. In contrast, the *d* spacing measured for the strongest ovine leather and bovine leathers was lower, at the boundary between the grain and the corium in the middle region, than on either side of this region (panels c and d of Figure 8), decreasing by as much as 1.8 nm for strong ovine and 2.2 nm for strong bovine leather.

Under tension, a markedly different change in *d* spacing was observed for weak ovine leather compared to both strong ovine and bovine leathers. The strain experienced by the fibrils in the weak leather was not uniformly distributed through the leather. Rather, the fibrils remained relatively unstressed in the middle section, while at the surface of the grain and in the bulk of the corium, the *d* spacing increased by up to 1.0 nm as the tension continued to increase. In fact, the profile of the weak ovine leather looked somewhat like that of strong ovine or bovine leather, with a dip in *d* spacing of 0.7 nm at the boundary between the corium and grain (but still less than half that for the strongest ovine or bovine leather). For the strongest ovine and strong bovine leathers, the shapes of the *d*-spacing profiles changed comparatively less when strained and retained the same basic shape throughout (panels c and d of Figure 8). This indicates a chemical and structural difference between strong and weak leathers related to the kind of collagen present, particularly in the corium.

The fibril orientation profiles for all of the ovine leather samples were fairly aligned, except for a slightly less aligned region in the grain close to the grain−corium boundary (panels a and b of Figure 9). In contrast, the fibrils of strong bovine leather were more strongly aligned than those of ovine leather, except at the outer edge of the corium (Figure 9c).

The greatest change in the shape and position of the OI profile occurred during the first one or two increments of stress. During those increases, regions of very low OI were brought generally into line with the rest of the thickness of the leather. The reorientation of fibrils toward greater alignment in the direction of the applied stress took place across the whole thickness of the leather. In addition, fibrils were more uniformly aligned through the whole thickness of the leather during the application of strain than they were before.

These observations provide some evidence of how strain is accommodated in collagen. Leather takes up strain first by reorienting the fibers/fibrils. This happens up to a strain of 15% and a stress of 0.3−0.5 N/mm^2. In the second stage, the fibrils stretch by up to 0.6% before the leather fibers start failing (large pieces of leather under tensile testing fail at strains up to 190%). During the fiber reorientation phase, the leather has a relatively low modulus of elasticity, but once the fibers are highly aligned and begin to individually stretch, the modulus of elasticity rises

dx.doi.org/10.1021/jf2039586 | *J. Agric.Food Chem.* 2012, 60, 1201−1208

as the reorientation mechanism is no longer available to the material.

In weak ovine leather, the fibrils across the thickness of the leather are subjected to a much more uneven tensile loading than in either strong ovine or bovine leathers, where the strain is distributed more evenly among the fibrils. This seems to be the most fundamental difference observed between these materials.

In the tear-strength test, which is considered by industry to give a good measure of strength in practical situations, the point of failure occurs at concentrated stress points. It is apparent from this study that the weak ovine leather was not able to spread stress from these concentrated sites throughout the tissue, and therefore, it failed at a lower force. The mechanism for this failure is therefore a progressive rupture of overstressed collagen fibers, leading to a catastrophic breakdown and tear.

This knowledge of the structural basis for strength in leather may lead to new strategies of leather processing and animal breeding to create leather of improved strength.

AUTHOR INFORMATION

Corresponding Author

*E-mail: r.haverkamp@massey.ac.nz.

Funding

This work was supported by the Ministry of Science and Innovation, New Zealand (Grant LSRX0801). The Australian Synchrotron provided travel funding and accommodations.

ACKNOWLEDGMENTS

This research was undertaken on the SAXS/WAXS beamline at the Australian Synchrotron, Victoria, Australia. Nigel Kirby, David Cookson, Adrian Hawley, and Stephen Mudie at the Australian Synchrotron assisted with data collection and processing. Katie Sizeland and Leah Graham of Massey University also assisted with data collection. Sue Hallas of Nelson assisted with editing the manuscript.

REFERENCES

(1) Jian-Bo, Q.; Chuan-Bo, Z.; Jian-Yan, F.; Fu-Tang, G. Natural and synthetic leather: A microstructural comparison. *J. Soc. Leather Technol. Chem.* **2008**, *92*, 8−13.

(2) Haines, B. M. The skin before tannage—Procters view and now. *J. Soc. Leather Technol. Chem.* **1984**, *68*, 57−70.

(3) Floden, E. W.; Malak, S.; Basil-Jones, M. M.; Negron, L.; Fisher, J. N.; Byrne, M.; Lun, S.; Dempsey, S. G.; Haverkamp, R. G.; Anderson, I.; Ward, B. R.; May, B. C. H. Biophysical characterization of ovine forestomach extracellular matrix biomaterials. *J. Biomed. Mater. Res., Part B* **2011**, *96B*, 67−75.

(4) Basil-Jones, M. M.; Edmonds, R. L.; Allsop, T. F.; Cooper, S. M.; Holmes, G.; Norris, G. E.; Cookson, D. J.; Kirby, N.; Haverkamp, R. G. Leather structure determination by small angle X-ray scattering (SAXS): Cross sections of ovine and bovine leather. *J. Agric. Food Chem.* **2010**, *58*, 5286−5291.

(5) Basil-Jones, M. M.; Edmonds, R. L.; Cooper, S. M.; Haverkamp, R. G. Collagen fibril orientation in ovine and bovine leather affects strength: A small angle X-ray scattering (SAXS) study. *J. Agric. Food Chem.* **2011**, *59*, 9972−9979.

(6) Sasaki, N.; Odajima, S. Stress-strain curve and Young's modulus of a collagen molecule as determined by the X-ray diffaction technique. *J. Biomech.* **1996**, *29*, 655−658.

(7) Sasaki, N.; Odajima, S. Elongation mechanisms of collagen fibils and force−strain relations of tendon at each level of structural hierarchy. *J. Biomech.* **1996**, *29*, 1131−1136.

(8) Burger, C.; Zhou, H. W.; Sics, I.; Hsiao, B. S.; Chu, B.; Graham, L.; Glimcher, M. J. Small-angle X-ray scattering study of intramuscular fish bone: Collagen fibril superstructure determined from equidistant meridional reflections. *J. Appl. Crystallogr.* **2008**, *41*, 252−261.

(9) Cedola, A.; Mastrogiacomo, M.; Burghammer, M.; Komlev, V.; Giannoni, P.; Favia, A.; Cancedda, R.; Rustichelli, F.; Lagomarsino, S. Engineered bone from bone marrow stromal cells: A structural study by an advanced X-ray microdiffraction technique. *Phys. Med. Biol.* **2006**, *51* (6), N109−N116.

(10) Goh, K. L.; Hiller, J.; Haston, J. L.; Holmes, D. F.; Kadler, K. E.; Murdoch, A.; Meakin, J. R.; Wess, T. J. Analysis of collagen fibril diameter distribution in connective tissues using small-angle X-ray scattering. *Biochim. Biophys. Acta* **2005**, *1722*, 183−188.

(11) Mollenhauer, J.; Aurich, M.; Muehleman, C.; Khelashvilli, G.; Irving, T. C. X-ray diffraction of the molecular substructure of human articular cartilage. *Connect. Tissue Res.* **2003**, *44*, 201−207.

(12) Fernandez, M.; Keyrilainen, J.; Karjalainen-Lindsberg, M.-L.; Leidenius, M.; Von Smitten, K.; Fiedler, S.; Suortti, P. Human breast tissue characterisation with small-angle X-ray scattering. *Spectroscopy* **2004**, *18*, 167−176.

(13) Liao, J.; Yang, L.; Grashow, J.; Sacks, M. S. The relation between collagen fibril kinematics and mechanical properties in the mitral valve anterior leaflet. *J. Biomech. Eng.* **2007**, *129*, 78−87.

(14) Liao, J.; Yang, L.; Grashow, J.; Sacks, M. S. The relation between collagen fibril kinematics and mechanical properties in the mitral valve anterior leaflet. *J. Biomech. Eng.* **2007**, *129*, 78−87.

(15) Liao, J.; Yang, L.; Grashow, J.; Sacks, M. S. Molecular orientation of collagen in intact planar connective tissues under biaxial stretch. *Acta Biomater.* **2005**, *1*, 45−54.

(16) Sturrock, E. J.; Boote, C.; Attenburrow, G. E.; Meek, K. M. The effect of the biaxial stretching of leather on fibre orientation and tensile modulus. *J. Mater. Sci.* **2004**, *39*, 2481−2486.

(17) Sellaro, T. L.; Hildebrand, D.; Lu, Q. J.; Vyavahare, N.; Scott, M.; Sacks, M. S. Effects of collagen fiber orientation on the response of biologically derived soft tissue biomaterials to cyclic loading. *J. Biomed. Mater. Res., Part A* **2007**, *80A* (1), 194−205.

(18) Williams, J. M. V. IULTCS (IUP) test methods—Measurement of tear load-double edge tear. *J. Soc. Leather Technol. Chem.* **2000**, *84*, 327−329.

(19) Williams, J. M. V. IULTCS (IUP) test methods—Sampling. *J. Soc. Leather Technol. Chem.* **2000**, *84*, 303−309.

(20) Cookson, D.; Kirby, N.; Knott, R.; Lee, M.; Schultz, D. Strategies for data collection and calibration with a pinhole-geometry SAXS instrument on a synchrotron beamline. *J. Synchrotron Radiat.* **2006**, *13*, 440−444.

(21) Chan, Y.; Cox, G. M.; Haverkamp, R. G.; Hill, J. M. Mechanical model for a collagen fibril pair in extracellular matrix. *Eur. Biophys. J.* **2009**, *38*, 487−493.

JOURNAL OF AGRICULTURAL AND FOOD CHEMISTRY

ARTICLE

pubs.acs.org/JAFC

Collagen Fibril Orientation in Ovine and Bovine Leather Affects Strength: A Small Angle X-ray Scattering (SAXS) Study

Melissa M. Basil-Jones,[†] Richard L. Edmonds,[‡] Sue M. Cooper,[‡] and Richard G. Haverkamp*[,†]

[†]School of Engineering and Advanced Technology, Massey University, Palmerston North, New Zealand 4442

[‡]Leather and Shoe Research Association, Palmerston North, New Zealand 4442

Supporting Information

ABSTRACT: There is a large difference in strength between ovine and bovine leather. The structure and arrangement of fibrous collagen in leather and the relationship between collagen structure and leather strength has until now been poorly understood. Synchrotron based SAXS is used to characterize the fibrous collagen structure in a series of ovine and bovine leathers and to relate it to tear strength. SAXS gives quantitative information on the amount of fibrous collagen, the orientation (direction and spread) of the collagen microfibrils, and the *d*-spacing of the collagen. The amount of collagen varies through the thickness of the leather from the grain to the corium, with a greater concentration of crystalline collagen measured toward the corium side. The orientation index (OI) is correlated strongly with strength in ovine leather and between ovine and bovine leathers. Stronger leather has the fibrils arranged mostly parallel to the plane of the leather surface (high OI), while weaker leather has more out-of-plane fibrils (low OI). With the measurement taken parallel to the animal's backbone, weak (19.9 N/mm) ovine leather has an OI of 0.422 (0.033), stronger (39.5 N/mm) ovine leather has an OI of 0.452 (0.033), and bovine leather with a strength of (61.5 N/mm) has an OI of 0.493 (0.016). The *d*-spacing profile through leather thickness also varies according to leather strength, with little variation being detected in weak ovine leather (average = 64.3 (0.5) nm), but with strong ovine leather and bovine leather (which is even stronger) exhibiting a dip in *d*-spacing (from 64.5 nm at the edges dropping to 62 nm in the center). This work provides a clear understanding of a nanostructural characteristic of ovine and bovine leather that leads to differences in strength.

KEYWORDS: leather, small angle X-ray scattering, SAXS, synchrotron, ovine, bovine, fiber structure, collagen, strength, orientation

INTRODUCTION

Ovine leather is traditionally a low-value product owing in part to its low strength relative to bovine leather. This low strength makes ovine leather unsuitable for footwear production, which is a major high-value use for leather. Whereas 4.6 billion pairs of footwear are made annually from bovine leather, no significant quantity of footwear is produced from sheep and goat leather.[1] Export trade in leather and footwear amounts to about $US 60 billion annually, with around 38% of bovine and 25% of ovine leather traded internationally. However, the raw material resource of ovine skins is large, with world annual production of sheep and goat leather being 5.3 billion square feet from 1.9 billion head of livestock (1.1 billion sheep, 0.8 billion goats), compared to 14 billion square feet of bovine leather from 1.5 billion head of livestock.[1] Clearly, the opportunity for shoe manufacture from ovine leather, were the leather sufficiently strong, is large.

It is not understood why ovine leather is weaker than bovine leather of the same thickness. However, it is clear that leather consists of a network of fibers based on collagens, a group of proteins that are responsible for the structure and physical properties of skin (and therefore leather) and several other animal tissues.[2] Leather structure is complex on several levels, including the microscopic scale as determined by the use of optical microscopy, scanning electron microscopy (SEM),[3−7] and atomic force microscopy (AFM).[6,8,9] These techniques generally provide qualitative information about fiber organization but may also give quantitative measurements.

The building blocks of collagen are pro-collagen molecules, each one a repeating sequence of $(\text{glycine-X-Y})_n$, where X and Y can be any amino acid, and *n* is the number of repeats (usually 100−400).[10] Three pro-collagen molecules that have combined in a coiled coil are a collagen molecule. Several collagen molecules aligned in a quarter-staggered array form a collagen microfibril, which has overlap and gap regions. Collections of microfibrils arranged in a parallel fashion, and connected by chemical cross-links, form collagen fibrils. These fibrils have characteristic banding patterns (observed with AFM or SEM) that result from the overlap and gap regions in the microfibrils comprising them.

Collagen fibrils can vary considerably among tissues. In skin, and therefore leather, the fibrils tend to vary only slightly in diameter and they form a somewhat random weblike structure.[11] The strength and softness of leather are believed to be related to a leather's internal structure[12,13] and its aesthetic properties to the internal fiber looseness.[14] In the leather-making process, it has been found that many collagens, in particular type I, III and VI collagens, are resistant to liming, bating and pickling[15] (skin/leather consists mostly of types 1 and III), and these collagen fibrils have a large inherent strength.

At a larger scale, fiber structure is responsible for the several distinct layers of leather. The outer "grain" layer and the "corium" layer found beneath it have visually different structures and impart specific properties to leather.[12,16,17] The cross-links (either natural

Received: June 29, 2011
Accepted: August 22, 2011
Revised: August 18, 2011
Published: August 22, 2011

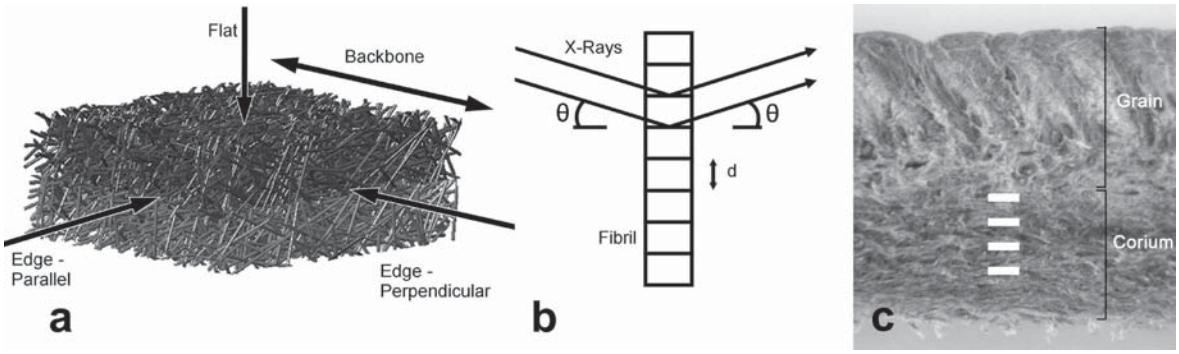

Figure 1. (a) Directions of X-ray beam with descriptors used in the text shown relative to the direction of the animal's backbone. (b) Interaction of X-rays with collagen fibril *d*-spacing. (c) Optical image of a cross section of ovine leather as seen by the SAXS X-ray beam. The rectangles indicate the size of the beam used to probe the sample and the approximate spacing.

or synthetic) between microfibrils also contribute to the differences observed between layers.[18−21]

In our earlier work, we showed how small-angle X-ray scattering (SAXS) investigations of leather can provide detailed structural information on the amount of fibrous collagen, the microfibril orientation, and the *d*-spacing.[22] Leather had previously been investigated using SAXS to identify fiber orientation in leather samples under strain,[23,24] although in these studies, the resolution appears to be rather limited (the collagen *d*-period is not easily discerned in the diffraction patterns). SAXS has also been used to investigate the structure of collagenous materials such as those found in tendons,[25,26] bone,[27,28] ligaments,[29] human articular cartliages,[30] breast tissue,[31] mitral valve leaflets[32] and materials for tissue regeneration scaffolds.[33]

Here, we report a study of the structure of ovine and bovine leather in which we attempted to understand the factors that contribute to the strength of leather and which account for the differences between strong and weak leather.

EXPERIMENTAL SECTION

Ovine pelts were from 5-month-old, early season lambs of breeds with "black face" lambs, which may include Suffolk, South Suffolk, and Dorset Down. The bovine hides were from 2- to 3-year-old cattle of a variety of breeds.

Leather was prepared from around 600 pelts. These leathers were generated with a variety of properties by deliberately using a range of processing parameters both during the conventional beamhouse process and then during the application of the conventional tanning processes to those pelts. Briefly, the pelts were depilated using a caustic treatment comprising sodium sulfide ranging from a slow acting paint containing 160 g/L flake sodium sulfide to a quick acting paint containing 200 g/L sulfide and a saturated solution of calcium hydroxide. Depilated slats were then processed to remove the residual wool in a solution of sodium sulfide ranging in concentration from 0.8 to 2.4% for a period ranging from 8 to 16 h at temperatures ranging from 16 to 24 °C. After this treatment the pelts were washed and treated to a proteolytic enzyme process containing either a bacterial enzyme (Tanzyme, Tryptec Biochemicals Ltd.) or pancreatic enzyme (Rohapon ANZ, Shamrock Ltd.) at concentrations ranging from 0.025% to 0.1%, followed, after washing, by pickling in 2% sulfuric acid and 10% sodium chloride solution. The pickled pelts were then pretanned using oxazolidine, degreased with an aqueous surfactant and then tanned using chromium sulfate. The resulting "wet blue" was then retanned using a mimosa vegetable extract and impregnated with lubricating oil prior to drying and mechanical softening.

Tear strengths of the crust leathers were tested using standard methods.[34] In brief, samples were cut from the leather at the official sampling positions (OSP).[35] The samples were then conditioned by holding at a constant temperature and humidity (20 °C and 65% relative humidity) for 24 h, after which time the samples were tested on an Instron strength testing device.

A selection of the 600 leather samples that had been prepared was chosen for the SAXS analysis, with a representative collection of strong and weak leathers. Sample preparation for SAXS analysis began by cutting strips of leather about 1 × 30 mm from the OSP from samples of tanned ovine and bovine leather. The bovine leather had been shaved, resulting in approximately 1.3-mm-thick samples consisting on average of 34% grain and 66% corium. Strips of leather were cut in two perpendicular directions. Each sample was mounted, without tension, in the X-ray beam to obtain spectra for each of three orthogonal directions through the leather (1). For the edge-on analyses (with strips cut in two perpendicular directions) the samples were analyzed from the grain to the corium, with measurements being made every either 0.25 mm or 0.2 mm (ca. 10 measurements in all, per edge). For when the beam was directed flat on (normal to) the surface of the leather, standard samples were cut parallel to the surface, producing a grain sample and a corium sample. These were mounted with the uncut face of the leather directed toward the X-ray beam (ca. four measurements made per sample, in a rectangular grid).

Diffraction patterns were recorded on the Australian Synchrotron SAXS/WAXS beamline, utilizing a high-intensity undulator source. Energy resolution of 10^{-4} is obtained from a cryocooled Si(111) double-crystal monochromator, and the beam size (fwhm focused at the sample) was 250 × 80 μm, with a total photon flux of about 2×10^{12} photons·s^{-1}. All diffraction patterns were recorded with an X-ray energy of either 8 or 11 keV using a Pilatus 1 M detector with an active area of 170 × 170 mm and a sample to detector distance of 3371 mm. Exposure time for diffraction patterns was 1 s, and data processing was carried out using the SAXS15ID software.[36]

The analysis of the spectra has been detailed previously,[22] but some key points are described here. The *d*-spacing was determined for each spectrum from Bragg's law by taking the central position of several of the collagen peaks, correcting these for the peak order (usually from $n = 5$ to $n = 10$) and averaging the resulting values.

The orientation index (OI) is defined as (90° − OA)/90° where OA is the minimum azimuthal angle range, centered at 180°, that contains 50% of the microfibrils. OI is used to give a measure of the spread of microfibril orientation (an OI of 1 indicates the microfibrils are completely parallel to each other and the leather surface; an OI of 0 indicates the microfibrils are completely randomly oriented). The OI is calculated from the spread in azimuthal angle of the most intense *d*-spacing peak (at around 0.059−0.060 Å^{-1}). Note that this differs from our previous use of the term orientation index in this context[22,33] where we had used the azimuthal angle range rather than this true index.

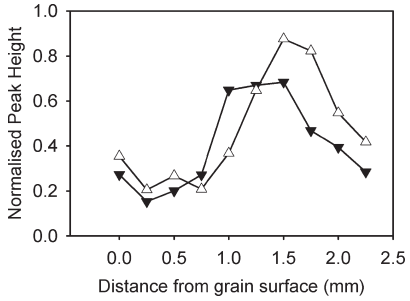

Figure 2. Amount of collagen through the thickness of ovine leather parallel to the backbone (averages of 12 samples each): (▼) strong leather; (△) weak leather.

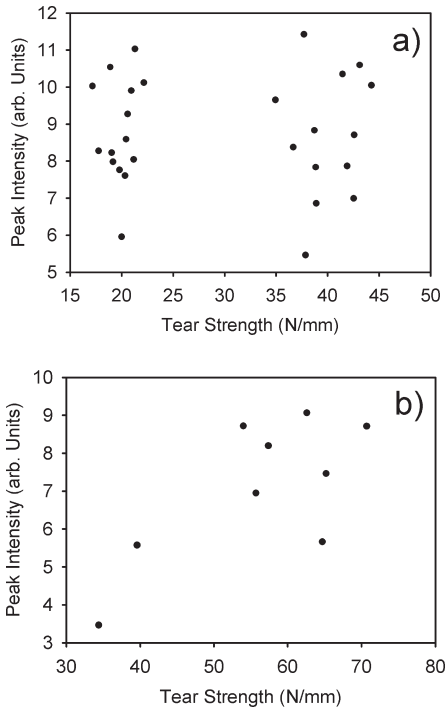

Figure 3. Amount of collagen determined from the intensity of the primary collagen *d*-spacing peak (at around 0.059−0.060 $Å^{-1}$) versus tear strength for (a) ovine leather; (b) bovine leather.

The amount of collagen was estimated by taking the area above the baseline of the fifth-order collagen *d*-spacing peak divided by the intensity of baseline under the peak.

For the plots of OI and *d*-spacing, each point on a plot represents the average of the four (normal) or about 10 (edge) measurements from different points on the sample (see above). For the plots of the amount of collagen (i.e., peak intensity), each point on the plot represents the average of measurements taken in the three orthogonal directions (which are in turn averages of four or 10 measurements as for the OI and *d*-spacing).

RESULTS AND DISCUSSION

Variation in Tear Strength of Leathers. A selection of leathers was chosen from those tested to have a representative sample of ovine leather of lower strength (17−22 N/mm), ovine leather of higher strength (35−44 N/mm) and bovine leather in the 32−71 N/mm strength range (although most of the last was predominantly in the upper end of this range). A list of tested samples is tabulated in the Supporting Information, and includes a sample's absolute strength, its thickness, and its relative strength (tear strength divided by thickness, which is the strength measurement used throughout this work).

Concentration of Crystalline Fibrillar Collagen. The amount of crystalline collagen varied through the thickness of ovine leather, with a greater concentration being measured toward the corium side (2). The corium is known to impart more strength to the leather than the grain,[16] and the above finding—of three or four times more fibrillar collagen in the corium region than in the grain region—may be part of the reason for this extra strength. However, the total amount of crystalline collagen in leather samples was not correlated with strength (Figure 3) (instead, strength was correlated with microfibril orientation; see below). An average value of about 8.8 was found for collagen, with no variation with strength. This finding was rather surprising as it is generally believed collagen is the structural material that contributes most to the strength of skin.

Orientation of Collagen Microfibrils Correlated with Tear Strength. The orientation and OI of the fibrils in leather are different when observed from different directions (Figure 4), making up a complex three-dimensional structure. Statistically significant differences in OI were observed between weak and strong ovine leather. Specifically, for ovine leather measured edge-on, the OI values were higher for the higher strength ovine leather. For ovine edge-parallel measurements, the average OI was 0.422 (variance = 0.033) for low strength (19.9 N/mm) ovine leather, which was significantly less than for high strength (39.5 N/mm) ovine leather (0.452 (0.033)) (*t*-stat = −2.06, *t*-crit =2.00, $P = 0.044$). Likewise, the OI of edge-perpendicular measurements of low-strength ovine leather was significantly less than of the corresponding high-strength leather (i.e., 0.578 (0.025) and 0.630 (0.016) respectively with *t*-stat = −3.21, *t*-crit = 2.01, $P = 0.0023$). These findings reveal that stronger ovine leather was characterized by having more collagen microfibrils that were in one plane (i.e., parallel to the surface), with fewer crossing between layers of the leather (referred to in the industry as a lower "angle of weave"). With the X-ray beam normal to the surface of the leather, the OI of ovine leather was around 0.248 (0.016) for grain and 0.329 (0.010) for corium, and it did not vary with strength (Figure 4c). In contrast, similar analysis of bovine leather yielded an average OI of 0.184 (0.026) in the grain and 0.364 (0.017) in the corium (Figure 4d). The microfibrils were aligned in the direction approximately parallel to the backbone of the animal (not shown). These OIs represent a moderate degree of alignment of the fibers in the direction of the backbone, with greater alignment in the corium in both ovine and bovine leather.

As for bovine leather, the OI measurements taken normal to the bovine leather surface were not strongly correlated with tear strength (Figure 4d), however, the greater alignment in the bovine corium is consistent with other observations described below. According to pooled edge-on measurements of bovine leather, strong bovine leather (61.5 N/mm) had a higher OI than strong ovine leather, of 0.493 (0.016) (*t*-stat = −2.20, *t*-crit = 2.01, $P = 0.03$) (Figure 5). There was not a strong trend visible within the limited bovine data (Figure 4b,d,f), however it is clear that the bovine leather was more aligned in one plane than was the ovine leather. This result, combined with the trend seen within the ovine leather, leads us to propose that fibril orientation is a determiner of strength in leather (and possibly, by analogy,

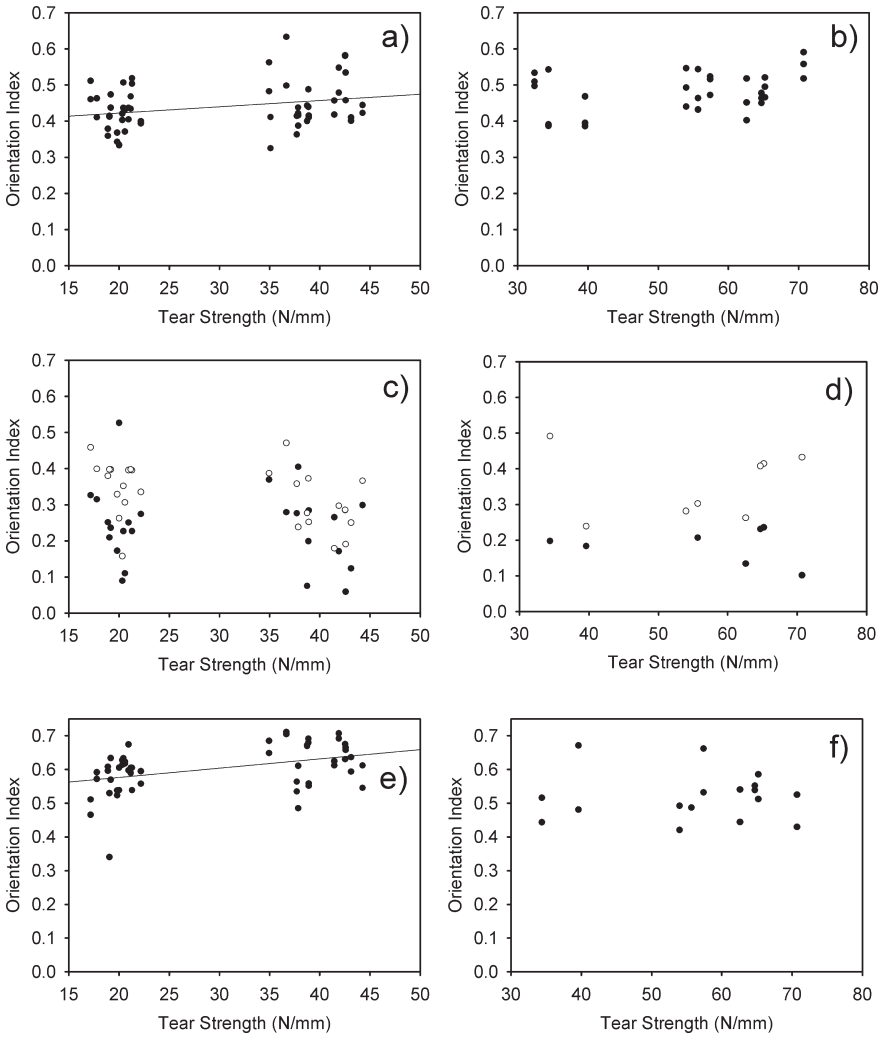

Figure 4. Orientation index versus tear strength for OSP samples of leather: (a) ovine, edge, parallel to backbone; (b) bovine, edge, parallel to backbone; (c) ovine, flat, (●) grain, (○) corium; (d) bovine, flat, (●) grain, (○) corium; (e) ovine, edge, perpendicular to backbone; (f) bovine, edge, perpendicular to backbone. A higher OI indicates a greater degree of fiber alignment.

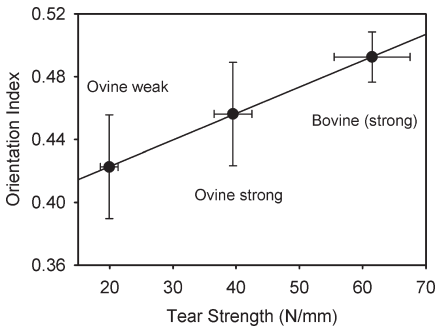

Figure 5. Orientation versus tear strength for the averages of each of the leather types measured through the edge parallel to the backbone. Error bars for one standard deviation.

in other tissues), and is not merely correlated with it. This is a key finding of this work.

A statistically significant difference was observed between ovine leather of low and high tear strength and collagen microfibril OI for edge-on measurements, with higher strength leather having a higher OI (Figure 4a, Figure 5). A similar correlation was found when the measurements for bovine leather were included in the data set. A regression line fitted to the averages of the three groups of data for OI and tear strength (low strength ovine, 15 samples, 228 analysis points; higher strength ovine, 14 samples, 249 analysis points; and bovine, 10 samples, 167 analysis points) has a slope of 1.708×10^{-3} mm/N, $r^2 = 0.20$, $p = 4.45 \times 10^{-5}$ (Figure 5). The relationship between OI and tear strength documented within species (i.e., sheep) is maintained between species (i.e., sheep and cattle). This finding points to a universal property of leather: that strength is determined by fibril orientation, such that stronger leather has the fibrils arranged mostly parallel to the plane of the leather surface (low angle of weave), while weaker leather has more out-of-plane fibrils (higher angle of weave) (Figure 6). It is possible that this relationship may extend to a large number of animal leathers. Work is currently underway to investigate this further.

There is likely to be a upper limit for OI because, with all fibers parallel, there might be little mechanical connection between the

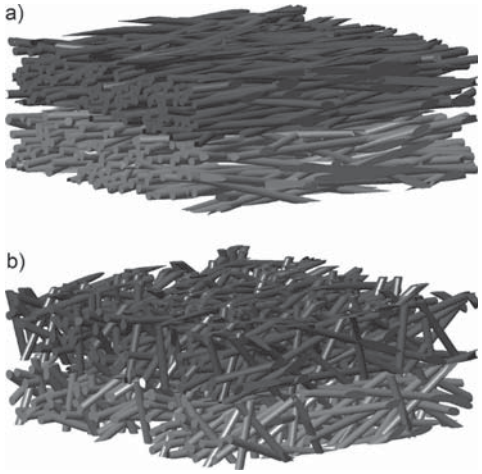

Figure 6. Sketch of fiber orientation in (a) stronger and (b) weaker leather. In the stronger leather the angle of weave is smaller (the fibers are contained more in planes parallel to the leather surface). The orientation change is exaggerated to better illustrate the difference.

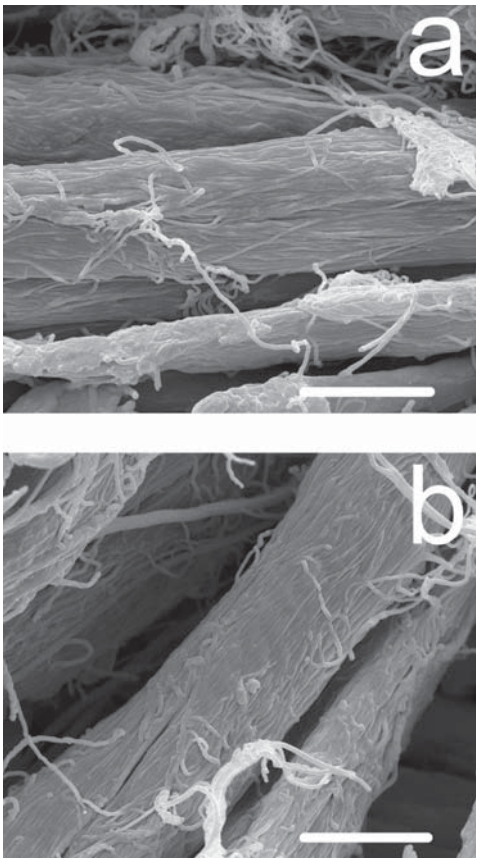

Figure 7. Representative SEM images of sections of leather observed parallel to the backbone: (a) weak ovine; (b) strong ovine. Scale bars 10 μm.

layers and delamination might be more likely. Other factors clearly are also important as the OI versus tear strength data have scatter.

SEM Images of Fibers and Crimp. We considered the possibility that spread of orientation we measure with SAXS may have a contribution from what is known as crimp, which consists

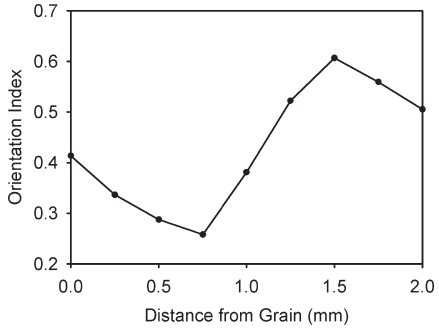

Figure 8. Average orientation index across the thickness of ovine leather measured parallel to the backbone. An average of 24 leather samples (1 measurement per sample).

of a wavy texture to the fibers with a period of several micrometers. One might imagine that increased crimp could result in a larger OI since the fibers and therefore the fibrils are tilted through a range of directions as they bend. We therefore used SEM to investigate ovine and bovine leathers with a range of OI determined by SAXS (Figure 7). The SEM images show no crimp for the ovine samples but some crimp in the bovine sample. Therefore if crimp were a significant contributor to the OI, then the trend on OI with strength would likely be in the opposite direction to that which we observe. We therefore believe that crimp is not a significant contributor to the measured OI and our observations on the correlation of OI to strength relate to overall fiber orientation rather than any effect of crimp.

Orientation of Collagen Microfibrils across the Thickness of Leather. Collagen microfibril alignment was found to vary considerably through the thickness of both ovine and bovine leather. Measured flat (normal to the surface) ovine leather is more aligned in the corium OI = 0.329 than the grain OI = 0.248 (t-stat = −3.7, t-crit = 2.1, P = 0.001) (Figure 4c); bovine leather is also more aligned in the corium OI = 0.364 than the grain OI = 0.184 (t-stat = −4.7, t-crit = 2.45, P = 0.003) (Figure 4d). The orientation was also measured edge-on parallel to the backbone with a series of points taken across the thickness of the leather (Figure 8). For ovine leather, the microfibrils were poorly aligned with each other edge-on in the grain (OI = 0.29−0.41), compared to the corium (OI = 0.50−0.61) (for ovine leather: t-stat = −12.9, t-crit = 2.05, $P = 2 \times 10^{-13}$). If, as suggested by our findings, leather strength depends on a high level of alignment of fibers within the plane of the leather, then these OIs suggest that the corium should be stronger than the grain in the ovine leather, as has been recognized by others.[16]

Internal Structure (d-Spacing) of Collagen Microfibrils Correlated with Tear Strength. Because of the nature of the molecular overlap in the collagen structure, the d-spacing gives a measure of the sum of the length of the collagen molecule plus the gap between two end-aligned molecules. Therefore, a difference in d-spacing indicates either a difference in the length of the molecules that make up the microfibrils or a difference in the amount of overlap of those molecules (less overlap means a longer d-spacing). d-Spacing varies with leather age.[37]

The d-spacing of ovine leather (64.3 (0.5) nm) differed significantly different from that of bovine leather (63.5 (0.9) nm) (t-stat = −11.58, t-crit = 2.04, $P = 1.34 \times 10^{-12}$).

For ovine edge-on measurements, there was no significant difference in the d-spacing between the weak and the stronger leathers (Figure 9). However, for normal ovine measurements of

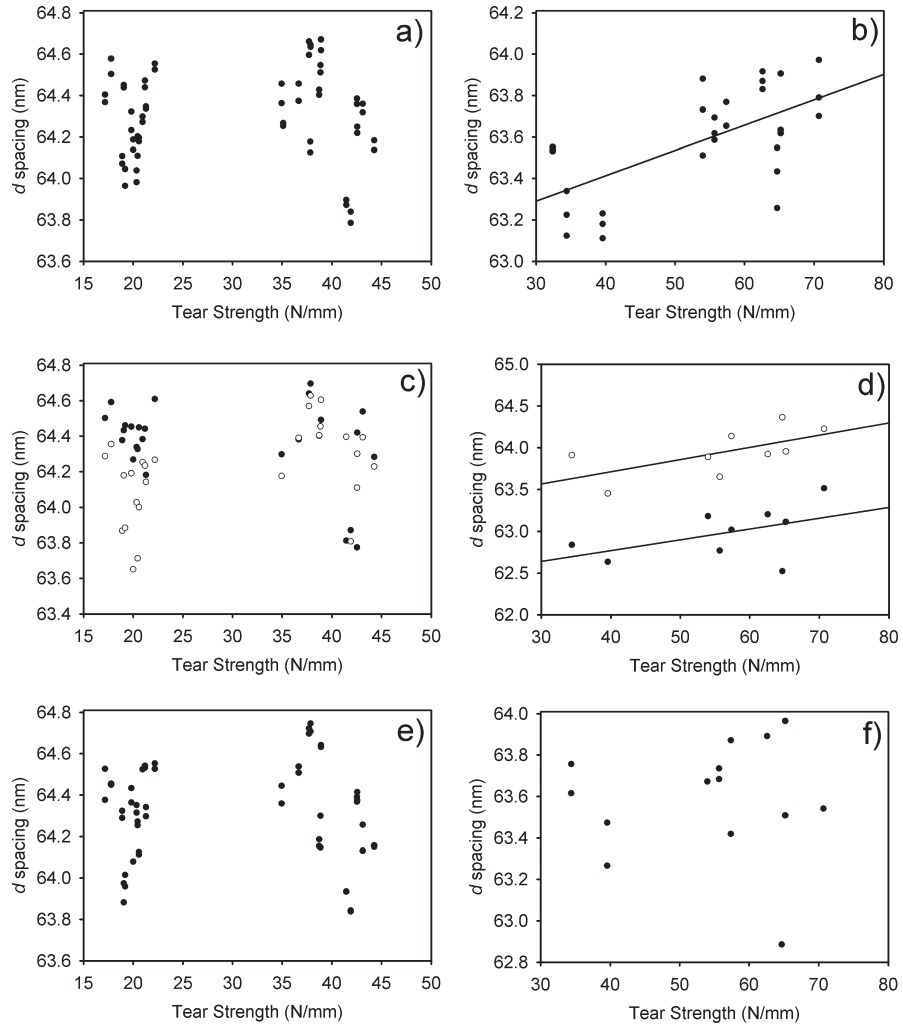

Figure 9. *d*-Spacing verses tear strength for (a) ovine, edge, parallel to backbone; (b) bovine, edge, parallel to backbone; (c) ovine, flat, (●) grain, (○) corium; (d) bovine, flat, (●) grain, (○) corium; (e) ovine, edge, perpendicular to backbone; (f) bovine, edge, perpendicular to backbone.

the weak leather, the *d*-spacing of the corium (64.1 nm) was significantly lower than that of the grain (64.4 nm) (*t*-stat = −5.08, *t*-crit = 2.06, $P = 2.75 \times 10^{-3}$). For the stronger ovine leather, the observed difference was not significant.

For bovine leather measured edge-on parallel, there was a consistent increase in *d*-spacing with increasing strength (least-squares fit slope = 0.014 nm·mm/N, $r^2 = 0.53$, $P = 2.98 \times 10^{-4}$), although the number of samples measured was fewer than for the ovine leather. For the normal bovine measurements, the corium had a larger *d*-spacing (63.9 (0.4) nm) than the grain (63.0 (0.3) nm) (*t*-stat = −6.91, *t*-crit = 2.12, $P = 3.49 \times 10^{-6}$), but bovine values were less than most ovine values. Least squares fits to the bovine data gave the following: for corium, slope = 0.015 nm·mm/N, $r^2 = 0.40$ and $P = 0.07$, and, for the grain, slope = 0.013 nm·mm/N, $r^2 = 0.25$ and $P = 0.17$ (this last suggesting that this correlation in the grain is not particularly significant). However, the changes in *d*-spacing across the bovine samples were not large compared to the differences between bovine and ovine leather.

There are advantages to calculating average *d*-spacing for each piece of leather, despite the fact that it obscures variation in leather across its thickness. Although each skin gave a different profile of

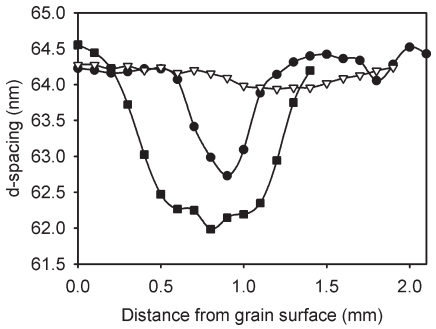

Figure 10. Variation in *d*-spacing through representative samples of (▽) weak ovine, (●) strong ovine and (■) bovine leathers.

d-spacing through the leather, a fairly consistent difference was observed between weak ovine, strong ovine and bovine leathers (Figure 10). Weaker leather had less variation in *d*-spacing compared to stronger leather, which had a dip of up to 3 nm in *d*-spacing in the central region of the leather. These differences in *d*-spacing may indicate differences in protein composition or fibril structure.

Our current research indicates that *d*-spacing responds to tensile stress applied to leather and gives a measure of the force applied to individual fibrils. We will present results from stress measurements on OI and *d*-spacing in leather in a subsequent paper.

The observed differences in *d*-spacing between ovine and bovine leathers cannot yet be ascribed to structures controlling leather strength. However, we expect that current tensile studies on these materials will provide further insight into the mechanisms of strength in collagen-based materials.

In summary, a correlation has been found between the tear strength in ovine leather and the orientation of collagen microfibrils in that leather. Stronger leather was found to have more fibrils aligned with the surface of the leather, with less crossover between layers, than weak leather (i.e., strong leather had a lower angle of weave). This trend was also apparent in bovine leather, which is stronger than ovine leather, with bovine leather having even more aligned fibrils. The total quantity of crystalline collagen was found, surprisingly, to not be correlated with strength. The *d*-spacing of bovine and ovine leather was found to be variable, reflecting differences in the molecular structure of collagen. A difference in the profile of the *d*-spacing was found between weak and strong ovine leather and between these leathers and bovine leather. We have not yet been able to ascribe these differences in *d*-spacing to structures that control leather strength. The discovery of the relationship between collagen microfibril alignment and leather tear strength has provided a clear understanding of a basis of the differences in strength between different leather types. We speculate that this relationship is a general one, which applies not only to skin of sheep and cattle but to skin of other animals also, including humans, and that this relationship may extend to other tissues.

■ ASSOCIATED CONTENT

Supporting Information. Table of tested leather samples and their absolute strength, thickness, and relative strength. This material is available free of charge via the Internet at http://pubs.acs.org.

■ AUTHOR INFORMATION

Corresponding Author

*E-mail: r.haverkamp@massey.ac.nz.

Funding Sources

The NZ Synchrotron Group Ltd is acknowledged for travel funding. This work was supported by the Foundation for Research Science and Technology grant number LSRX0801.

■ ACKNOWLEDGMENT

This research was undertaken on the SAXS/WAXS beamline at the Australian Synchrotron, Victoria, Australia. Nigel Kirby and David Cookson at the Australian Synchrotron assisted with data collection and processing. Katie Sizeland and Leah Graham of Massey University also assisted with data collection. Doug Hopcroft of the Manawatu Microscopy Centre assisted with the SEM images.

■ REFERENCES

(1) *World statistical compendium for raw hides and skins, leather and leather footwear 1990−2009*; Commodities and Trade Division, Food and Agriculture Organization of The United Nations: Rome, Italy, 2010.

(2) Fratzl, P., *Collagen: structure and mechanics*; SpringerScience +Business Media: New York, 2008; pp 1−13.

(3) Barlow, J. R. Scanning electron-microscopy of hides, skins and leather. *J. Am. Leather Chem. Assoc.* **1975**, *70*, 114–128.

(4) Dempsey, M. *Hide, skin and leather defects: a guide to their microscopy*; New Zealand Leather and Shoe Association: Palmerston North, 1984.

(5) Haines, B. M. The skin before tannage - procters view and now. *J. Soc. Leather Technol. Chem.* **1984**, *68*, 57–70.

(6) Deb Choudhury, S.; Haverkamp, R. G.; DasGupta, S.; Norris, G. E. Effect of oxazolidine E on collagen fibril formation and stabilization of the collagen matrix. *J. Agric. Food Chem.* **2007**, *55*, 6813–6822.

(7) Kielty, C. M.; Shuttleworth, C. A. Microfibrillar elements of the dermal matrix. *Microsc. Res. Tech.* **1997**, *38*, 413–427.

(8) Reich, G.; Bradt, J.; Mertig, M.; Pompe, W.; Taeger, T. Scanning probe microscopy - a useful tool in leather research. *J. Soc. Leather Technol. Chem.* **1998**, *82*, 11–14.

(9) Edmonds, R. L.; Deb Choudhury, S.; Haverkamp, R. G.; Birtles, M.; Allsop, T. F.; Norris, G. E. Using proteomics, immunohistology, and atomic force microscopy to characterize surface damage to lambskins observed after enzymatic dewooling. *J. Agric. Food Chem.* **2008**, *56*, 7934–7941.

(10) Bailey, A. J.; Paul, R. G. Collagen: a not so simple protein. *J. Soc. Leather Technol. Chem.* **1999**, *82*, 104–110.

(11) Gathercole, L. J.; Shah, J. S.; Nave, C. Skin-tendon differences in collagen d-period are not geometric or stretch-related artifacts. *Int. J. Biol. Macromol.* **1987**, *9*, 181–183.

(12) Russell, A. E. Stress-strain relationships in leather and the role of fiber structure. *J. Soc. Leather Technol. Chem.* **1988**, *72*, 121–134.

(13) Michel, A. Tanners' dilemma: vertical fibre defect. *Leather Int.* **2004**, *206* (4750), 36–37.

(14) Rabinovich, D. Seeking soft leathers with a tight grain. *WORLD Leather* **2001**, *14* (5), 27–32.

(15) Stephens, L. J.; Werkmeister, J. A.; Ramshaw, J. A. M. Changes in bovine hides during leather processing. *J. Soc. Leather Technol. Chem.* **1993**, *77*, 71–74.

(16) Vera, V. D.; Cantera, C. S.; Dominguez, D. O.; Bernardi, C. In *Modern soft leather influence of the relationship grain/corium on the topography of some physical properties*; 22th IULTCS Congress Proceedings, Porto Alegra, 1993; pp 560−569.

(17) Bavinton, J. H.; Peters, D. E.; Stephens, L. J. A comparative morphology of kangaroo and bovine leathers. *J. Am. Leather Chem. Assoc.* **1987**, *82*, 197–199.

(18) Folkhard, W.; Geercken, W.; Knorzer, E.; Mosler, E.; Nemetschek-Gansler, H.; Nemetschek, T.; Koch, M. H. J. Structural dynamic of native tendon collagen. *J. Mol. Biol.* **1987**, *193*, 405–407.

(19) Folkhard, W.; Mosler, E.; Geercken, W.; Knorzer, E.; Nemetschek-Gansler, H.; Nemetschek, T.; Koch, M. H. J. Quantitative analysis of the molecular sliding mechanism in native tendon collagen - time-resolved dynamic studies using synchrotron radiation. *Int. J. Biol. Macromol.* **1987**, *9*, 169–175.

(20) Chan, Y.; Cox, G. M.; Haverkamp, R. G.; Hill, J. M. Mechanical model for a collagen fibril pair in extracellular matrix. *Eur. Biophys. J.* **2009**, *38*, 487–493.

(21) Cuq, M. H.; Palevody, C.; Delmas, M. Fundamental study of cross-linking of collagen with chrome tanning agents in traditional and Cr.AB processes. *J. Soc. Leather Technol. Chem.* **1999**, *83*, 233–238.

(22) Basil -Jones, M. M.; Edmonds, R. L.; Allsop, T. F.; Cooper, S. M.; Holmes, G.; Norris, G. E.; Cookson, D. J.; Kirby, N.; Haverkamp, R. G. Leather structure determination by small angle X-ray scattering (SAXS): cross sections of ovine and bovine leather. *J. Agric. Food Chem.* **2010**, *58*, 5286–5291.

(23) Boote, C.; Sturrock, E. J.; Attenburrow, G. E.; Meek, K. M. Psuedo-affine behaviour of collagen fibres during the uniaxial deformation of leather. *J. Mater. Sci.* **2002**, *37*, 3651–3656.

(24) Sturrock, E. J.; Boote, C.; Attenburrow, G. E.; Meek, K. M. The effects of the biaxial stretching of leather on fibre orientation and tensile modulus. *J. Mater. Sci.* **2004**, *39*, 2481–2486.

(25) Sasaki, N.; Odajima, S. Stress-strain curve and Young's modulus of a collagen molecule as determined by the X-ray diffaction technique. *J. Biomech.* **1996**, *29*, 655–658.

(26) Sasaki, N.; Odajima, S. Elongation mechanisms of collagen fibils and force-strain relations of tendon at each level of structural hierarchy. *J. Biomech.* **1996**, *29*, 1131–1136.

(27) Burger, C.; Zhou, H. W.; Sics, I.; Hsiao, B. S.; Chu, B.; Graham, L.; Glimcher, M. J. Small-angle X-ray scattering study of intramuscular fish bone: collagen fibril superstructure determined from equidistant meridional reflections. *J. Appl. Crystallogr.* **2008**, *41*, 252–261.

(28) Cedola, A.; Mastrogiacomo, M.; Burghammer, M.; Komlev, V.; Giannoni, P.; Favia, A.; Cancedda, R.; Rustichelli, F.; Lagomarsino, S. Engineered bone from bone marrow stromal cells: a structural study by an advanced X-ray microdiffraction technique. *Phys. Med. Biol.* **2006**, *51* (6), N109–N116.

(29) Goh, K. L.; Hiller, J.; Haston, J. L.; Holmes, D. F.; Kadler, K. E.; Murdoch, A.; Meakin, J. R.; Wess, T. J. Analysis of collagen fibril diameter distribution in connective tissues using small-angle X-ray scattering. *Biochim. Biophys. Acta* **2005**, *1722*, 183–188.

(30) Mollenhauer, J.; Aurich, M.; Muehleman, C.; Khelashvilli, G.; Irving, T. C. X-Ray diffraction of the molecular substructure of human articular cartilage. *Connect. Tissues Res.* **2003**, *44*, 201–207.

(31) Fernandez, M.; Keyrilainen, J.; Karjalainen-Lindsberg, M. L.; Leidenius, M.; von Smitten, K.; Fiedler, S.; Suortti, P. Human breast tissue characterisation with small-angle X-ray scattering. *Spectroscopy* **2004**, *18*, 167–176.

(32) Liao, J.; Yang, L.; Grashow, J.; Sacks, M. S. The relation between collagen fibril kinematics and mechanical properties in the mitral valve anterior leaflet. *J. Biomech. Eng.* **2007**, *129*, 78–87.

(33) Floden, E. W.; Malak, S. F. F.; Basil-Jones, M. M.; Negron, L.; Fisher, J. N..; Lun, S.; Dempsey, S. G.; Haverkamp, R. G.; Ward, B. R.; May, B. C. H. Biophysical characterization of ovine forestomach extracellular matrix biomaterials. *J. Biomed. Mater. Res., Part B* **2011**, *96B*, 67–75.

(34) Williams, J. M. V. IULTCS (IUP) test methods—measurement of tear load-double edge tear. *J. Soc. Leather Technol. Chem.* **2000**, *84*, 327–329.

(35) Williams, J. M. V. IULTCS (IUP) test methods—sampling. *J. Soc. Leather Technol. Chem.* **2000**, *84*, 303–309.

(36) Cookson, D.; Kirby, N.; Knott, R.; Lee, M.; Schultz, D. Strategies for data collection and calibration with a pinhole-geometry SAXS instrument on a synchrotron beamline. *J. Synchrotron Radiat.* **2006**, *13*, 440–444.

(37) Scott, J. E.; Orford, C. R.; Hughes, E. W. Proteoglycan-collagen arrangements in developing rat tail tendon—an electron-microscopical and biochemical investigation. *Biochem. J.* **1981**, *195*, 573–584.

Biophysical characterization of ovine forestomach extracellular matrix biomaterials

Evan W. Floden,[1] Sharif F. F. Malak,[2] Melissa M. Basil-Jones,[3] Leonardo Negron,[1] James N. Fisher,[1] Stan Lun,[1] Sandi G. Dempsey,[1] Richard G. Haverkamp,[3] Brian R. Ward,[1] Barnaby C. H. May[1]

[1]Mesynthes Limited, Lower Hutt 5040, New Zealand
[2]Auckland Bioengineering Institute, University of Auckland, Auckland 1010, New Zealand
[3]School of Engineering and Advanced Technology, Massey University, Palmerston North 4442, New Zealand

Received 13 May 2010; revised 19 July 2010; accepted 17 August 2010
Published online 4 November 2010 in Wiley Online Library (wileyonlinelibrary.com). DOI: 10.1002/jbm.b.31740

Abstract: Ovine forestomach matrix (OFM) is a native and functional decellularized extracellular matrix biomaterial that supports cell adhesion and proliferation and is remodeled during the course of tissue regeneration. Small angle X-ray scattering demonstrated that OFM retains a native collagen architecture (*d* spacing = 63.5 ± 0.2 nm, orientation index = 20°). The biophysical properties of OFM were further defined using ball-burst, uniaxial and suture retention testing, as well as a quantification of aqueous permeability. OFM biomaterial was relatively strong (yield stress = 10.15 ± 1.81 MPa) and elastic (modulus = 0.044 ± 0.009 GPa). Lamination was used to generate new OFM-based biomaterials with a range of biophysical properties. The resultant multi-ply OFM biomaterials had suitable biophysical characteristics for clinical applications where the grafted biomaterial is under load. © 2010 Wiley Periodicals, Inc. J Biomed Mater Res Part B: Appl Biomater 96B: 67–75, 2011.

Key Words: extracellular matrix, forestomach propria submucosa, SAXS, biophysical, tissue engineering, wound healing

INTRODUCTION

Synthetic meshes (e.g., polypropylene) have historically been used in a number of clinical applications where the graft must support load, for example, hernioplasty. However, the suitability of synthetic meshes has been under scrutiny in light of the increased infection and rejection rates associated with these materials. Consequently, there has been a move towards native biomaterials, particularly those composed of decellularized extracellular matrix (dECM), for example human acellular dermis (HAD, Alloderm®, LifeCell Corporation, NJ) and acellular small intestinal submucosa (SIS, Cook Biotech, IN). The clinical uptake of dECM-based biomaterials has been such that it is expected that these biomaterials will account for >50% of the market value of implantable meshes by 2011.[1] These dECM-based biomaterials are prepared from suitable source tissues that are decellularized and delaminated, typically by exposure to detergents, to yield an intact dECM.[2] dECM-based biomaterials retain the complexity of native tissue ECM, with an intact collagen framework consisting of structural proteins, as well as, associated cell signaling and adhesion molecules.[3] In this way, exogenous dECM can stimulate, support, and host cell colonization of the tissue deficit leading to regeneration. No chronic inflammatory response is observed with native dECM-based biomaterials. Instead, the observed inflammatory response is one associated with constructive remodeling, whereby the biomaterial is degraded and replaced by a new collagenous framework as part of normal tissue remodeling.[4,5] Increased vascularization, as well as, reduced scar tissue and capsule formation have been noted with the use of dECM-based biomaterials following implantation. Importantly, due to their biophysical properties, either inherent or engineered, these biomaterials can physically bridge large tissue deficits to allow tension free repair of adjacent tissues and therefore replace synthetic meshes in certain clinical applications.

Biomaterials must be engineered with suitable biophysical properties to allow successful clinical use. For example, hernia grafts must withstand the load bearing stresses exerted by the contents of the abdominal cavity, retain sutures used to secure the graft, and provide sufficient elasticity to mimic natural tissue movement. Numerous technologies have been developed to modify the biophysical properties of collagen-based biomaterials to match certain clinical applications. Chemical crosslinking (e.g., 1-ethyl-3-(3-dimethylaminopropyl) carbodiimide or glutaraldehyde) is one such approach that covalently crosslinks adjacent collagen fibers to increase matrix density, strength and persistence. However, confidence in this approach has decreased due to the chronic inflammatory response that is associated with crosslinked biomaterials.[4,5] Other approaches have attempted to introduce new biophysical properties to collagen scaffolds

Additional Supporting Information may be found in the online version of this article.
Correspondence to: B. C. H. May; e-mail: barnaby.may@mesynthes.com

by combining or layering biomaterials such that the properties of the hybrid biomaterial benefits from the properties of the individual components. For example, composite biomaterials comprising urinary bladder matrix (UBM)/polyglycolic acid (PGA),[6] heparinized poly(vinyl alcohol)/SIS,[7] collagen/hydroxyapitate,[8] collagen/hyaluronan/chitosan,[9] collagen/silica,[10] and collagen/polypropylene,[11] have been reported. Although the introduction of synthetic components to tune the physical properties of collagen-based biomaterials can be effective, these advantages may be offset by the risk of introducing non-native components that may not undergo constructive remodeling. Additionally, in order for these hybrid biomaterials to properly serve as templates for regeneration they must adequately recapitulate structural features of native ECM.

As part of efforts directed at developing materials as biomimetics of native ECM, a dECM termed ovine forestomach matrix (OFM) has been developed for applications in tissue regeneration, including the treatment of chronic and acute wounds and in the form of implantable grafts for soft tissue reconstruction. OFM comprises the decellularized propria submucosa isolated from ovine forestomach tissue. Previous studies[12] have shown that OFM is primarily composed of collagens I and III, and retains the collagen microarchitecture of native ECM. Additional ECM-associated macromolecules (e.g., fibronectin and fibroblast growth factor basic) were also present in OFM, as were remnant basement membrane components (e.g. laminin and collagen IV) on the luminal surface and in native vascular channels. These secondary molecules, working in concert with the collagenous framework, were shown to support cell attachment, infiltration and stimulate cell differentiation.[11] OFM was developed as a means of addressing shortcomings with existing dECM-based biomaterials. Namely, the disease risk associated with porcine, bovine- and human-sourced dECM, the cultural and religious objections to collagens sourced from these raw materials, and the limited biophysical properties of current dECM-based biomaterials. The aim of this study was to understand the physical properties of OFM, and a series of new laminated OFM biomaterials whose properties were tunable through a process of lamination.

MATERIALS AND METHODS

General

OFM was prepared from ovine forestomach propria submucosa according to established procedures by Mesynthes Limited using proprietary methods.[12] All experiments were conducted at room temperature unless otherwise indicated. Strength testing was conducted using an Instron 5800 series electromechanical tester (Instron, MA). All samples were rehydrated in phosphate buffered saline (PBS) for at least 5 minutes prior to testing and testing was conducted within 30 minutes of rehydration. The thickness of materials was determined using a micrometer (Mitutoyo, Japan).

Small angle X-ray scattering analysis

Lyophilized samples of OFM were characterized using small angle X-ray scattering (SAXS) according to the method described in Basil-Jones et al.[13] Single SAXS images were taken from a spot 80 $\times$ 250 μm in size. SAXS diffraction patterns were recorded on the Australian Synchrotron SAXS/WAXS beamline, utilizing a high-intensity undulator source.

Lamination

Thicker OFM biomaterials were created by lamination either via lyophilization, with or without additional sewing, or through adhesion of lyophilized OFM sheets using a collagen gel. All lamination procedures used a perforated stainless steel tray that allowed adequate vapor flow from the multiply laminates during lyophilization. Lamination via lyophilization proceeded as follows; a sheet of wet OFM was laid flat on a perforated stainless steel surface. Additional sheets of wet OFM were added to the top of the first to create a multilaminate stack. Care was taken to remove any air bubbles between each of the sheets. The stack of wet OFM sheets, up to eight sheets in total, was freeze dried according to proprietary procedures. The lyophilized laminates were sewn using PGA absorbable suture, 4-0 or 5-0 gauge (Foosin Medical Supplies, Shandong, China). OFM laminates were additionally created using a collagen gel prepared from powdered OFM. OFM was powdered using a spice grinder and liquid nitrogen. The powdered material was placed in PBS 10% w/v and heated at 90°C for 1.5 hours, then centrifuged at 4000 rpm for 20 minutes. The supernatant was shown to reversibly gel on cooling, and thus the gel was maintained at 37°C during application. The collagen gel was applied as a continuous layer (~25–100 μm thick) to a single sheet of lyophilized OFM. A second layer of lyophilized OFM was applied to the layer of gel and this procedure repeated to build up a laminate of the desired thickness (up to 8-ply). Care was taken to remove any air bubbles between each of the sheets. The multi-ply stack was oven dried at 37°C for 24 hours prior to use during which time the collagen gel dried to adhere adjacent layers.

Ball-burst testing

Materials were tested using an adaption to the ball burst method described in ASTM D 3787-07 "Standard Test Method for Bursting Strength of Knitted Goods, Constant-Rate-of-Traverse Ball-burst Test."[14] A materials testing machine was equipped with a 1 kN load cell and fitted with a custom built ball-burst compression apparatus consisting of an orifice and a 25.4-mm stainless steel ball. Test samples measuring ~10 $\times$ 10 cm were centered over the orifice and clamped in place. The stainless steel ball was pushed through the test material at a constant feed rate of 305 mm/min and the compression load of failure was recorded.

Uniaxial strength

Materials were cut with a die to "dumbbell" shaped samples with widths of 6 mm and 25 mm along the gauge length and specimen ends, respectively. The specimen ends were fixed to the grips of a materials testing machine, ensuring a grip-to-grip distance of 75 mm. The samples were tested to failure, whilst the tensile load was measured using a 100 N load cell and a constant feed-rate of 25.4 mm/min. Maximum

tangential stiffness was calculated from the slope of the load (N) versus elongation (mm curve). The load versus elongation curve was transformed to a stress (N/m^2) versus strain curve, using the cross-sectional area calculated from the thickness and the width of the sample. The slope of this latter curve at its linear transition was used to calculate the modulus of elasticity, or Young's modulus (GPa).

Suture retention test

OFM biomaterials were tested for suture retention using an adaptation of 'ANSI/AAMI VP20-1994 Guidelines for Cardiovascular Implants Vascular Prostheses Measured in Newtons. A 5 mm diameter loop of suture material (4-0, Vicryl®, Ethicon) was added to the middle of the shorter edge of OFM samples measuring 2 × 4 cm. The two ends of the suture material were knotted together using a surgeon's knot. Sutures were positioned with a bite-depth (distance from the site of the suture to the edge of the sample) of 2 mm. A 3-mm diameter round stainless steel bar was fed through the suture loops and suspended by two parallel hooks. The opposing suture-free end of the samples were held in a vice grip. The sutures were pulled through the sample at a constant feed rate of 20 mm/min and the load to failure measured with a 100 N load cell. Load at failure was defined as a 90% reduction in the observed load.

Preparation of cross-linked OFM

OFM materials were cross-linked according to established procedures.[15] Briefly, sheets of hydrated OFM were prepared and cut to ~400 cm^2 and soaked in a solution of 0.6% *N*-hydroxysuccinimide in water (100 mL) for 5 minutes. The OFM sheets were removed and individually laid over rigid 5-mm plastic boards (400 cm^2) with the luminal side facing up. A 1.15% solution of 1-ethyl-3-(3-dimethylaminopropyl)carbodiimide in water (20 mL) was added directly to the surface of the OFM sheet, ensuring that the entire surface was covered. Two similarly treated pieces of OFM were joined such that their luminal surfaces were in contact. The 'sandwich' was compressed and incubated at 37°C overnight. The 2-ply laminates were removed from the plastic sandwich, rinsed with RO H_20 (3 × 250 mL), then PBS (2 × 250 mL), and finally freeze-dried using proprietary procedures. The dried materials were cut to size and tested for uniaxial strength, as described earlier.

Permeability

Permeability indices (PI) were determined using a custom built hydrostatic permeability test rig, according to established procedures.[16] Test specimens measuring ~8 × 8 cm were clamped into an orifice with an internal diameter of 22 mm, such that the surface area of the test sample was 3.8 cm^2. A column of distilled water was maintained with a height of 163.2 cm above the sample to achieve a pressure head of 120 mmHg. This pressure was maintained throughout the experiment. A valve that separated the water column and the sample orifice was opened at the start of the experiment allowing water to come in contact with and flow through the sample. Water passing through the sample was collected over a period of time using a pre-weighed plastic tube. The weight of water collected (g) was converted into volume (mL), assuming density of water = 1.0 g/mL. PI were calculated using the formula; PI (120 mmHg) = volume collected (mL)/[area orifice (cm^2) × time (min)]. Bovine dura was isolated from a two-year old Angus cow following slaughter (Ashurst Meat Processing, Ashurst, New Zealand). The skull was cut longitudinally and the brain tissue removed to expose the underlying dura. The dura was carefully separated from the skull and placed in sterile saline at 4°C. Dura was tested for permeability within 24 hours of harvesting.

RESULTS

SAXS analysis

SAXS analysis of OFM provided insight into the structure and orientation of the collagen fibrils. The periodicity in the collagen overlaps is apparent with the rings in the scattering pattern [Figure 1(A)] which, when integrated around all azimuthal angles showed distinct peaks representing the collagen overlap spacing [Figure 1(B)]. The *d* period spacing is the measurement of the collagen fibril repeating unit, termed "axial periodicity." The average *d* period was obtained from the *q* position of the peaks in Figure 1(B), and was measured in OFM as 63.5 ± 0.2 nm. Information about larger collagen structures was gained from the lower *q* regions (<0.03 $Å^{-1}$). The slope at low *q* for the OFM SAXS profile [Figure 1(B)] is $q^{-3.7}$ which corresponds quite closely with a Porod's law slope (of q^{-4}) and indicates that distinct boundaries exist between the collagen fibrils, which is another indicator of native collagen structure. The scattering pattern observed from the higher *q* ranges (0.04–0.1 $Å^{-1}$) showed the non-isotropic nature of the collagen fibrils present in OFM [Figure 1(B)]. This non-isotropy is apparent in the significantly higher intensities of the Bragg peaks in the azimuthal region Ψ = 150°–210°, and 330°–30°compared with Ψ = 60°–120° and 240°–300° showing the orientation approximately through 0°–180°. The range of orientations in the collagen fibrils was determined by plotting the azimuthal angle versus relative intensities for a Bragg peak. A single 5° meridional arc at $q \sim 0.06$ $Å^{-1}$ represents only one Bragg peak, and the variation in intensity of this peak through 360° provides information on the orientation of collagen [Figure 1(C)]. OFM showed only one preferred fibril orientation that goes through ~0° and 180°. The fibril orientation index (OI), defined as the minimum angle which contains 50% of the fibrils, was calculated as 20°.

Preparation of laminated OFM biomaterials

OFM was manufactured from ovine forestomach tissue according to established procedures[12] and were prepared as sheets in sizes up to approximately 40 x 40 cm. There was relatively small variation in the thickness of the material, with an average thickness of 0.25 ± 0.01 mm and a range of 0.14–0.41 mm [Figure 3 (B) and Supplementary Table 1]. Before testing samples were rehydrated in saline. Generally, the biomaterials fully rehydrated in 1–5 minutes, consistent with the reported rehydration rates of other dECMs.[17] Rehydration improved the handling and physical properties of OFM

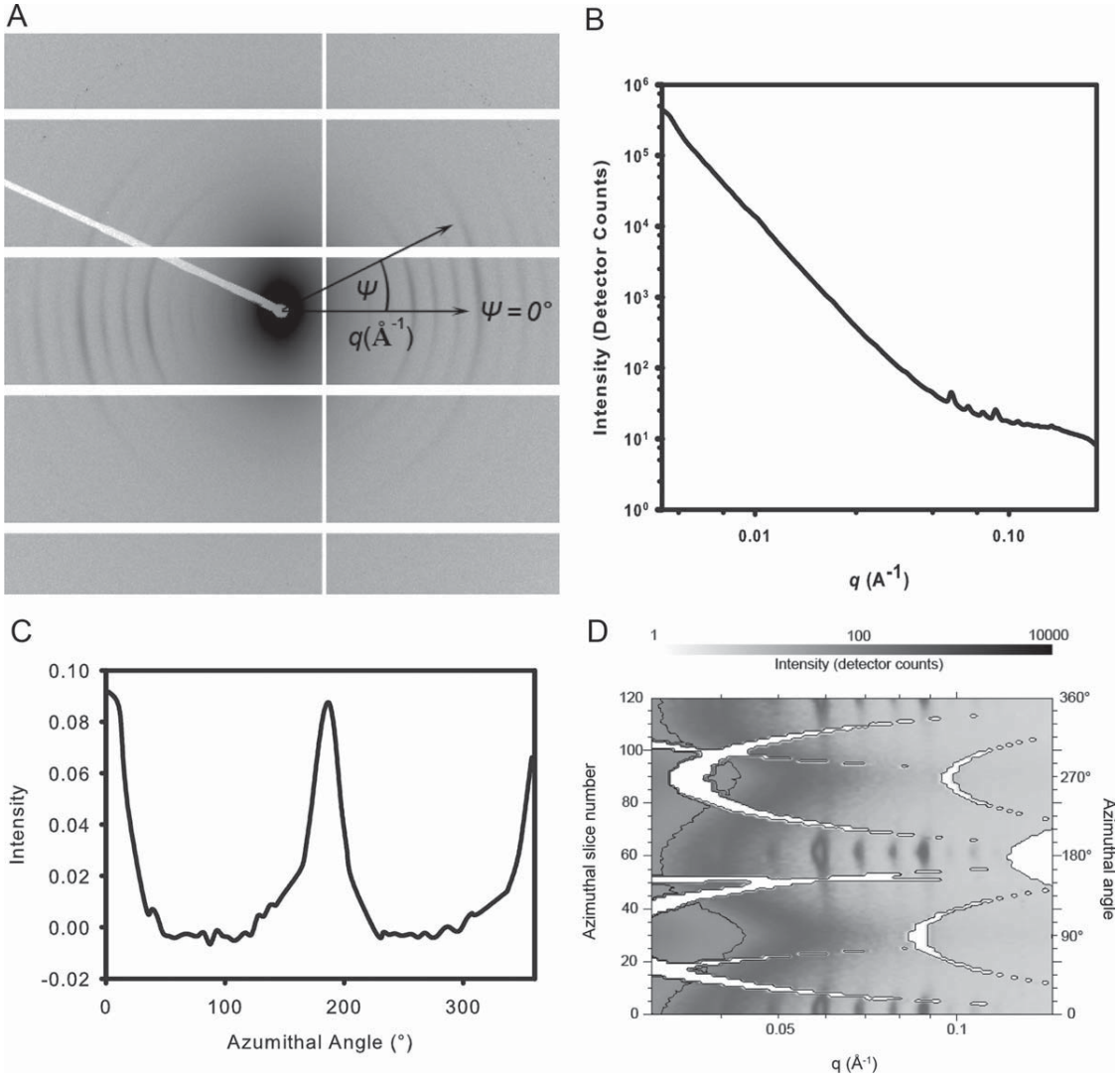

FIGURE 1. A. SAXS diffraction pattern for OFM. B. SAXS profile of OFM showing q versus intensity. C. Azimuthal angle plot from the Bragg peak $q \sim 0.06$ Å^{-1} with arbitrary intensity scale and offset. D. Gray shade plot of q versus azimuthal angle for OFM. The white arcs on the image represent the gaps in the detector. The dark vertical bands centered vertically on the azimuth angle of 0° and 180° are the collagen d spacing Bragg peaks. SAXS intensity is given by the gray scale.

consistent with the observations of Whitson et al.[17] The three methods of laminating OFM sheets all gave biomaterials of similar handling characteristics, including the ability to bunch and fold, and to be deformed. Use of lyophilization or the collagen gel adhesive did not grossly impact on the cosmetic features of the resultant OFM multilaminates. Sewing the lyophilized laminates was explored as a means of providing additional structural cohesiveness over-and-above that achieved by simply lyophilizing. In this instance, samples were sewn using a quilting pattern, comprising a series of stitch lines running perpendicular to each other [Figure 2(A)].

Comparison of the biophysical properties OFM biomaterials prepared with collagen gel

The OFM biomaterials were tested to the point of catastrophic failure using ball-burst, uniaxial, and suture retention testing. In all cases, the biophysical properties where compared for a series of OFM biomaterials prepared using a collagen gel to laminate adjacent sheets. As expected, there was a dramatic increase in the strength of OFM biomaterials as the thickness was increased by adding additional sheets to produce the series of multi-ply biomaterials (up to 8-ply). The ball-burst test measured resistance to force applied equally in all directions. When considering implanted biomaterials, the ball-burst test may be considered more predictive than the uniaxial strength test, as the test load is distributed in all directions across the surface of the biomaterial. In comparison, uniaxial strength determines load at failure in one direction only. Under ball-burst testing, the 8-ply OFM biomaterial had a maximum burst strength of 941.89 ± 48.75 N, whereas single-ply OFM was significantly weaker, with a maximum burst strength of 92.84 ± 12.73 N [Figure 2(B) and Supplementary Table 1].

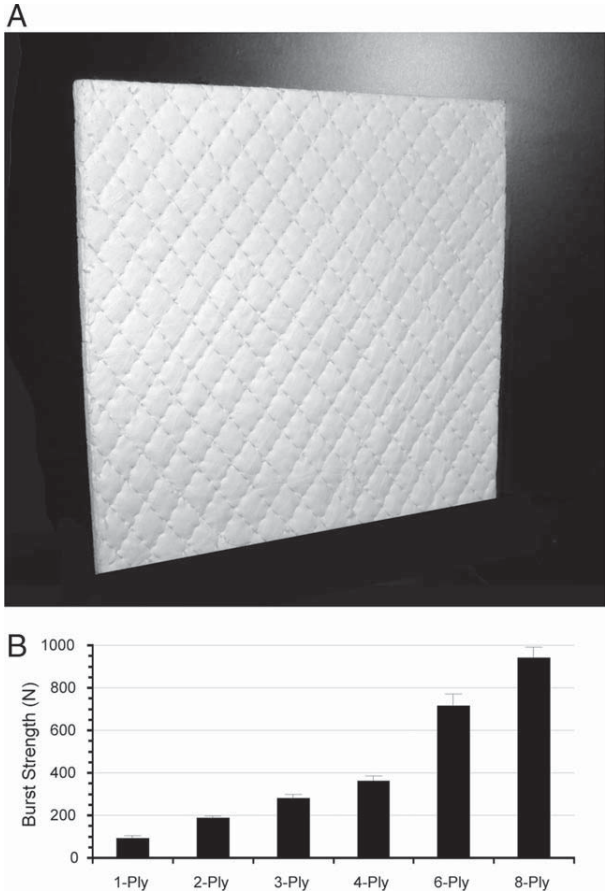

FIGURE 2. A. Representative image of a 6-ply OFM laminate sewn with PGA suture. B. Ball-burst strength—burst strength at failure (N) of a series of multilaminate OFM biomaterials. See Supplementary Table 1 for sample sizes (*n*). Error bars represent standard error.

A comparison of the uniaxial strength properties of the OFM biomaterials is presented in Figure 3, and Supplementary Table 1. A representative bimodal stress-strain curve derived from the elongation versus force curve is shown in Figure 3(A). Stress-strain curves were characterized by a "toe region," a transition through a linear elastic deformation region and a well-defined yield point. There was good agreement between the relative strengths of biomaterials tested under uniaxial and ball-burst methods. As expected, increasing the thickness [Figure 3(B)] of the biomaterial by increasing the lamination state significantly increased the maximum load [Figure 3(C)]. For example, the maximum load at failure of 8-ply material was 65.13 ± 4.37 N, whereas the single-ply material was 15.07 ± 2.68 N. Yield stress [Figure 3(F)] was determined by normalizing the maximum load to the cross sectional area of the sample. Yield stress was ~10 MPa, irrespective of the thickness. This is to be expected given that the material composition of the laminates did not change with increasing the lamination state. There was no increase in the observed yield stress of the 2-ply (9.77 ± 1.68 MPa) material relative to the single-ply (10.15 ± 1.81 MPa) material suggesting that the OFM determined the strength of the biomaterial rather than the collagen gel used during lamination. Lamination did not increase the maximum elongation (~20 mm), but the maximum tangential stiffness increased between the single- and multi-ply laminates [Figure 3(D)]. The modulus of elasticity (Young's modulus) is an intrinsic property and describes the tendency of a material to be deformed elastically. The modulus increased between the single and multi-ply biomaterials [Figure 3(C)]. For example, the modulus of elasticity of the single-ply material was 0.044 ± 0.009 GPa, whereas the 8-ply material was 0.085 ± 0.006 GPa. The observed increase in the modulus and the increase in the maximum tangential stiffness suggest that the thicker biomaterials (e.g. 6- and 8-ply) prepared with collagen gel would be less elastic than thinner OFM biomaterials laminated using this approach.

Suture retention strength measures a material's resistance to suture pull-out under uniaxial load. Suture retention strength increased relative to the thickness of the material. For example, the maximum load at failure of the single-ply and 8-ply laminates were 5.91 ± 0.60 N and 16.85 ± 2.46 N, respectively (Supplementary Table I). It was possible to normalize the suture retention strength to the thickness of the biomaterial (Supplementary Table 1). Normalized suture retention did not change with the increasing thickness of the laminated biomaterials.

Comparison of laminated OFM biomaterials

The 6-Ply OFM laminated biomaterials were created by either lyophilization, sewing a lyophilized laminate, or by use of a collagen gel to bond adjacent lyophilized OFM sheets. Sewn laminates were prepared with either 4-0 or 5-0 gauge PGA suture material. The thickness of the 6-ply collagen gel laminated biomaterial was ~30% of the other laminated 6-ply biomaterials (Table I). There were no obvious differences seen in the relative strengths of the various materials using ball-burst testing and any differences might be accounted for by the natural variations seen in the OFM biomaterial, rather than the influence of the lamination technique. Indeed, under uniaxial load the 6-ply biomaterials had essentially equivalent failure points (~50 N). Differences in the relative thicknesses of the laminates (Table I) meant the collagen gel laminated biomaterial had the highest yield stress (14.81 ± 0.94 MPa). Sewn laminates had a lower average modulus of elasticity (0.047 ± 0.003 and 0.033 ± 0.006 GPa) relative to the other laminates tested. It was difficult to distinguish the biophysical properties of laminates sewn with either the 4-0 or 5-0 suture on the basis of uniaxial testing. This suggests that the contribution of the sutures to the biophysical properties of the corresponding biomaterials was low, which is consistent with the observations that the collagen gel did not significantly contribute to the performance characteristics of the gel laminated biomaterials, as described earlier. Alternatively, there may be little to distinguish the biophysical properties of 4-0 versus 5-0 suture material such that these two materials are essentially identical under the testing performed here.

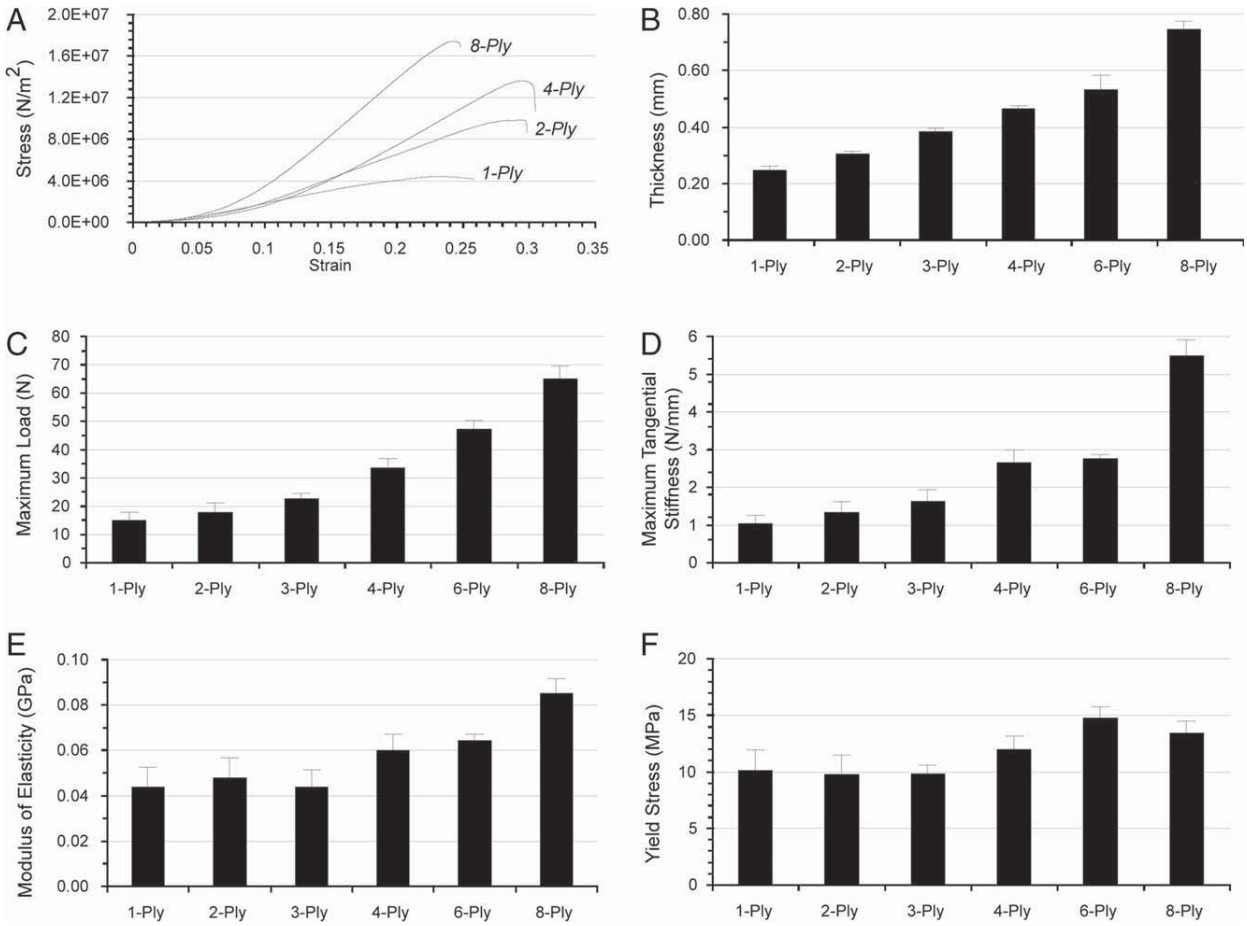

FIGURE 3. Uniaxial strength of multilaminate OFM biomaterials. A. Representative stress-strain curve. B. Thickness of collagen laminated OFM biomaterials. C. Maximum load at failure (N). D. Maximum tangential stiffness (N/mm). E. Young's Modulus (GPa). F. Yield stress (MPa). See Supplementary Table 1 for sample sizes (*n*). Error bars represent standard error.

We additionally prepared cross-linked OFM biomaterials and tested these under uniaxial testing. The uniaxial strength of crosslinked OFM was reduced relative to 2-ply laminates created using a collagen gel (yield stress, 6.22 ± 0.76 and 9.77 ± 1.68, respectively). Additionally, there was a significant increase in the elasticity of the crosslinked

TABLE I. Biophysical Properties of 6-Ply OFM Laminated Biomaterials Prepared Using a Collagen Gel, Lyophilization and by Sewing with Either 4-0 or 5-0 PGA Suture

		6-Ply Laminate Construction			
		Collagen Gel	Lyophilized	Sewn (4-0)	Sewn (5-0)
Thickness (mm)		0.53 ± 0.05 ($n = 6$)	1.16 ± 0.03 ($n = 6$)	1.10 ± 0.09	1.26 ± 0.10 ($n = 6$)
Ball-Burst	Burst strength (N)	714.90 ± 48.75	534.83 ± 75.28	343.37 ± 43.17	455.96 ± 23.68
Uniaxial Strength	Maximum load (N)	47.31 ± 2.99 ($n = 6$)	57.93 ± 6.05 ($n = 6$)	44.72 ± 8.18	43.44 ± 6.91 ($n = 6$)
	Maximum elongation (mm)	31.36 ± 2.04 ($n = 6$)	22.44 ± 2.59 ($n = 6$)	18.16 ± 0.77	24.15 ± 1.93 ($n = 6$)
	Maximum tangential stiffness (N/mm)	2.77 ± 0.10 ($n = 6$)	4.90 ± 0.89 ($n = 6$)	4.16 ± 0.52	3.21 ± 0.38 ($n = 6$)
	Modulus of elasticity (GPa)	0.065 ± 0.002 ($n = 6$)	0.054 ± 0.011 ($n = 6$)	0.047 ± 0.003	0.033 ± 0.006 ($n = 6$)
	Yield stress (Mpa)	14.81 ± 0.94 ($n = 6$)	8.33 ± 0.87 ($n = 6$)	6.76 ± 1.24	5.75 ± 0.3 ($n = 6$)
Suture Retention	Maximum load (N)	12.95 ± 0.92	16.96 ± 1.83	13.33 ± 1.22	11.62 ± 1.58
	Normalized maximum load (N)	24.43 ± 1.73	14.62 ± 1.58	12.12 ± 1.11	10.32 ± 1.40

Five samples were tested, unless otherwise specified (*n*). Errors represent standard error.

TABLE II. Permeability of Single-Ply OFM, Laminated OFM Biomaterials and Bovine Dura

Permeability Index (mL/min/cm^2)	1-Ply	2-Ply Laminate Construction			Bovine Dura
		Collagen Gel	Lyophilized	Sewn (4-0)	
Luminal→abluminal	0.0031 ± 0.0005 (n = 10)	0.0002 ± 0.0001 (n = 7)	0.0007 ± 0.0003 (n = 7)	128.57 ± 28.56 (n = 12)	0.0022 ± 0.0003 (n = 6)
Abluminal→luminal	0.0025 ± 0.0006 (n = 8)				

Single-ply OFM is anisotropic and was tested in both directions. 2-Ply OFM laminates are isotropic and were tested in one direction only. Sample sizes are as indicated (n). Errors represent standard error.

material relative to the collagen gel laminate (modulus, 0.044 ± 0.009 and 0.028 ± 0.002, respectively).

Permeability of OFM laminates

Previously, OFM was shown to be anisotropic having a distinct luminal and abluminal surface.[12] The luminal surface has been shown to retain remnants of the basement membrane that underlies the epithelial surface of forestomach tissue. In contrast to the smooth continuous luminal surface, the abluminal surface has a more open reticular surface. Given the differences in surface morphology of the OFM biomaterial, and the function of forestomach tissue in adsorption of nutrients from the ingesta, we investigated whether the aqueous permeability of OFM was directional. Using a custom fabricated permeability test-rig, the PI of OFM was assessed, both in the luminal→abluminal and in the abluminal→luminal directions (Table II). OFM was shown to be permeable to aqueous solutions; however, there was no statistical difference in the flow rates from either the luminal or abluminal surfaces.

To understand the effect of the various lamination techniques on the aqueous permeability of OFM laminates we quantified the permeability of various 2-ply OFM biomaterials (Table II). As expected the sewn laminate was highly permeable (128.57 ± 28.6 mL/min/cm^2) owing to the needle tracks that allowed free flow of solutions across the material. The laminates prepared with either a collagen gel or via lyophilization (0.0002 ± 0.0001 and 0.0007 ± 0.0003 mL/min/cm^2, respectively) were significantly less permeable than the sewn laminates and were approximately half as permeable as single-ply OFM. To our knowledge, the permeability of human dura has not been established under similar testing conditions. Therefore, in an effort to identify a biologically relevant frame of reference, bovine dura was isolated and tested for aqueous permeability. Bovine and human dura are known to have similar mechanical properties,[18] and both comprise an especially dense arrangement of collagen fibers. Under identical testing procedures bovine dura had an aqueous permeability of 0.0022 ± 0.0003 mL/min/cm^2 equivalent to single-ply OFM.

DISCUSSION

Scanning electron microscopy has previously been used to confirm that the collagen matrix of OFM grossly resembles a native structure,[12] and we present here a SAXS analysis of the collagen arrangement at the molecular level. SAXS analysis can be used to resolve structural features of collagen fibers, and therefore interrogate the structural integrity of collagen-containing biomaterials. As the arrangement of collagen fibers within dECM-based biomaterials largely dictates their biophysical properties, SAXS analysis is also complementary to more traditional biophysical strength testing (e.g., uniaxial or ball-burst testing). High-resolution SAXS diffraction data for dECM-based biomaterials have not previously been published, however SAXS analysis has been presented for tendon,[19] bone,[20] colonic submucosa,[21] and leather.[13] It is expected that colonic submucosa would be structurally similar to forestomach propria submucosa as both include submucosa derived from the digestive tract and contain similar collagen I/III ratios. As such, SAXS analysis of colonic submucosa provides a convenient indicator of the expected "native" collagen structure of OFM. Axial periodicity values for native collagen tissues are between 63 nm and 68 nm.[21] For example, the observed d period for colonic submucosa has been reported as 64.7 nm.[21] In comparison, the axial periodicity OFM was 63.5 nm. The close agreement between the expected axial periodicity of native submucosal ECM, as determined from colonic submucosa, and the observed axial periodicity of OFM suggests that the native fibril structure is retained in OFM. SAXS analysis revealed the OFM fibril orientation index (OI) was 20° demonstrating a highly orientated fibril network. Similarly, the fiber orientation of the dECM-based biomaterials SIS and acellular UBM have been reported using small angle lights scattering as 25°[22] and 46°,[23] respectively. Therefore, there is strong evidence from SAXS and scanning electron microscopy analysis that the collagen fiber matrix in OFM is highly ordered and resembles a native collagen matrix.

Several deficiencies in the use of dECM-based biomaterials have been identified. These include laxity (bulging) due to elastic potential, seroma formation within dead space in delaminated implants, and incomplete cellular infiltration due to the thickness of the material. Being composed of decellularized human dermis, HAD is highly elastic allowing for ~50% increase in the surface area of the material.[24] As such, graft laxity can be problematic following the use of HAD in complex hernia and abdominal repair,[24,25] and it has been suggested that HAD be prestretched before implantation.[26,27] This is reflected in the modulus of elasticity of HAD, ~0.01 GPa.[28] In comparison the elasticity of OFM (0.044 ± 0.009 GPa) was shown to be comparable with the reported modulus of SIS (0.026 ± 0.014 GPa).[29] Biophysical testing of the OFM biomaterial additionally demonstrated that this native dECM is relatively strong (yield stress, 10.15 ± 1.81 MPa) and is

consistent with the typical yield stress of implantable synthetic meshes (10 GPa or greater[30]). In comparison, the yield stress of UBM is ~2 MPa.[31] OFM (92.8 ± 12.7 N) additionally out-performed the reported burst strength of both UBM (11.19 ± 3.39 N)[31] and SIS (20.32 ± 1.88 N).[32] One caveat to these comparisons is that the dECM-based biomaterials have not been tested in side-by-side experiments, such that the observed differences (and similarities) may reflect subtle differences in experimental conditions.

The load bearing performance characteristics of biologic implants can be improved by increasing the thickness of the graft. For example, HAD is available in a range of thicknesses (~0.3−3.3 mm, www.lifecell.com) reflecting the diversity of donor cadaveric dermis, whereas SIS is available in 1-, 4- and 8-ply formats. However, increasing the thickness of biologic implants to improve absolute strength can introduce additional problems. For example, thicker grafts are less likely to fully recellularize following implantation, a pathology that has been noted for both HAD and multi-ply SIS.[24,33] Delamination of laminated SIS has been noted following its use in hernia repair[34] and has been associated with intra-graft seroma between adjacent sheets of the laminated material.[24] Seroma formation within laminated grafts can be largely overcome by ensuring that the graft remains intact so that fluid cannot accumulate within the graft. Additionally, fenestration has been used to ensure that fluid can drain freely from within the graft and underlying tissues. To increase the absolute strength of OFM-based biomaterials various methods were explored to combine multiple layers in a process of lamination. These approaches endeavored to retain as much of the native structure and function encoded in OFM, and as such, did not explore methods that relied on chemical modification or the introduction of non-native polymers. To our knowledge, sewn dECM laminates have not previously been reported in the scientific literature and this approach offers a simple solution to modifying the biophysical properties of dECM laminated biomaterials. Chemical crosslinking has been explored as a method of improving the tensile strength of decellularized biologics, and there are a number of crosslinked biologic implants commercially available.[3] To understand if there were biophysical advantages to crosslinking OFM biomaterials we created 2-ply crosslinked OFM laminates using established procedures.[15] Chemically crosslinked OFM biomaterials demonstrated increased elasticity and reduced strength. These findings suggest that crosslinking may be associated with some denaturation of the collagen scaffold leading to a weakened matrix structure with increased elasticity, consistent with previous findings.[35] Given that crosslinked dECM-based biomaterials are known to illicit a foreign body response and that crosslinking does not significantly improve the biophysical performance of the OFM biomaterial, we would suggest that the applications of cross-linked OFM biomaterials are limited.

Being derived from natural tissues rather than a reconstituted collagen source, dECM-based biomaterials typically have macroscopic and microscopic differences reflecting natural variation in the source tissue. These differences are also demonstrated in the biophysical properties of the materials. For example, Sacks and Gloeckner[36] have shown mechanical anisotropy in single-ply SIS reflecting a collagen fiber alignment that runs parallel to the long axis of the intestine. Anisotropy is also evident in multi-ply SIS biomaterials and HAD.[28] A benefit of laminating dECM-based biomaterials is that the process of lamination has the potential to average any morphological differences seen in the materials. In this way, local biophysical differences within a sheet of material, or differences between two sheets of material are averaged out to increase homogeneity. For example, Freytes and co-workers[14] have overcome physical differences in the longitudinal and traverse directions of SIS by creating laminates whereby successive sheets were oriented 45° from each other. OFM is anisotropic having distinct luminal and abluminal surfaces.[12] The luminal surface arises from separation of the lamina epithelias from the propria submucosa and is characterized by protrusions resulting from remnants of the epithelial papillae. Additionally, the luminal surface is known to contain remnants of basement membrane components (e.g., laminin and collagen IV). In contrast, the abluminal surface is relatively smooth. In preparing the laminated OFM presented here, opposing layers of OFM were orientated in a luminal-luminal and abluminal-abluminal fashion, such that in all cases the exposed surfaces were the smoother abluminal face. In this way, the resulting laminated biomaterial is isotropic. It is equally possible to create OFM laminates by placing successive sheets in a luminal-abluminal orientation, such that the resultant laminates have both a luminal and abluminal surface exposed and the anisotropic characteristics of single-ply OFM are retained. Lamination also provides a route to creating larger format dECM-based biomaterials.[14] The ovine forestomach is a relatively large tissue source for isolating intact dECM, with sheets of up to 40 × 40 cm available. However, for certain applications, lamination of overlapping sheets and subsequent sewing of the laminate, would provide a means of generating laminated biomaterials in sizes in excess of current limitations.

There is a current need for dECM-based biomaterials with biophysical properties tailored for various clinical applications. The native collagen fiber structure of OFM imparts excellent biophysical properties to this biomaterial and these properties can be extended and tuned using lamination. It has been demonstrated that it is possible to generate a range of OFM biomaterials with various thicknesses, strengths, and permeabilities. This flexibility in the OFM biomaterial opens up a range of potential applications.

ACKNOWLEDGMENTS

We acknowledge the Foundation for Research Science and Technology (New Zealand) MSMA0701 for funding this project. SAXS analysis was undertaken on the SAXS/WAXS beamline at the Australian Synchrotron, Victoria, Australia.
Author Disclosure: E.W.F., S.L., B.R.W., and B.C.H.M. are shareholders of Mesynthes Limited.

REFERENCES

1. US Markets for Soft Tissue Repair 2008: Millenium Research Group.
2. Gilbert TW, Sellaro TL, Badylak SF. Decellularization of tissues and organs. Biomaterials 2006;27:3675–3683.

3. Badylak SF, Freytes DO, Gilbert TW. Extracellular matrix as a biological scaffold material: Structure and function. Acta Biomater 2009;5:1–13.
4. Badylak SF, Gilbert TW. Immune response to biologic scaffold materials. Semin Immunol 2008;20:109–116.
5. Valentin JE, Stewart-Akers AM, Gilbert TW, Badylak SF. Macrophage Participation in the Degradation and Remodeling of ECM Scaffolds. Tissue Eng Part A 2009;15:1687–1694.
6. Eberli D, Freitas Filho L, Atala A, Yoo JJ. Composite scaffolds for the engineering of hollow organs and tissues. Methods 2009;47: 109–115.
7. Jiang T, Wang G, Qiu J, Luo L, Zhang G. Heparinized poly(vinyl alcohol)—small intestinal submucosa composite membrane for coronary covered stents. Biomed Mater 2009;4:25012.
8. Al-Munajjed AA, Plunkett NA, Gleeson JP, Weber T, Jungreuthmayer C, Levingstone T, Hammer J, O'Brien FJ. Development of a biomimetic collagen-hydroxyapatite scaffold for bone tissue engineering using a SBF immersion technique. J Biomed Mater Res B Appl Biomater 2009;90:584–591.
9. Lin YC, Tan FJ, Marra KG, Jan SS, Liu DC. Synthesis and characterization of collagen/hyaluronan/chitosan composite sponges for potential biomedical applications. Acta Biomater 2009;5:2591–2600.
10. Heinemann S, Heinemann C, Bernhardt R, Reinstorf A, Nies B, Meyer M, Worch H, Hanke T. Bioactive silica-collagen composite xerogels modified by calcium phosphate phases with adjustable mechanical properties for bone replacement. Acta Biomater 2009;5:1979–1990.
11. van't Riet M, Burger JW, Bonthuis F, Jeekel J, Bonjer HJ. Prevention of adhesion formation to polypropylene mesh by collagen coating: A randomized controlled study in a rat model of ventral hernia repair. Surg Endosc 2004;18:681–685.
12. Lun S, Irvine SM, Johnson KD, Fisher NJ, Floden EW, Negron L, Dempsey SG, McLaughlin RJ, Vasudevamurthy M, Ward BR, May BC. A functional extracellular matrix biomaterial derived from ovine forestomach. Biomaterials 2010;31:4517–4529.
13. Basil-Jones MM, Edmonds RL, Allsop TF, Cooper SM, Holmes G, Norris GE, Cookson DJ, Kirby N, Haverkamp RG. Leather structure determination by small-angle X-ray scattering (SAXS): Cross sections of ovine and bovine leather. J Agric Food Chem 2010;58: 5286–5291.
14. Freytes DO, Badylak SF, Webster TJ, Geddes LA, Rundell AE. Biaxial strength of multilaminated extracellular matrix scaffolds. Biomaterials 2004;25:2353–2361.
15. Lee JM, Edwards HHL, Pereira CA, Samii SI. Crosslinking of tissue-derived biomaterials in 1-ethyl-3-(3-dimethylaminopropyl) carbodiimide (EDC). J Mat Sci Mat Med 1996;7:531–541.
16. Guidoin R, King M, Marceau D, Cardou A, de la Faye D, Legendre JM, Blais P. Textile arterial prostheses: Is water permeability equivalent to porosity? J Biomed Mater Res 1987;21:65–87.
17. Whitson BA, Cheng BC, Kokini K, Badylak SF, Patel U, Morff R, O'Keefe CR. Multilaminate resorbable biomedical device under biaxial loading. J Biomed Mater Res 1998;43:277–281.
18. Runza M, Pietrabissa R, Mantero S, Albani A, Quaglini V, Contro R. Lumbar dura mater biomechanics: Experimental characterization and scanning electron microscopy observations. Anesth Analg 1999;88:1317–1321.
19. Sasaki N, Odajima S. Stress-strain curve and Young's modulus of a collagen molecule as determined by the X-ray diffraction technique. J Biomech 1996;29:655–658.
20. Cedola A, Mastrogiacomo M, Burghammer M, Komlev V, Giannoni P, Favia A, Cancedda R, Rustichelli F, Lagomarsino S. Engineered bone from bone marrow stromal cells: A structural study by an advanced x-ray microdiffraction technique. Phys Med Biol 2006;51:N109–N116.
21. Cameron GJ, Alberts IL, Laing JH, Wess TJ Structure of type I and type III heterotypic collagen fibrils: An X-ray diffraction study. J Struct Biol 2002;137:15–22.
22. Nguyen TD, Liang R, Woo SL, Burton SD, Wu C, Almarza A, Sacks MS, Abramowitch S. Effects of cell seeding and cyclic stretch on the fiber remodeling in an extracellular matrix-derived bioscaffold. Tissue Eng Part A 2009;15:957–963.
23. Gilbert TW, Wognum S, Joyce EM, Freytes DO, Sacks MS, Badylak SF. Collagen fiber alignment and biaxial mechanical behavior of porcine urinary bladder derived extracellular matrix. Biomaterials 2008;29:4775–4782.
24. Gupta A, Zahriya K, Mullens PL, Salmassi S, Keshishian A. Ventral herniorrhaphy: Experience with two different biosynthetic mesh materials. Surgisis and Alloderm. Hernia 2006;10:419–425.
25. Lin HJ, Spoerke N, Deveney C, Martindale R. Reconstruction of complex abdominal wall hernias using acellular human dermal matrix: A single institution experience. Am J Surg 2009;197: 599–603; discussion 603.
26. Morgan AS, McIff T, Park DL, Tsue TT, Kriet JD. Biomechanical properties of materials used in static facial suspension. Arch Facial Plast Surg 2004;6:308–310.
27. Vural E, McLaughlin N, Hogue WR, Suva LJ. Comparison of biomechanical properties of alloderm and enduragen as static facial sling biomaterials. Laryngoscope 2006;116:394–396.
28. Yoder JH, Elliott DM. Nonlinear and anisotropic tensile properties of graft materials used in soft tissue applications. Clin Biomech (Bristol, Avon) 2010;25:378–382.
29. Raghavan D, Kropp BP, Lin HK, Zhang Y, Cowan R, Madihally SV. Physical characteristics of small intestinal submucosa scaffolds are location-dependent. J Biomed Mater Res A 2005;73:90–96.
30. Barber FA, Aziz-Jacobo J. Biomechanical testing of commercially available soft-tissue augmentation materials. Arthroscopy 2009; 25:1233–1239.
31. Freytes DO, Tullius RS, Valentin JE, Stewart-Akers AM, Badylak SF. Hydrated versus lyophilized forms of porcine extracellular matrix derived from the urinary bladder. J Biomed Mater Res A 2008;87:862–872.
32. Badylak JS, Voytik SL, Brightman AO, Tullius B; Purdue Research Foundation, assignee. Stomach submucosa derived tissue graft. USA. 2000.
33. Misra S, Raj PK, Tarr SM, Treat RC. Results of AlloDerm use in abdominal hernia repair. Hernia 2008;12:247–250.
34. Sandor M, Xu H, Connor J, Lombardi J, Harper JR, Silverman RP, McQuillan DJ. Host response to implanted porcine-derived biologic materials in a primate model of abdominal wall repair. Tissue Eng Part A 2008;14:2021–2031.
35. Naimark WA, Pereira CA, Tsang K, Lee JM. HMDC crosslinking of bovine pericaridal tissue: A potential role of the solvent environment in the design of bioprosthetic materials. J Mat Sci Mat Med 1995;6:235–241.
36. Sacks MS, Gloeckner DC. Quantification of the fiber architecture and biaxial mechanical behavior of porcine intestinal submucosa. J Biomed Mater Res 1999;46:1–10.

5286 J. Agric. Food Chem. 2010, 58, 5286–5291
DOI:10.1021/jf100436c

JOURNAL OF AGRICULTURAL AND FOOD CHEMISTRY
ARTICLE

Leather Structure Determination by Small-Angle X-ray Scattering (SAXS): Cross Sections of Ovine and Bovine Leather

Melissa M. Basil-Jones,[†] Richard L. Edmonds,[§] Timothy F. Allsop,[§] Sue M. Cooper,[§] Geoff Holmes,[§] Gillian E. Norris,[‡] David J. Cookson,[⊥] Nigel Kirby,[⊥] and Richard G. Haverkamp*,[†]

[†]School of Engineering and Advanced Technology, and [‡]Institute of Molecular Biosciences, Massey University, Palmerston North, New Zealand 4442, [§]Leather and Shoe Research Association, Palmerston North, New Zealand 4442, and [⊥]Australian Synchrotron, Melbourne, Australia

SAXS has been applied to structural determination in leather. The SAXS beamline at the Australian Synchrotron provides 6 orders of magnitude dynamic range, enabling a rich source of structural information from scattering patterns of leather sections. SAXS patterns were recorded for q from 0.004 to 0.223 Å^{-1}. Collagen d spacing varied across ovine leather sections from 63.8 nm in parts of the corium up to 64.6 nm in parts of the grain. The intensity of the collagen peak at q = 0.06 Å^{-1} varied by 1 order of magnitude across ovine leather sections with the high-intensity region in the corium and the low intensity in the grain. The degree of fiber orientation and the dispersion of the orientation has been quantified in leather. It is shown how the technique provides a wealth of useful information that may be used to characterize and compare leathers, skin, and connective tissue.

KEYWORDS: Leather; small-angle X-ray scattering; SAXS; synchrotron; ovine; bovine; fiber structure; collagen

INTRODUCTION

The value of leather depends on the physical and aesthetic properties of the material. The leather industry is large, with global production of about 1.7 billion square meters of leather per year with a value of around $40 billion. About 65% of the world production of leather goes into footwear, worth an estimated $150 billion at wholesale prices. Other major uses include upholstery (including automotive) and clothing.

The properties of leather ultimately depend on the properties of the component fibers and their structure. Leather consists of a network of collagen fibrils interlinked with natural and synthetic chemical bonds. The collagens are a group of proteins that are responsible for providing structure and desirable physical properties to a number of tissues in the body (*1*).

Collagen is almost always present in its characteristic hierarchical structure (*2*). At its primary level, pro-collagen molecules are characterized by the repetitive chain sequence of $(Gly\text{-}X\text{-}Y)_n$, where Gly is glycine, X and Y can be any amino acid, and n is the number of repeats, usually 100−400 (*3*). A collagen molecule is composed of three of these chains, which combine in a coiled-coil structure, due to the chain's repetitive sequence. These molecules align to form microfibrils, in a quarter-staggered array which results in the formation of overlap and gap regions. These regions are responsible for the characteristic banding pattern observed in collagen fibrils with atomic force or scanning electron microscopy. The period of this repeating sequence is known as the d period. The microfibrils arrange in a parallel fashion and through cross-links form collagen fibrils.

Collagen fibril arrangement can vary significantly between different tissues. In skin, collagen fibrils tend to have a low variation in diameter (*4*) and form a random web-like structure (*5*). It has been found that many collagens, in particular type I, III, and VI collagens, are resistant to liming, bating, and pickling (*6*). Collagen fibrils have a large inherent strength, and the arrangements of collagen fibrils are crucial to the final physical properties of the leather. The strength and softness of leather are believed to be related to the internal structure of the leather (*7*, *8*) and aesthetic properties to the internal fiber looseness (*9*).

Leather has a complex hierarchical structure with a number of distinct layers. The grain layer found at the leather outer surface and the corium layer found beneath have visually different structures and impart different properties to the final leather (*10*). The physical properties of those layers are strongly related to the fiber structure of which they are made up. The organization of these layers and the resulting physical properties are also influenced by cross-linking, either natural or modified (*11*−*14*).

Differences between fiber structures have been determined through the use of optical microscopy, scanning electron microscopy (SEM) (*15*−*19*), and atomic force microscopy (AFM) (*18*, *20*, *21*). The microscopic techniques generally give qualitative measurement of fiber organization but may also give quantitative measurement of fiber dimensions and d period.

*To whom correspondence should be addressed. E-mail: r.haverkamp@massey.ac.nz.

 Published on Web 03/25/2010

X-ray diffraction is a powerful technique for investigating material structures. The study by X-ray diffraction techniques of long-range structural order, with repeat distances on the order of 0.1−10 nm, is particularly useful for protein assemblages, such as collagen. Such measurements require small diffraction angles, θ, typically less than 10 degrees and are often referred to as small angle X-ray scattering (SAXS). The scattering momentum q ($q = 4\pi(\sin\theta)/\lambda$, where λ is the X-ray wavelength used) is generally used rather than θ in SAXS plots, as it allows direct comparison of SAXS measured at different incident X-ray wavelengths. SAXS can provide information on macromolecules either in solution or in solid materials (*22*, *23*) and has been used to investigate the structure of collagen (*24*) and collagenous materials such as tendon (*2*, *25*), bone (*26*, *27*), and human articular cartilage (*28*). SAXS provides a quantitative measurement of both fibril orientation and the average d spacing of collagen within the irradiated volume of sample.

Leather has previously been investigated using SAXS. Fiber orientation was identified in leather samples under strain (*29*, *30*), although in these studies the resolution appears to be rather limited with collagen d period not easily observed in the diffraction patterns.

In this work, we describe how modern high-sensitivity SAXS may be applied to the study of leather using the wealth of information available in a two-dimensional SAXS pattern. We describe the use of some of this information and show, using examples, how it may be applied to characterize leather. Some of this information can be directly related to existing industry tests, while other information is new to the field. The use of these techniques to infer important structural differences in different leathers will be the subject of subsequent publications.

EXPERIMENTAL SECTION

SAXS diffraction patterns were recorded on the Australian Synchrotron SAXS/WAXS beamline, utilizing a high-intensity undulator source. An energy resolution of 10^{-4} is obtained from a cryo-cooled Si(111) double-crystal monochromator, and the beam size (fwhm focused at the sample) was 250×80 μm with a total photon flux of about 2×10^{12} photons s^{-1}. All diffraction patterns were recorded with an X-ray energy of either 8 or 11 keV using a Pilatus 1 M detector with an active area of 170×170 mm and a sample to detector distance of 3371 mm. The exposure time for diffraction patterns was in the range of 1−5 s, and data processing was carried out using the SAXS15ID software (*31*). Intensities displayed are all absolute detector counts (one X-ray detected one detector count), except where stated otherwise.

Leather was prepared from pelt leather using conventional beamhouse and tanning processes. Briefly, the pelts were depilated using a caustic treatment comprising sodium sulfide and a saturated solution of calcium hydroxide followed, after washing, by pickling in sulfuric acid and sodium chloride to a pH of less than 2. The pickled pelts were then pretanned using oxazolidine, degreased with an aqueous surfactant, and then tanned using chromium sulfate. The resulting "wet blue" was then retanned using a mimosa vegetable extract and impregnated with lubricating oil prior to drying and mechanical softening.

Strips of leather about 1 mm thick and 30 mm long were cut at selected positions from samples of tanned ovine and bovine leather. The leather was mounted in the beam horizontally without tension. Samples were mounted on a support which held up to 36 samples and which could be manipulated remotely, which enabled rapid profiling across a sample of leather and quick sample changing (**Figure 1**).

Analyses were performed across the section of each strip of leather starting at the region of the grain and progressing through to the corium (**Figure 2**). Steps of either 0.25 or 0.05 mm were made between analysis points. The rectangles shown on **Figure 2** show the beam probe size and scan spacing, demonstrating that the smaller step size was comparable with the fwhm of the beam at the sample. Analyses were also performed normal to the surface of the leather.

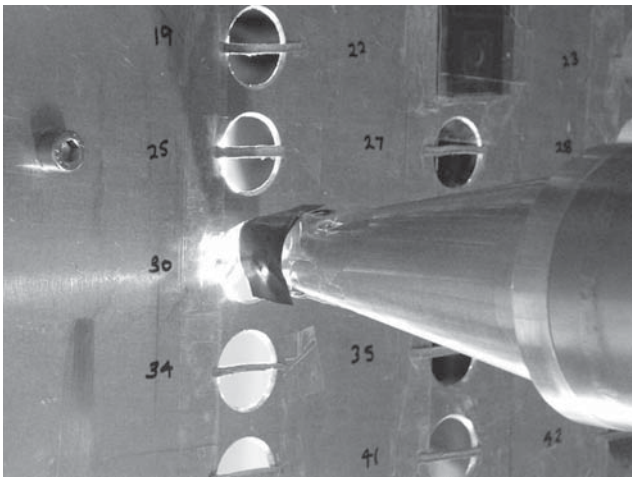

Figure 1. Image of leather samples mounted on sample holder with camera entrance cone in position. Holes are 25 mm diameter.

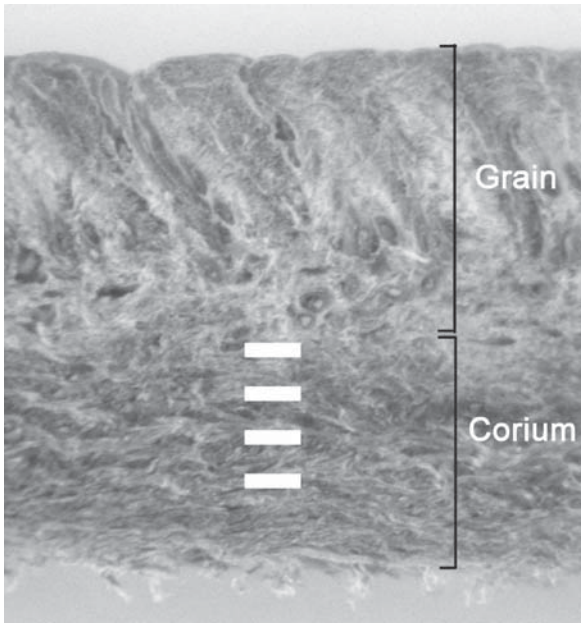

Figure 2. Optical image of a cross section of ovine leather as seen by the SAXS X-ray beam. The height (leather thickness) of the section shown is 2.2 mm but varies between samples. The rectangles indicate the size of the beam used to probe the sample (shown at 0.25 mm spacing, for 0.05 mm spacing the analysis area overlaps by 30%).

Thin sections parallel to the surface of the leather were also made by sectioning the leather strips into three layers, one containing just grain, one with the middle part, and one with just corium. These were mounted with the face of the leather toward the X-ray beam.

RESULTS AND DISCUSSION

Diffraction Pattern. Diffraction images of leather recorded on Pilatus detector with the Australian Synchrotron provide remarkable resolution (**Figure 3**). Previous synchrotron SAXS studies failed to show the same level of detail (*29*, *30*). However, on the data recorded on the Pilatus detector it is possible to record across

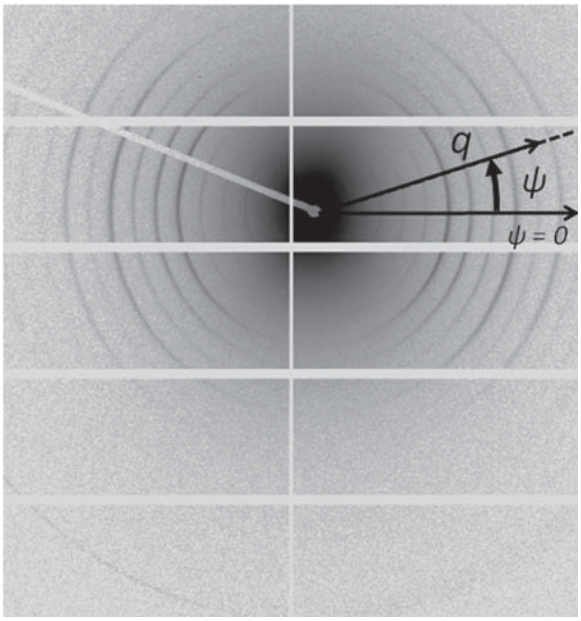

Figure 3. SAXS image of ovine leather. The image extends to q = 0.223 A^{-1} at the bottom left-hand corner. Note that q is calculated from the scattering angle and that the azimuthal angle ψ is measured anticlockwise from the horizontal.

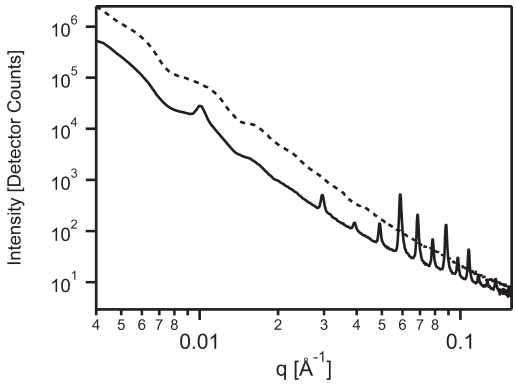

Figure 4. SAXS profiles of an example of ovine leather using two azimuthal angle ranges. The dashed line shows profiles integrated from ψ = 60 to 120°, while the solid line shows ψ = −30 to 30°.

6 orders of magnitude of intensity enabling the Bragg peaks from the collagen d period to be easily observed (at q = 0.04−0.1 $Å^{-1}$) while simultaneously measuring to low q (0.004 $Å^{-1}$), where the signal intensity is much greater (**Figure 4**).

From a single SAXS image taken of a leather sample, information relating to fiber and fibril structure, collagen concentration, and orientation can be readily obtained. The positions of the series of prominent rings correspond to the Bragg peaks from the collagen d period, the region at low q yields information on fiber morphology, the intensity of the collagen rings relates to the collagen concentration, the broadness of these rings relates to crystallinity, and the angular distribution of the rings provides information on fibril orientation. We will discuss some of these parameters in turn below. All the figures shown, with the exception of **Figure 10**, are for spectra recorded with the X-ray beam parallel to the original leather surface.

Radial Integration of Scattering Pattern. Most SAXS scattering patterns from leather samples are highly nonisotropic, meaning that a plot of intensity (I) versus q will give significantly different

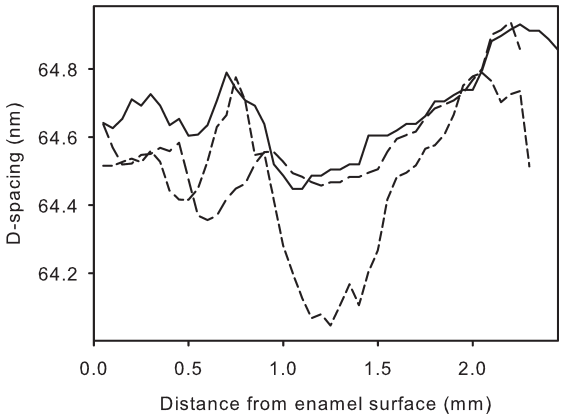

Figure 5. Variation of collagen d period through ovine leather (for three samples).

profiles depending on the azimuthal range of integration. The I versus q profile changes when integrating over the meridional arcs (ψ = −30 to 30°) or over the region without the arcs (ψ = 60 to 120°), as illustrated in **Figure 4**. For the former azimuthal region the profile shows a series of peaks at q in the range 0.04−0.1 $Å^{-1}$ corresponding to periodicity of molecular overlap in the collagen fibrils. Around 15 of these arcs can be observed in the raw diffraction pattern. Measuring the q position for the center of any one of these peaks provides a quantitative measure of the collagen molecule overlap or d period. The sixth Bragg peak was generally used, as it was the most intense, although it was found that any of the other intense peaks would provide the same information.

In addition, structural information can be obtained from the region of low q (below 0.03 $Å^{-1}$). This lower angle region provides information on the larger structures, the fibers in the material (*32*). The slope of this line when plotted on a log−log scale indicates the nature of the boundary between the organized fibers and the disorganized medium. In this case there is a clear oscillation in the profile in both azimuthal regions—with an average envelope slope of 4 ± 0.1 on the log−log plot. This means that the general decay of intensity at lower q goes as q^{-4}, which conforms to Porod's law. A Porod law slope indicates that there is a sharp well-defined (smooth) boundary between the fibrils and their nearest neighboring fibrils and/or surrounding air and amorphous material.

Structure of Collagen. Upon analysis of the position of the collagen peaks (**Figure 4**), a large variation in collagen d period can be observed through the thickness of leather samples (**Figure 5**). The d period is seen to decrease in the corium compared with the grain layer (**Figure 5**). Differences in d period between different tissues has previously been observed, using other methods, with skin having a lower d period (65 nm) than tendon (67 nm) (*5*). The shorter d period is closer to that which we observe here in leather. The differences in d period have proposed to not be related to stretch or crimp but rather may be due to the intrafibrillar texture in the tissues (*5*). It has also been suggested that for collagen with a helical inner structure the d spacing only appears to be shorter due to the projection of this structure along the fibril axis (*4*). The d spacing has been correlated with fibril diameter, with small diameter fibrils having a smaller d period (*4*, *5*).

Reproducibility and Variability. Leather is potentially a nonhomogenous material at the scale of the SAXS analysis (80 μm × 250 μm spot). This can be used to advantage by imaging the variation across a cross section. However, for the simple tests we are presenting here, an assurance is needed that this variation is

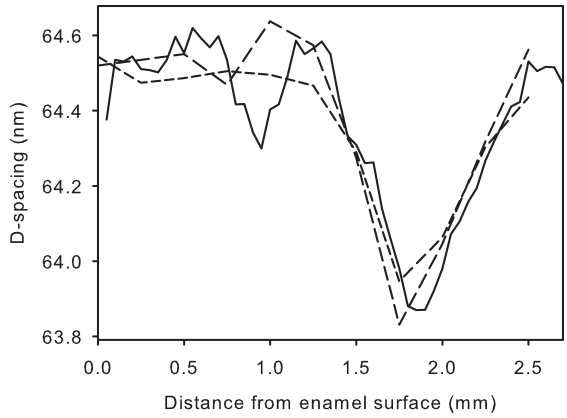

Figure 6. Example of reproducibility of *d* period measurement in adjacent regions on one sample: (solid line) 5 s exposure, 0.05 mm sampling; (dashed lines) 1 s exposure, 0.25 mm sampling.

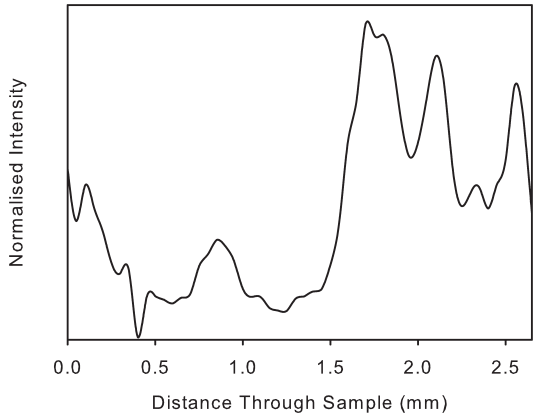

Figure 7. Example of the intensity of the primary collagen *d* spacing peak (at around 0.059−0.06 $Å^{-1}$) through ovine leather, normalized for total scattering at low *q*, taken at 0.05 mm steps. The grain surface is at 0 mm.

not so large as to make a scan of a series of points across the sample nonrepresentative. We have therefore made several point scans across samples and calculated the intensity and *d* period across these scans (**Figure 6**). The variation from one series of points to the next is small compared with the variation across the thickness of the sample or the variation between samples, which gives some confidence that the measurement is useful. Similarly, the orientation parameters are similar from one scan across a section to another on the same sample (not shown).

Concentration of Crystalline Fibrillar Collagen across the Leather. By measuring the intensity (integrated area) of a selected collagen diffraction peak across the profile of the leather sample, it is possible to quantify the concentration of crystalline fibrillar collagen in the sample. First it is necessary to correct for any variation in sample thickness and density across the area of analysis. This can be done by normalizing with respect to the total scattering in the low *q* region. The variation of intensity of the Bragg peaks for collagen observed for a sample of ovine leather (**Figure 7**) is nearly 1 order of magnitude, with the most intense region across the corium, the region known to provide most of the strength to leather (*33*).

It is well recognized that the grain layer of leather is weak compared with the corium, with the grain having perhaps as little as 20% of the tearing strength of corium. It has been suggested that these differences in strength between the two strata of leather are associated with the greater ability of the corium layer's fiber

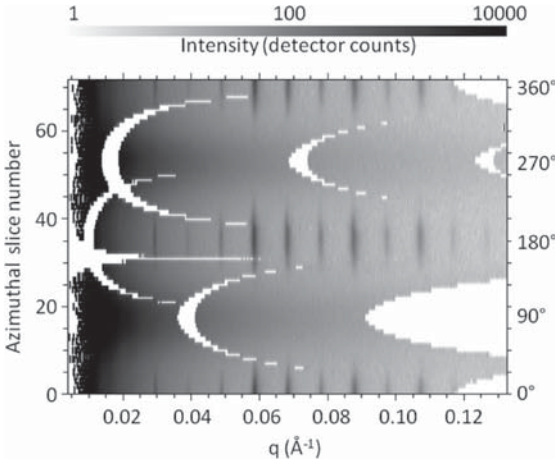

Figure 8. Gray shade plot of *q* versus azimuthal angle for an ovine leather. The white arcs on the left of the image represent the gaps in the detector. The dark vertical bands centered vertically on the azimuth angle of 0 and 180° are the collagen *d* spacing Bragg peaks. SAXS intensity is given by the gray scale.

structure to impede propagating tears by means of tear tip blunting and fiber pull out (*33*). The measure of fibrilar collagen content could therefore be a guide to leather strength, with high concentrations of structured fibrilar collagen corresponding with regions of high strength (**Figure 7**).

It may also be possible to measure the "crystallinity" of the collagen. This can be done by measuring the intensity of the higher order peaks relative to lower order peaks. These higher order peaks would be expected to decay in intensity more quickly when the *d* spacing is poorly conserved. We have not yet investigated this aspect.

Orientation of Collagen. The orientation of collagen fibrils in the plane normal to the irradiating X-ray beam can be obtained from the azimuthal distribution of the diffraction arcs. The samples are taken parallel to the backbone of the animals, and this direction represents 0° on the plots for all samples. For standard samples 90° represents the direction from the grain to the corium. For the thin surface parallel sections 90° is the direction at right angles to the backbone and parallel to the surface.

A series of profiles from azimuthal subregions 5° wide around the entire 360° range of an image can be used to generate a composite image of arcs (vertical dark lines) that can be readily analyzed for intensity, position, and length (**Figure 8**).

By selection of a small enough *q* range a single meridional arc can be selected and analyzed in detail. In **Figure 9** a single meridional arc in the region $q \approx 0.06$ $Å^{-1}$ is compared between example samples of bovine and ovine leather (not the same sample as in **Figure 4**). The arcs from the bovine sample indicate only one preferred direction (a peak at 0 and 180° azimuth), while the arcs in the particular ovine sample shown indicate two preferred directions (peaks at 0, 90, 180, and 270°). Both leather cross-sectional samples were cut parallel to the backbone (0, 180°).

The spread of fibril orientation can be quantified by the width of the peaks in the azimuthal angle plots (**Figure 9**). In the case of the collagen peaks of bovine leather illustrated this was 72° and for ovine illustrated 44° in the primary direction of orientation and 35° for some fibrils at right angles. This particular bovine sample, therefore, could be said to have a greater spread of fibril orientation around the preferred direction than the ovine sample. The ovine sample has a narrower distribution in the preferred direction, but it also has some fibrils running at right angles to the line of the backbone.

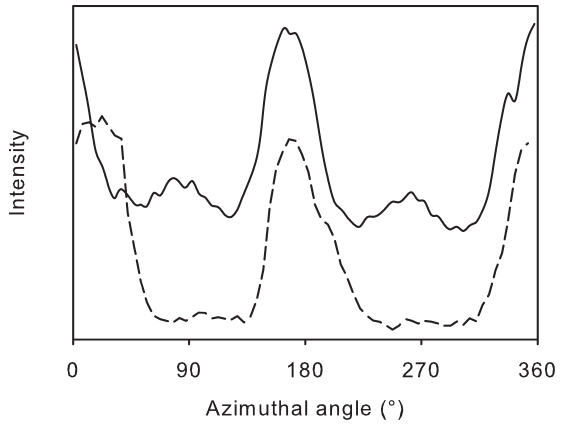

Figure 9. Examples of azimuthal angle plots of bovine leather at ~0.6 Å^{-1} (dashed line) and ovine leather at ~0.6 Å^{-1} (solid line), with arbitrary intensity scale and offset. Note that the narrow dips on the sides of some peaks are artifacts caused by gaps in the detector.

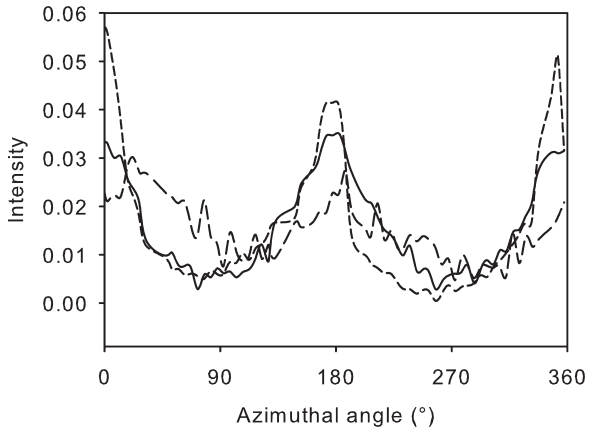

Figure 10. Azimuthal angle plots of ovine leather at the collagen *d* spacing peak around 0.059−0.06 Å^{-1} for SAXS taken of sections parallel to an ovine leather surface: (solid line) grain; (long dash) middle; (short dash) corium. The X-ray beam was normal to the original leather surface.

The sections of leather cut parallel to the leather surface, each about one-third of the thickness of the leather, also show a collagen orientation aligned at 0 and 180° (i.e., parallel to the backbone), as shown in **Figure 10**, but with a greater spread in that plane than in the plane of a cross section (**Figure 9**). The strongest orientation is observed in the corium.

The azimuthal distribution of the collagen diffraction rings can be plotted across the thickness of the leather samples in a three-dimensional representation to visualize the variation of orientation with position in the leather (**Figure 11**). A plot of the absolute magnitude of these diffraction peaks (**Figure 11a**) may be a useful indicator of the possible contribution of the combined effect of the amount of collagen and its orientation on the physical properties of the leather. Or, by normalizing the data at each position to a constant intensity, the effect of varying collagen concentration is removed so that just the orientation data is displayed (**Figure 11b**).

The orientation of the collagen within leather falls into two regions: highly oriented in the corium and poorly oriented in the grain. It is well-known that the corium is stronger than the grain. Therefore, there is a correlation between orientation and strength (as there is between the amount of collagen and strength and between *d* spacing and strength). It may therefore be useful to

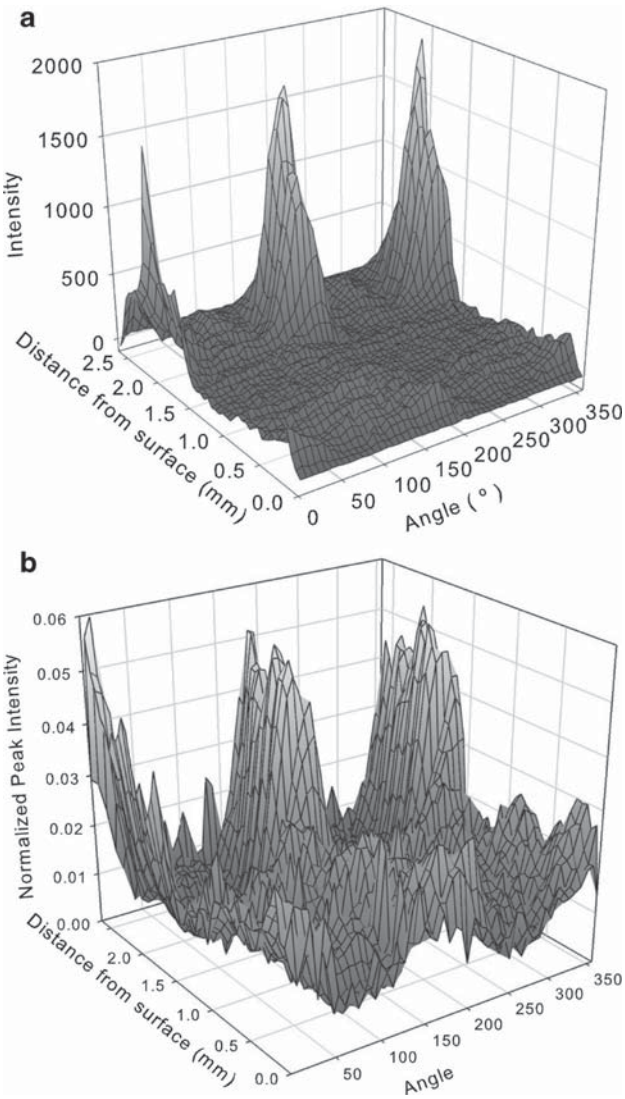

Figure 11. Azimuthal angle through ovine leather at the collagen *d* spacing peak around 0.059−0.06 Å^{-1}: (a) absolute intensity; (b) intensity normalized to an equal sum at each sample position, therefore showing only relative orientation.

investigate this correlation to determine if a greater degree of orientation in collagen is a contributing factor for higher strength. This method may provide a more reliable quantitative measure of fiber orientation than the existing industry methods which use optical microscopy to measure individual fiber orientation in samples of leather and therefore have poorer sampling statistics than the SAXS method. These examples given are illustrative only and demonstrate the orientation information that may readily be obtained.

Usefulness of the Technique. Leather is a structured material with clearly measurable differences between the corium and the grain. The corium contains, relative to the grain, a greater concentration of collagen which is more highly oriented and has a shorter *d* spacing. The corium is known to be stronger than the grain (although less elastic), and these measured differences are likely to contribute to the differences in mechanical properties.

We have shown that this technique provides quantitative information on the leather structure. The three parameters we have measured, *d* spacing, collagen orientation, and amount of collagen, all correlate with strength in the samples we have analyzed (*33*). They are therefore confounded and it is not

possible to say with any certainty what each of their individual contributions are to the strength of leather. We are now conducting a detailed SAXS-based comparison of leathers with different physical properties to quantitatively evaluate the relationship between the SAXS-derived parameters and the mechanical properties.

In combination with traditional and emerging testing methods such as light microscopy, scanning electron microscopy, and atomic force microscopy, SAXS provides complementary information that will be increasingly important in the characterization of leather, with the prospect of allowing us insight into how such characteristics could be improved in this complex composite material. Synchrotron SAXS allows these studies to be done quickly, for a wide range of samples and with an unparalleled degree of spatial precision.

ACKNOWLEDGMENT

This research was undertaken on the SAXS/WAXS beamline at the Australian Synchrotron, Victoria, Australia.

LITERATURE CITED

(1) Fratzl, P. *Collagen: Structure and Mechanics*; SpringerScience+ Business Media: New York, 2008.
(2) Sasaki, N.; Odajima, S. Elongation mechanisms of collagen fibils and force-strain relations of tendon at each level of structural hierarchy. *J. Biomech.* **1996**, *29* (9), 1131–1136.
(3) Bailey, A. J.; Paul, R. G. Collagen: a not so simple protein. *J. Soc. Leather Technol. Chem.* **1999**, *82*, 104–110.
(4) Ottani, V.; Raspanti, M.; Ruggeri, A. Collagen structure and functional implications. *Micron* **2001**, *32*, 252–260.
(5) Gathercole, L. J.; Shah, J. S.; Nave, C. Skin-tendon differences in collagen D-period are not geometric or stretch-related artefacts. *Int. J. Biol. Macromol.* **1987**, *9*, 181–183.
(6) Stephens, L. J.; Werkmeister, J. A.; Ramshaw, J. A. M. Changes in bovine hides during leather processing. *J. Soc. Leather Technol. Chem.* **1993**, *77* (3), 71–74.
(7) Russell, A. E. Stress-strain relationships in leather and the role of fibre structure. *J. Soc. Leather Technol. Chem.* **1988**, *72* (4), 121–134.
(8) Michel, A. Tanners' dilemma: Vertical fibre defect. *Leather Int.* **2004**, *206* (4750), 36–37.
(9) Rabinovich, D. Seeking soft leathers with a tight grain. *WORLD Leather* **2001**, *14* (5), 27–32.
(10) Vera, V. D.; Cantera, C. S.; Dominguez, D. O.; Bernardi, C. In *Modern Soft Leather Influence of the Relationship Grain/Corium on the Topography of Some Physical Properties*; 22nd IULTCS Congress Proceedings, Porto Alegra, ABQTIC: Porto Alegre, Brazil, 1993; pp 560−569.
(11) Folkhard, W.; Geercken, W.; Knorzer, E.; Mosler, E.; Nemetschek-Gansler, H.; Nemetschek, T.; Koch, M. H. J. Structural dynamic of native tendon collagen. *J. Mol. Biol.* **1987**, *193*, 405–407.
(12) Folkhard, W.; Geercken, W.; Knorzer, E.; Nemetschek-Gansler, H.; Nemetschek, T.; Koch, M. H. J. Quantitative analysis of the molecular sliding mechanism in native tendon collagen - time-resolved dynamic studies using synchrotron radiation. *Int. J. Biol. Macromol.* **1987**, *9* (3), 169–175.
(13) Chan, Y.; Cox, G. M.; Haverkamp, R. G.; Hill, J. M. Mechanical model for a collagen fibril pair in extracellular matrix. *Eur. Biophys. J. Biophys.* **2009**, *38* (4), 487–493.
(14) Cuq, M. H.; Palevody, C.; Delmas, M. Fundamental study of cross-linking of collagen with chrome tanning agents in traditional and Cr.A.B processes. *J. Soc. Leather Technol. Chem.* **2000**, *83*, 233–238.
(15) Barlow, J. R. Scanning Electron-Microscopy of hides, skins and leather. *J. Am. Leather Chem. Assoc.* **1975**, *70* (3), 114–128.
(16) Dempsey, M., *Hide, Skin and Leather Defects: A Guide to Their Microscopy*; New Zealand Leather and Shoe Association: Palmerston North, New Zealand, 1984.
(17) Haines, B. M. Twentieth Procter memorial lecture: the skin before tannage - Procter's view and now. *J. Soc. Leather Technol. Chem.* **1984**, *68*, 57–70.
(18) Deb Choudhury, S.; Haverkamp, R. G.; DasGupta, S.; Norris, G. E. Effect of oxazolidine E on collagen fibril formation and stabilization of the collagen matrix. *J. Agric. Food Chem.* **2007**, *55* (17), 6813–6822.
(19) Cay, M.; Kiety, C.; Shuttleworth, A. Microfibrillar elements of the dermal matrix. *Microsc. Res. Tech.* **1997**, *38* (4), 413–427.
(20) Reich, G.; Bradt, J.; Mertig, M.; Pompe, W.; Taeger, T. Scanning probe microscopy a useful tool in leather research. *J. Soc. Leather Technol. Chem.* **1999**, *82*, 11–14.
(21) Edmonds, R. L.; Deb Choudhury, S.; Haverkamp, R. G.; Birtles, M.; Allsop, T. F.; Norris, G. E. Using proteomics, immunohistology, and atomic force microscopy to characterize surface damage to lambskins observed after enzymatic dewooling. *J. Agric. Food Chem.* **2008**, *56* (17), 7934–7941.
(22) Bernado, P.; Mylonas, E.; Petoukhov, M. V.; Blackledge, M.; Svergun, D. I. Structural characterization of flexible peoteins using small-angle X-ray scattering. *J. Am. Chem. Soc.* **2007**, *129* (17), 5656–5664.
(23) Tsutakawa, S. E.; Hura, G. L.; Frankel, K. A.; Cooper, P. K.; Tainer, J. A. Structural analysis of flexible proteins in solution by small angle x-ray scattering combined with crystallography. *J. Struct. Biol.* **2007**, *158* (2), 214–223.
(24) Cameron, G. J.; Alberts, I. L.; Laing, J. H.; Wess, T. J. Structure of type I and type III heterotypic collagen fibrils: an x-ray diffaction study. *J. Struct. Biol.* **2002**, *137*, 15–22.
(25) Sasaki, N.; Odajima, S. Stress-strain curve and youngs modulus of a collagen molecule as determined by the x-ray diffaction technique. *J. Biomech.* **1996**, *29* (5), 655–658.
(26) Burger, C.; Zhou, H. W.; Sics, I.; Hsiao, B. S.; Chu, B.; Graham, L.; Glimcher, M. J. Small-angle X-ray scattering study of intramuscular fish bone: collagen fibril superstructure determined from equidistant meridional reflections. *J. Appl. Crystallogr.* **2008**, *41*, 252–261.
(27) Cedola, A.; Mastrogiacomo, M.; Burghammer, M.; Komlev, V.; Giannoni, P.; Favia, A.; Cancedda, R.; Rustichelli, F.; Lagomarsino, S., Engineered bone from bone marrow stromal cells: A structural study by an advanced x-ray microdiffraction technique. *Phys. Med. Biol.* **2006**, *51* (6), N109−N116.
(28) Mollenhauer, J.; Aurich, M.; Muehleman, C.; Khelashvilli, G.; Irving, T. C. X-Ray Diffraction of the Molecular Substructure of Human Articular Cartilage. *Connect. Tissue Res.* **2003**, *44* (5), 201–207.
(29) Boote, C.; Sturrock, E. J.; Attenburrow, G. E.; Meek, K. M. Psuedo-affine behaviour of collagen fibres during the uniaxial deformation of leather. *J. Mater. Sci.* **2002**, *37*, 3651–3656.
(30) Sturrock, E. J.; Boote, C.; Attenburrow, G. E.; Meek, K. M. The effect of the biaxial stretching of leather on fibre orientation and tensile modulus. *J. Mater. Sci.* **2004**, *39*, 2481–2486.
(31) Cookson, D.; Kirby, N.; Knott, R.; Lee, M.; Schultz, D. Strategies for data collection and calibration with a pinhole-geometry SAXS instrument on a synchrotron beamline. *J. Synchrotron Radiat.* **2006**, *13*, 440–444.
(32) Roe, R.-J. *Methods of X-ray and Neutron Scattering in Polymer Science*; Oxford University Press: Oxford, U.K., 2000.
(33) O'Leary, D. N.; Attenburrow, G. E. Differences in strength between the grain and corium layers of leather. *J. Mater. Sci.* **1996**, *31*, 5677–5682.

Received for review February 3, 2010. Revised manuscript received March 10, 2010. Accepted March 15, 2010. The NZ Synchrotron Group Ltd. is acknowledged for travel funding. This work was supported by the Foundation for Research Science and Technology Grant No. LSRX0801.

[1]"SAXS Structural Studies of Collagen Materials"

Richard G. Haverkamp, Katie H. Sizeland, Melissa M. Basil-Jones, Sue M. Cooper, Richard L. Edmonds

Fibrous collagen is the basis of leather and of tissues used in medical applications such as pericardium for heart valve repair. The structure of such materials contributes to their mechanical properties. We used small angle X-ray scattering to characterise the structure of fibrous collagen materials. The two dimensional small angle scattering pattern provides information on the internal fibril structure and the fibril arrangement. Leathers of different strengths were characterized as were juvenile and adult bovine pericardium. It is shown that greater collagen alignment leads to stronger material. The structural response to dynamic loads varies between strong and weak material. Under tension fibrils reorient at low strain then individual fibrils stretch at higher strain. Stronger material has more uniform strain throughout the thickness and greater extension of fibrils is achieved. Processing treatments affect the response of these tissues to strain. These studies provide an insight into the structural basis of strength in fibrous collagen materials and the behaviour of these materials under stress.

[1] Abstract for presentation at the Australian Synchrotron User Meeting, Melbourne, 29-30 December 2012

[1]"SAXS of Leather Reveals a Structural Basis for Strength"

Katie H. Sizeland, Melissa M. Basil-Jones, Richard L. Edmonds, Richard G. Haverkamp

Leather is a processed material made from fibrous collagen. The physical properties of leather are due in large part to the arrangement of the collagen fibrils. We have used small angle X-ray scattering to characterize leather from seven species of animal with widely different mechanical properties. The two dimensional small angle scattering pattern provides information on the internal fibril structure and the fibril arrangement. It is shown that the strongest leather has fibrils which are highly aligned within parallel planes with few fibrils crossing between planes. Weak leather contains fibrils that are less aligned. Tear strengths for the selection of leathers fell in the range 20–110 N/mm with orientation indices ranging from 0.420–0.633. There is a direct relationship between orientation index and strength. This understanding provides a new insight into structure – property relationships in leather and may be extended to other tissues for biological and medical applications.

[1] Abstract for poster presented at the Australian Synchrotron User Meeting, Melbourne, 29-30 December 2012

[1]Alignment and Stretching of Collagen Fibrils in Leather

Richard G. Haverkamp[1], Melissa M. Basil-Jones[1], Richard L. Edmonds[2], Gillian E. Norris[3]

[1]School of Engineering and Advanced Technology, Massey University, Private Bag 11222, Palmerston North 4442, r.haverkamp@massey.ac.nz
[2]Leather and Shoe Research Association, Palmerston North 4442
[3]Institute of Molecular Biosciences, Massey University, Palmerston North, New Zealand 4442

Leather is composed of collagen fibrils. The strength and other physical properties of leather depend on the structure and arrangement of these fibrils. Small angle X-ray scattering (SAXS) can be used to measure the alignment and tension in these fibrils. A stretching device was mounted in the SAXS beam line at the Australian Synchrotron and samples of ovine and bovine leather were stretched while spectra were recorded edge-on to the leather at points from the corium to the grain. Under strain the fibrils initially reorient, becoming more aligned. At higher strain (over 5-10%) the fibrils begin to stretch indicated by the d-spacing increasing, with little further reorientation of the fibrils. These changes are not uniform through the cross section of leather, and differ between leathers of different strengths. The stresses are taken up more evenly through the leather cross section in stronger leathers in comparison to weaker leathers where stresses tended to be concentrated during strain. These observations contribute to our understanding of the internal strains and structural changes that take place in leather under stress.

[1] Abstract for presentation at the Australian Synchrotron Users Conference, Melbourne, 3-4 December 2011

A SAXS STUDY OF THE RELATIONSHIP OF COLLAGEN FIBRIL ORIENTATION IN LEATHER WITH STRENGTH

Richard G. Haverkamp[1], Melissa M. Basil-Jones[1], Richard L. Edmonds[2]
[1]*School of Engineering and Advanced Technology, Massey University, Private Bag 11222, Palmerston North 4442, r.haverkamp@massey.ac.nz*
[2]*Leather and Shoe Research Association, Palmerston North 4442*

The main structural component of leather and many other tissues is fibrous collagen. Synchrotron based SAXS was used to characterize the fibrous collagen structure and arrangement in a series of ovine and bovine leathers and to relate it to tear strength[1,2]. SAXS gives quantitative information on the amount of fibrous collagen, the orientation (direction and spread) of the collagen microfibrils, and the d-spacing of the collagen. There is a large difference in tear strength between ovine and bovine leather. The orientation index (OI) is correlated strongly with strength in ovine and bovine leathers. Stronger leather has the fibrils arranged mostly parallel to the plane of the leather surface (high OI), while weaker leather has more out-of-plane fibrils (low OI). With the SAXS measurements taken parallel to the animal's backbone, weak (19.9 N/mm) ovine leather has an OI of 0.422 (0.033), stronger (39.5 N/mm) ovine leather has an OI of 0.452 (0.033), and bovine leather with a strength of (61.5 N/mm) has an OI of 0.493 (0.016). The d-spacing profile through leather thickness also varies according to leather strength. This work provides an understanding of a structural characteristic of ovine and bovine leather that leads to differences in strength and may have implications for other tissues and collagen based materials[3].

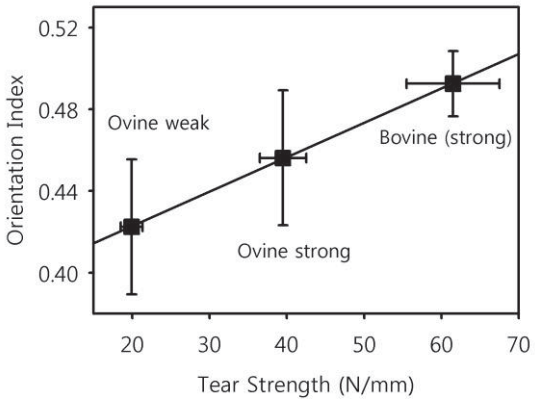

References:

1. Melissa M. Basil-Jones, Richard L. Edmonds, Sue M. Cooper, Richard G. Haverkamp, "Collagen Fibril Orientation in Ovine and Bovine Leather Affects Strength: A Small Angle X-ray Scattering (SAXS) Study*" J Agric Food Chem* DOI: 10.1021/jf202579b (2011)
2. Melissa M. Basil-Jones, Richard L. Edmonds, Richard G. Haverkamp " Collagen Fibril Alignment and Deformation during Tensile Strain of Leather: A SAXS Study" *J Agric. Food Chem* **58** (9) 5286–5291 (2010)
3. Evan W. Floden, Sharif Malak, Melissa M. Basil-Jones, Leonardo Negron, James N. Fisher, Michael Byrne, Stan Lun, Sandi G. Dempsey, Richard G. Haverkamp, Iain Anderson, Brian R. Ward, Barnaby C. H. May "Biophysical Characterization of Ovine Forestomach Extracellular Matrix Biomaterials" J. Biomed. Mat. Res. B **96B** (1) 67-75 (2011)

[1] Abstract for presentation at the NZIC conference, Hamilton, 27 November – 1 December 2011

[1]A novel low sulphide processing regime with improved product quality

Richard Edmonds[1], Tim Allsop[1], Geoff Holmes[1], Sue Cooper[1], Melissa Basil Jones[2] and Richard Haverkamp[2]

[1]New Zealand Leather and Shoe Research Association, 69 Dairy Farm Road, Palmerston North, New Zealand, Phone: 64-6-3559028, Fax: 64-6-3541185, e-mail: richard.edmonds@lasra.co.nz
[2]School of Engineering and advanced technology, Massey University, Palmerston North, New Zealand, Phone: 64-6-3569099 x 81056, e-mail: r.haverkamp@massey.ac.nz

Abstract

Applied research carried out at LASRA has indicated the importance of processing conditions early on in processing on the ultimate strength of ovine leather. Experiments were carried out which confirmed the value of pH control during the liming process and resulted in the generation of ovine leather with remarkably high strength attributes.

Through rationalisation of the depilation and liming process total sulphide use has been able to be reduced by up to 90% and through controlled liming with no additional sulphide leathers have been produced that have remarkable physical properties. In some instances the leather strength rivalled that of conventional bovine shoe upper leather.

The causes behind the increase in strength is being investigated through a research consortium funded by the New Zealand foundation for research science and technology.

During leather making, changes are made to the basic collagen molecule through chemical interactions with process reagents and to the skin structure through the removal of other matrix components such as glycosaminoglycans and water and also by the addition of crosslinking, filling and lubricating agents. These changes result in ovine leather with insufficient strength for footwear manufacture. Understanding how the process regimes used cause changes to the structural proteins and to the matrix in which they reside will allow a targeted response to this issue which has not been possible before.

Cutting edge techniques have been used to analyse the leather components and relate the results to differences in physical property outcomes and finally to changes in the skin processing regime.

[1] Abstract for presentation at the XXXI IULTCS Congress, Valencia, 27-30 September 2011

[1]Fibrillar Collagen Structure Determination of Ovine Leather using Small Angle X-ray Scattering (SAXS)

Melissa M. Basil-Jones,[†] Richard L. Edmonds,[§] Timothy F. Allsop,[§] Sue M. Cooper,[§] Geoff Holmes,[§] Gillian E. Norris,[‡] David J. Cookson,[⊥] Nigel Kirby,[⊥] and Richard G. Haverkamp,[†]

[†]School of Engineering and Advanced Technology, and [‡]Institute of Molecular Biosciences, Massey University, Palmerston North, New Zealand 4442, [§]Leather and Shoe Research Association, Palmerston North, New Zealand 4442, and [⊥]Australian Synchrotron, Melbourne, Australia

Introduction

Overview and Importance: Leather contains of a network of collagen fibrils interlinked with natural and synthetic chemical bonds. Collagen fibrils have a large inherent strength, and the arrangements of collagen fibrils are crucial to the final physical properties of the leather. Leather contains two main layers; the grain layer found at the leather outer surface and the corium layer found beneath. These layers have different structures and impart different properties to the final leather. Currently techniques used to analyse leather include optical microscopy, scanning electron microscopy, and atomic force microscopy. These techniques generally give qualitative measurements of fiber organisation but may not give quantitative measurement of fiber dimensions, orientation or *d* period.

Goal: Small Angle X-ray scattering is a powerful technique that can determine long range structural order. The goal of this work was to apply this technique to the characterising of the fibrillar collagen structure.

Experimental

Leather was prepared from pelt using the conventional beamhouse and tanning processes. Strips of leather 1mm thick and 30mm long were cut from samples of ovine leather at selected positions. SAXS diffraction patterns were recorded on the Australian Synchrotron SAXS/WAXS beamline, with a beam size of 250 × 80 µm, a total photon flux of 2×10^{12} photons s^{-1}, and an X-ray energy of 8 or 11keV. The leather samples were mounted in the beam horizontally without tension at a sample to detector distance of 3371mm. Exposure time for diffraction patterns was in the range of 1-5s. Analyses were performed across the section of each strip of leather starting at the region of the grain and progressing through the corium. Steps of either 0.25 or 0.05mm were made between analysis points.

Results

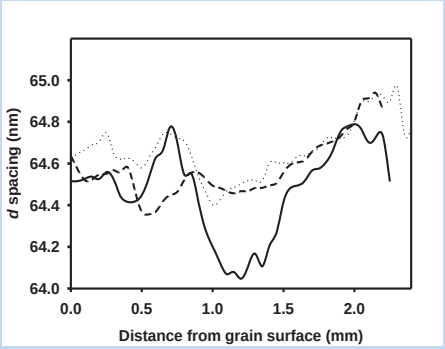

Figure 1: Variation of collagen *d* period through ovine leather cross section (for three samples)

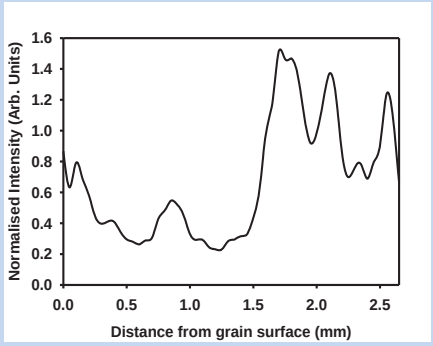

Figure 2: Intensity of the primary collagen *d* spacing peak (at around 0.059-0.060 $Å^{-1}$) through ovine leather cross section, normalised for total scattering at low q.

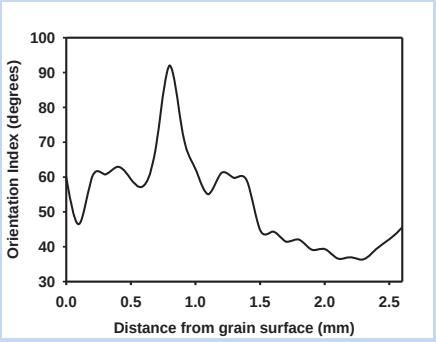

Figure 3: Graph of Orientation Index (%) versus distance through ovine leather cross section.

Discussion

Ovine leather has measurable differences between the fibrillar collagen structure of the grain and corium. The corium, relative to the grain, contains a greater proportion of fibrillar collagen which is more highly orientated and has a shorter *d* spacing.

Conclusion

Our study shows that Small Angle X-ray Scattering can provide quantitative information on the structure of ovine leather.

Acknowledgements

This research was undertaken on the SAXS/WAXS beamline at the Australian Synchrotron, Victoria, Australia. This research was supported by a grant from the Foundation for Research Science and Technology.

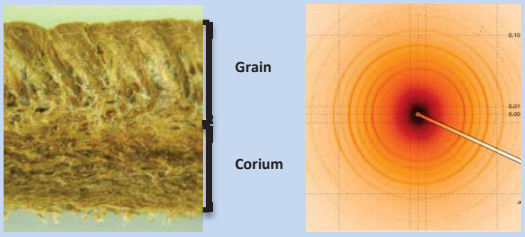

Figure 4: (a) Optical image of a cross section of ovine leather; (b) SAXS image of ovine leather.

MASSEY UNIVERSITY
TE KUNENGA KI PŪREHUROA

[1]Copy of poster presented at Pacifichem 2010, Honolulu, 15-20 December 2010

LASRA®

MASSEY UNIVERSITY
GRADUATE RESEARCH SCHOOL

STATEMENT OF CONTRIBUTION TO DOCTORAL THESIS CONTAINING PUBLICATIONS

(To appear at the end of each thesis chapter/section/appendix submitted as an article/paper or collected as an appendix at the end of the thesis)

We, the candidate and the candidate's Principal Supervisor, certify that all co-authors have consented to their work being included in the thesis and they have accepted the candidate's contribution as indicated below in the *Statement of Originality*.

Name of Candidate: Melissa Basil-Jones

Name/Title of Principal Supervisor: Prof Richard Haverkamp

Name of Published Research Output and full reference: Sizeland K.H., Basil-Jones M.M., Edmonds R.L., Cooper S.M., Kirby, N., Hawley A., Haverkamp R.G. (2013) Collagen Orientation & Leather Strength for Selected Mammals. J Agric Food Chem. DOI 10.1021/jf3043067

In which Chapter is the Published Work: Appendix

Please indicate either:

- **The percentage of the Published Work that was contributed by the candidate:** _____

  ~~and~~ / or

- **Describe the contribution that the candidate has made to the Published Work:**

  Performed part of the synchrotron experiments & part of the data processing. Assisted with the paper preparation.

Melissa Basil-Jones
Candidate's Signature

3/2/13
Date

Principal Supervisor's signature

28/1/13
Date

MASSEY UNIVERSITY
GRADUATE RESEARCH SCHOOL

STATEMENT OF CONTRIBUTION TO DOCTORAL THESIS CONTAINING PUBLICATIONS

(To appear at the end of each thesis chapter/section/appendix submitted as an article/paper or collected as an appendix at the end of the thesis)

We, the candidate and the candidate's Principal Supervisor, certify that all co-authors have consented to their work being included in the thesis and they have accepted the candidate's contribution as indicated below in the *Statement of Originality*.

Name of Candidate: Melissa Basil-Jones

Name/Title of Principal Supervisor: Prof. Richard Haverkamp

Name of Published Research Output and full reference: Basil-Jones, M.M., Norris, G.E., Edmonds, R.L., Haverkamp, R.G., (2012) Collagen Fibril Alignment and Deformation during Tensile Strain of Leather: A SAXS Study. Journal of Agricultural and Food, 60(5), 1201-1208

In which Chapter is the Published Work: Appendix, chapter 7

Please indicate either:

- **The percentage of the Published Work that was contributed by the candidate:** 90%

  and / or

- **Describe the contribution that the candidate has made to the Published Work:**

I performed all synchrotron based experimental work, data processing and analysis. I prepared samples from material supplied by LASRA. I co-wrote the paper with my supervisor and with input from other authors.

Melissa Basil-Jones — Candidate's Signature

3/2/13 — Date

Principal Supervisor's signature

28/1/13 — Date

MASSEY UNIVERSITY
GRADUATE RESEARCH SCHOOL

STATEMENT OF CONTRIBUTION TO DOCTORAL THESIS CONTAINING PUBLICATIONS

(To appear at the end of each thesis chapter/section/appendix submitted as an article/paper or collected as an appendix at the end of the thesis)

We, the candidate and the candidate's Principal Supervisor, certify that all co-authors have consented to their work being included in the thesis and they have accepted the candidate's contribution as indicated below in the *Statement of Originality*.

Name of Candidate: Melissa Basil-Jones

Name/Title of Principal Supervisor: Prof. Richard Haverkamp

Name of Published Research Output and full reference: Basil-Jones, M.M, Norris G.E., Edmonds, R.L., Cooper, S.M., Haverkamp, R.G., (2011) Collagen fibril Orientation in Ovine and Bovine Leather Affects Strength: A small Angle X-ray Scattering (SAXS) study. Journal of Agricultural and Food Chemistry 59 (18), 9972-9979

In which Chapter is the Published Work: Appendix, chapter 4

Please indicate either:

- **The percentage of the Published Work that was contributed by the candidate:** 85%

  and / or

- **Describe the contribution that the candidate has made to the Published Work:**
  I performed all synchrotron based experimental work, the data processing and analysis. I assisted in SEM imaging of samples. I prepared samples from material supplied by LASRA. I co-wrote the paper with my supervisor and with input from the other authors

Melissa Basil-Jones
Candidate's Signature

3/2/13
Date

Principal Supervisor's signature

28/1/13
Date

MASSEY UNIVERSITY
GRADUATE RESEARCH SCHOOL

STATEMENT OF CONTRIBUTION TO DOCTORAL THESIS CONTAINING PUBLICATIONS

(To appear at the end of each thesis chapter/section/appendix submitted as an article/paper or collected as an appendix at the end of the thesis)

We, the candidate and the candidate's Principal Supervisor, certify that all co-authors have consented to their work being included in the thesis and they have accepted the candidate's contribution as indicated below in the *Statement of Originality*.

Name of Candidate: Melissa Basil-Jones

Name/Title of Principal Supervisor: Prof. Richard Haverkamp

Name of Published Research Output and full reference: Floden, E.W., Malak, S., Basil-Jones, M.M., Negron, L., Fisher, J.N., [redacted], Lun, S., Dempsey, S.G. Haverkamp, R.G., Ward, B.R., May, B.C. (2011) Biophysical Characterization of Ovine Forestomach Extracellular Matrix Biomaterials. Journal of Biomedical Materials Research Part B, 96B(1), 67-75

In which Chapter is the Published Work: Appendix, Chapter 8

Please indicate either:

- **The percentage of the Published Work that was contributed by the candidate:** _____

  ~~and~~ / or

- **Describe the contribution that the candidate has made to the Published Work:**

I performed the synchrotron part of the work and the associated data processing and analysis I assisted in the preparation of the manuscript

Melissa Basil-Jones
Candidate's Signature

3/2/13
Date

Principal Supervisor's signature

28/1/13
Date

MASSEY UNIVERSITY
GRADUATE RESEARCH SCHOOL

STATEMENT OF CONTRIBUTION TO DOCTORAL THESIS CONTAINING PUBLICATIONS

(To appear at the end of each thesis chapter/section/appendix submitted as an article/paper or collected as an appendix at the end of the thesis)

We, the candidate and the candidate's Principal Supervisor, certify that all co-authors have consented to their work being included in the thesis and they have accepted the candidate's contribution as indicated below in the *Statement of Originality*.

Name of Candidate: Melissa Basil-Jones

Name/Title of Principal Supervisor: Prof. Richard Haverkamp

Name of Published Research Output and full reference: Basil-Jones, M.M., Edmonds, R.L., Allspp, T.F., Cooper, S.M., Holmes, G., Norris, G.E., Cookson, D.J., Kirby, N., Haverkamp, R.G. (2010) Leather Structure Determination by Small Angle X-ray Scattering (SAXS): Cross Sections of Ovine and Bovine Leather. Journal of Agricultural and Food Chemistry, 58(9), 5286-5291

In which Chapter is the Published Work: Appendix, Chapter 3

Please indicate either:

- **The percentage of the Published Work that was contributed by the candidate:** 80%

  and / or

- **Describe the contribution that the candidate has made to the Published Work:** I performed all synchrotron based experimental work, data processing and analysis. I prepared samples from material supplied by LARA. I co-wrote the paper with my supervisor and will input from the other authors.

Melissa Basil-Jones
Candidate's Signature

3/2/13
Date

Principal Supervisor's signature

28/1/13
Date

10.2 Appendix II: Sample Information

10.2.1 Information for Samples included in Chapter 4

Table 10.1: Sample information for cross-sections of ovine leather cut from the OSP parallel to the backbone.

Sax skin Number	Thickness mm	Absolute strength N	Relative strength N/mm	Tensile Force N/mm²	Tensile Extension %	Sample Name
1	1.20	24.69	20.34	9.69	82.1	Ov004
2	1.34	27.59	20.59	13.48	83.8	Ov008
3	1.77	35.01	19.81	9.24	82.2	Ov012
4	1.30	24.50	18.90	10.48	104.4	Ov016
5	1.21	50.07	41.46	15.01	74.3	Ov020
6	1.21	46.66	38.74	13.72	82.9	Ov024
7	1.25	53.67	43.12	14.36	114.1	Ov028
8	1.71	32.77	19.18	7.90	85.9	Ov032
9	1.71	34.23	20.01	11.18	81.5	Ov036
10	1.34	50.39	37.85	12.30	122.7	Ov040
11	1.21	51.52	42.57	13.64	109.0	Ov044
12	1.23	25.69	20.94	10.19	74.1	Ov048
14	1.24	46.82	37.71	12.09	97.9	Ov056
15	1.79	39.59	22.17	8.59	100.7	Ov060
16	1.27	27.13	21.30	9.88	78.4	Ov064
17	1.23	21.90	17.78	8.09	70.2	Ov068
18	1.25	26.45	21.17	10.93	68.1	Ov072
19	1.38	26.04	19.05	11.28	83.3	Ov076
20	1.23	25.09	20.44	9.42	65.3	Ov080
21	1.25	55.13	44.26	13.26	89.2	Ov084
22	0.96	40.86	42.53	13.84	73.4	Ov088
23	1.28	49.04	38.91	10.27	95.3	Ov092
24	1.82	31.01	17.18	9.27	115.3	Ov096
25	1.25	47.40	37.86	9.57	74.5	Ov100
26	0.96	33.60	34.96	12.02	71.2	Ov104
27	0.98	38.08	38.86	12.93	80.6	Ov108
28	0.98	36.02	36.67	10.72	93.4	Ov112
29	0.92	32.30	35.10	10.59	81.4	Ov116
30	1.32	55.42	41.90	17.68	77.2	Ov120

Table 10.2: Sample information for cross-sections of bovine leather cut from the OSP parallel to the backbone.

Sax skin Number	Thickness mm	Absolute strength N	Relative strength N/mm	Tensile Force N/mm²	Tensile Extension %	Sample Name
31	1.2	47.6	39.6			Bo121
32	1.23	80.8	65.2			Bo122
33	1.26	67.9	54			Bo123
34	1.26	69.8	55.7			Bo124
35	1.31	81.8	62.6			Bo125
36	1.29	91.3	70.7			Bo126
37	1.34	45.9	34.4			Bo127
38	1.21	69.8	57.4			Bo128
39	1.35	87	64.7			Bo129
40	1.25	40.4	32.4			Bo130

Table 10.3: Sample information for flat samples of the grain of ovine leather cut from the OSP parallel to the backbone.

Sax skin Number	Thickness mm	Absolute strength N	Relative strength N/mm	Tensile Force N/mm²	Tensile Extension %	Sample Name
1	1.20	24.69	20.34	9.69	82.1	401
2	1.34	27.59	20.59	13.48	83.8	404
3	1.77	35.01	19.81	9.24	82.2	407
4	1.30	24.50	18.90	10.48	104.4	410
5	1.21	50.07	41.46	15.01	74.3	413
6	1.21	46.66	38.74	13.72	82.9	416
7	1.25	53.67	43.12	14.36	114.1	419
8	1.71	32.77	19.18	7.90	85.9	422
9	1.71	34.23	20.01	11.18	81.5	425
10	1.34	50.39	37.85	12.30	122.7	428
11	1.21	51.52	42.57	13.64	109.0	431
12	1.23	25.69	20.94	10.19	74.1	434
14	1.24	46.82	37.71	12.09	97.9	437
15	1.79	39.59	22.17	8.59	100.7	440
16	1.27	27.13	21.30	9.88	78.4	443
17	1.23	21.90	17.78	8.09	70.2	446
18	1.25	26.45	21.17	10.93	68.1	449
19	1.38	26.04	19.05	11.28	83.3	452
20	1.23	25.09	20.44	9.42	65.3	455
21	1.25	55.13	44.26	13.26	89.2	458
22	0.96	40.86	42.53	13.84	73.4	461
23	1.28	49.04	38.91	10.27	95.3	464
24	1.82	31.01	17.18	9.27	115.3	467
25	1.25	47.40	37.86	9.57	74.5	470
26	0.96	33.60	34.96	12.02	71.2	473
27	0.98	38.08	38.86	12.93	80.6	476
28	0.98	36.02	36.67	10.72	93.4	479
29	0.92	32.30	35.10	10.59	81.4	482
30	1.32	55.42	41.90	17.68	77.2	485

Table 10.4: Sample information for flat samples of the grain of bovine leather cut from the OSP parallel to the backbone.

Sax skin Number	Thickness mm	Absolute strength N	Relative strength N/mm	Tensile Force N/mm²	Tensile Extension %	Sample Name
31	1.2	47.6	39.6			488
32	1.23	80.8	65.2			491
33	1.26	67.9	54			494
34	1.26	69.8	55.7			497
35	1.31	81.8	62.6			500
36	1.29	91.3	70.7			503
37	1.34	45.9	34.4			506
38	1.21	69.8	57.4			509
39	1.35	87	64.7			512

Table 10.5: Sample information for flat samples of the corium of ovine leather cut from the OSP parallel to the backbone.

Sax skin Number	Thickness mm	Absolute strength N	Relative strength N/mm	Tensile Force N/mm²	Tensile Extension %	Sample Name
1	1.20	24.69	20.34	9.69	82.1	402
2	1.34	27.59	20.59	13.48	83.8	405
3	1.77	35.01	19.81	9.24	82.2	408
4	1.30	24.50	18.90	10.48	104.4	411
5	1.21	50.07	41.46	15.01	74.3	414
6	1.21	46.66	38.74	13.72	82.9	417
7	1.25	53.67	43.12	14.36	114.1	420
8	1.71	32.77	19.18	7.90	85.9	423
9	1.71	34.23	20.01	11.18	81.5	426
10	1.34	50.39	37.85	12.30	122.7	429
11	1.21	51.52	42.57	13.64	109.0	432
12	1.23	25.69	20.94	10.19	74.1	435
14	1.24	46.82	37.71	12.09	97.9	438
15	1.79	39.59	22.17	8.59	100.7	441
16	1.27	27.13	21.30	9.88	78.4	444
17	1.23	21.90	17.78	8.09	70.2	447
18	1.25	26.45	21.17	10.93	68.1	450
19	1.38	26.04	19.05	11.28	83.3	453
20	1.23	25.09	20.44	9.42	65.3	456
21	1.25	55.13	44.26	13.26	89.2	459
22	0.96	40.86	42.53	13.84	73.4	462
23	1.28	49.04	38.91	10.27	95.3	465
24	1.82	31.01	17.18	9.27	115.3	468
25	1.25	47.40	37.86	9.57	74.5	471
26	0.96	33.60	34.96	12.02	71.2	474
27	0.98	38.08	38.86	12.93	80.6	477
28	0.98	36.02	36.67	10.72	93.4	480
29	0.92	32.30	35.10	10.59	81.4	483
30	1.32	55.42	41.90	17.68	77.2	486

Table 10.6: Sample information for flat samples of the corium of bovine leather cut from the OSP parallel to the backbone.

Sax skin Number	Thickness mm	Absolute strength N	Relative strength N/mm	Tensile Force N/mm²	Tensile Extension %	Sample Name
31	1.2	47.6	39.6			489
32	1.23	80.8	65.2			492
33	1.26	67.9	54			495
34	1.26	69.8	55.7			498
35	1.31	81.8	62.6			501
36	1.29	91.3	70.7			504
37	1.34	45.9	34.4			507
38	1.21	69.8	57.4			510
39	1.35	87	64.7			513

Table 10.7: Sample information for cross-sections of ovine leather cut from the OSP perpendicular to the backbone.

Sax skin Number	Thickness mm	Absolute strength N	Relative strength N/mm	Tensile Force N/mm²	Tensile Extension %	Sample Name
1	1.20	24.69	20.34	9.69	82.1	400
2	1.34	27.59	20.59	13.48	83.8	403
3	1.77	35.01	19.81	9.24	82.2	406
4	1.30	24.50	18.90	10.48	104.4	409
5	1.21	50.07	41.46	15.01	74.3	412
6	1.21	46.66	38.74	13.72	82.9	415
7	1.25	53.67	43.12	14.36	114.1	418
8	1.71	32.77	19.18	7.90	85.9	421
9	1.71	34.23	20.01	11.18	81.5	424
10	1.34	50.39	37.85	12.30	122.7	427
11	1.21	51.52	42.57	13.64	109.0	430
12	1.23	25.69	20.94	10.19	74.1	433
14	1.24	46.82	37.71	12.09	97.9	436
15	1.79	39.59	22.17	8.59	100.7	439
16	1.27	27.13	21.30	9.88	78.4	442
17	1.23	21.90	17.78	8.09	70.2	445
18	1.25	26.45	21.17	10.93	68.1	448
19	1.38	26.04	19.05	11.28	83.3	451
20	1.23	25.09	20.44	9.42	65.3	454
21	1.25	55.13	44.26	13.26	89.2	457
22	0.96	40.86	42.53	13.84	73.4	460
23	1.28	49.04	38.91	10.27	95.3	463
24	1.82	31.01	17.18	9.27	115.3	466
25	1.25	47.40	37.86	9.57	74.5	469
26	0.96	33.60	34.96	12.02	71.2	472
27	0.98	38.08	38.86	12.93	80.6	475
28	0.98	36.02	36.67	10.72	93.4	478
29	0.92	32.30	35.10	10.59	81.4	481
30	1.32	55.42	41.90	17.68	77.2	484

Table 10.8: Sample information for cross-sections of bovine leather cut from the OSP perpendicular to the backbone.

Sax skin Number	Thickness mm	Absolute strength N	Relative strength N/mm	Tensile Force N/mm²	Tensile Extension %	Sample Name
31	1.2	47.6	39.6			222
32	1.23	80.8	65.2			223
33	1.26	67.9	54			224
34	1.26	69.8	55.7			536
35	1.31	81.8	62.6			225
36	1.29	91.3	70.7			226
37	1.34	45.9	34.4			537
38	1.21	69.8	57.4			227
39	1.35	87	64.7			228

10.2.2 Information for Samples included in Chapter 5

Table 10.9: Sample information for cross-sections of ovine leather cut from the neck parallel to the backbone.

Sax skin Number	Thickness mm	Absolute strength N	Relative strength N/mm	Sample Name
1	1.73	43.51	25.22	Ov001
2	1.85	43.75	23.64	Ov005
3	2.67	68.11	25.52	Ov009
4	1.88	53.40	28.66	Ov013
5	1.54	49.94	32.59	Ov017
6	1.47	54.16	36.92	Ov021
7	1.57	68.51	43.51	Ov025
8	1.84	34.47	18.72	Ov029
9	2.16	42.82	19.81	Ov033
10	2.08	59.06	28.48	Ov037
11	1.64	60.51	36.90	Ov041
12	1.67	40.80	24.31	Ov045
14	1.77	55.73	31.24	Ov053
15	2.73	62.10	22.90	Ov057
16	1.71	47.20	27.63	Ov061
17	1.86	41.41	22.38	Ov065
18	1.53	40.01	26.14	Ov069
19	1.59	42.98	27.24	Ov073
20	1.56	37.65	24.13	Ov077
21	1.96	64.66	33.10	Ov081
22	1.23	49.87	40.54	Ov085
23	2.15	68.26	31.84	Ov089
24	2.48	69.68	28.19	Ov093
25	1.46	31.27	21.47	Ov097
26	1.69	55.83	33.14	Ov101
27	1.58	42.69	27.10	Ov105
28	1.77	41.47	24.15	Ov109
29	1.19	33.76	28.48	Ov113
30	2.06	65.59	31.92	Ov117

Table 10.10: Sample information for cross-sections of ovine leather cut from the belly parallel to the backbone.

Sax skin Number	Thickness mm	Absolute strength N	Relative strength N/mm	Sample Number
1	1.02	35.41	34.80	Ov002
2	1.08	26.65	24.79	Ov006
3	1.22	37.13	30.34	Ov010
4	1.49	22.23	16.09	Ov014
5	1.14	53.38	47.20	Ov018
6	0.88	34.03	39.07	Ov022
7	1.16	50.75	43.81	Ov026
8	1.28	35.18	27.73	Ov030
9	1.47	33.75	23.47	Ov034
10	1.20	46.91	39.08	Ov038
11	1.06	42.43	39.96	Ov042
12	1.12	29.75	26.65	Ov046
14	1.08	33.32	30.79	Ov054
15	1.41	40.06	28.35	Ov058
16	0.91	25.77	27.95	Ov062
17	1.10	15.75	14.32	Ov066
18	0.87	30.18	34.77	Ov070
19	0.88	21.18	24.15	Ov074
20	1.03	21.14	20.52	Ov078
21	1.02	52.14	51.75	Ov082
22	0.80	30.03	37.88	Ov086
23	1.32	38.30	28.96	Ov090
24	1.33	50.45	38.03	Ov094
25	0.88	28.08	32.15	Ov098
26	0.88	44.20	50.61	Ov102
27	0.89	36.93	41.83	Ov106
28	0.86	36.59	42.39	Ov110
29	0.84	26.85	32.29	Ov114
30	1.21	54.11	44.76	Ov118

Table 10.11: Sample information for cross-sections of ovine leather cut from the butt perpendicular to the backbone.

Sax skin Number	Thickness mm	Absolute strength N	Relative strength N/mm	Sample Number
1	1.48	35.33	23.95	Ov003
2	1.65	44.26	27.05	Ov007
3	1.67	35.87	21.60	Ov011
4	2.01	33.83	16.76	Ov015
5	1.55	56.03	36.08	Ov019
6	1.30	51.88	39.99	Ov023
7	1.87	65.49	35.07	Ov027
8	1.75	44.33	25.33	Ov031
9	1.45	35.11	24.25	Ov035
10	1.61	56.31	34.97	Ov039
11	1.47	59.26	40.40	Ov043
12	1.54	37.18	24.17	Ov047
14	1.44	47.94	33.22	Ov055
15	1.78	43.07	24.06	Ov059
16	1.28	30.89	24.18	Ov063
17	1.55	22.06	14.27	Ov067
18	2.87	63.72	22.21	Ov071
19	1.07	28.36	26.40	Ov075
20	2.24	41.25	18.61	Ov079
21	1.81	40.12	22.15	Ov083
22	1.20	39.67	33.17	Ov087
23	1.57	57.19	36.51	Ov091
24	2.02	48.15	25.20	Ov095
25	1.32	29.32	22.28	Ov099
26	1.26	44.67	35.37	Ov103
27	1.13	40.78	36.05	Ov107
28	1.17	41.11	35.09	Ov111
29	0.90	26.90	29.89	Ov115
30	1.71	63.83	37.14	Ov119

Table 10.12: Sample information for cross-sections of ovine leather cut from the OSP parallel to the backbone.

Sax skin Number	Thickness mm	Absolute strength N	Relative strength N/mm	Sample Number
1	1.26	37.60	29.82	Ov004
2	1.27	33.48	26.41	Ov008
3	1.68	36.57	21.74	Ov012
4	1.23	22.65	18.37	Ov016
5	1.21	43.36	35.95	Ov020
6	1.07	40.39	37.81	Ov024
7	1.28	43.54	34.08	Ov028
8	1.55	29.94	19.28	Ov032
9	1.55	30.78	19.84	Ov036
10	1.41	42.79	30.72	Ov040
11	1.32	41.41	31.49	Ov044
12	1.20	28.14	23.45	Ov048
14	1.41	44.59	31.73	Ov056
15	1.73	37.20	21.53	Ov060
16	1.14	24.92	21.93	Ov064
17	1.15	20.85	18.16	Ov068
18	1.31	33.05	25.32	Ov072
19	1.48	20.70	14.00	Ov076
20	1.24	23.88	19.34	Ov080
21	1.19	54.04	45.58	Ov084
22	1.10	39.17	35.65	Ov088
23	1.26	40.14	31.89	Ov092
24	1.74	47.30	27.18	Ov096
25	1.07	27.06	25.35	Ov100
26	1.04	32.03	30.98	Ov104
27	0.98	38.92	39.91	Ov108
28	1.04	37.83	36.43	Ov112
29	0.99	27.80	28.19	Ov116
30	1.43	51.79	36.26	Ov120

Table 10.13: Sample information for cross-sections of ovine leather cut from the OSP perpendicular to the backbone.

Sax skin Number	Thickness mm	Absolute strength N	Relative strength N/mm	Sample Number
1	1.33	30.61	23.04	400
2	1.27	31.94	25.24	403
3	1.82	43.71	23.98	406
4	1.33	36.53	27.57	409
5	1.26	42.19	33.35	412
6	1.13	46.25	41.01	415
7	1.31	51.21	39.04	418
8	1.69	43.45	25.71	421
9	1.65	36.03	21.88	424
10	1.48	52.13	35.26	427
11	1.35	56.27	41.60	430
12	1.32	35.87	27.15	433
14	1.50	59.02	39.24	436
15	1.76	51.01	28.95	439
17	1.22	25.17	20.59	445
18	1.32	33.24	25.18	448
19	1.38	28.71	20.73	451
20	1.32	27.02	20.53	454
21	1.19	53.84	45.30	457
22	1.19	37.92	31.91	460
24	1.98	54.30	27.39	466
25	1.17	31.96	27.20	469
26	1.10	44.91	40.80	472
27	1.13	41.36	36.61	475
28	1.07	39.01	36.46	478
29	1.05	36.81	35.13	481
30	1.52	65.63	43.03	484

10.2.3 Information for Samples included in Chapter 6

Table 10.14: Sample information for cross-sections of ovine partially processed leather cut from the butt perpendicular to the backbone.

Sample Type	Sample Number
Pickle	131
Pickle	132
Pickle	133
Pickle	134
Wet Blue	135
Wet Blue	136
Wet Blue	137
Wet Blue	138
Pretanned	139
Pretanned	140
Pretanned	141
Pretanned	142
Retanned	143
Retanned	144
Retanned	145
Retanned	146
Salted Green Skin	147
Salted Green Skin	148
Salted Green Skin	149
Salted Green Skin	150

10.2.4 Information for Samples included in Chapter 7

Table 10.15: Sample information for samples of leather cut from the OSP parallel to the backbone used for stretching experiments.

Skin Type (Species)	SAXS Skin Number	Sample Cut	Thickness (mm)	Absolute strength (N)	Relative strength (N/mm)	Sample Number
Ovine	11	Cross-section	1.21	51.52	42.57	202
Ovine	19	Cross-section	1.38	26.04	19.05	208
Ovine	27	Cross-section	0.98	38.08	38.86	221
Ovine	18	Flat-Grain	1.25	26.45	21.17	828
Ovine	18	Flat-Corium	1.25	26.45	21.17	829
Ovine	21	Flat-Grain	1.25	55.13	44.26	843
Ovine	21	Flat-Corium	1.25	55.13	44.26	844
Bovine	36	Cross-section	1.29	90.30	70.70	884

10.3 Appendix III: Raw Data

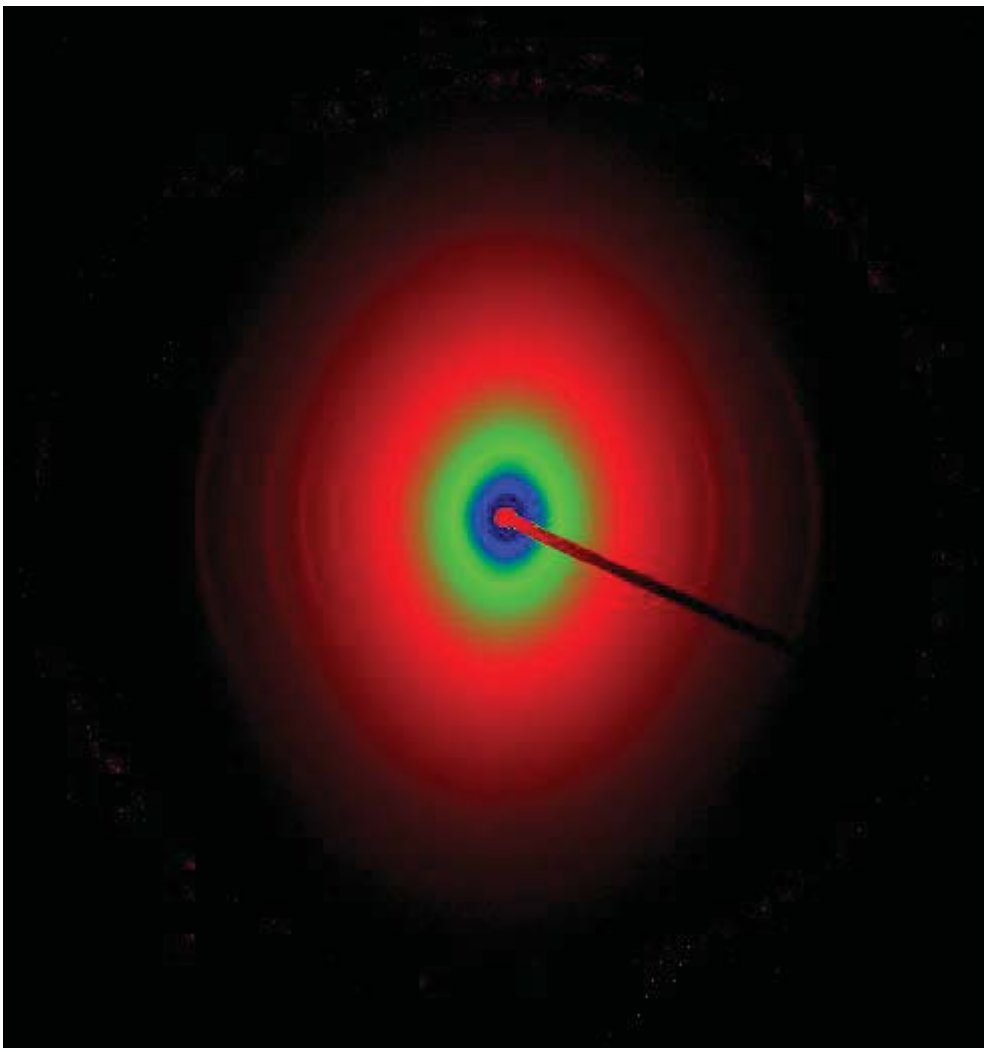

Figure 10.1: Example of a SAXS image for a leather sample with a high level of preferred orientation (orientation index was calculated to be 0.81).

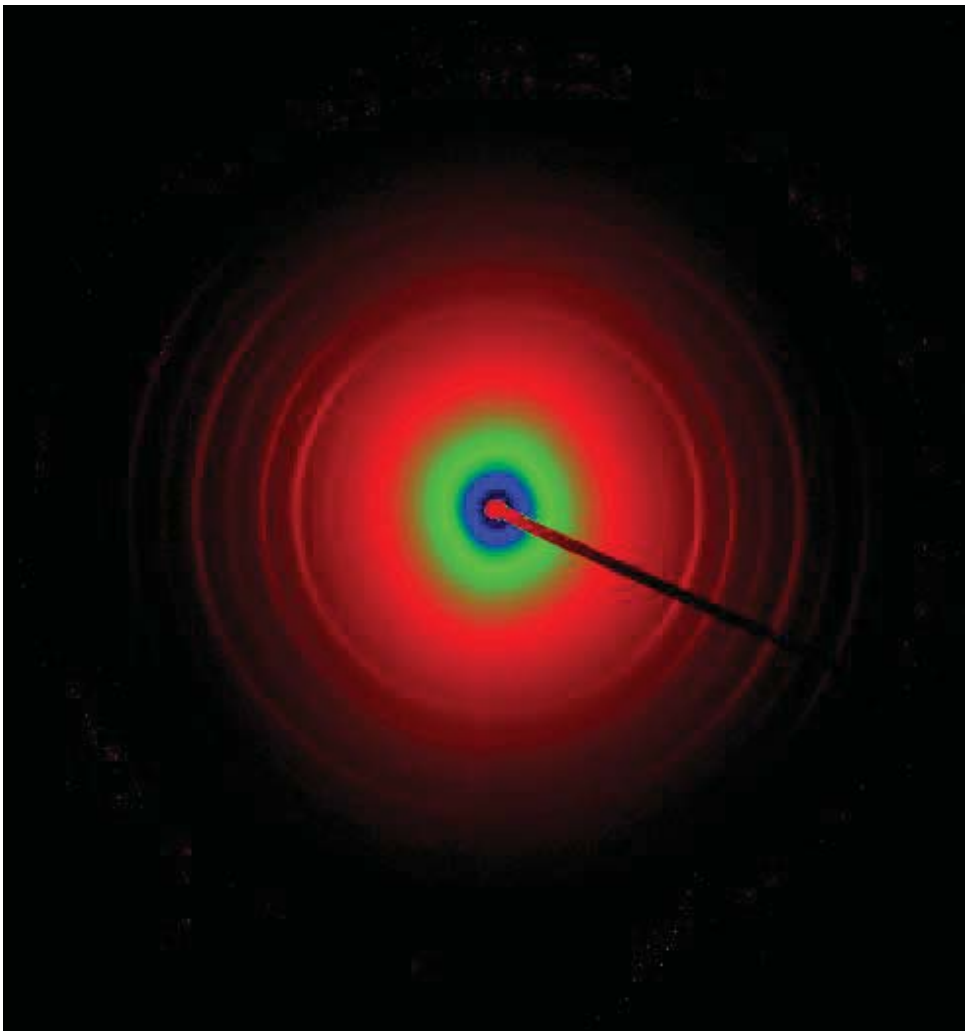

Figure 10.2: Example of a SAXS image for a leather sample with a medium level of preferred orientation (orientation index was calculated to be 0.50).

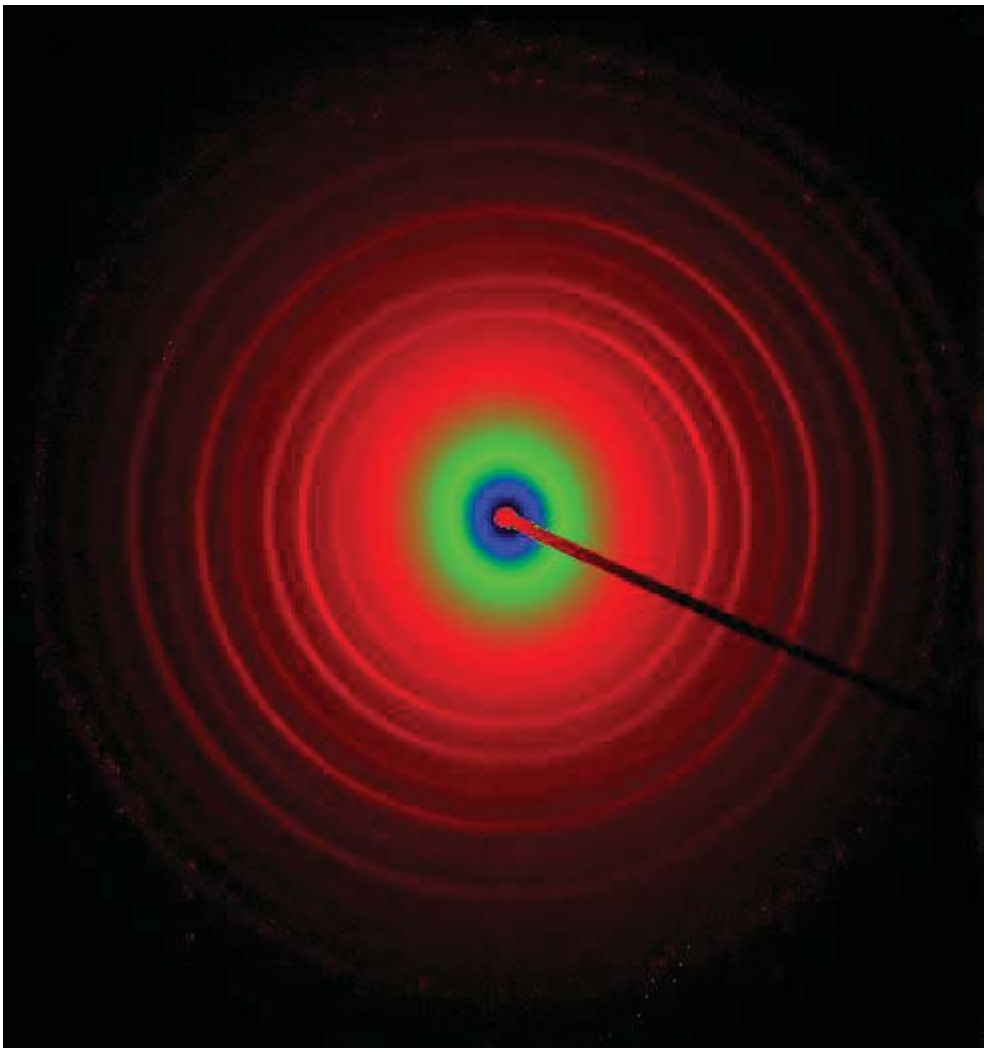

Figure 10.3: Example of a SAXS image for a leather sample with a low level of preferred orientation (orientation index was calculated to be 0.19).

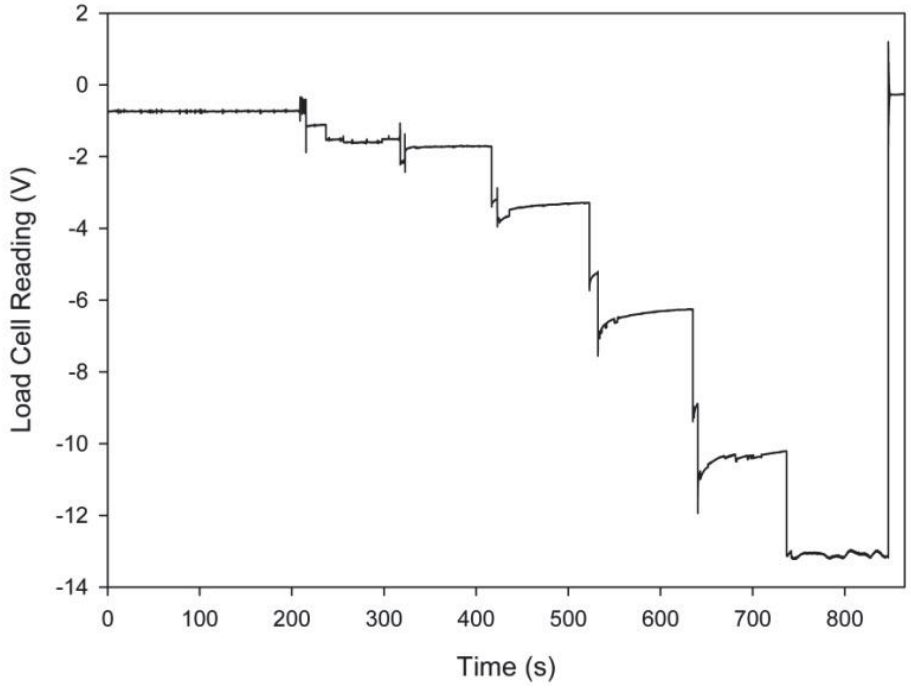

Figure 10.4: An example of the data recorded by the load cell during stretching of leather while mounted in the SAXS X-ray beam.

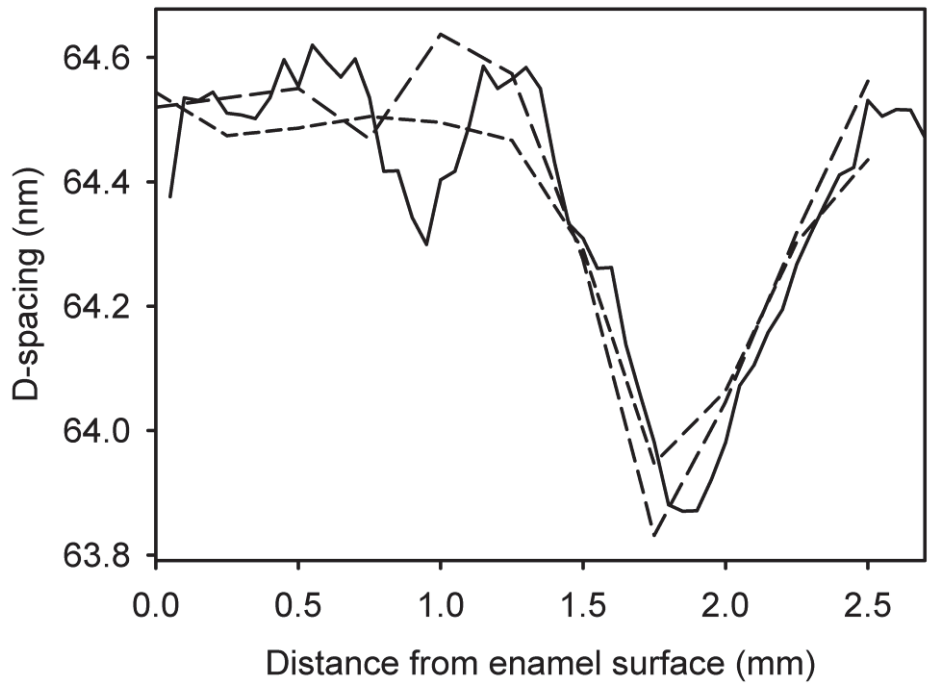

Figure 10.5: Example of reproducibility of *d* period measurement in adjacent regions on one sample. Solid line, 5s exposure, 0.05 mm sampling; Dashed lines, 1s exposure, 0.25 mm sampling.

10.4 Appendix IV: Additional Processed Data

This appendix contains additional processed data which, for reasons of clarity and consensus, have not been included in the main body of the thesis. As will be apparent from an inspection of this appendix, there is a large body of processed data. The data that was selected for inclusion in the body of this thesis are those which illustrate the major findings from this work. The remainder, which is contained in this appendix, consist of additional material on a wider range of samples or of duplicates, or of data which does not illustrate an interesting new finding.

10.4.1 Extra Data Relating to Chapter 4

10.4.1.1 Additional SEM Images

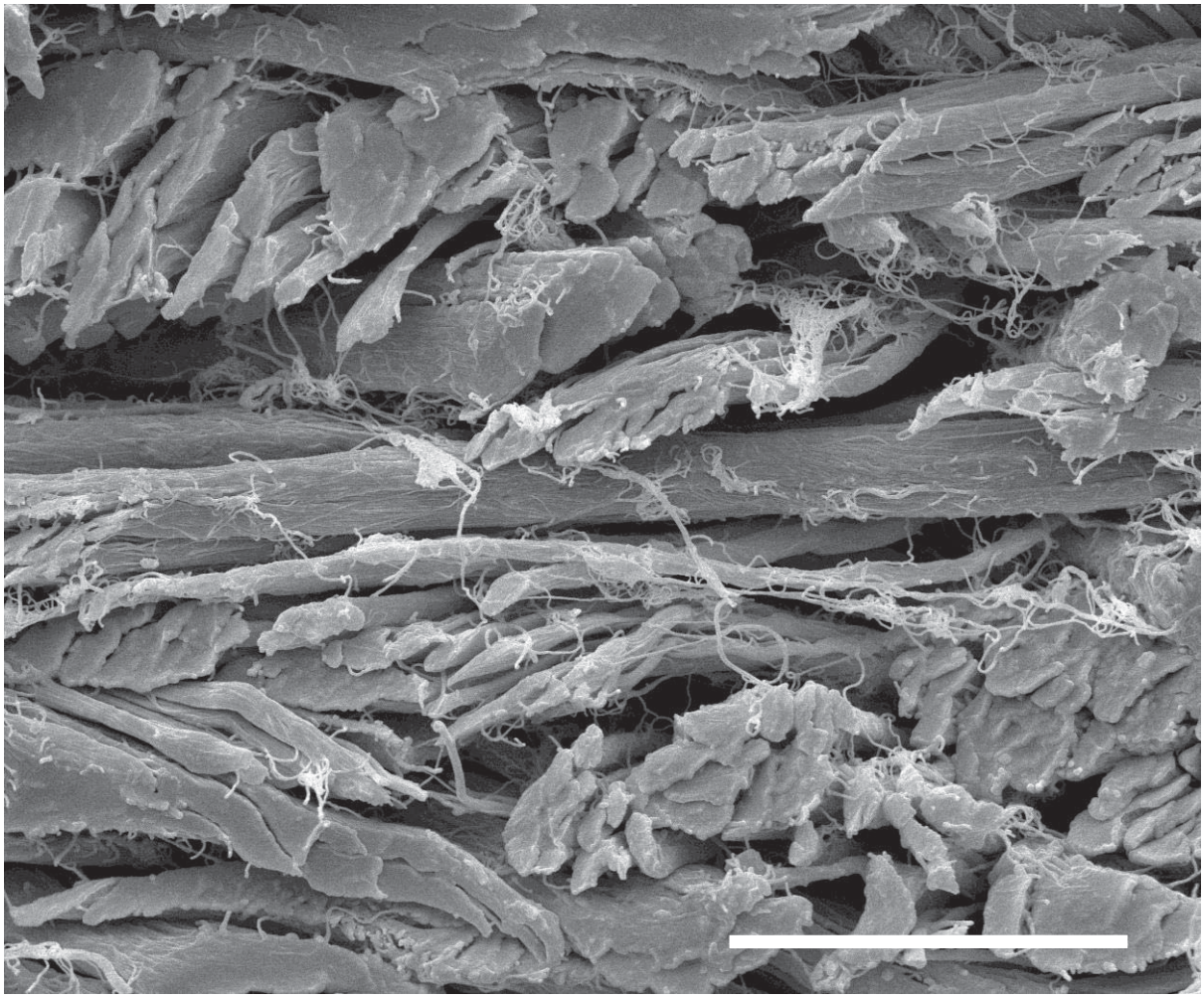

Figure 10.6: Representative SEM image of a cross-section of weak ovine leather observed parallel to the backbone. Scale bar 50 μm.

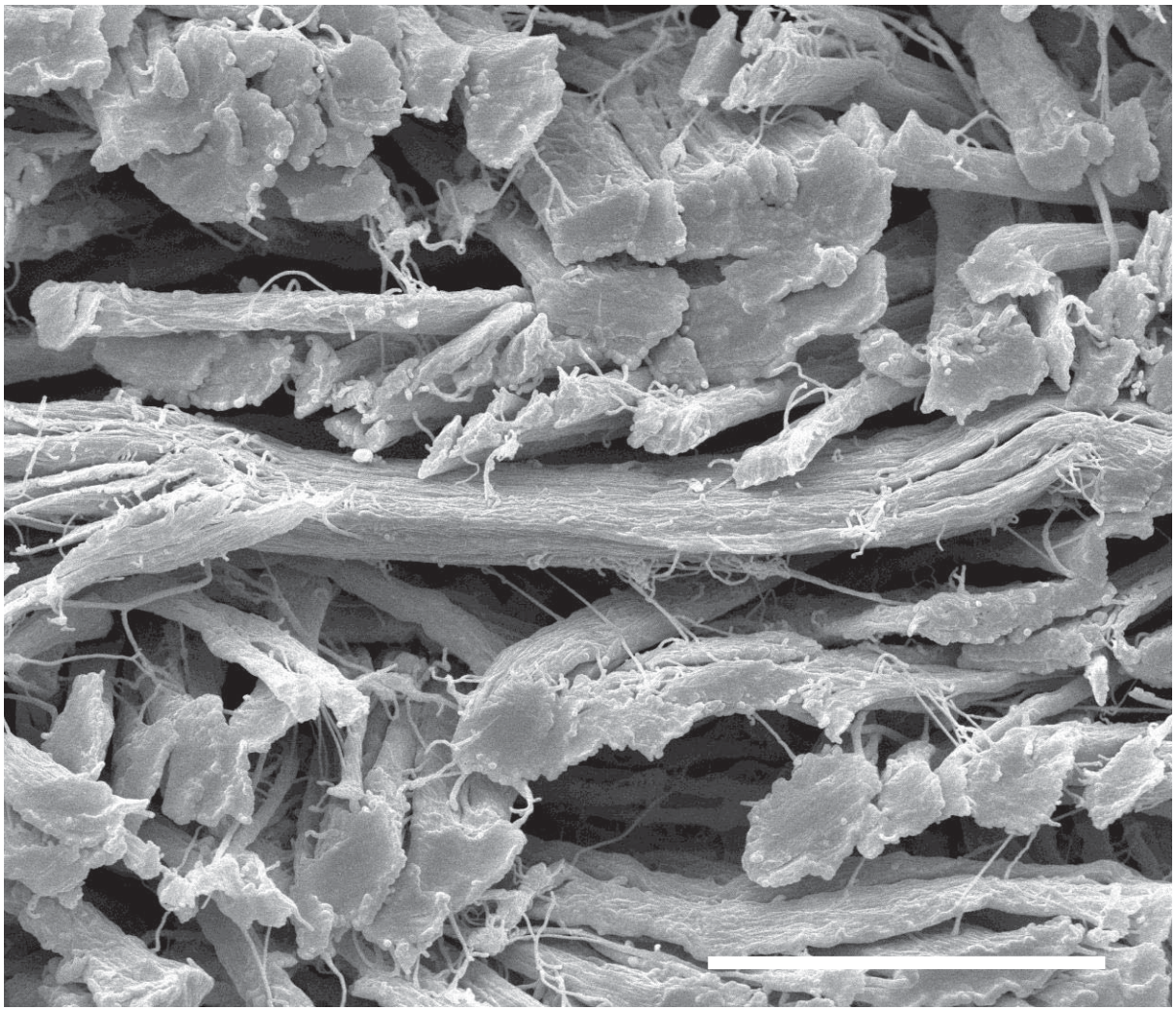

Figure 10.7: Representative SEM image of a cross-section of strong ovine leather observed parallel to the backbone. Scale bar 50 μm.

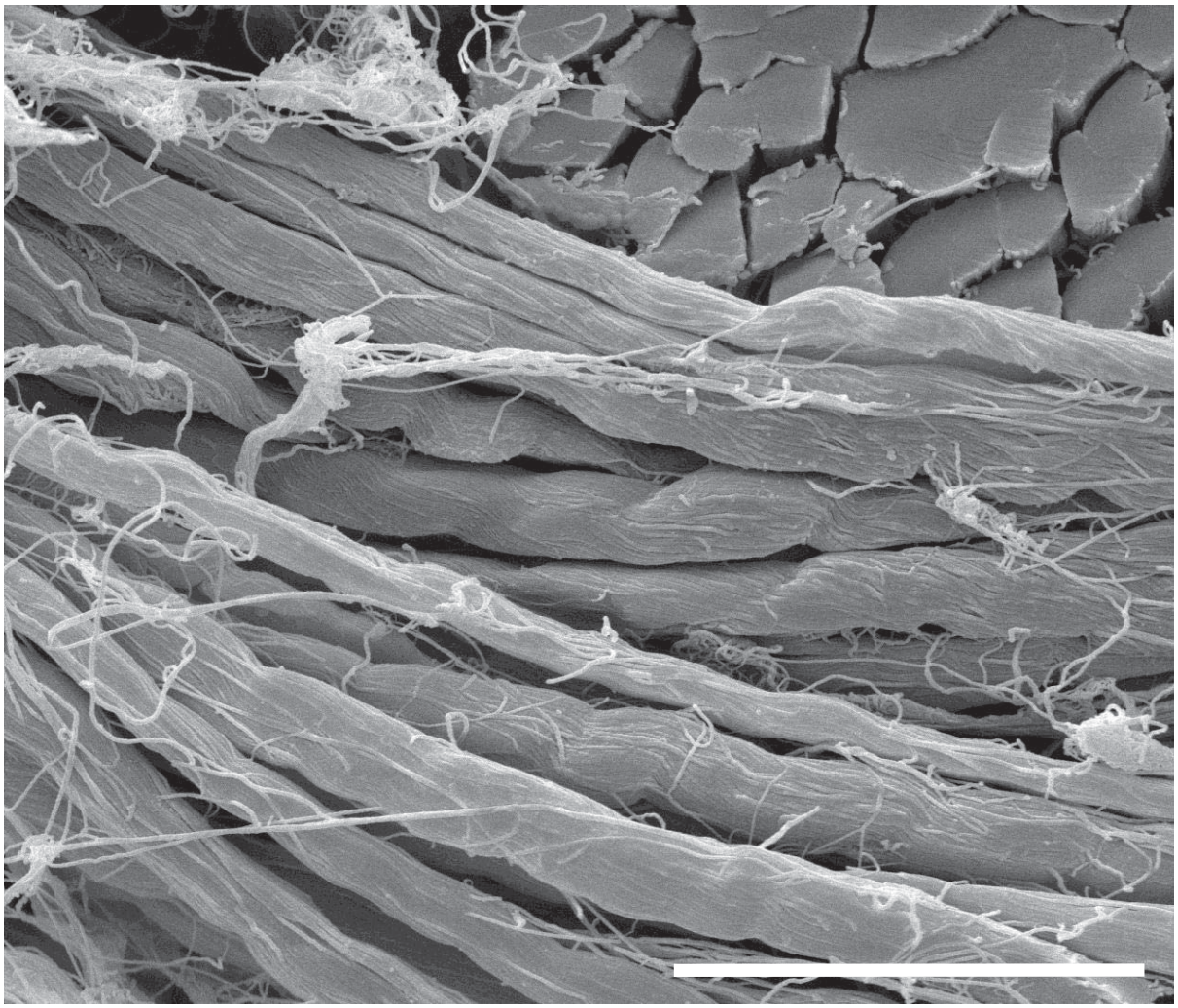

Figure 10.8: Representative SEM image of a cross-section of bovine leather observed parallel to the backbone. Scale bar 30 μm.

10.4.1.2 Absolute Tear Strength

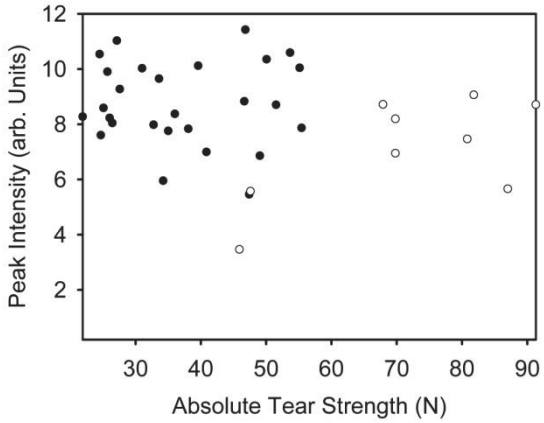

Figure 10.9: Amount of collagen determined from the intensity of the primary collagen *d* spacing peak (at around 0.059–0.060 $Å^{-1}$) versus absolute tear strength for both ovine - closed circle, and bovine - open circle, samples.

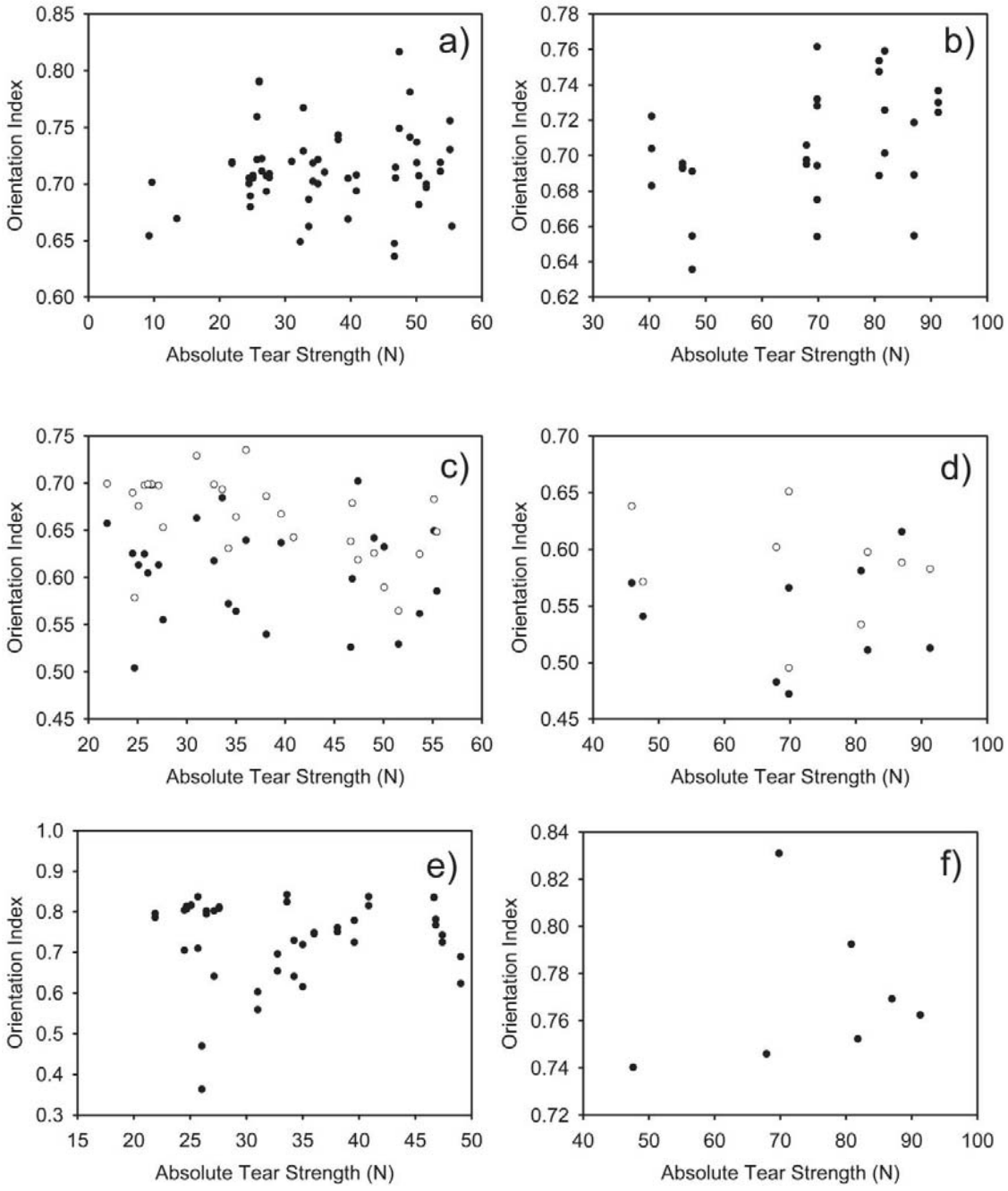

Figure 10.10: Orientation index versus absolute tear strength for OSP samples of leather. a) Ovine cross-section cut parallel to backbone; b) bovine cross-section cut parallel to backbone; c) ovine, flat, grain - closed circle, corium - open circle, ; d) bovine, flat, grain - closed circle, corium - open circle, ; e) ovine cross-section cut perpendicular to backbone; f) bovine cross-section cut perpendicular to backbone.

There is a statistically significant relationship between absolute tear strength and the *d* spacing of bovine cross-sections cut parallel to the backbone (Figure 10.11). A linear regression analysis of the results produced a slope of 43 N/nm, $r^2 = 0.35$ and $P = 3.1 \times 10^{-4}$. There is also a statistically significant relationship between absolute tear strength and the

d spacing of flat corium samples. A linear regression analysis of the results for bovine samples produced a slope of 40 N/nm, $r^2 = 0.41$ and P = 0.038. While analysis of the results for ovine samples produced a slope of 17 N/nm, $r^2 = 0.13$ and P = 0.039.

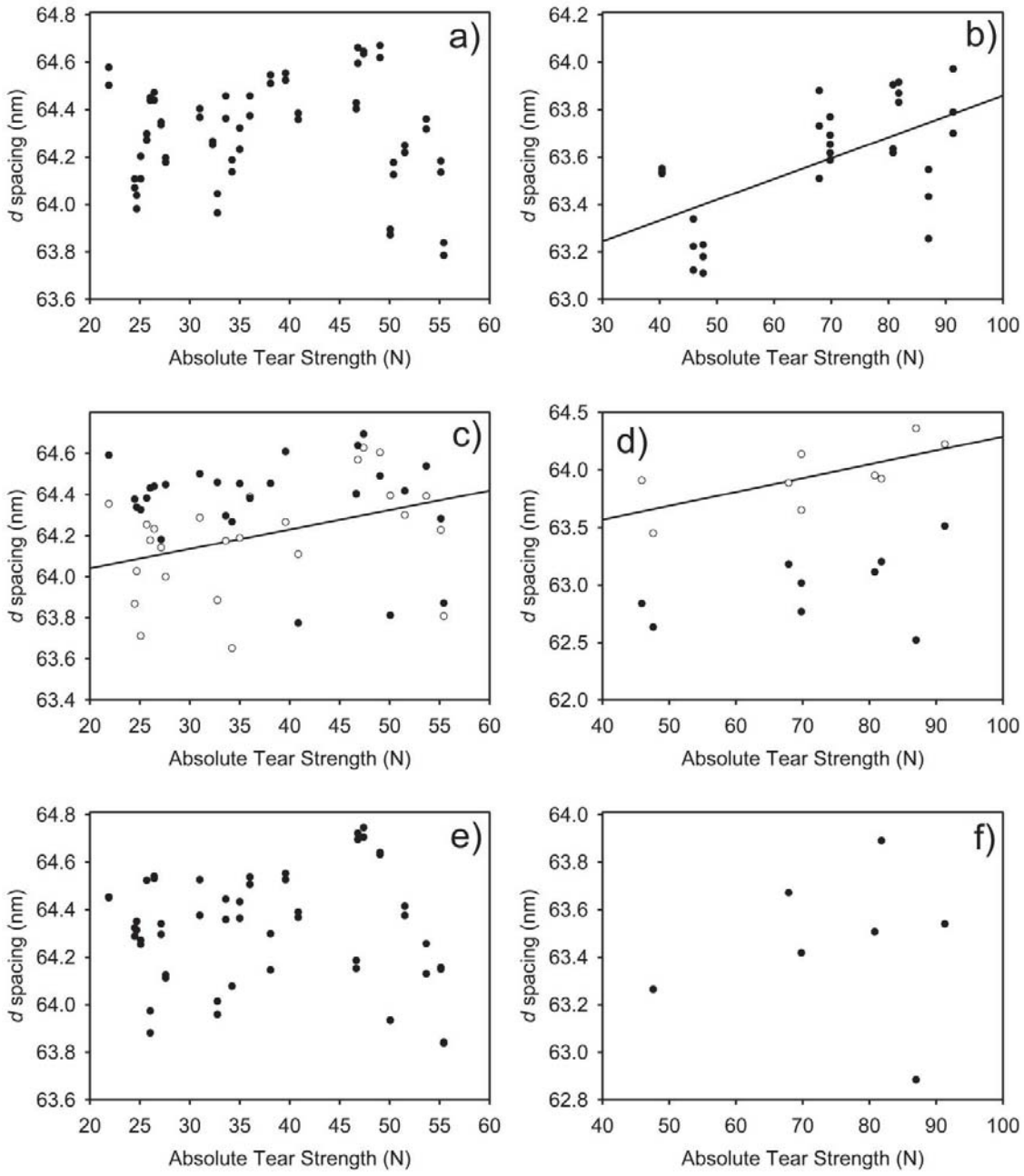

Figure 10.11: *d* spacing versus absolute tear strength for OSP samples of leather. a) Ovine cross-section cut parallel to backbone; b) bovine cross-section cut parallel to backbone; c) ovine, flat, grain - closed circle, corium - open circle, ; d) bovine, flat, grain - closed circle, corium - open circle, ; e) ovine cross-section cut perpendicular to backbone; f) bovine cross-section cut perpendicular to backbone. Trend lines indicate significant relationships.

10.4.1.3 Tensile Strength

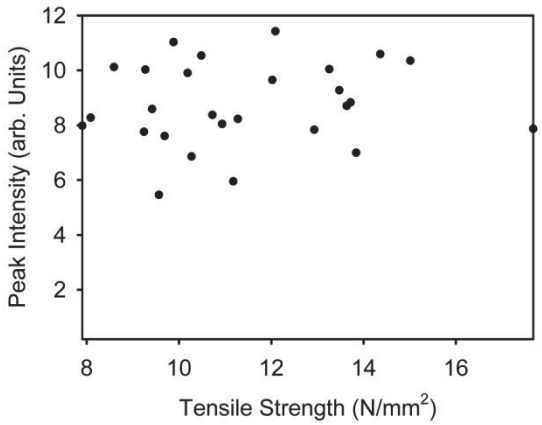

Figure 10.12: Amount of collagen determined from the intensity of the primary collagen *d* spacing peak (at around 0.059–0.060 $Å^{-1}$) versus tensile strength.

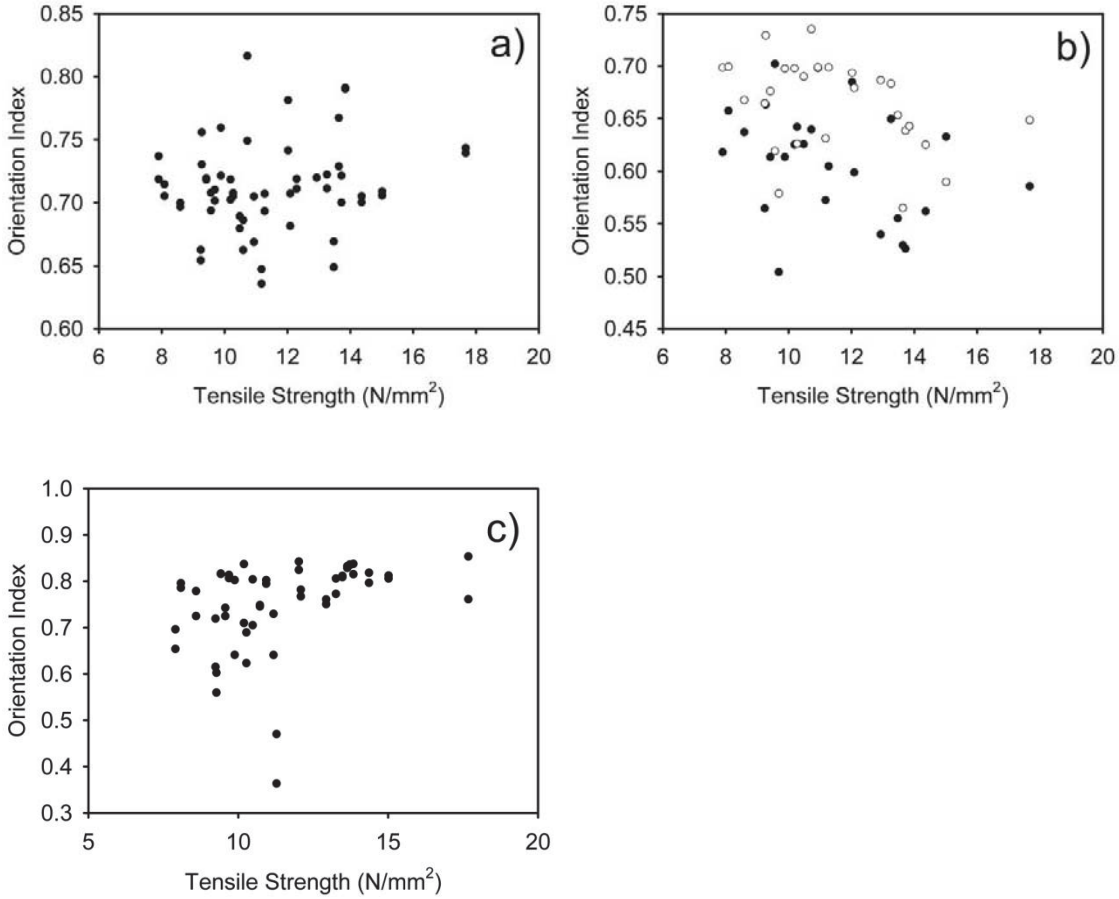

Figure 10.13: Orientation index versus tensile strength for OSP samples of leather. a) Ovine cross-section cut parallel to backbone; b) ovine, flat, grain - closed circle, corium - open circle, and c) ovine cross-section cut perpendicular to backbone.

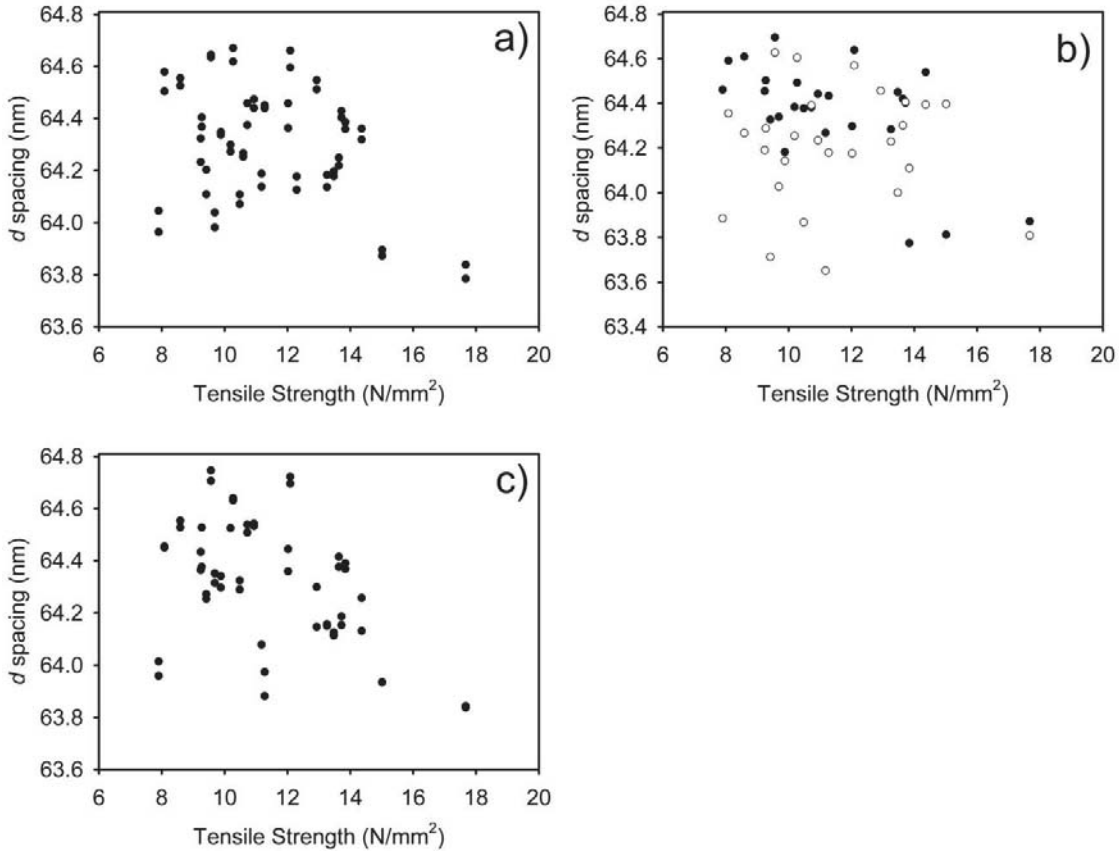

Figure 10.14: *d* spacing versus tensile strength for OSP samples of leather. a) Ovine cross-section cut parallel to backbone; b) ovine, flat, grain - closed circle, corium - open circle, and c) ovine cross-section cut perpendicular to backbone.

10.4.1.4 Tensile Extension

There is a statistically significant relationship between tensile extension and the average amount of fibrillar collagen (Figure 10.15). A linear regression analysis of the results produced a slope of 3.511 arb. Units/%, $r^2 = 0.147$ and $P = 0.048$

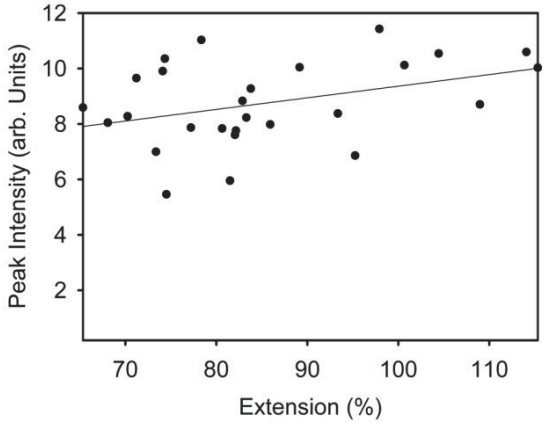

Figure 10.15: Amount of collagen determined from the intensity of the primary collagen *d* spacing peak (at around 0.059–0.060 $Å^{-1}$) versus tensile extension.

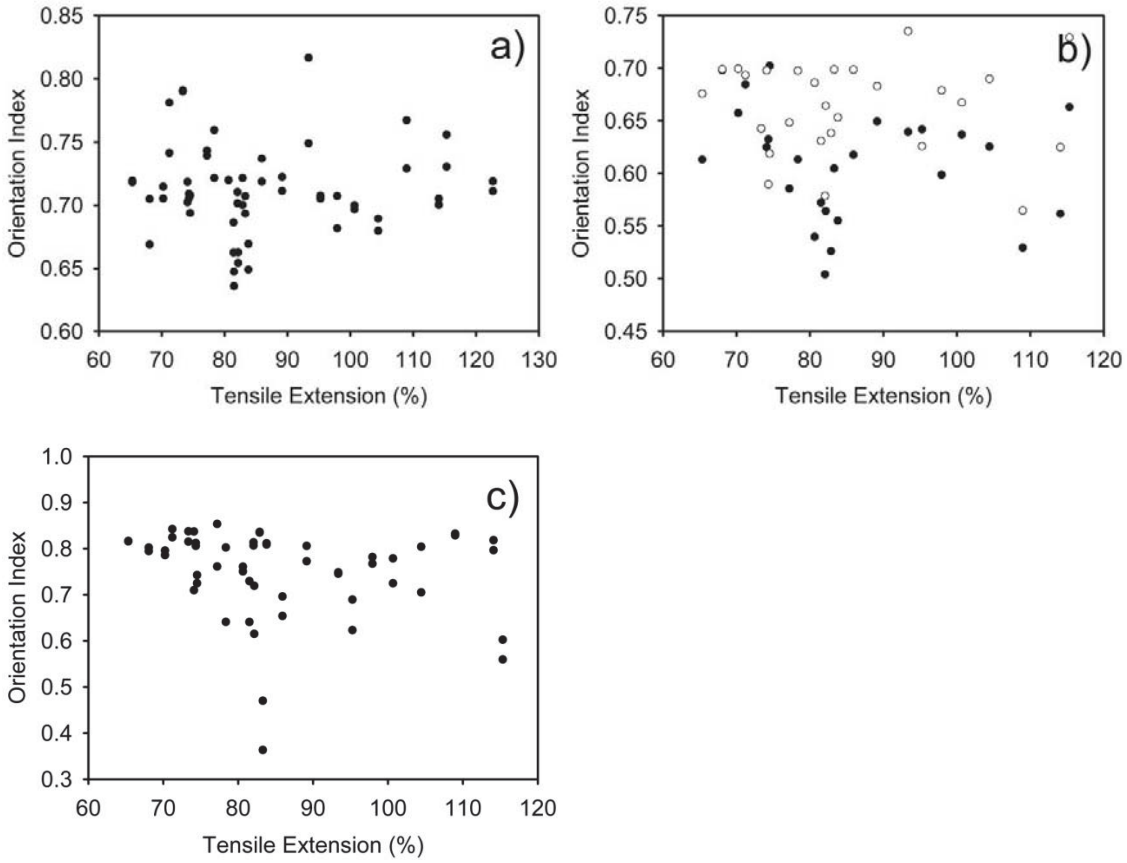

Figure 10.16: Orientation index versus tensile extension for OSP samples of leather. a) Ovine cross-section cut parallel to backbone; b) ovine, flat, grain - closed circle, corium - open circle, and c) ovine cross-section cut perpendicular to backbone.

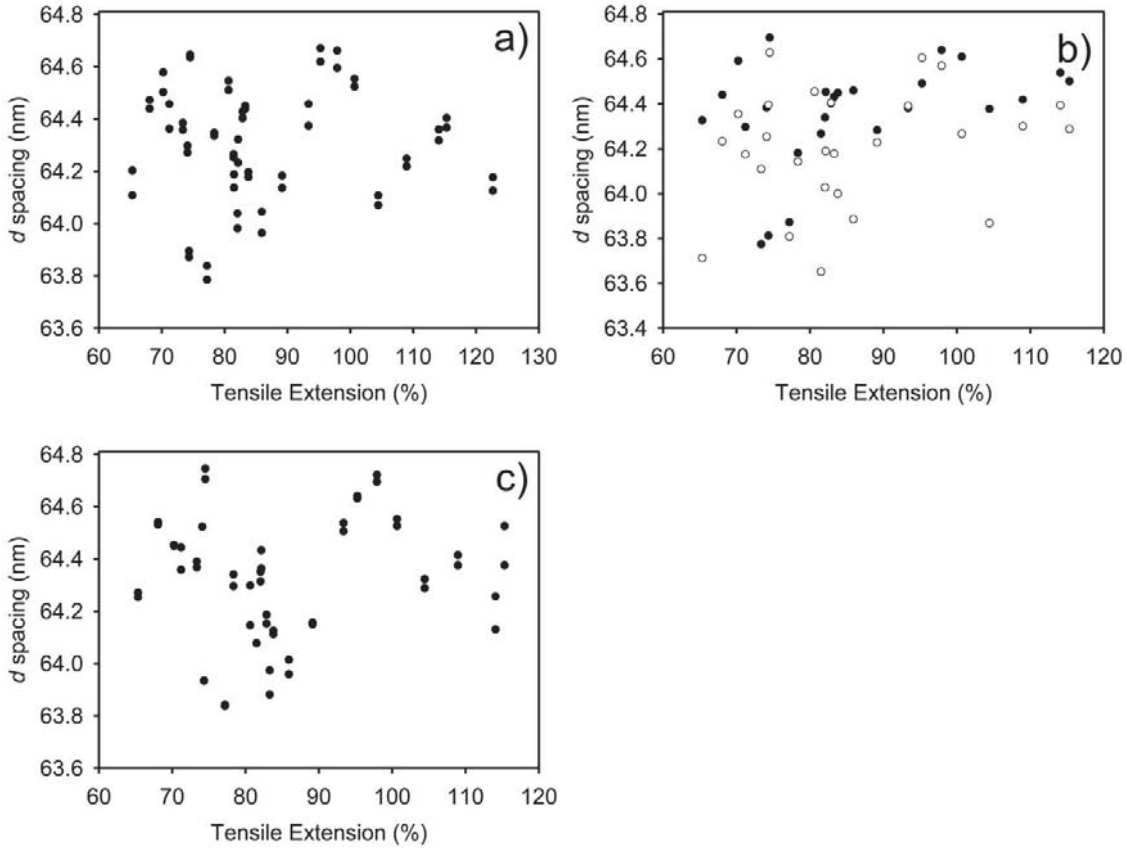

Figure 10.17: *d* spacing versus tensile extension for OSP samples of leather. a) Ovine cross-section cut parallel to backbone; b) ovine, flat, grain - closed circle, corium - open circle, and c) ovine cross-section cut perpendicular to backbone.

10.4.2 Extra Data Relating to Chapter 7

Table 10.16: Information on stretched cross-sectional samples cut from the OSP parallel to the backbone.

SAXS Skin No	Skin Type (Species)	Thickness Mm	Absolute strength N	Relative strength N/mm	Tensile Force N/mm²	Tensile Extension %	Sample No.
1	Ovine	1.20	24.69	20.34	9.69	82.05	198
3	Ovine	1.77	35.01	19.81	9.24	82.15	199
4	Ovine	1.30	24.50	18.90	10.48	104.44	200
6	Ovine	1.21	46.66	38.74	13.72	82.87	201
11	Ovine	1.21	51.52	42.57	13.64	108.97	202
17	Ovine	1.23	21.90	17.78	8.09	70.24	206
18	Ovine	1.25	26.45	21.17	10.93	68.07	207
21	Ovine	1.25	55.13	44.26	13.26	89.15	212
22	Ovine	0.96	40.86	42.53	13.84	73.36	216
35	Bovine	1.31	81.80	62.60			881
38	Bovine	1.21	69.80	57.40			887
39	Bovine	1.35	87.00	64.70			890

Table 10.17: Information on stretched flat samples cut from the OSP parallel to the backbone.

SAXS Skin No	Sample Cut	Thickness Mm	Absolute strength N	Relative strength N/mm	Tensile Force N/mm²	Tensile Extension %	Sample No.
1	Grain	1.20	24.69	20.34	9.69	82.05	801
1	Corium	1.20	24.69	20.34	9.69	82.05	802
3	Grain	1.77	35.01	19.81	9.24	82.15	804
3	Corium	1.77	35.01	19.81	9.24	82.15	805
22	Grain	0.96	40.86	42.53	13.84	73.36	855
22	Corium	0.96	40.86	42.53	13.84	73.36	856
24	Grain	1.82	31.01	17.18	9.27	115.33	867
24	Corium	1.82	31.01	17.18	9.27	115.33	868

10.4.2.1 Cross-sections

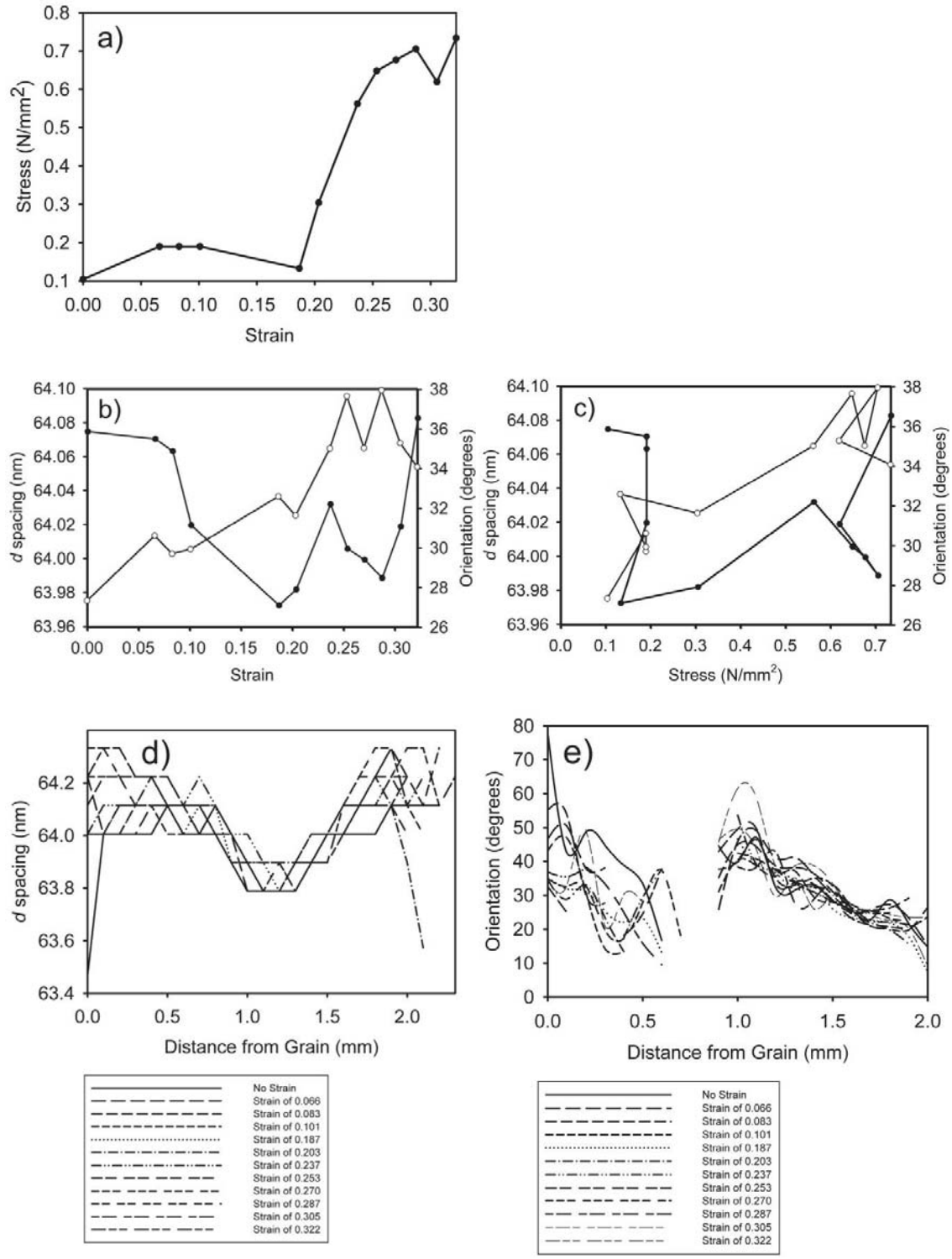

Figure 10.18: Stretching results for sample Ov198 with a tear strength of 20 N/mm a) stress versus strain; b) *d* spacing and orientation versus strain. *d* spacing: open circle; orientation: closed circle,; c) *d* spacing and orientation versus stress measured. *d* spacing: open circle; orientation: closed circle,; d) *d* spacing through the thickness of the leather and change in *d* spacing as a consequence of increasing strain; e) orientation through the thickness of the leather versus strain and change in orientation as a consequence of increasing strain.

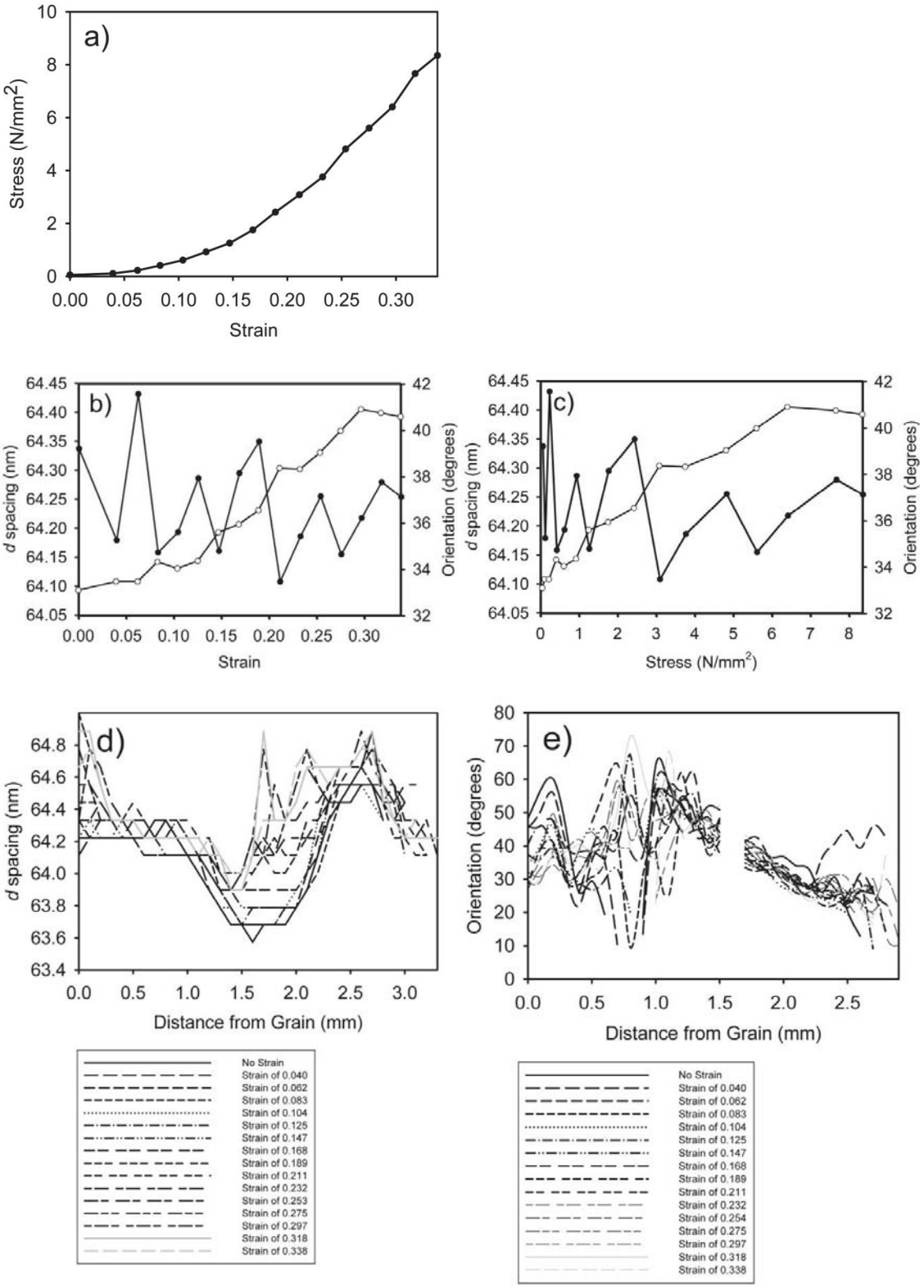

Figure 10.19: Stretching results for sample Ov199 with a tear strength of 20 N/mm a) stress versus strain; b) *d* spacing and orientation versus strain. *d* spacing: open circle; orientation: closed circle,; c) *d* spacing and orientation versus stress measured. *d* spacing: open circle; orientation: closed circle,; d) *d* spacing through the thickness of the leather and change in *d* spacing as a consequence of increasing strain; e) orientation through the thickness of the leather versus strain and change in orientation as a consequence of increasing strain.

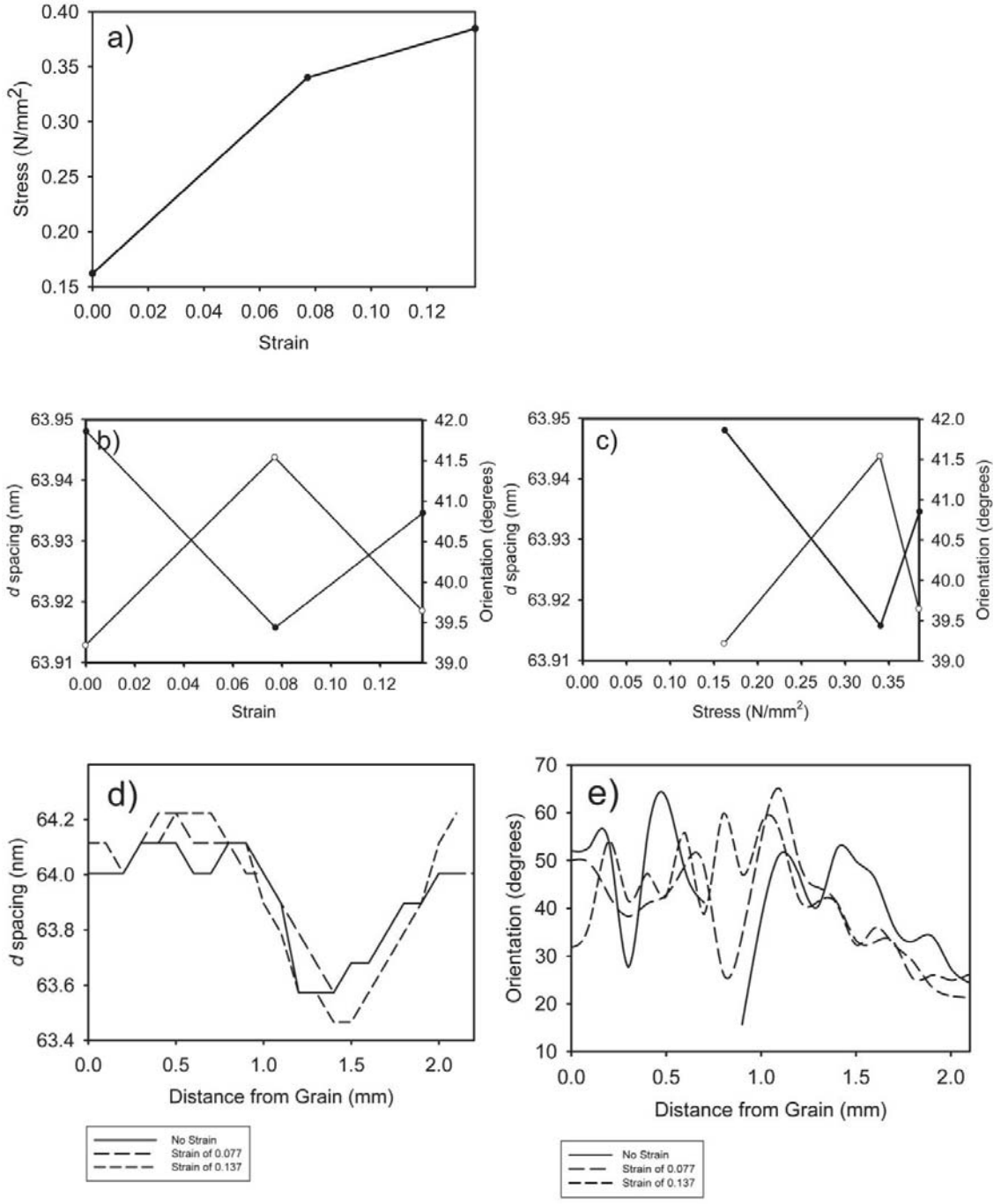

Figure 10.20: Stretching results for sample Ov200 with a tear strength of 19 N/mm a) stress versus strain; b) *d* spacing and orientation versus strain. *d* spacing: open circle; orientation: closed circle,; c) *d* spacing and orientation versus stress measured. *d* spacing: open circle; orientation: closed circle,; d) *d* spacing through the thickness of the leather and change in *d* spacing as a consequence of increasing strain; e) orientation through the thickness of the leather versus strain and change in orientation as a consequence of increasing strain.

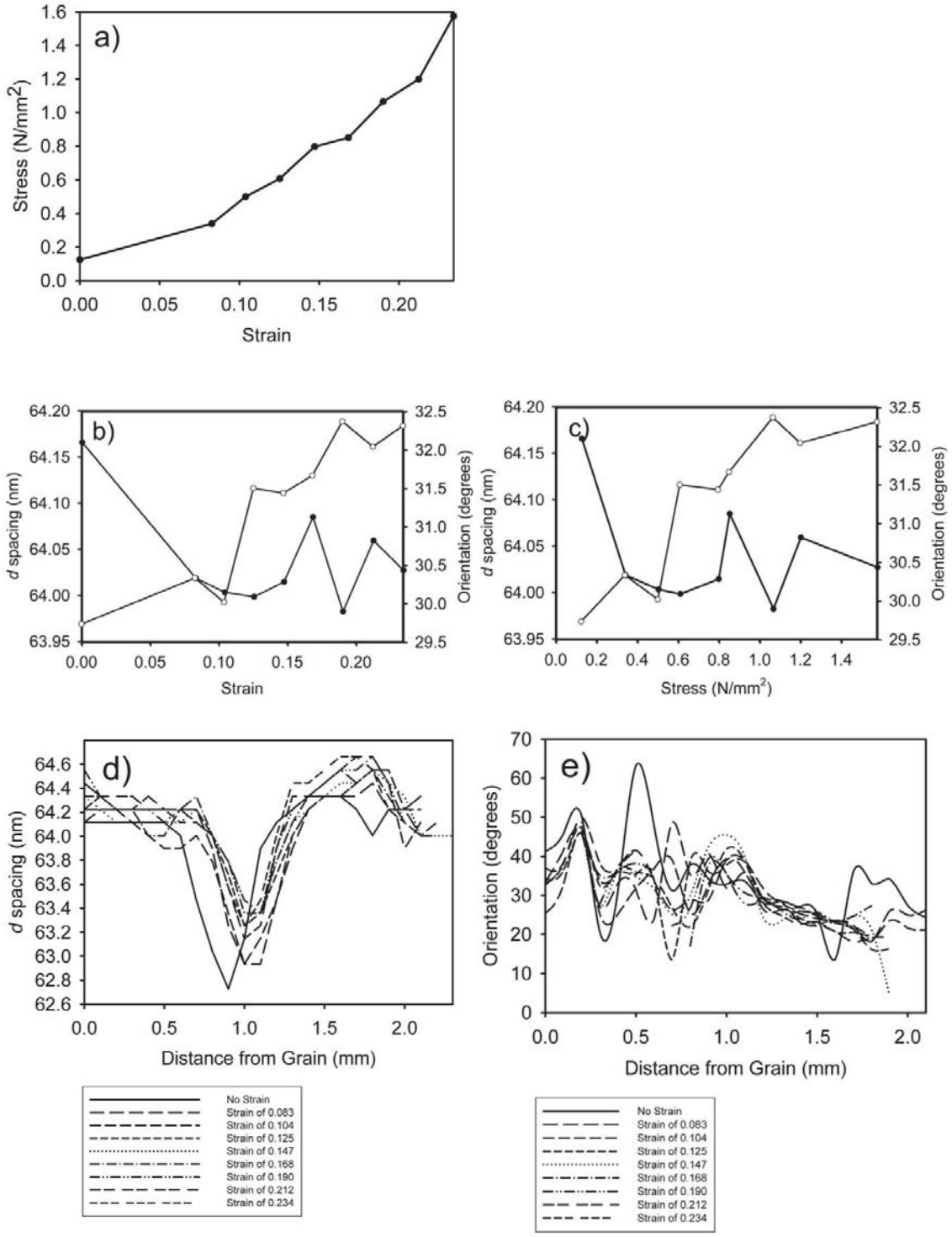

Figure 10.21: Stretching results for sample Ov201 with a tear strength of 39 N/mm a) stress versus strain; b) *d* spacing and orientation versus strain. *d* spacing: open circle; orientation: closed circle,; c) *d* spacing and orientation versus stress measured. *d* spacing: open circle; orientation: closed circle,; d) *d* spacing through the thickness of the leather and change in *d* spacing as a consequence of increasing strain; e) orientation through the thickness of the leather versus strain and change in orientation as a consequence of increasing strain.

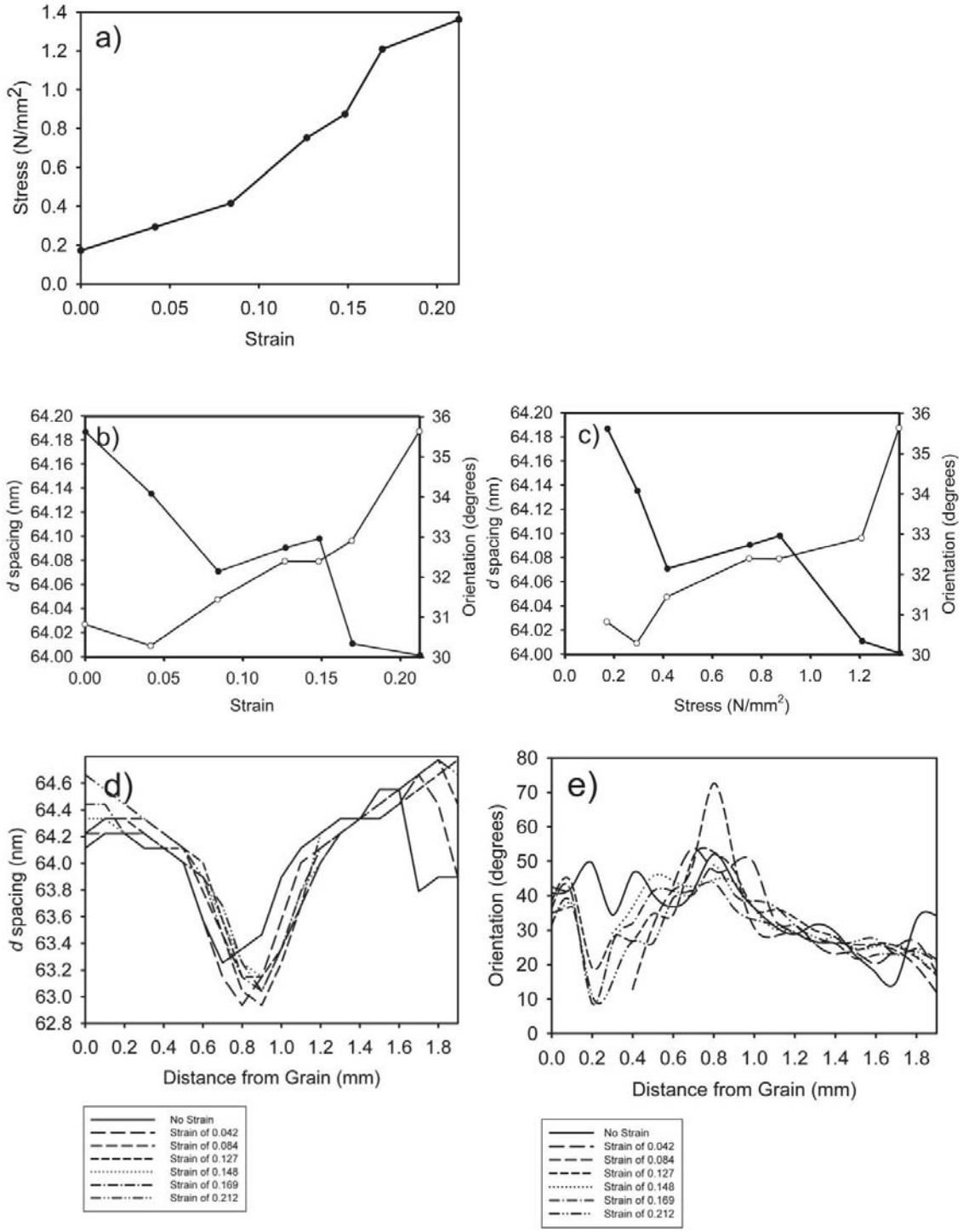

Figure 10.22: Stretching results for sample Ov202 with a tear strength of 43 N/mm a) stress versus strain; b) *d* spacing and orientation versus strain. *d* spacing: open circle; orientation: closed circle,; c) *d* spacing and orientation versus stress measured. *d* spacing: open circle; orientation: closed circle,; d) *d* spacing through the thickness of the leather and change in *d* spacing as a consequence of increasing strain; e) orientation through the thickness of the leather versus strain and change in orientation as a consequence of increasing strain.

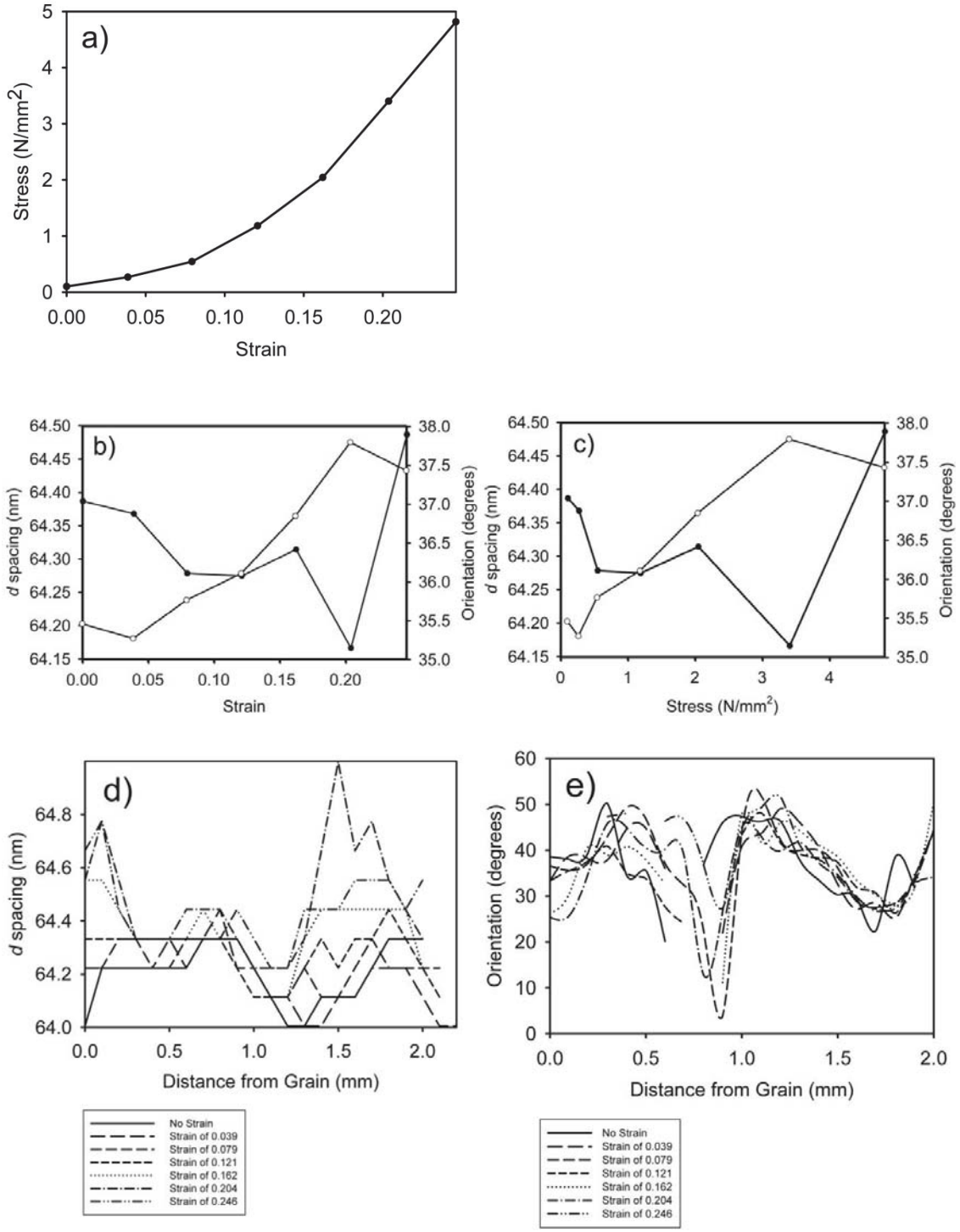

Figure 10.23: Stretching results for sample Ov206 with a tear strength of 18 N/mm a) stress versus strain; b) *d* spacing and orientation versus strain. *d* spacing: open circle; orientation: closed circle,; c) *d* spacing and orientation versus stress measured. *d* spacing: open circle; orientation: closed circle,; d) *d* spacing through the thickness of the leather and change in *d* spacing as a consequence of increasing strain; e) orientation through the thickness of the leather versus strain and change in orientation as a consequence of increasing strain.

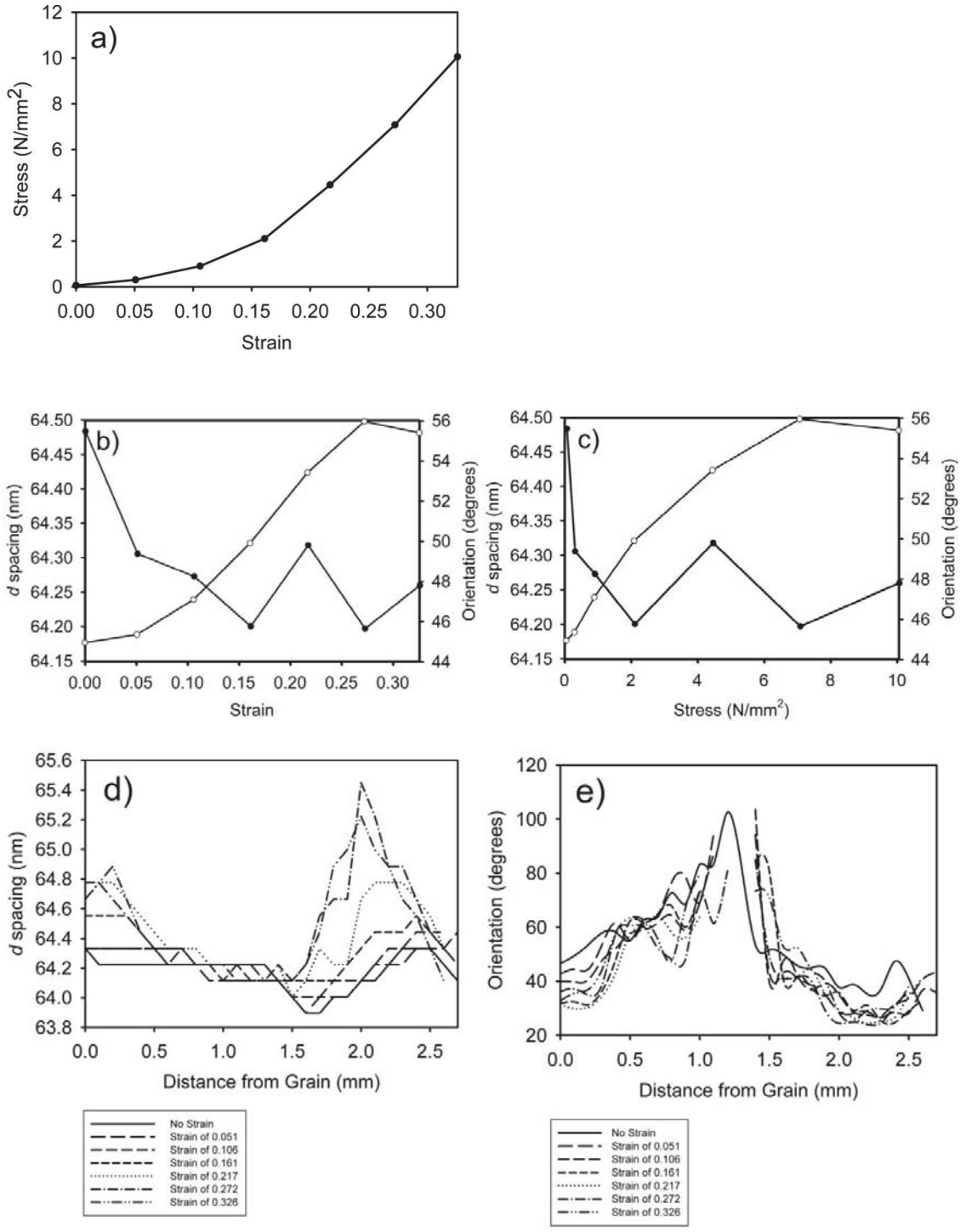

Figure 10.24: Stretching results for sample Ov207 with a tear strength of 21 N/mm a) stress versus strain; b) *d* spacing and orientation versus strain. *d* spacing: open circle; orientation: closed circle,; c) *d* spacing and orientation versus stress measured. *d* spacing: open circle; orientation: closed circle,; d) *d* spacing through the thickness of the leather and change in *d* spacing as a consequence of increasing strain; e) orientation through the thickness of the leather versus strain and change in orientation as a consequence of increasing strain.

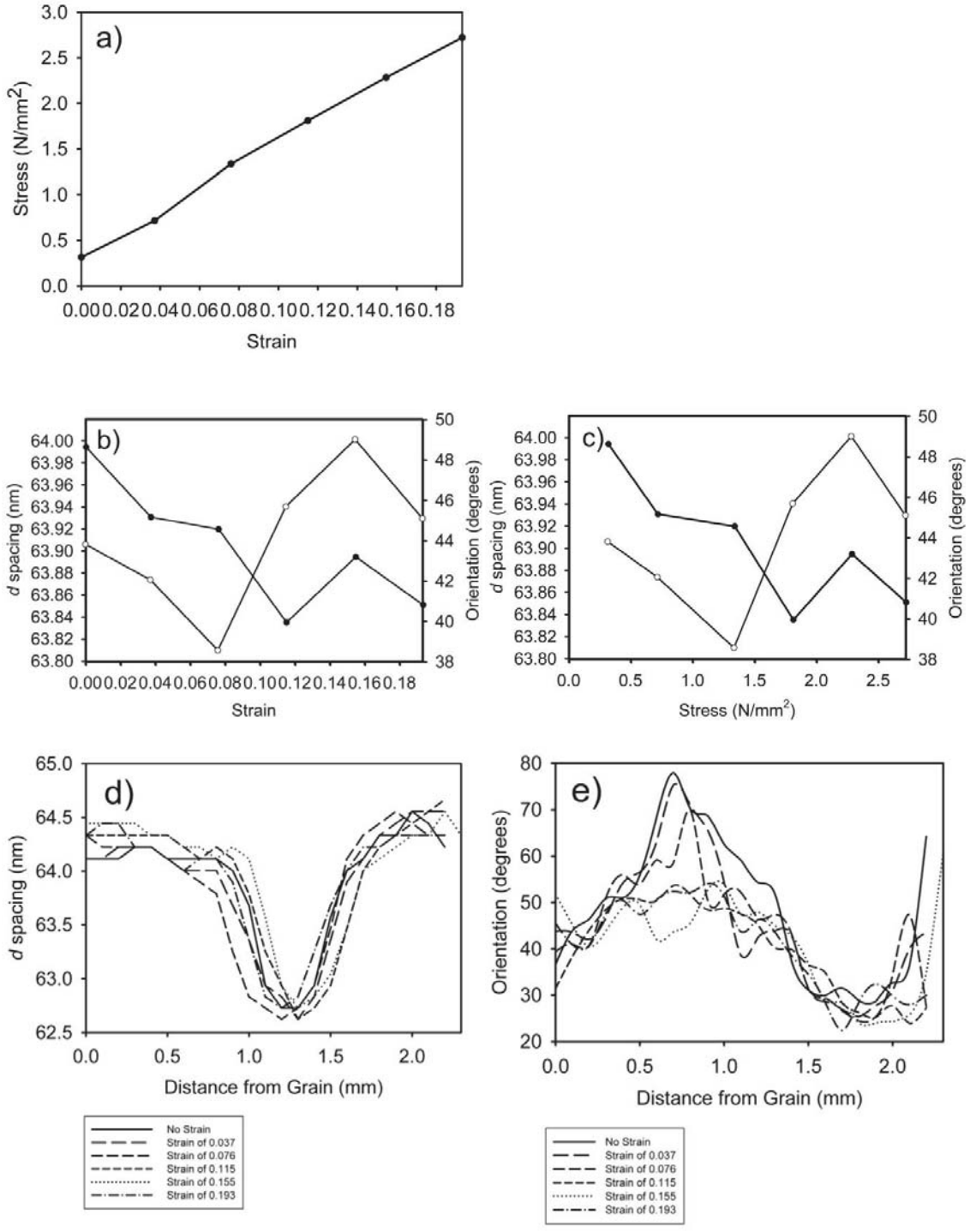

Figure 10.25: Stretching results for sample Ov212 with a tear strength of 44 N/mm a) stress versus strain; b) *d* spacing and orientation versus strain. *d* spacing: open circle; orientation: closed circle,; c) *d* spacing and orientation versus stress measured. *d* spacing: open circle; orientation: closed circle,; d) *d* spacing through the thickness of the leather and change in *d* spacing as a consequence of increasing strain; e) orientation through the thickness of the leather versus strain and change in orientation as a consequence of increasing strain.

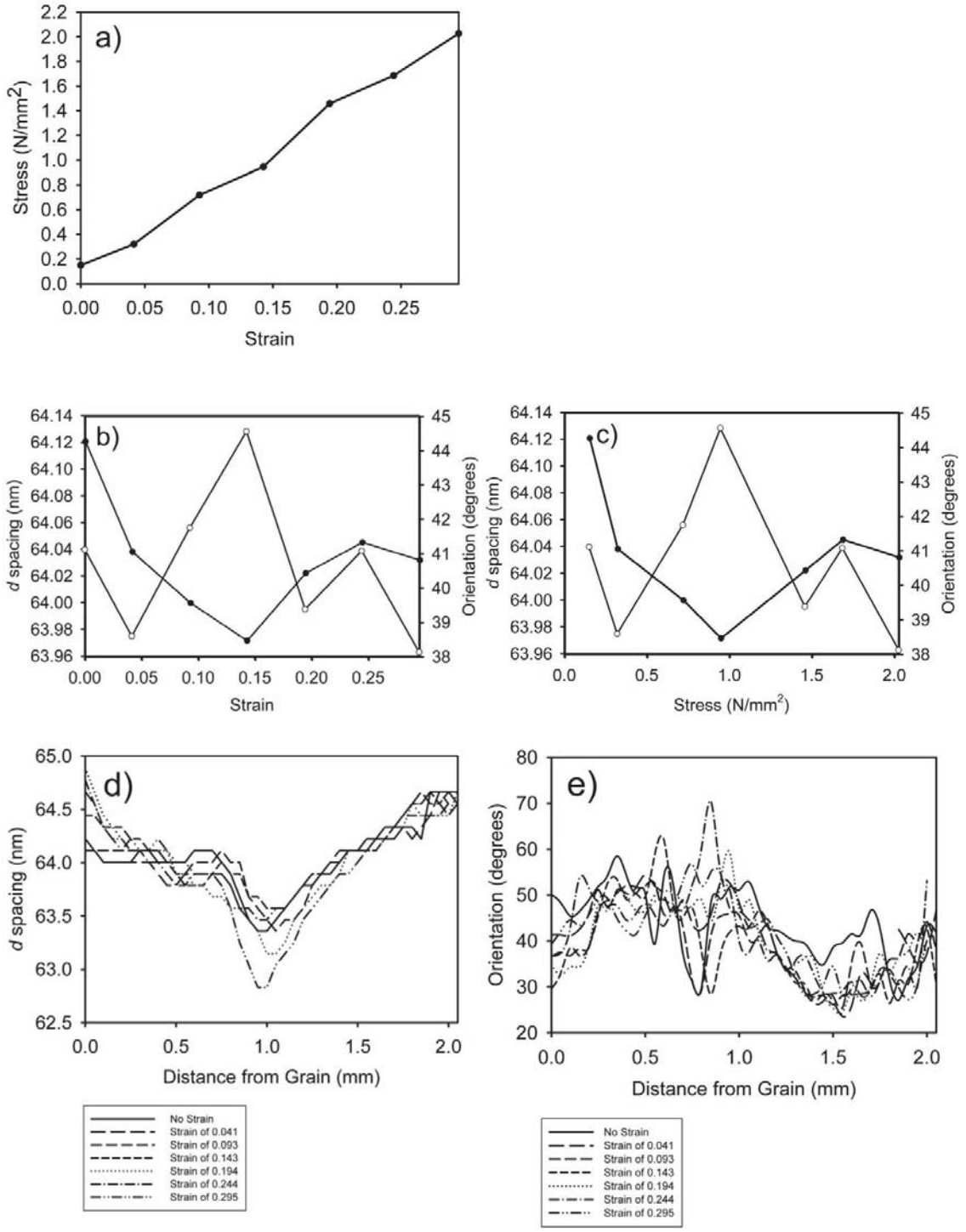

Figure 10.26: Stretching results for sample Ov216 with a tear strength of 43 N/mm a) stress versus strain; b) *d* spacing and orientation versus strain. *d* spacing: open circle; orientation: closed circle,; c) *d* spacing and orientation versus stress measured. *d* spacing: open circle; orientation: closed circle,; d) *d* spacing through the thickness of the leather and change in *d* spacing as a consequence of increasing strain; e) orientation through the thickness of the leather versus strain and change in orientation as a consequence of increasing strain.

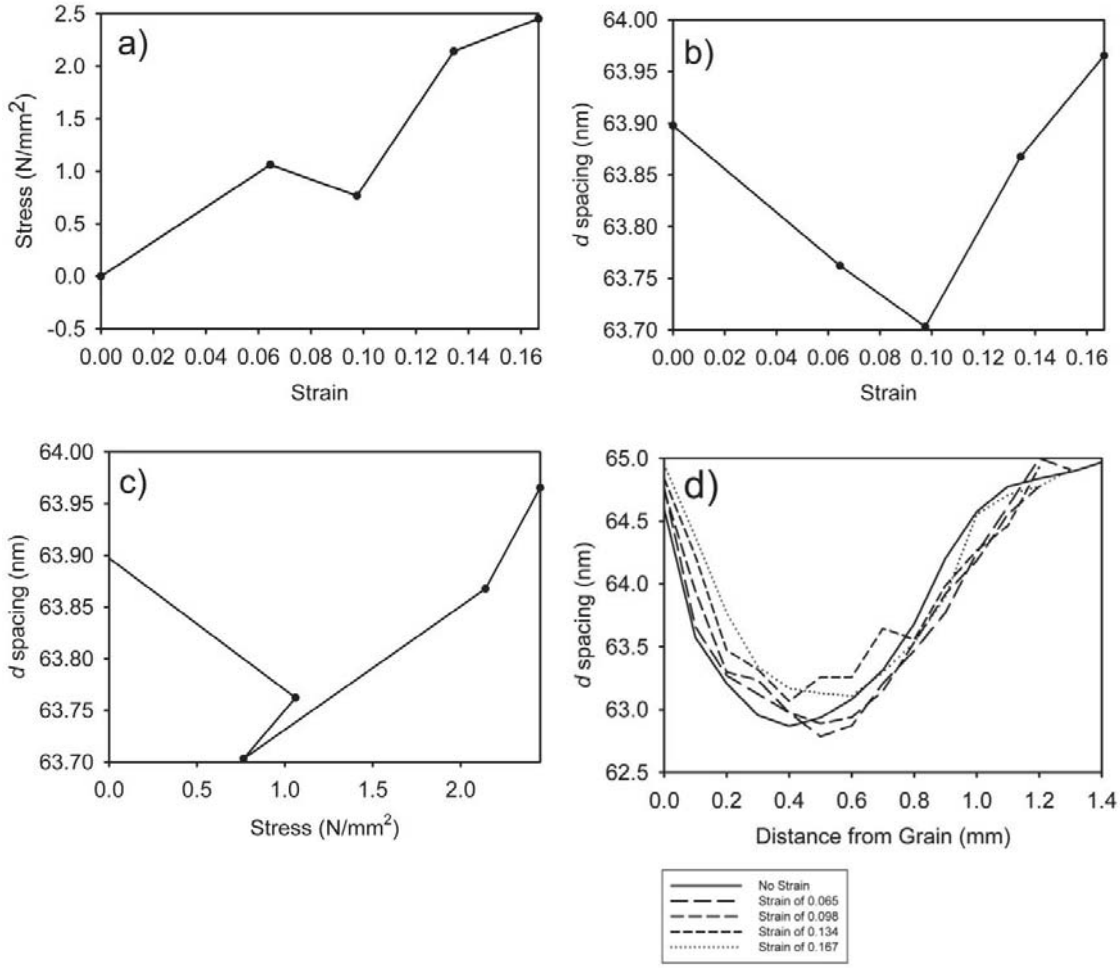

Figure 10.27: Stretching results for sample Bo881 with a tear strength of 63 N/mm a) stress versus strain; b) *d* spacing versus strain; c) *d* spacing versus stress measured; d) *d* spacing through the thickness of the leather and change in *d* spacing as a consequence of increasing strain.

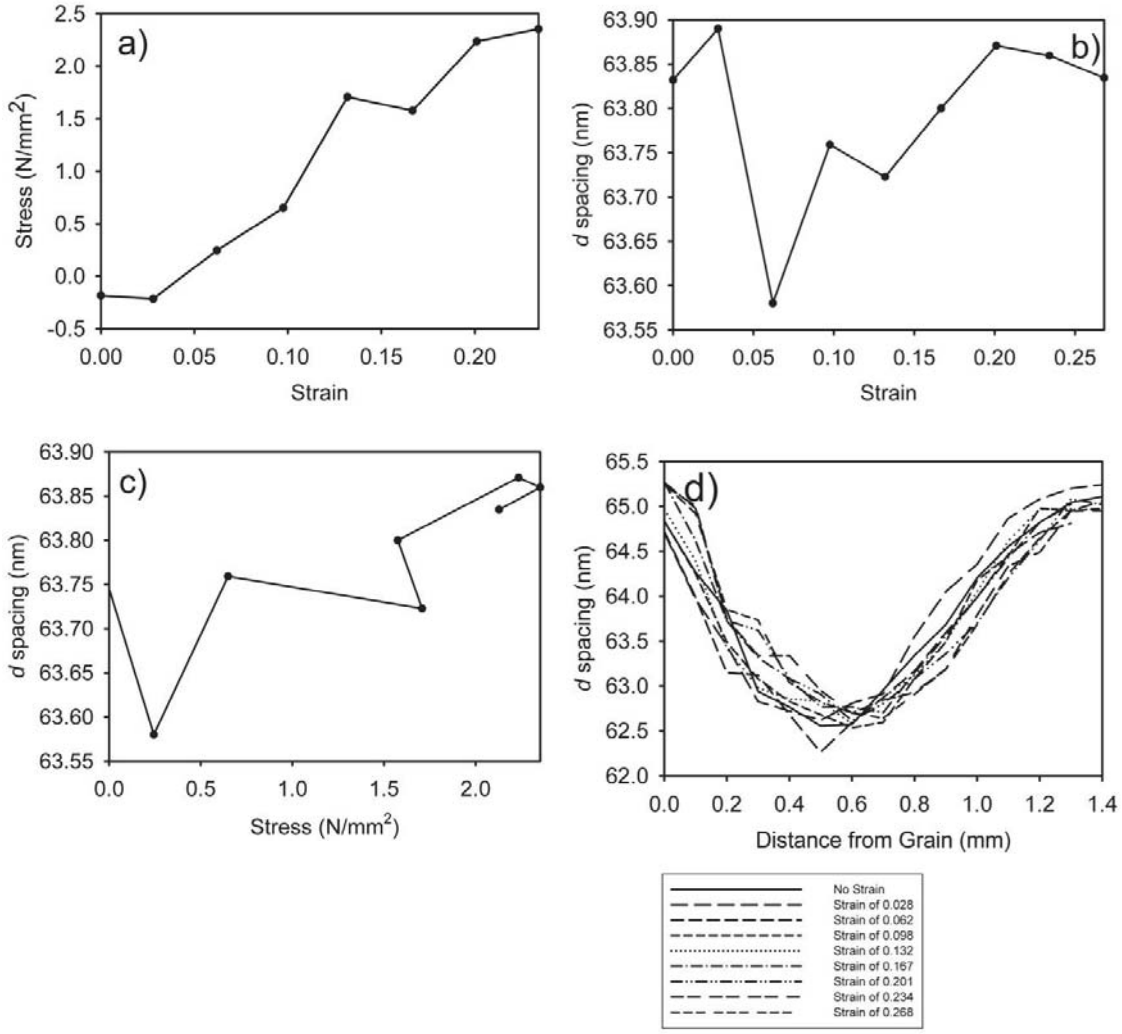

Figure 10.28: Stretching results for sample Bo887 with a tear strength of 57 N/mm a) stress versus strain; b) *d* spacing versus strain; c) *d* spacing versus stress measured; d) *d* spacing through the thickness of the leather and change in *d* spacing as a consequence of increasing strain.

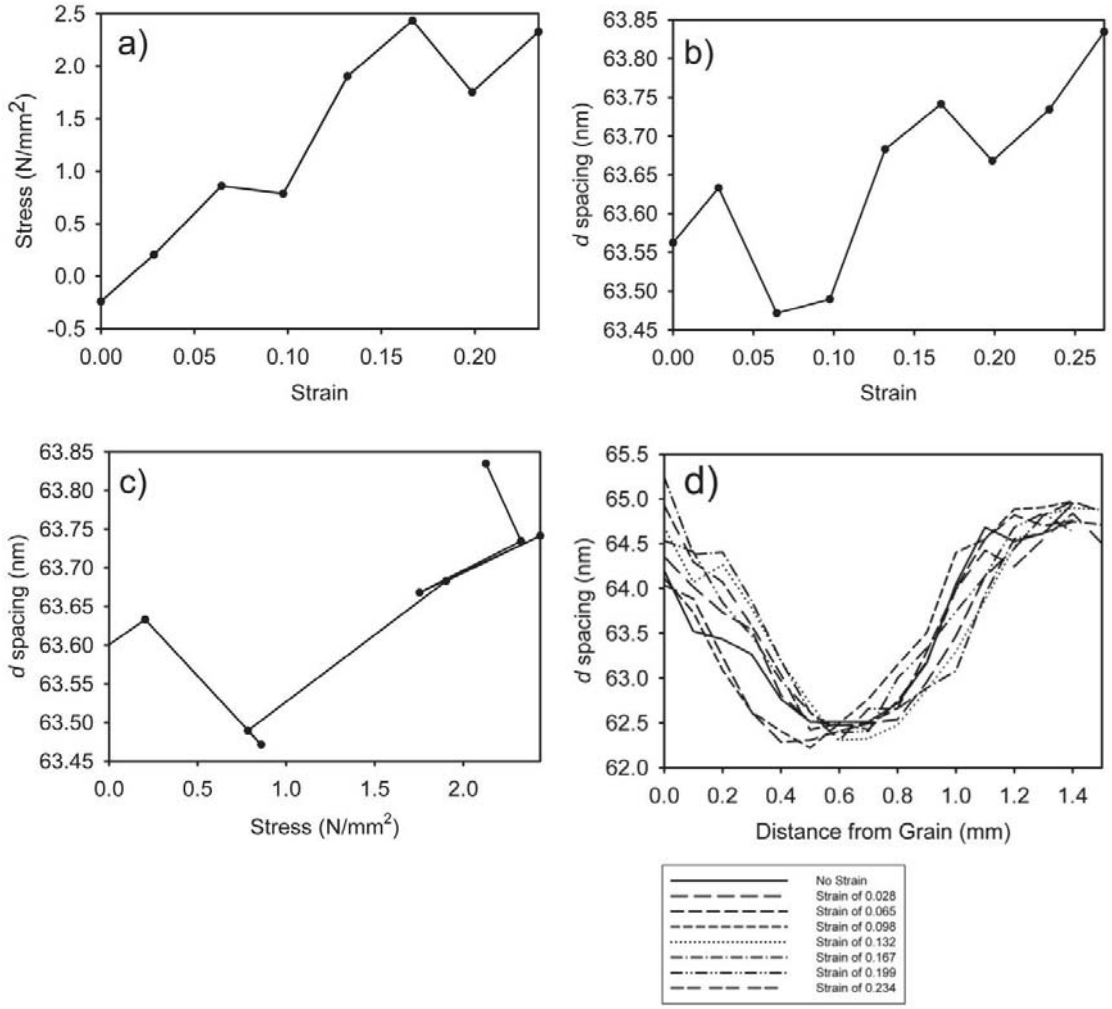

Figure 10.29: Stretching results for sample Bo887 with a tear strength of 57 N/mm a) stress versus strain; b) *d* spacing versus strain; c) *d* spacing versus stress measured; d) *d* spacing through the thickness of the leather and change in *d* spacing as a consequence of increasing strain.

10.4.2.2 Flat Samples

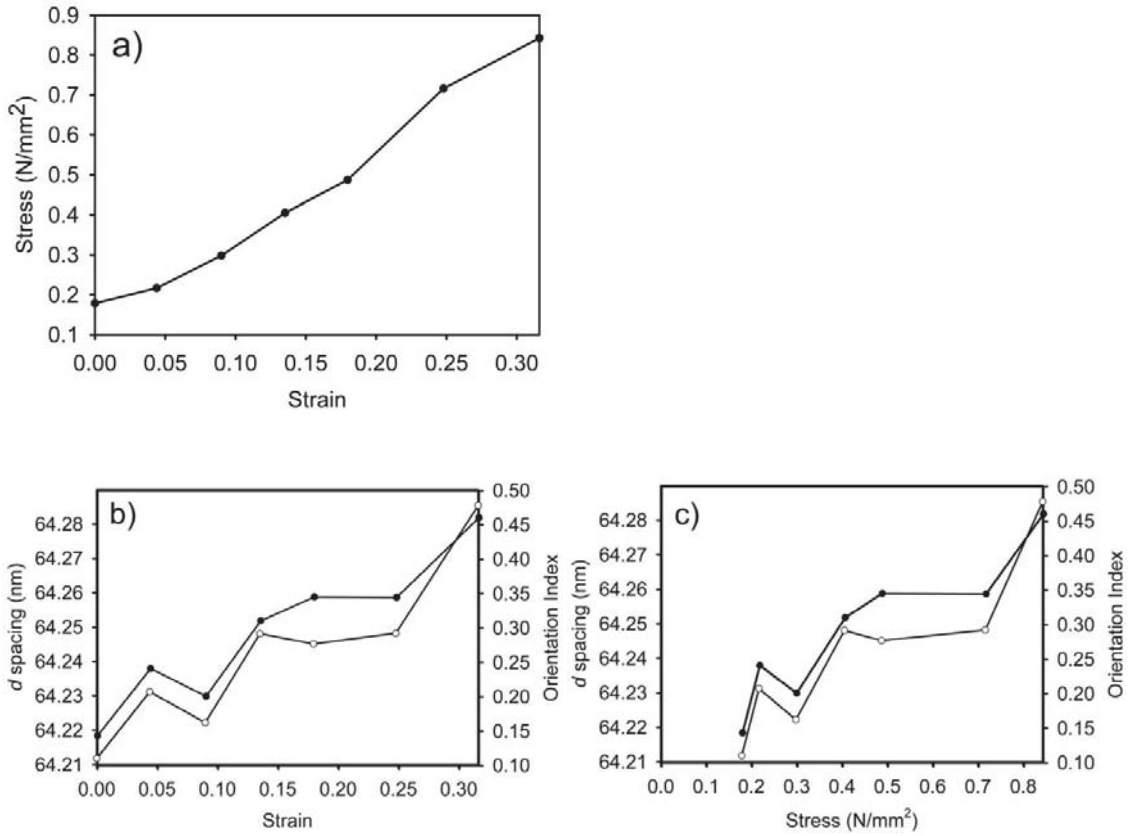

Figure 10.30: Stretching results for flat grain sample Ov801 with a tear strength of 20 N/mm a) stress versus strain; b) *d* spacing and orientation versus strain. *d* spacing: open circle; orientation: closed circle,; c) *d* spacing and orientation versus stress measured. *d* spacing: open circle; orientation: closed circle.

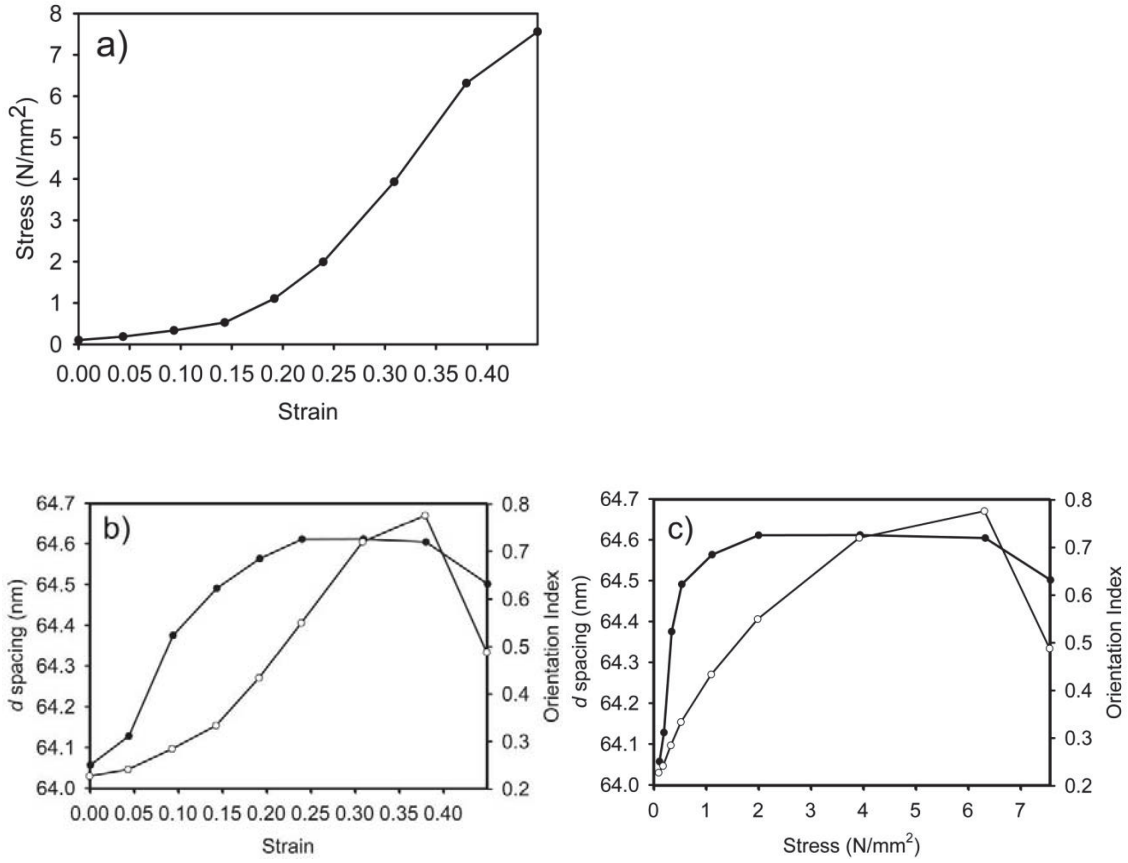

Figure 10.31: Stretching results for flat corium sample Ov802 with a tear strength of 20 N/mm a) stress versus strain; b) *d* spacing and orientation versus strain. *d* spacing: open circle; orientation: closed circle,; c) *d* spacing and orientation versus stress measured. *d* spacing: open circle; orientation: closed circle.

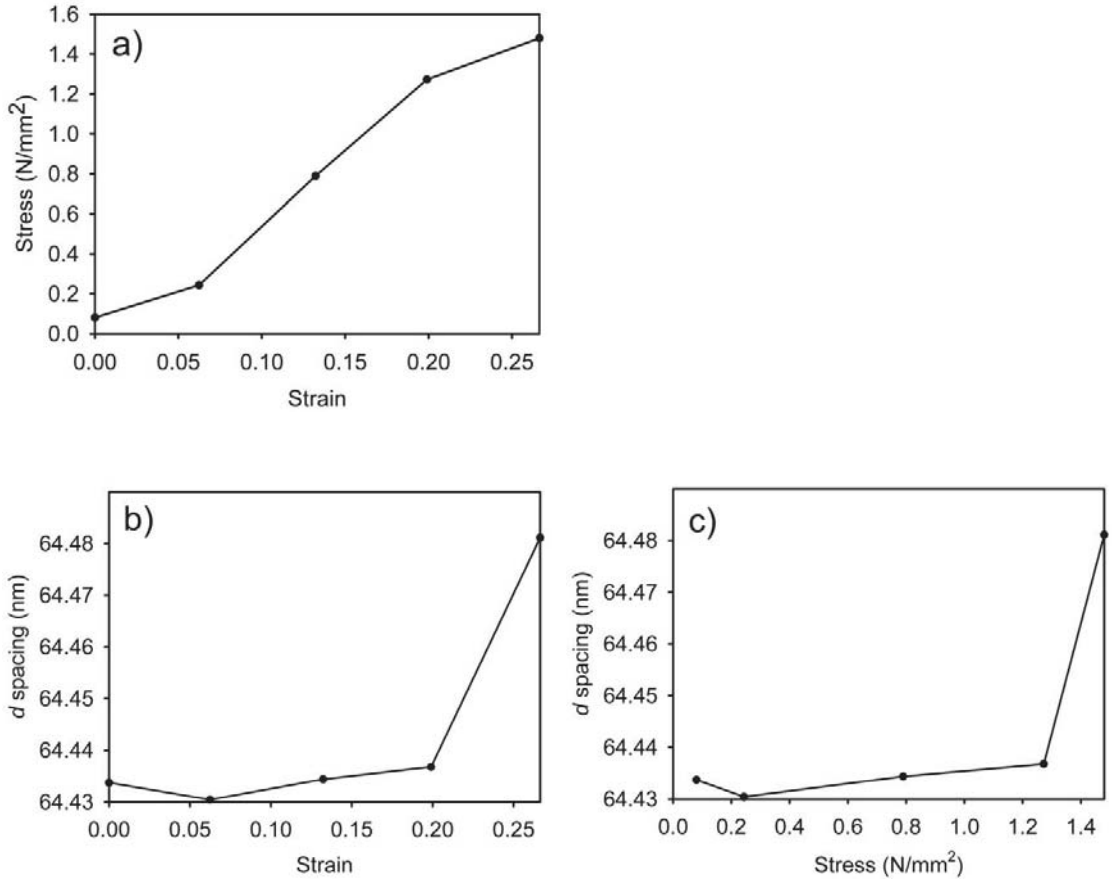

Figure 10.32: Stretching results for flat grain sample Ov804 with a tear strength of 20 N/mm a) stress versus strain; b) *d* spacing versus strain; c) *d* spacing versus stress measured.

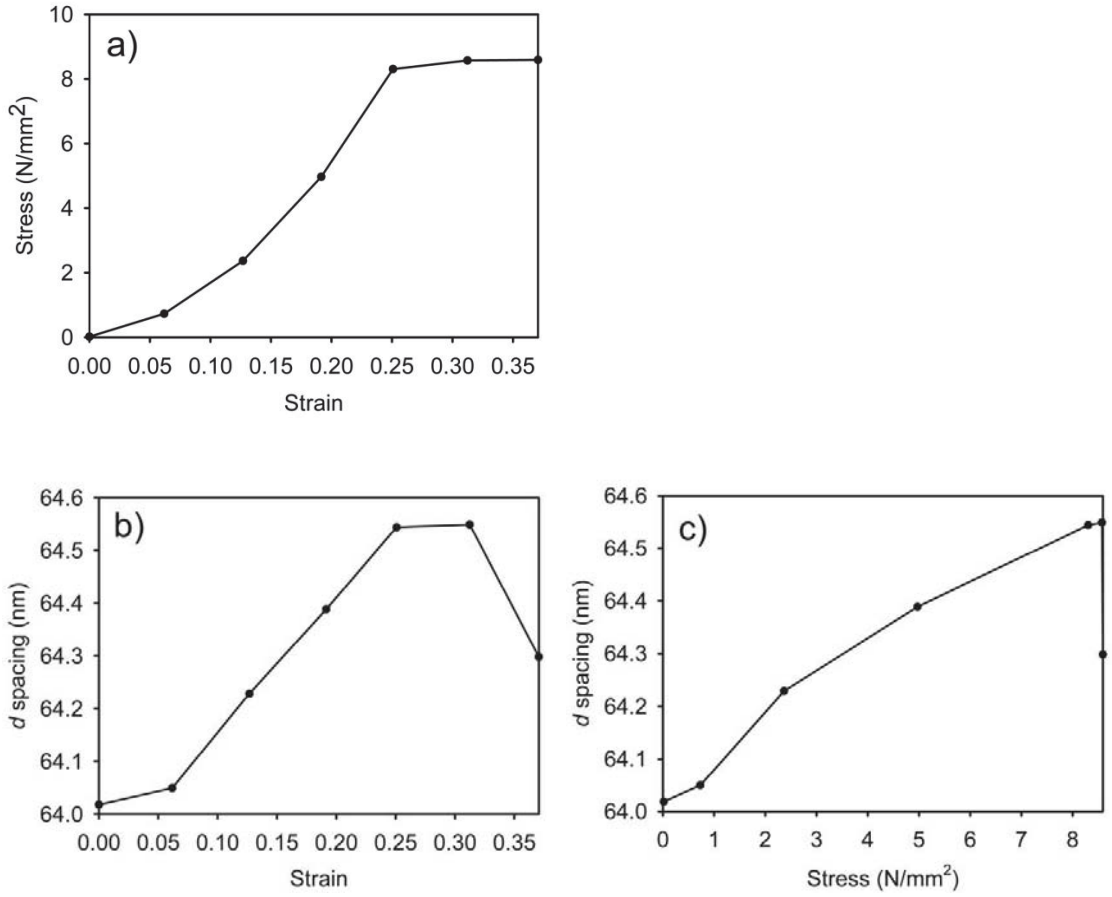

Figure 10.33: Stretching results for flat corium sample Ov805 with a tear strength of 20 N/mm a) stress versus strain; b) *d* spacing versus strain; c) *d* spacing versus stress measured.

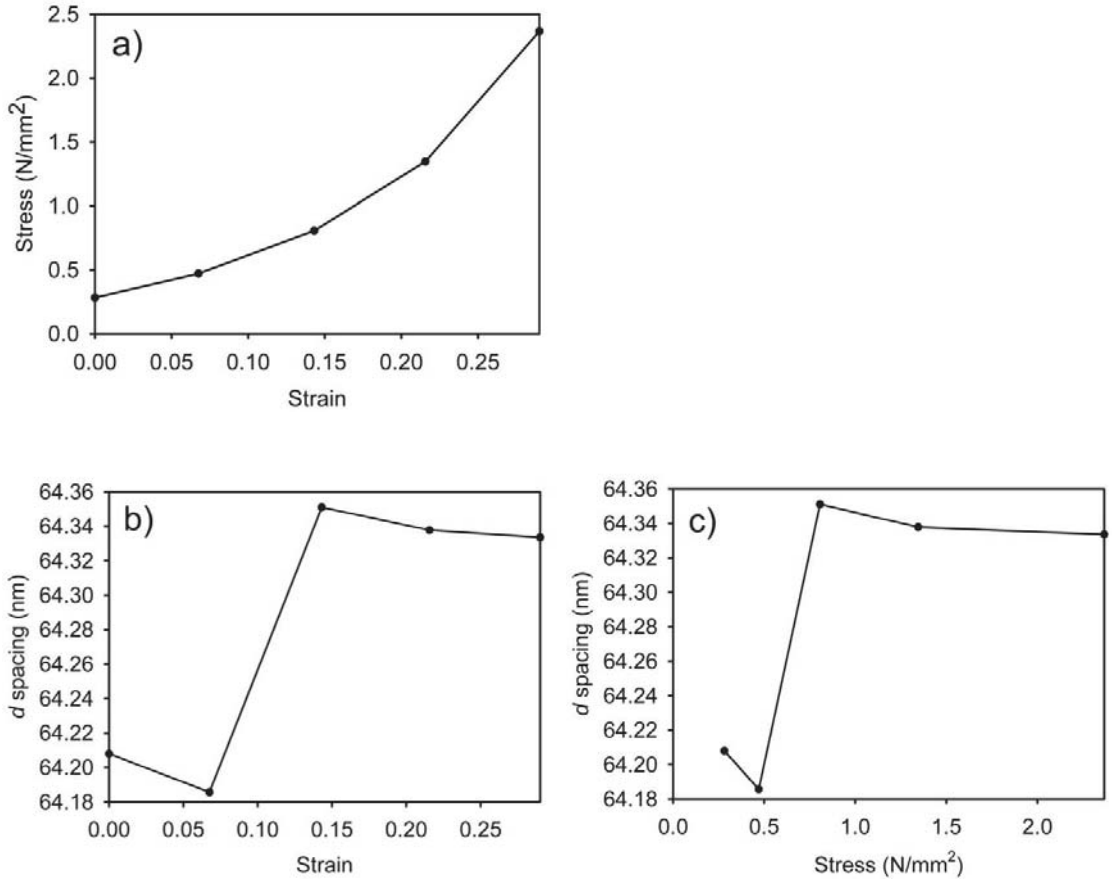

Figure 10.34: Stretching results for flat grain sample Ov855 with a tear strength of 43 N/mm a) stress versus strain; b) *d* spacing versus strain; c) *d* spacing versus stress measured.

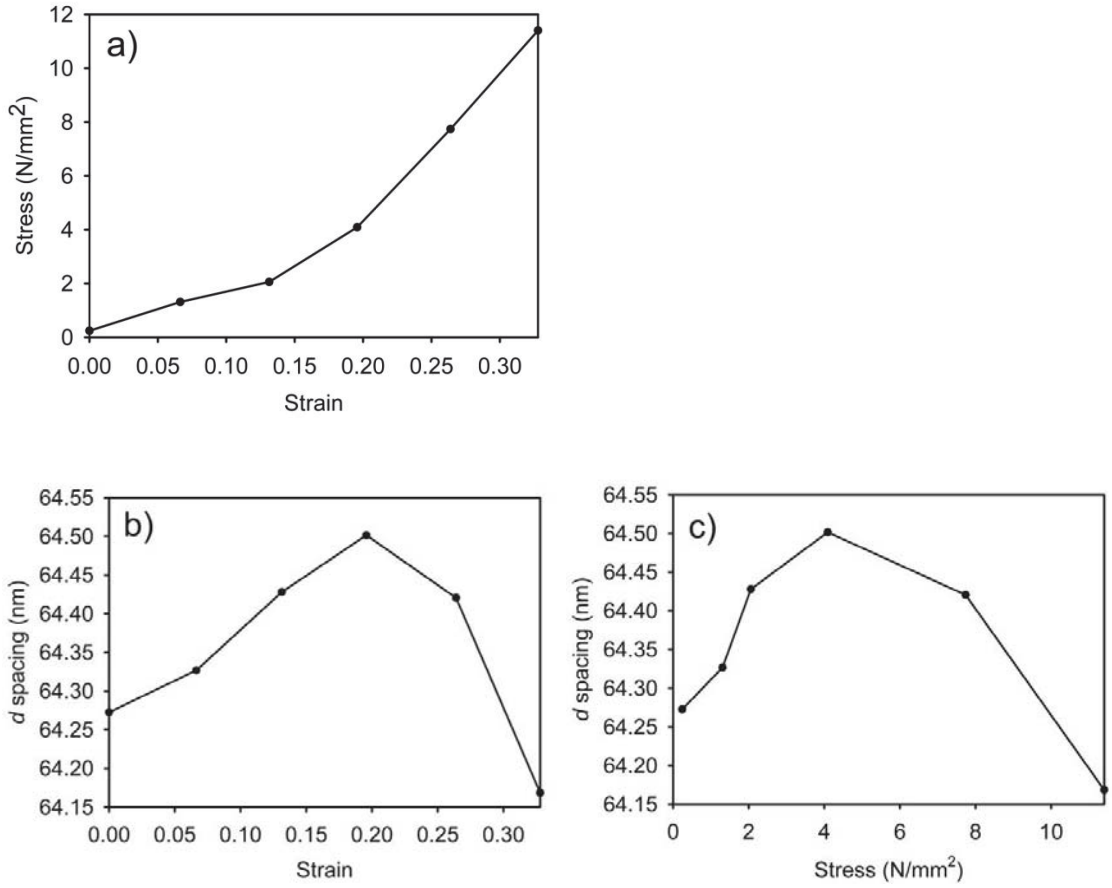

Figure 10.35: Stretching results for flat corium sample Ov856 with a tear strength of 43 N/mm a) stress versus strain; b) *d* spacing versus strain; c) *d* spacing versus stress measured.

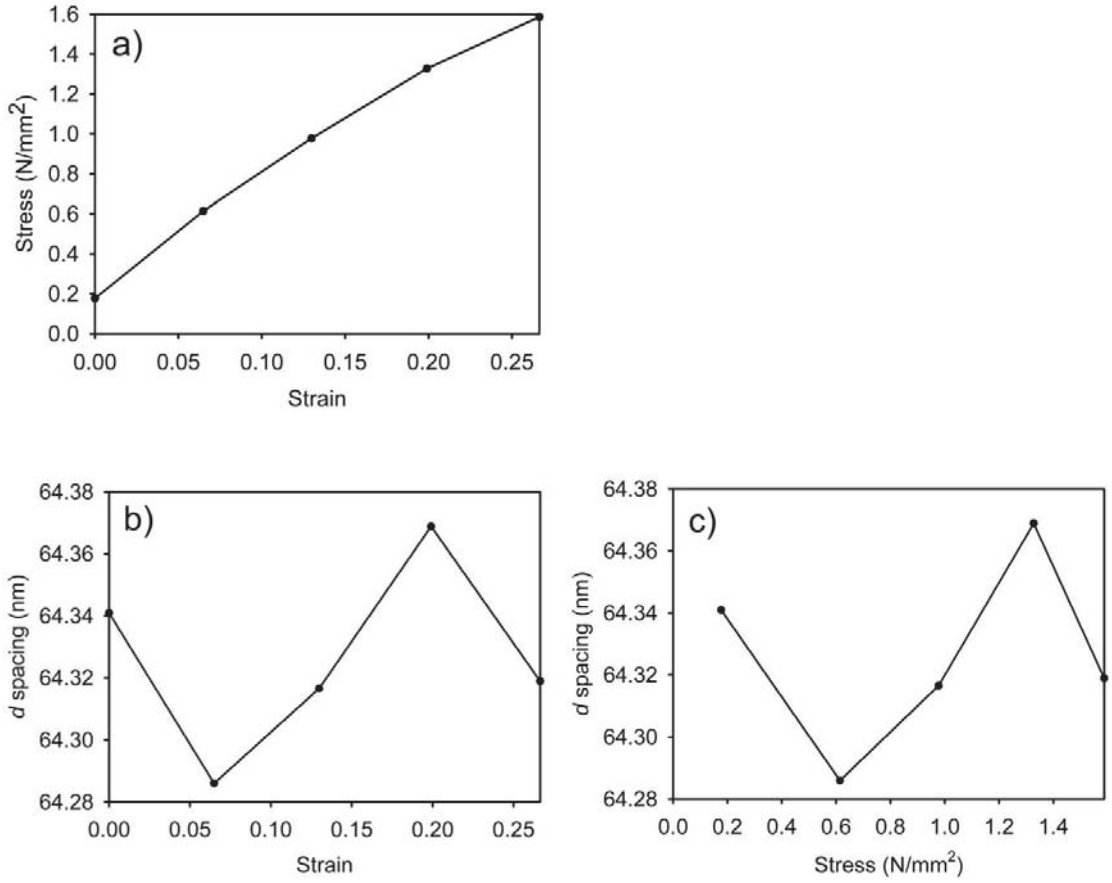

Figure 10.36: Stretching results for flat grain sample Ov867 with a tear strength of 17 N/mm a) stress versus strain; b) *d* spacing versus strain; c) *d* spacing versus stress measured.

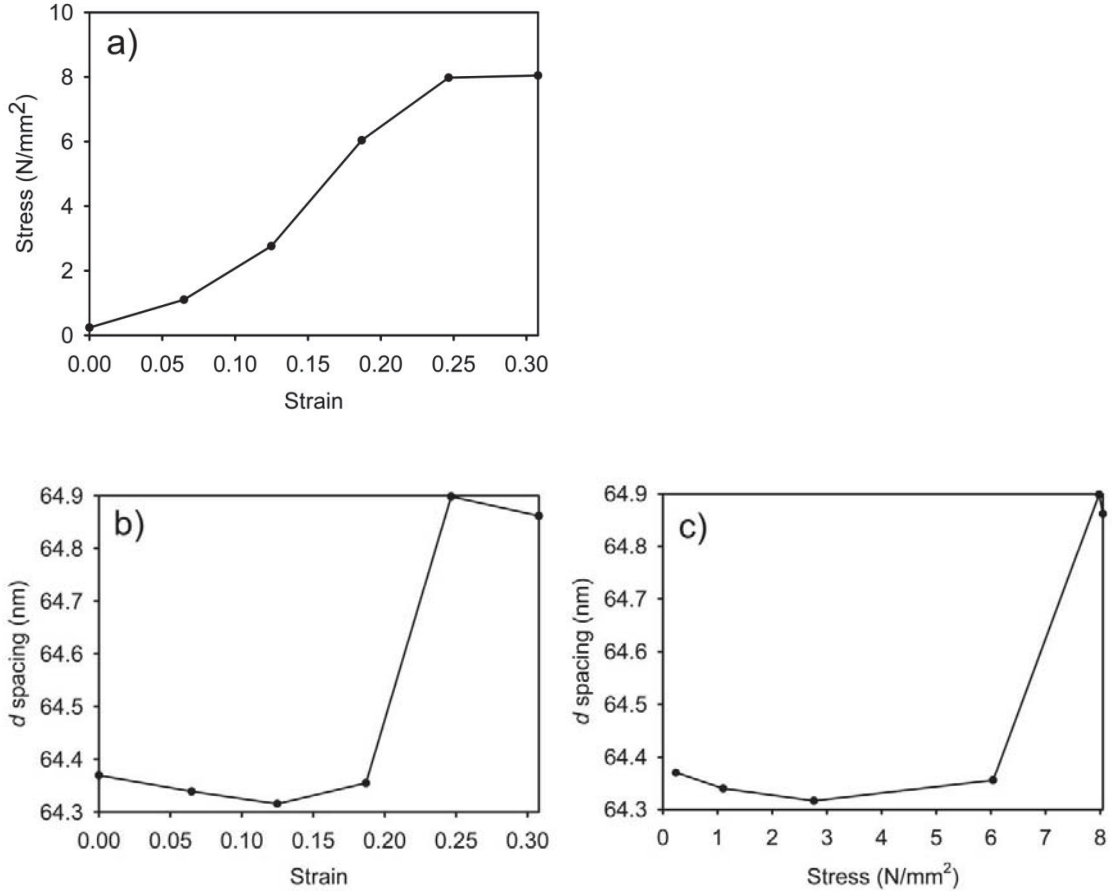

Figure 10.37: Stretching results for flat corium sample Ov868 with a tear strength of 17 N/mm a) stress versus strain; b) *d* spacing versus strain; c) *d* spacing versus stress measured.

10.4.3 Extra Data Relating to Chapter 8

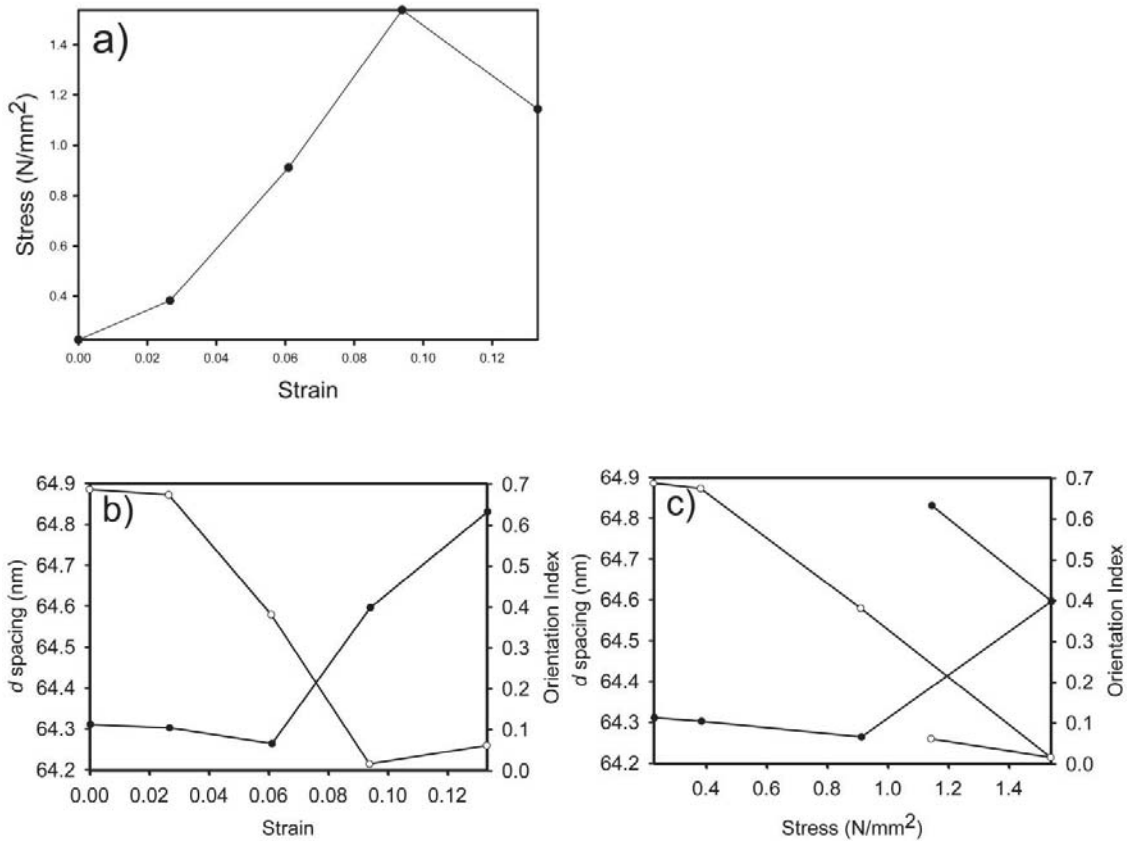

Figure 10.38: Stretching results for OFM a) stress versus strain; b) *d* spacing and orientation versus strain. *d* spacing: open circle; orientation: closed circle,; c) *d* spacing and orientation versus stress measured. *d* spacing: open circle; orientation: closed circle.

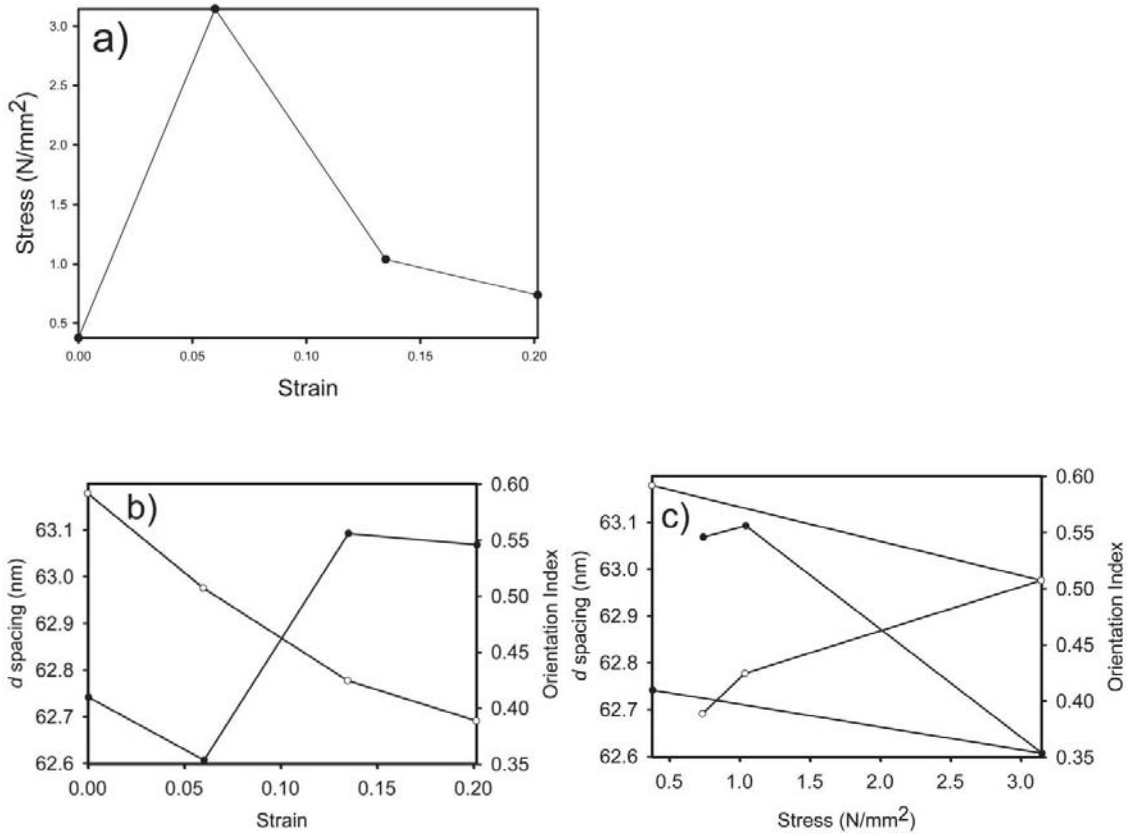

Figure 10.39: Stretching results for OFM a) stress versus strain; b) *d* spacing and orientation versus strain. *d* spacing: open circle; orientation: closed circle,; c) *d* spacing and orientation versus stress measured. *d* spacing: open circle; orientation: closed circle.

CHAPTER 11 LIST OF REFERENCES

Aebi, U., W. E. Fowler, P. Rew and T. I. Sun (1983). "The fibrillar substructure of keratin filaments unravelled." Journal of Cell Biology **97**: 1131-1143

Allsop, T., S. M. Cooper, S. DasGupta, M. Birtles, R. L. Edmonds and A. Passman (2006). "Elastin in lamb pelts - its role in leather quality." Leather International **208**(4763): 41-46.

Arumugam, V., M. D. Naresh, N. Somanathan and R. Sanjeevi (1995). "Effect of strain rate on crosslinked collagen fibres." Journal of the Society of Leather Technologists and Chemists **79**: 143-147.

Attenburrow, G. E. (1993). "The rheology of leather - a review." Journal of the Society of Leather Technologists and Chemists **77**: 107-114.

Badylak, S. F. (2007). "The extracellular matrix as a biologic scaffold material." Biomaterials **28**: 3587-3593.

Badylak, S. F., D. O. Freytes and T. W. Gilbert (2009). "Extracellular matrix as a biological scaffold material: structure and function." Acta Biomaterialia **5**: 1-13.

Bailey, A. J. and R. G. Paul (1998). "Collagen: a not so simple protein." Journal of the Society of Leather Technologists and Chemists **82**: 104-110.

Bailey, A. J., R. G. Paul and L. Knott (1998). "Mechanisms of maturation and ageing of collagen." Mechanisms of Ageing and Development **106**: 1-56.

Barlow, J. R. (1975). "Scanning Electron-Microscopy of hides, skins and leather." Journal of the American Leather Chemists Association **70**(3): 114-128.

Barrick, B., E. J. Campbell and C. A. Owen (1999). "Leukocyte proteinases in wound healing: roles in physiologic and pathologic processes." Wound Repair and Regeneration **7**(6): 410-422.

Basil-Jones, M. M., R. L. Edmonds, G. E. Norris and R. G. Haverkamp (2012). "Collagen fibril alignment and deformation during tensile strain of leather: a small-angle X-ray scattering study." Journal of Agricultural and Food Chemistry **60**(5): 1201-1208.

Basil-Jones, M. M., R. L. Edmonds, S. M. Cooper and R. G. Haverkamp (2011). "Collagen fibril orientation in ovine and bovine leather affects strength: a small angle X-ray (SAXS) study." Journal of Agricultural and Food Chemistry **59**: 9972-9979.

Basil-Jones, M. M., R. L. Edmonds, T. F. Allsop, S. M. Cooper, G. Holmes, G. E. Norris, D. J. Cookson, N. Kirby and R. G. Haverkamp (2010). "Leather Structure

Determination by Small-Angle X-ray Scattering (SAXS): Cross Sections of Ovine and Bovine Leather." Journal of Agricultural and Food Chemistry **58**(9): 5286-5291.

Bernado, P., E. Mylonas, M. V. Petoukhov, M. Blackledge and D. I. Svergun (2007). "Structural characterization of flexible proteins using small-angle X-ray scattering." Journal of the American Leather Chemists Association **129**(17): 5656-5664.

Birk, D. E., J. M. Fitch, J. P. Babiarz, K. J. Doane and T. F. Linsenmayer (1990). "Collagen fibrillogenesis *in vitro*: interaction of types I and V collagen regulates fibril diameter." Journal of Cell Science **95**: 649-657.

Bishop, S. M., M. Walker, A. A. Rogers and Chen, W. Y. J (2003). "Moisture balance: optimising the wound-dressing interface." Journal of Wound Care **12**: 125-128.

Boote, C., E. J. Sturrock, G. E. Attenburrow and K. M. Meek (2002). "Psuedo-affine behaviour of collagen fibres during the uniaxial deformation of leather." Journal of Materials Science **37**: 3651-3656.

Brodsky, B., E. F. Eikenberry and K. Cassidy (1980). "An unusual collagen periodicity in skin." Biochimica et Biophysica Acta **621**: 162-166.

Burger, C., H. W. Zhou, I. Sics, B. S. Hsiao, B. Chu, L. Graham and M. J. Glimcher (2008). "Small-angle X-ray scattering study of intramuscular fish bone: collagen fibril superstructure determined from equidistant meridional reflections." Journal of Applied Crystallography **41**: 252-261.

Burgeson, R. E. (1988). "New collagens, new concepts." Annual Review of Cell Biology **4**: 551-577

Cameron, G. J., I. L. Alberts, J. H. Laing and T. J. Wess (2002). "Structure of type I and type III heterotypic collagen fibrils: an X-ray diffraction study." Journal of Structural Biology **137**: 15-22.

Cedola, A., M. Mastrogiacomo, M. Burghammer, V. Komlev, P. Giannoni, A. Favia, R. Cancedda, F. Rustichelli and S. Lagomarsino (2006). "Engineered bone from bone marrow stromal cells: A structural study by an advanced X-ray microdiffraction technique." Physics in Medicine and Biology **51**(6): N109-N116.

Chan, Y., G. M. Cox, R. G. Haverkamp and J. M. Hill (2009). "Mechanical model for a collagen fibril pair in extracellular matrix." European Biophysics Journal **38**(4): 487-493.

Costa, M., N. Benseny-Cases, M. Cócera, C.V. Teixeira, M. Alsina, J. Cladera, O. López, M. Fernández and M. Sabés (2009) "Diagnosis Applications of Non-Crystalline Diffraction of Collagen Fibres: Breast Cancer and Skin Diseases." Lecture Notes in Physics Volume **776**: 265-280.

Covington, A. D., G. S. Lampard, O. Menders, A. V. Chadwick, G. Rafeletos and P. O'Brien (2001). "Extanded X-ray absorption fine structure studies of the role of chromium in leather tanning." Polyhedron **20**: 461-466.

Craig, A. S. and D. A. D. Parry (1981). "Growth and development of collagen fibrils in immature tissues from rat and sheep." Proceedings of the Royal Society B **212**(1186): 85-92.

Crapo, P. M., T. W. Gilbert and S. F. Badylak (2011). "An overview of tissue and whole organ decellularization processes." Biomaterials **32**: 3233-3243.

Cuq, M. H., C. Palevody and M. Delmas (2000). "Fundamental study of cross-linking of collagen with chrome tanning agents in traditional and Cr.A.B processes." Journal of the Society of Leather Technologists and Chemists **83**: 233-238.

Daniels, R. (2002). "Back to basics: preparation for tanning (i)." WORLD Leather **15**(3): 56.

Daniels, R. (2002). "Back to basics: preparation for tanning (ii)." WORLD Leather **15**(4): 53.

Daniels, R. (2002). "Back to basics: raw material and preservation." WORLD Leather **15**(2): 52-53.

Daniels, R. (2002). "Back to basics: the tanning process (i)." WORLD Leather **15**(5): 28.

Daniels, R. (2003). "Back to basics: drying and pre-tanning operations." WORLD Leather **16**(1): 36.

Daniels, R. (2003). "Back to basics: retanning, dyeing and softening." WORLD Leather **15**(8): 58.

Deb Choudhury, S., T. Allsop, A. Passman and G. E. Norris (2006). "Use of a proteomics approach to identify favourable conditions for production of good quality lambskin leather." Analytical and Bioanalytical Chemistry **384**: 723-735.

Deb Choudhury, S., R. G. Haverkamp, S. DasGupta and G. E. Norris (2007). "Effect of Oxazolidine E on collagen fibril formation and stabilization of the collagen matrix." Journal of Agricultural and Food Chemistry **55**: 6813-6822.

Debelle, L. and A. M. Tamburro (1999). " Elastin: molecular description and function." The International Journal of Biochemistry & Cell Biology **31**: 261-272.

Dempsey, M. (1984). Hide, Skin and Leather Defects: A Guide to Their Microscopy. Palmerston North, New Zealand Leather and Shoe Association.

Diamant, J., A. Keller, E. Baer, M. Litt and R. G. C. Arridge (1972). "Collagen; ultrastructure and its relation to mechanical properties as a function of ageing." Proceedings of the Royal Society B **180**: 293-315.

Edmonds, R. L., S. Deb Choudhury, R. G. Haverkamp, M. Birtles, T. Allsop and G. E. Norris (2008). "Using proteomics, immunohistology, and atomic force microscopy to characterize surface damage to lambskins observed after enzymatic dewooling." Journal of Agricultural and Food Chemistry **56**: 7934-7941.

Eyre, D. R. and J.J. Wu (2005). "Collagen cross-links." Topics in Current Chemistry **247**: 207-229.

Fathima, N. N., M. P. Kumar, J. R. Rao and B. U. Nair (2010). "A DSC investigation on the changes in the pore structure of skin during leather processing." Thermochimica Acta **501**: 98-102.

Fennen, J. (1999). "Molecular modelling of tanning processes." Journal of the Society of Leather Technologists and Chemists **82**: 5-10.

Floden, E. W., S. Malak, M. M. Basil-Jones, L. Negron, J. N. Fisher, S. Lun, S. G. Dempsey, R. G. Haverkamp, B. R. Ward and B. C. H. May (2011). "Biophysical characterization of ovine forestomach extracellular matrix biomaterials." Journal of Biomedical Materials Research Part B: Applied Biomaterials **96B**: 67-75.

Folkhard, W., W. Geercken, E. Knorzer, E. Mosler, H. Nemetschek-Gansler, T. Nemetschek and M. H. J. Koch (1987). "Structural dynamic of native tendon collagen." Journal of Molecular Biology **193**: 405-407.

Folkhard, W., W. Geercken, E. Knorzer, H. Nemetschek-Gansler, T. Nemetschek and M. H. J. Koch (1987). "Quantitative analysis of the molecular sliding mechanism in native tendon collagen - time-resolved dynamic studies using synchrotron radiation." International Journal of Biological Macromolecules **9**(3): 169-175.

Fraser, R. D. B., T. P. MacRae, A. Miller and E. Suzuki (1983). "Molecular conformation and packing in collagen fibrils." Journal of Molecular Biology **167**: 497-521.

Fraser, R. D. B., T. P. MacRae and E. Suzuki (1979). The molecular and fibrillar structure of collagen. Fourth International Conference on Fibrous Proteins, Palmerston North, New Zealand, Academic Press Inc.

Fratzl, P., Ed. (2008). Collagen: Structure and Mechanics. New York, Springer Science+Business Media.

Fratzl, P., N. Fratzl-Zelman and K. Klaushofer (1993). "Collagen packing and mineralization: an x-ray scattering investigation of turkey leg tendon." Biophysical Journal **64**: 260-266.

Fratzl, P., K. Misof, I. Zizak, G. Rapp, H. Amenitsch and S. Bernstorff (1997). "Fibril structure and mechanical properties of collagen." Journal of Structural Biology **122**: 119-122.

Gathercole, L. J., J. S. Shah and C. Nave (1987). "Skin-tendon differences in collagen D-period are not geometric or stretch-related artifacts." International Journal of Biological Macromolecules **9**: 181-183.

Gautieri, A., S. Vesentini, A. Redaelli and M. J. Buehler (2011). "Hierarchical structure and nanomechanics of collagen microfibrils from the atomistic scale up." Nano Letters **11**: 757-766.

Gayatri, R., A. K. Sharma, R. Rajaram and T. Ramasami (2001). "Chromium(III)-induced structural changes and self-assembly of collagen." Biochemical and Biophysical Research Communications **283**: 229-235.

Glanville, R. W. and K. Kuhn (1979). The primary structure of collagen. Fourth International Conference on Fibrous Proteins, Palmerston North, New Zealand, Academic Press.

Glatter, O. and O. Kratky (1982). Small Angle X-ray Scattering. London, Academic Press Inc..

Haines, B. M. (1984). "Twentieth Procter memorial lecture: the skin before tannage - Procter's view and now." Journal of the Society of Leather Technologists and Chemists **68**: 57-70.

Heidemann, E. (1979). The current state of collagen chemistry in relation to the manufacture of leather. Fourth International Conference on Fibrous Proteins, Massey, University, Academic Press.

Hulmes, D. J. S., A. Miller, D. A. D. Parry, K. A. Peiz and J. Woodhead-Galloway (1973). "Analysis of the primary structure of collagen for the origins of molecular packing." Journal of Molecular Biology **79**: 137-148.

Hulmes, D. J. S., T. J. Wess, D. J. Prockop and P. Fratzl (1995). "Radial packing, order, and disorder in collagen fibrils." Biophysical Journal **68**: 1661-1670.

Hulmes, D. J. S (2008). Collagen Diversity, synthesis and assembly. Collagen: Structure and Mechanics. P. Fratzl. New York, Springer Science+Business Media: 15-41.

Iozzo, R. V. (1998). "Matrix proteoglycans: from molecular design to cellular function." Annual Review of Biochemistry **67**: 609-652.

IULTCS (2002). Leather - Chemical, physical and mechanical and fastness tests. Sampling location. Switzerland, ISO. **BS EN ISO 2418:2002(E).**

IULTCS (2002). Leather - Physical and mechanical tests. Determination of tear load - Part 2: Double edge tear. Switzerland, ISO. **BS EN ISO 3377-2:2002(E).**

IULTCS (2012). Leather - Physical and mechanical tests. Sample preparation and conditioning. Switzerland, ISO. **BS EN ISO 2419:2012(E).**

James, V. J., J. F. McConnell and M. Capel (1991). "The d-spacing of collagen from mitral heart-valves changes with aging, but not with collagen type-III content." Biochemica et Biophysica Acta **1078**(1): 19-22.

Kadler, K. E., C. Baldock, J. Bella and R. P.Boot-Handford (2007). "Collagens at a glance." Journal of Cell Science **120**(12): 1955-1958

Kajava, A. V. (1991). "Molecular packing in type I collagen fibrils: a model with neighbouring collagen molecules aligned in axial register." Journal of Molecular Biology **218**: 815-823.

Kanagy, J. R., W. H. Leser, E. B. Randall, T. J. Carter and C. W. Mann (1952). "Influence of splitting on the strength of chrome-tanned steer sides." Journal of the American Leather Chemists Association **47**: 329-350.

Kanagy, J. R., C. W. Mann and J. Mandel (1952). "Study of the variation of the physical and chemical properties of chrome-tanned leather and the selection of a sampling location." Journal of the Society of Leather Technologists and Chemists **36**: 231-252.

Kanagy, J. R., E. B. Randall, T. J. Carter, R. A. Kinmonth and C. W. Mann (1952). "Variation of physical and chemical properties within and between vegetable retanned cow and steer sides." Journal of the American Leather Chemists Association **47**(10): 726-748.

Keene, D. R., M. P. Marinkovich and L. Y. Sakai (1997). "Immunodissection of the connective tissue matrix in human skin." Microscopy Research and Technique **38**: 394-406.

Kielty, C. M. and C. A. Shuttleworth (1997). "Microfibrillar elements of the dermal matrix." Microscopy Research and Technique **38**: 413-427.

Kronick, P. L., B. E. Maleeff and M. P. Dahms (1991). "Removal of collagen-VI and collagen-XII by beamhouse chemistry." Journal of the American Leather Chemists Association **86**(6): 209-224.

Kroschwitz, J. I. (1989). Leather. Encyclopedia of Polymer Science and Engineering. H. F. Mark, N. Bikales, C. G. Overberger, G. Menges and J. I. Kroschwitz. USA, John Wiley & Sons, Inc. **Supplement Volume:** 362-379.

Light, N. D. and A. J. Bailey (1979). Covalent crosslinks in collagen: characterisation and relationships to connective tissue disorders. Fourth International Conference on Fibrous Proteins, Palmerston North, New Zealand, Academic Press Inc.

Linsenmayer, T. F., E. Gibney, F. Igoe, M. K. Gordon, J. M. Fitch, L. I. Fessler and D. E. Birk (1993). "Type V collagen: molecular structure and fibrillar organization of the chicken α1(V) NH_2-terminal domain, a putative regulator of corneal fibrillogenesis." The Journal of Cell Biology **121**: 1181-1189.

Liu, C.K. and M. D. McClintick (1999). "Tearing behaviour of chrome-tanned leather." Journal of the American Leather Chemists Association **94**: 129-145.

Lun, S., S. M. Irvine, K. D. Johnson, N. J. Fisher, E. W. Floden, L. Negron, S. G. Dempsey, R. J. McLaughlin, M. Vasudevamurthy, B. R. Ward and B. C. H. May (2010) "A functional extracellular matrix biomaterial derived from ovine forestomach." Biomaterials **31**(16): 4517-4529.

Maeser, M. (1960). "The effect of hide location and cutting direction on the tensile properties of upper leathers." Journal of the American Leather Chemists Association **55**: 501-530.

Mann, C. W., E. B. Randall, J. Mandel and T. J. Kilduff (1951). "The sampling of side upper leather." Journal of the American Leather Chemists Association **46**(3): 248-263.

Mantysalo, E., M. Marjoniemi and E. Kemppinen (1991). "Anisotrophy of physical-characteristic functions of fur leather." Journal of the American Leather Chemists Association **86**: 133-139.

Maxwell, C. A., T. J. Wess and C. J. Kennedy (2006). "X-ray diffraction study into the effects of liming on the structure of collagen." Biomacromolecules **7**: 2321-2326.

Mayne, R. and R. E. Burgeson, Eds. (1987). Structure and Function of Collagen Types. Florida, Academic Press, Inc.

Menderes, O., A. D. Covington, E. R. Waite and M. J. Collins (2000). "The mechanism and effects of collagen amide group hydrolysis during liming." Journal of the Society of Leather Technologists and Chemists **83**: 107-110.

Menkart, J., J. H. Dillom, K. Beurling, J. G. Fee and E. F. Mellon (1962). "Mechanical properties of steerhides and constituent collagen fiber aggregates." Journal of the American Leather Chemists Association **57**: 318-342.

Michel, A. (2004). "Tanners' dilemma: Vertical fibre defect." Leather International **206**(4750): 36-37.

Mier, P. D. and D. W. K. Cotton (1976). The molecular biology of skin. London, Blackwell Scientific Publications.

Misof, K., G. Rapp and P. Fratzl (1997). "A new molecular model for collagen elasticity based on synchrotron x-ray scattering evidence " Biophysical Journal **72**: 1376-1381.

Mithieux, S. M. and A. S. Weiss (2005). Elastin. Advances in Protein Chemistry, Volume 70: Fibrous Proteins: Coiled-Coils, Collagen and Elastomers. D. A. D. Parry and J. M. Squire. USA, Elserier Academic Press.

Mollenhauer, J., M. Aurich, C. Muehleman, G. Khelashvilli and T. C. Irving (2003). "X-ray diffraction of the molecular substructure of human articular cartilage." Connective Tissue Research **44**: 201-207.

Mosler, E., W. Folkhard, E. Knorzer, H. Nemetschek-Gansler, T. Nemetschek and M. H. J. Koch (1985). "Stress-induced molecular rearrangement in tendon collagen." Journal of Molecular Biology **182**: 589-596.

Nimni, M. E., E. de Guia and L. A. Bavetta (1966). "Collagen, Hexosamine and tensile strength of rabbit skin during aging." Journal of Investigative Dermatology **47**(2): 156-158.

O'Leary, D. N. and G. E. Attenburrow (1996). "Differences in strength between the grain and corium layers of leather." Journal of Materials Science **31**: 5677-5682.

Orgel, J. P. R. O., T. C. Irving, A. Miller and T. J. Wess (2006). "Microfibrillar structure of type I collagen *in situ*." PNAS **103**(24): 9001-9005.

Osaki, S. (1999). "Distribution map of collagen fiber orientation in a whole calf skin." The Anatomical Record **254**: 147-152.

Ottani, V., M. Raspanti and A. Ruggeri (2001). "Collagen structure and functional implications." Micron **32**: 251-260.

Parry, D. A. D., A. S. Craig and G. R. G. Barnes (1979). Fibrillar collagen in connective tissue. Fourth International Conference on Fibrous Proteins, Palmerston North, New Zealand, Academic Press Inc.

Parry, D.A.D. and A. S. Craig (1984). "Growth and development of collagen fibrils in connective tissue." In: Ruggeri, A., Motta, P. (Eds.). Ultrastructure of the connective tissue matrix, Martinus Nijhoff, The Hague, pp.34–64.

Prathiba, V. and P. D. Gupta (2000). "Cutaneous wound healing: significance of proteoglycans in scar formation." Current Science **78**(6): 697-701.

Purslow, P. P., T. J. Wess and D. W. L. Hukins (1998). "Collagen orientation and molecular spacing during creep and stress-relaxation in soft connective tissues." The Journal of Experimental Biology **201**: 135-142.

Puxkandl, R., I. Zizak, O. Paris, J. Keckes, W. Tesch, S. Bernstorff, P. Purslow and P. Fratzl (2002). "Viscoelastic properties of collagen: synchrotron radiation investigations and structural model." Philosophical Transactions of the Royal Society **357**: 191-197.

Rabinovich, D. (2001). "Seeking soft leathers with a tight grain." WORLD Leather **14**(5): 27-32.

Randall, E. B., T. J. Carter, T. J. Kilduff, C. W. Mann and J. R. Kanagy (1952). "The variation of the physical and chemical properties of split and unsplit chrome-tanned leathers." Journal of the American Leather Chemists Association **47**: 404-425.

Raspanti, M., V. Ottani and A. Ruggeri (1989). "Different architectures of the collagen fibril: morphological aspects and functional implications." International Journal of Biological Macromolecules **11**: 367–371.

Reed, C. C. and R. V. Iozzo (2003). "The role of decorin in collagen fibrillogenesis and skin homeostasis." Glycoconjugate Journal **19**: 249-255.

Reich, G., J. Bradt, M. Mertig, W. Pompe and T. Taeger (1998). "Scanning probe microscopy a useful tool in leather research." Journal of the Society of Leather Technologists and Chemists **82**: 11-14.

Reich, G. (1999). "The structural changes of collagen during the leather making processes 1998 Atlin memorial lecture." Journal of the Society of Leather Technologists and Chemists **83**: 63-79.

Russell, A. E. (1985). Stress-strain relationships in leather and the role of fibre structure LIRI Research Bulletin.

Russell, A. E. (1988). "Stress-strain relationships in leather and the role of fibre structure." Journal of the Society of Leather Technologists and Chemists **72**: 121-134.

Sasaki, N. and S. Odajima (1996). "Elongation mechanisms of collagen fibils and force-strain relations of tendon at each level of structural hierarchy." Journal of Biomechanics **29**(9): 1131-1136.

Sasaki, N. and S. Odajima (1996). "Stress-strain curve and young's modulus of a collagen molecule as determined by the X-ray diffraction technique." Journal of Biomechanics **29**(5): 655-658.

Scott, J. E. (1980). "Collagen-proteoglycan interactions: localization of proteoglycans in tendon by electron microscopy." Biochemical Journal **187**: 887-891

Sizeland, K. H., M. M. Basil-Jones, R. L. Edmonds, S. M. Cooper, N. Kirby, A. Hawley and R. G. Haverkamp (2013). "Collagen orientation and leather strength for selected mammals." Journal of Agricultural and Food Chemistry **61**(4): 887-892.

Sherratt, M. J. (2009). "Tissue elasticity and the ageing elastic fibre." AGE **31**: 305-325.

Shoulders, M. D. and R. T. Raines (2009). "Collagen structure and stability." Annal Review of Biochemistry **78**: 929-58.

Stephens, L. J. and D. E. Peters (1989). "The physical properties of leather from kangaroo skins II: variation in properties with sampling position." Journal of the American Leather Chemists Association **84**: 143-149.

Stephens, L. J., J. A. Werkmeister and J. A. M. Ramshaw (1993). "Changes in bovine hides during leather processing." Journal of the Society of Leather Technologists and Chemists **77**(3): 71-74.

Sturrock, E. J., C. Boote, G. E. Attenburrow and K. M. Meek (2004). "The effect of the biaxial stretching of leather on fibre orientation and tensile modulus." Journal of Materials Science **39**: 2481-2486.

Suzuki, E., R. D. B. Fraser and T. P. MacRae (1980). "Role of hydroxyproline in the stabilization of the collagen molecule via water-molecules." International Journal of Biological Macromolecules **2**(1): 54-56.

Thomas, S. and P. Fram (2001). "The development of a novel technique for predicting the exudates handling properties of modern wound dressings." Journal of Tissue Viability **11**(4): 145-53, 156-60.

Thyberg, J., S. Lohmander and D. Heinegard (1975). "Proteoglycans of hyaline cartilage – electron- microscopic studies on isolated molecules." Biochemical Journal **151**(1): 157-166.

Trengove, N. J., M. C. Stacey, S. MacAuley, N. Bennett, J. Gibson, F. Burslem, G. Murphy and G. Schultz (1999). "Analysis of the acute and chronic wound environments: the role of proteases and their inhibitors." Wound Repair and Regeneration **7**(6): 442-452.

Tsutakawa, S. E., G. L. Hura, K. A. Frankel, P. K. Cooper and J. A. Tainer (2007). "Structural analysis of flexible proteins in solution by small angle X-ray scattering combined with crystallography." Journal of Structural Biology **158**(2):214-23.

United Nations (2010). World statistical compendium for raw hides and skins, leather and leather footwear 1990-2009. Rome, Italy, Commodities and Trade Division, Food and Agriculture Organization of the United Nations.

Vera, V. D., C. S. Cantera, D. O. Dominguez and C. Bernardi (1993). Modern soft leather influence of the relationship grain/corium on the topography of some physical properties. 22th IULTCS Congress Proceedings, Porto Alegra.

Waller, J. M. and H. I. Maibach (2006). "Age and skin structure and function, a quantitative approach (II): protein, glycosaminoglycan, water, and lipid content and structure." Skin Research and Technology **12**: 145-154.

Wang, Y., Z. Li, M. Chen, H. Cheng and L. Liao (2005). "Study on the changes of collagen fibril structure in pigskin tissue after enzyme treatment." Journal of the Society of Leather Technologists and Chemists **89**(2): 47-56.

Wainwrigth, S.A., W. D. Biggs, J. D. Currey and J. M. Gosline (1976). Mechanical Design in Organisms, New Jersey, Princeton University Press.

Wess, T. J., A. P. Hammersley, L. Wess and A. Miller (1998). "A consensus model for molecular packing of type I collagen." Journal of Structural Biology **122**: 92-100.

Woodhead-Galloway, J. (1980). Collagen: the Anatomy of a Protein. London, Edward Arnold (Publishers) Ltd.

Wysocki, A. B., A. O. Kusakabe, S. Chang and T. L. Tuan (1999). "Temporal expression of urokinase plasminogen activator, plasminogen activator inhibitor and gelatinase-B in chronic wound fluid switches from a chronic to acute wound profile with progression to healing." Wound Repair and Regeneration **7**(3): 154-165.

Yager, D. R. and B. C. Nwomeh (1999). "The proteolytic environment of chronic wounds." Wound Repair and Regeneration **7**(6): 433-41.